

UC Berkeley
SEMM Reports Series

Title

Refined Finite Element Analysis of Linear and Nonlinear Two-Dimensional Structures

Permalink

<https://escholarship.org/uc/item/56p2c0sw>

Author

Felippa, Carlos

Publication Date

1966-10-01

NISEE/COMPUTER APPLICATIONS
DAVIS HALL
UNIVERSITY OF CALIFORNIA
BERKELEY, CALIFORNIA 94720
(415) 642-5113

REFINED FINITE ELEMENT
ANALYSIS OF LINEAR AND
NONLINEAR TWO-DIMENSIONAL
STRUCTURES

by

CARLOS A. FELIPPA

Structures and Materials Research
Department of Civil Engineering

Structural Engineering Laboratory
University of California
Berkeley, California

Report No. SESM 66-22

October 1966

TABLE OF CONTENTS

	<u>Page</u>
ABSTRACT	vi
INTRODUCTION	vii
NOTATION AND LIST OF SYMBOLS	xii
ACKNOWLEDGEMENTS	xviii
I. CONSTRUCTION OF DISPLACEMENT FIELDS OF COMPATIBLE FINITE ELEMENTS BY INTERPOLATION FORMULAS	1
I.1 FINITE ELEMENT ANALYSIS BY DISPLACEMENT MODELS	2
I.1.1 Summary of the Direct Stiffness Method	2
I.1.2 Types of Compatibility Requirements	5
I.1.3 Selection of Nodal Point Systems	7
I.1.4 Polynomial Displacement Functions	10
I.2 GENERAL INTERPOLATION FORMULAS FOR FINITE ELEMENTS	13
I.2.1 The General Concept of Interpolation	13
I.2.2 Interpolation for Vector and Matrix Functions	15
I.3 COORDINATE SYSTEMS FOR PLANE TRIANGLES	17
I.3.1 Cartesian and Triangular Coordinates	17
I.3.2 Relations between Coordinate Systems	20
I.4 POLYNOMIAL INTERPOLATION FORMULAS FOR TRIANGLES	23
I.4.1 Polynomial Expressions in Triangular Coordinates	23
I.4.2 Determination of Complete Polynomials from Boundary Conditions	24
I.4.3 List of Interpolation Formulae for Complete Polynomials of the First Three Orders	26

I.5	AREA INTEGRATION OF FUNCTIONS IN TRIANGULAR COORDINATES	33
I.5.1	Formulas for Polynomial Expressions	33
I.5.2	Numerical Integration	37
II.	DERIVATION OF CONVENTIONAL STIFFNESS MATRICES FOR PLANE ELEMENTS	40
II.1	BASES FOR THE CONSTRUCTION OF STIFFNESS MATRICES	41
II.1.1	The Conventional Ritz Technique and the Finite Element Method	41
II.1.2	Selection of Displacement Functions	43
II.1.3	Introduction of Additional Modes	47
II.2	GENERAL DERIVATION OF CONVENTIONAL STIFFNESS MATRICES	50
II.2.1	Validity	50
II.2.2	Displacement Functions	51
II.2.3	Strain-Displacement Relations	52
II.2.4	Constitutive Law	53
II.2.5	Generalized Force-Displacement Relations	54
II.3	PRACTICAL CONSTRUCTION OF STIFFNESS MATRICES	56
II.3.1	Selection of Nodal System for Element Functions	56
II.3.2	Stiffness Matrix	59
II.4	PRACTICAL GENERATION OF CONSISTENT FORCE VECTORS AND MASS MATRICES	64
II.4.1	Surface Loads	64
II.4.2	Body Forces	66
II.4.3	Consistent Mass Matrix	68

II.5	THERMOELASTIC PROBLEMS	69
II.5.1	Solution by the Initial Stress Method	69
II.5.2	Computation of Initial Thermal Loads	70
III.	TRIANGULAR ELEMENT STIFFNESS MATRICES FOR LINEAR PROBLEMS - POLYNOMIAL ORDERS $n = 1, 2$ and 3	73
III.1	THE CONSTANT STRAIN TRIANGULAR ELEMENT (CST)	74
III.1.1	Displacement and Strain Fields	74
III.1.2	Stiffness Matrix	75
III.1.3	Consistent Nodal Forces and Mass Matrix	76
III.2	THE LINEARLY VARYING STRAIN TRIANGULAR ELEMENT (LST)	77
III.2.1	Motivation	77
III.2.2	Displacement Functions	77
III.2.3	Strain-Displacement Equations	78
III.2.4	Stress-Strain Law	81
III.2.5	Strain Energy Integration	82
III.2.6	Stiffness Matrix	84
III.2.7	Kinematically Equivalent Force Vectors	87
III.2.8	Consistent Mass Matrix	91
III.2.9	Restraint Thermal Forces	91
III.3	THE QUADRATICALLY VARYING STRAIN TRIANGULAR ELEMENT (QST)	93
III.3.1	Displacement Functions	93
III.3.2	Strain-Displacement Relations	94
III.3.3	Strain Energy Integration	96

III.3.4	Stiffness Matrix	98
III.3.5	Kinematically Equivalent Force Vectors	101
III.3.6	Possibilities of the QST	105
IV.	ANALYSIS OF NONLINEAR PROBLEMS	108
IV.1	GENERAL FORMULATION	109
IV.1.1	Classification of Nonlinear Effects	109
IV.1.2	Solution Procedures	110
IV.1.3	Variational Formulation of the Incremental Method	113
IV.1.4	Instantaneous Stiffness Matrix	119
IV.1.5	Numerical Integration Procedures	122
IV.2	ANALYSIS OF ELASTOPLASTIC PROBLEMS	123
IV.2.1	Scope	123
IV.2.2	Summary of Fundamental Constitutive Relations of Elastoplasticity	124
IV.2.3	Matrix Expressions of Incremental Relations for Three-Dimensional Continua	130
IV.2.4	Incremental Law for Plane Stress and Plane Strain (Von Mises criterion)	133
IV.2.5	LST Plane Stress Elements for Elastoplastic Analysis	136
IV.3	FINITE DEFORMATION ANALYSIS FOR ARBITRARY ELEMENTS	147
IV.3.1	Geometrically Nonlinear Problems	147
IV.3.2	Practical Generation of Geometric Stiffness Matrices	150
IV.3.3	Examples: Stringer, Beam-Column	153

IV.4	GEOMETRIC STIFFNESSES OF PLANE STRESS TRIANGULAR ELEMENTS	159
IV.4.1	General Derivation	159
IV.4.2	Constant Strain Triangle	163
IV.4.3	Linear Strain Triangle	164
V.	APPLICATION OF THE LINEAR STRAIN TRIANGLE	165
V.1	LINEAR ELASTIC PROBLEMS	166
V.1.1	Procedure	166
V.1.2	Cantilever Beam	166
V.1.3	Circular Hole in Tension Plate	168
V.1.4	Circular Disk Diametrically Loaded	169
V.1.5	Buried Concrete Pipe	170
V.2	ELASTOPLASTIC PROBLEMS	170
V.2.1	Procedure	170
V.2.2	Plastic Hinge Formation (Small Displacements)	189
V.2.3	Plastic Buckling (Finite Displacements)	191
V.3	ELASTIC STABILITY PROBLEMS	205
V.3.1	Procedure	205
V.3.2	Simply Supported Column	207
	REFERENCES	209
	APPENDIX I. CONSTITUTIVE EQUATIONS FOR LINEAR ELASTIC MATERIALS	213
	APPENDIX II. COMPARISON BETWEEN DIFFERENT TYPES OF QUADRILATERALS ASSEMBLED WITH TRIANGULAR ELEMENTS	221
	APPENDIX III. COMPUTER PROGRAM FOR LINEAR ELASTIC ANALYSIS USING LST ELEMENTS	226
	APPENDIX IV. COMPUTER PROGRAM FOR ELASTOPLASTIC ANALYSIS USING LST ELEMENTS	285

ABSTRACT

The purpose of this report is to study the application of refined displacement finite elements for the direct stiffness analysis of linear and nonlinear problems of structural mechanics.

A systematic procedure to construct polynomial displacement fields based on the use of interpolation formulas in natural coordinates is applied to plane triangles of linear elastic material using the first three complete polynomial expansions.

Geometrically and physically nonlinear problems are formulated in the general form of a step-by-step matrix displacement analysis by means of an incremental variational principle. The derivation of geometric stiffness matrices for finite displacement and stability analysis and of incremental conventional stiffnesses for elastoplastic material is carried out for arbitrary three-dimensional elements and then specialized for plane stress triangles.

Digital computer programs for the linear strain triangle are described and examples of application presented.

INTRODUCTION

Historical Background

The development of general discrete methods of structural mechanics began in the early 1950's, parallel to the advent and extending usage of high-speed digital computers. A formal but important step was the development of the matrix formulation of the transformation theory of structures, after the fundamental work of Argyris [1]. The clear and elegant matrix representation not only shed light on the structure and dual formulation of the two fundamental solution methods, but provided a powerful way of organizing the automatic computation as well.

These techniques were originally applied to the analysis of highly redundant aircraft structures, whose idealization is immediate. Load-displacement relations were usually constructed by direct application of the unit-load or the unit-displacement methods. In the light of present knowledge, some of the early difficulties encountered in representing a correct kinematic behavior are not important, but nevertheless instructive.

The first two-dimensional compatible displacement field, the constant strain triangle [2], provided a means of analyzing arbitrary plane problems. Although the original derivation made use of a one-dimensional model representation, it was soon recognized that the fundamental characteristic of a displacement-consistent finite element is the assumed kinematic field. Extension to rectangular plates [3,4], shells of revolution [5], axisymmetric bodies [6,7], and general three-dimensional continua [6,8], was also successful.

The stiffness formulation and the displacement method of solution were found to be ideally suited for this type of displacement mode analysis, and the direct stiffness method [9] which combined these characteristics with an efficient automatic assembly procedure, soon overshadowed other solution techniques.

Meanwhile, a theory establishing necessary and sufficient conditions to guarantee convergence to the true solution was lacking. Such requirements were considered much later, especially after the work of Melosh [10,11]. The derivation of the load-displacement equations was shown to be equivalent to a piecewise Rayleigh-Ritz procedure applied to the variational principle of minimum potential energy. The basic conditions for a successful generation of displacement fields; continuity (interelement compatibility) and completeness (inclusion of kinematic rigid body modes and uniform strain states) were summarized by Irons [12].

The failure of early attempts [13] to construct satisfactory triangular plate elements may be attributed not only to the lack of compatibility, but to the derivation in cartesian coordinates (a non-natural system) leading to lack of invariance in general. Similar cartesian expansions were successful for non-compatible rectangular plate elements.

With a firmly established basis for the generation of higher order displacement fields, a systematic development of refined elements is now possible. This tendency has been observed recently [14,15,29]. The application of such elements to geometrically and physically nonlinear problems, originally restricted to framed structures [16] or constant strain triangles [17,18], is very promising

A recent development concerns the possibility of systematic usage of other types of finite elements. De Veubeke [15,19] has advocated the use of equilibrium elements formulated by means of stress assumptions on the minimum complementary energy principle to obtain upper bounds on the influence coefficients; the dual aspects of the derivation have been stressed. Simple equilibrium elements (spar, shear panels, etc.) have been used for a long time; however, more refined two or three dimensional elements do not seem to have been employed in significant scale.

Mixed models, generated by partial assumptions on displacements and stresses, might also be extremely useful for many problems. Governing variational principles yielding the field equations as Euler equations on the primary variables, must be constructed for each problem and a general theory is still lacking. The most important application so far concerns incompressible solids [20] where stresses are determined by the distortions only up to an hydrostatic pressure depending on stress boundary conditions. An assumed transverse displacement-moment thick plate element has also been developed [21].

Finally it should be stressed that the finite element technique is by no means restricted to the solution of structural problems; it may be applied to the solution of general field problems which can be cast into a variational form. Zienkiewicz and Cheung [22] have recently applied this procedure to solve second order problems such as stationary heat flow and torsion.

Past experience has shown that the success of the analysis depends on the adequacy of the finite element behavior. The establishment of the set of equations and their solution is a practically important, but formal application of matrix algebra and numerical analysis.

Purposes and Scope

This report deals with the systematic generation of compatible finite elements and their specific application to the analysis of linear and nonlinear plane problems. The general character of the derivations is stressed; computations and examples for particular cases are intended to illustrate the method.

A concise and elegant derivation of the load-displacement relations can only be achieved through the use of natural coordinates, which are intrinsically related to the element geometry. Compatible displacement fields may be systematically constructed by interpolation functions in natural coordinates. The tedious process of inverting transformation matrices and the endless evaluation of integrals in cartesian coordinates is completely avoided.

The formulation of the general step-by-step matrix displacement analysis for nonlinear problems is carried out for arbitrary elements. This generality is necessary since past presentations have been either limited to specific problems or obscured by unnecessary intuitive arguments. An incremental variational principle provides macroscopic equilibrium equations in the deformed geometry and uncouples physical and geometric nonlinearities.

Specific examples and the included computer programs illustrate the application of the linear strain triangle (LST) for linear and nonlinear two-dimensional problems. A significant improvement of both displacement and stress patterns with respect to the constant strain element is observed.

The techniques described in this report have also been applied to the development of successful triangular plate elements; compatible displacement fields may be obtained by assembling several triangles [23]. Application to linear and nonlinear plate problems will be the matter of a forthcoming publication.

NOTATION AND LIST OF SYMBOLS

Notation Rules

The following rules concerning notation are observed:

- 1) Vectors and matrices are represented by bold-type characters.
- 2) A tilde on top of a vector or matrix symbol is used when necessary to distinguish a function of spatial coordinates from its nodal point values arranged as a vector or matrix.
- 3) Summation convention holds for component expressions unless specifically suppressed. It does not apply to indexed matrix or vector symbols.

List of General Symbols

A list of the most commonly used symbols and their general meaning follows. Specific usage and indexing is explained in the context of the report.

a) Scalars

a,b	Generalized coordinates. Global dimensions of a triangle.
c	Elements of matrix of material constants.
d	Differential symbol. Projection of a corner of a triangle over opposite side.
f	General Function. Body forces. Yield surface equation.
g	Function used in plasticity theory (IV-30).
h	Thickness. Triangle heights. Function used in plasticity theory (IV-30).
k	Elements of stiffness matrix in terms of nodal displacements.
i,j,...s	Used as subscripts or integer constants.

l	Triangle side lengths.
m	Mass (dm = mass element).
n	Normal to boundary. Elements of stiffness matrix in terms of nodal strains.
p	Distributed in-plane loading on triangles. Derivatives of hardening parameter K with respect to plastic strains.
q	Elements of weight matrix Q . Derivatives of yield surface with respect to stress components.
r	Components of nodal displacement vector.
s	Triangle side directions. Deviatoric stress components, Arc length (ds = line element).
t	Stress-temperature material constants.
u	X-displacement component. Displacements in general derivations.
v	Y-displacement component.
w	Z-displacement component. Weights in numerical integration formulas.
x,y,z	Local coordinate system and coordinates.
A	Area of two-dimensional finite elements (dA = area element). Cross sectional area of one-dimensional elements.
B,S	Boundary of finite element (dS = surface element for three-dimensional regions).
C	Components of fourth-order stress-strain tensor (instantaneous moduli in general derivations).
D,V	Volume of finite element (dV = volume element).
E	Direct or Young's moduli (technical constants). Components of Cauchy's finite strain tensor.
F	Body forces in general derivations. Work-hardening function with dimension of stress.

G	Shear moduli (technical constants).
J	Invariants of stress deviator.
H	Work-hardening function with dimension of (stress) ² (=F ²). Height.
I	Integral. Moment of inertia.
L	Length.
M	Moment.
(N)	Nodal point system.
P	Potential of prescribed loads. Force.
Q	Second differential of the strain energy U.
R	Components of nodal force vector.
S	Components of fourth-order strain-stress tensor (compliances in general derivations).
T	Surface tractions in general derivations.
U	Strain energy.
V	Total potential energy (U-P).
W	Work (W_e = external work, W_i = internal work, W_p = plastic work, etc).
X,Y,Z	Global coordinate system and coordinates.
α	Coefficient of thermal expansion.
$\alpha, \beta, \epsilon, \psi, \dots$	General coefficients.
γ	Total shear strain. Angles of triangle sides and the x-axis.
ϵ	Components of infinitesimal or linear strain tensor.
δ	Variation symbol. Specific displacement. Kronecker s delta.
ζ	Natural coordinates.
η	Components of quadratic strain tensor.

θ	Temperature variation. Rotation angles.
K	Work-hardening parameter.
λ	Load parameter. $d\lambda$ = coefficient of proportionality in flow rule of plasticity.
μ	Coefficient of influence between shear strains and direct stresses.
ν	Poisson's ratio.
ξ	Reduced or dimensionless thickness.
ρ	Density.
σ, τ	Stress components: τ is used in general derivations for actual stress, $\bar{\tau}$ for stress referred to initial area.
ϕ	Interpolation functions.
φ	Coordinate functions.
χ	Plastic/elastic modulus ratio in tension test.
ω	Components of the infinitesimal rotation tensor.
Γ	Position parameter.
Ω	Function space basis.
\mathcal{V}	General function space.
\mathcal{P}	Polynomial space
\mathcal{S}	Structure (\mathcal{S}^* = actual; \mathcal{S} = discretized).

b) Vectors and matrices

$\langle \dots \rangle$	Row vector.
$\left\{ \begin{array}{c} \vdots \\ \vdots \end{array} \right\}$	Column vector.
$[]$	Matrix.

a	Vector of generalized coordinates
f	Nodal vector for a general function. Body force vector.
h	Nodal thickness vector.
p	Nodal vector for in-plane distributed force on plane triangle. Vector of p's used in plasticity analysis.
q	Vector of q's used in plasticity analysis.
r	Nodal displacement vector.
u,v,w	Subvectors of r including specific (x,y,z) components.
A	Transformation matrix.
B	Strain-nodal displacement matrix.
C	General stress-strain matrix.
D	Nodal stress-nodal strain matrix.
F	Flexibility matrix.
I	Identity matrix.
J	Geometric stiffness in terms of nodal strains.
K	Stiffness matrix in terms of nodal displacements (for an element or the entire structure).
K_C, K_G	Conventional and geometric stiffness matrices, where distinction is necessary.
L	Numerical matrices resulting from area integrals of triangular interpolation functions. Lower triangular matrix.
M	Mass matrix.
N	Stiffness matrix in terms of nodal strains.
O	Null vector or matrix.
Q	Weighting matrix resulting from strain energy integration over an element (\bar{Q} = numerical blocks of Q).

R	Nodal forces.
S	Applied nodal forces when necessary to differentiate from R (internal nodal forces). Compliance matrix.
T	Transformation matrix.
U, V, W	Submatrices of the strain-nodal displacement matrix B .
α	Thermal coefficient vector.
ϵ	Infinitesimal strain vector.
θ	Nodal temperature vector.
ζ	Natural coordinate vector.
ξ	Reduced thickness vector.
ϕ	Interpolation function vector.
σ, τ	Stress vector.
Φ	Interpolation function matrix.
Λ	Numerical matrix relating strains at the nodal stress system and nodal strains.
Ω	Incremental plastic strain-incremental total strain matrix.

ACKNOWLEDGEMENTS

The research reported herein was carried out during the author's graduate study for the Ph.D. degree in Civil Engineering at the University of California, Berkeley.

The author wishes to express his deepest gratitude to Professor R. W. Clough, under whose supervision the work was conducted, and to Professors E. L. Wilson and B. Parlett, members of his thesis committee, for their helpful guidance and assistance.

This work was sponsored by the National Science Foundation by Grant GK-75. The Berkeley Computer Center provided their facilities for the computer work.

Mrs. M. French did the final typing of the report.

I. CONSTRUCTION OF DISPLACEMENT FIELDS OF
COMPATIBLE FINITE ELEMENTS BY INTERPOLATION FORMULAS

I.1 FINITE ELEMENT ANALYSIS BY DISPLACEMENT MODELS

I.1.1. Summary of the Direct Stiffness Method

The direct stiffness method, described by Turner [9] in his 1959 AGARD paper, is at the present the most powerful and developed subclass of the general finite element methods of structural mechanics. Since this procedure has been extensively covered elsewhere [24,25], only a summary of the relevant steps will be presented:

(a) Structure Discretization. The behavior of the actual structure \mathcal{S}^* is assumed to be approximated by that of a "discretized structure" \mathcal{S} formed by an assemblage

$$\mathcal{S} = \bigcup_K D_K \quad (U \equiv \text{union of})$$

of bounded, simply connected domains D_k called "finite elements". Since for practical reasons the geometry of the elements must be simple, the geometry of \mathcal{S}^* is, in general, only approximated by \mathcal{S} .

(b) Displacement Field Discretization. Every element displacement field is constrained to belong to a finite class or space of functions continuous in D_k and satisfying deformation continuity across element interfaces. The coordinate functions $\{\psi_j\}$, component of a basis Ω for the element displacement function space, will be called "displacement modes" or "displacement shapes;" their amplitudes are the "generalized coordinates" or "generalized displacements" with respect to Ω and may be considered as kinematic degrees of freedom.

The whole displacement field of the connected discretized structure *S* is then continuous, piecewise differentiable and can be made to satisfy kinematic boundary conditions.

This type of displacement field assumption defines a "compatible element" or "displacement model." Two other types of structural finite elements may be constructed; equilibrium or stress-assumed models, and mixed or displacement-stress assumed models (see Table 1).

(c) Derivation of Element Stiffnesses. The element stiffness matrix expresses, in a compact form, the relations between generalized coordinates and associated generalized forces; it is a function of the geometric and constitutive properties of the element. Stiffness matrices associated with different coordinate bases are related by simple congruent transformations.

The derivation of these relations must be based on the governing variational principle. For the compatible element defined in (b), the general variational principle of Hu-Washizu [26,27] reduces to the ordinary principle of variations of displacements expressing the minimum of the total potential energy [15]. This is actually a form of the Rayleigh-Ritz technique applied to the network of finite elements (see II.1.1).

(d) Assembly of the Stiffness of the Complete Structure. To make the combination of the individual stiffnesses possible, the assumed displacement modes are defined by their values at special points - called "nodal points" or simple "nodes" - located usually on the element interfaces. The generalized

coordinates become "nodal displacements" and the components of the associated orthonormal basis are referred to as "interpolating functions" or "shape functions" (1.2.1). Interelement compatibility requires that the displacements of any surface B_{kl} common to two elements "k" and "l" be completely specified in terms of nodal displacements on B_{kl} .

The element stiffness matrices, expressed in terms of nodal displacements and associated nodal forces, must be transformed to a common coordinate system at each nodal point; usually this system is the same for the entire structure ("global" reference frame). The formation of the complete stiffness of \mathcal{S} proceeds now by direct addition at all interface nodes. Finally kinematic constraints are introduced.

The resulting system of equations (linear or nonlinear), may be interpreted as "global" equilibrium equations for the discretized structure connected only at the nodal points; however, this physical picture may fail when high order gradients are selected as generalized nodal displacements.

(e) Displacement Solution. Any problem analyzed by the stiffness procedure may be solved either by the force or by the displacement method (see Table 1). The terms "stiffness method of analysis" and "displacement method of solution" should not be taken as synonyms; for instance, the force method may be the best one for the solution of problems involving equilibrium elements. However, the topology of the element connections is such that the displacements are by far the best choices in a displacement model analysis; the matrix of the equilibrium equation set is then the complete stiffness matrix, which is

usually well-conditioned, sparsely populated and (with adequate arrangement of the equations) narrowly banded. These properties permit a very efficient automatic assembly and solution of large systems, and explain the power of the direct stiffness technique.

(f) Stress Computation. The best stresses resulting from a displacement-mode analysis are those associated with the strain field derived from the displacement solution, as pointed out by De Veubeke [15]. Other procedures such as least-square fitting, etc., to which certain amount of literature has been devoted, are unnecessarily complicated nonsense. Of course, element stresses should be interpreted with care when using very restricted displacement expansions such as linear ones; certain averaging procedures have to be developed for the interfaces.

In summary, the direct stiffness method is the analysis of displacement finite element idealizations, solved by the displacement method. The term "direct" refers to the particular way of assembling the complete stiffness matrix of the unconstrained elements in common nodal systems, before imposing kinematic constraints, and avoiding inefficient transformations with location or "Boolean" matrices [18].

1.1.2 Types of Compatibility Requirements

For general three-dimensional elements, only the displacement field need to be continuous across element interfaces; this will be referred to as "type C-0" of compatibility. Frequently we can reduce a problem to two dimensions if a displacement law of order "q" is assumed to hold in the third

Table 1. Classification of Finite Element Methods

Subdivision based on	Id.	Name	Description
Finite Element Model	I	Displacement or Compatible	Assumed compatible displacement field
	II	Equilibrium	Assumed equilibrium stress field
	III	Mixed	Partial assumptions on displacement and stresses
Element Relations Between Generalized Forces and Displacements	A	Stiffness	Generalized forces from generalized displacements
	B	Flexibility	Generalized displacements from generalized forces
Method of Solution	a	Displacement	Displacement as unknowns
	b	Force	Forces as unknowns
	c	Mixed	Displacements and Forces as unknowns

- Notes:
1. There are 18 possible combinations.
 2. A-B refer to the original derivation of relations for the element; they may be inverted if necessary to match with the method of solution.
 3. Only the choice of model determines the results; other steps constitute formal matrix algebra.
 4. The transfer matrix method is a special mixed method of solution.

direction; then the satisfaction of three-dimensional compatibility requires that normal gradients of the transversal components, up to the "q-th" order, should be continuous at the interelement boundaries; this is "type C-q" of compatibility. The same definition may be extended to one-dimensional elements. In summary:

- (a) C-0 compatibility: all displacement components u_i ($i = 1, 2, 3$) are continuous on all B_{kl} ;
- (b) C-q compatibility: includes C-0, plus for $i = 3$ (two-dimensional elements) or $i = 2, 3$ (one-dimensional elements) $\partial^r u_i / \partial n^r$ ($r = 1, 2, \dots, q$) continuous on all B_{kl} , where n is the normal to B_{kl} .

For brevity we shall often refer to displacement models satisfying "C-k" compatibility as "C-k elements". Three-dimensional, plane "membrane" and truss members are of C-0 type. Bending elements, when shear distortion is neglected, should be C-1. Specific examples may be found in Table 2.

The construction of two-dimensional C-q ($q \geq 1$) elements is much more difficult than simple three-dimensional C-0 elements. For that reason, plate and shell elements which satisfy only C-0 compatibility have been often used, sometimes with success.

I.1.3 Selection of Nodal Point Systems

Let

(N) = element nodal point system for the displacement field;

\mathbf{r} = corresponding vector of "m" nodal displacements.

where the components r_i ($i = 1, 2, \dots, m$) may be actual displacements or displacement gradients of any order, provided their selection satisfies the conditions indicated in I.2.1.

We may partition (N) into

$$\begin{aligned} (N) &= (N)_c + (N)_a \\ \mathbf{r}^t &= \langle \mathbf{r}_c^T ; \mathbf{r}_a^T \rangle \end{aligned} \tag{I-1}$$

where $(N)_c$ is the fundamental nodal system containing the " m_c " kinematic degrees of freedom \mathbf{r}_c necessary and sufficient to accomplish interface compatibility requirements; these will be referred to as external or fundamental degrees of freedom;

$(N)_a$ is the nodal system containing additional " m_a " degrees of freedom \mathbf{r}_a , not necessary for compatibility purposes. This set $(N)_a$ may be empty, i.e., $m_a \cong 0$.

A second subdivision of (N) is

$$\begin{aligned} (N) &= (N)_B + (N)_I \\ \text{and } \mathbf{r}^T &= \langle \mathbf{r}_B^T ; \mathbf{r}_I^T \rangle \end{aligned} \tag{I-2}$$

where $(N)_B$: nodal point system on the boundary B; these will be called external nodal points;

$(N)_I$: nodal point system in the interior of D (internal nodal points); each one including nodal displacement subvectors \mathbf{r}_B and \mathbf{r}_I with " m_B " and " m_I " components. Again m_I may be zero.

Fundamental requirements for $(N)_c$ are

(a) All fundamental degrees of freedom must be specified on the boundary, i.e.,

$$(N)_c \in (N)_B \quad (I-3)$$

(b) The displacements of any portion of the boundary B_{kl} common to elements "k" and "l" must be completely defined by nodal points on B_{kl} .

This condition includes (a).

Additional properties are

(c) Some additional degrees of freedom may be specified on the boundary, i.e.,

$$(N)_a = (N)_{aB} + (N)_{aI}$$

with associated displacement subvectors with " m_{aB} " and " m_{aI} " components, respectively.

(d) All additional degrees of freedom specified at internal nodes may be eliminated in the formation of the external stiffness matrix by the condensation procedure described in II.1.3; provided the generalized nodal forces \mathbf{R}_I associated with \mathbf{r}_I are known a priori (this may not occur in dynamic linear problems if the frequencies are unknown).

(e) Additional degrees of freedom specified on the boundary \mathbf{r}_{aB} may be condensed or retained; therefore the order of the final stiffness matrix may vary between " m_c " and $m_B = m_c + m_{aB}$. In general the best policy is to eliminate all additional boundary modes since their inclusion introduces

unnecessary compatibility relations and stiffens the structure. For example: a beam element may be given two fifth order additional modes specified by the end curvatures; if they are included in the external stiffness, we impose a continuous transmission of moments even at the meeting of several of such members.

I.1.4 Polynomial Displacement Functions

Polynomial expansions have been used nearly exclusively in the generation of all types of finite element models. This preference is based on their simplicity and convenience for automatic computation; moreover, the investigation of compatibility satisfaction is simplified.

The space \mathcal{P}_n of all polynomials of degree $\leq n$ in the Euclidean space \mathcal{E}_s contains

$$m = \binom{n+s}{s} = \frac{(n+s)!}{n! s!} \quad (\text{I-4})$$

independent functions, i.e., has dimension m . We call \mathcal{P}_n a complete polynomial space of order "n" and a general $P_n(x_1) \in \mathcal{P}_n$ a complete n-th order polynomial. Evidently \mathcal{P}_n contains all \mathcal{P}_r , ($r \leq n$) as linear subspaces. If "j" constraints are imposed on the class of polynomials spanning \mathcal{P}_n , we get an incomplete polynomial space \mathcal{P}_n^{m-j} of order "n" and dimension $(m-j)$.

The importance of the concept of the complete polynomial lies in the fact that \mathcal{P}_∞ is a complete function space for the class of continuous functions [28] (Weierstrass theorem).

Table 2. Examples of Compatible Polynomial Displacement Fields

Displacement Function Order	Dim.	Comp. Type	Fundam. degrees of freedom (local system)	No. of distinct Nodes	Complete Polynomial?	Domain	Description	Ref.
Linear	1	C-0	2	2	Yes	Segment	Stringer or Truss Member	
	2	C-0	6	3	Yes	Triangle	Constant Strain Triangle	2
	2	C-0	6	3	Yes	Triang. Ring	Axisymmetric Const. Strain Ring Element	6
	3	C-0	12	4	Yes	Tetrahedron	Constant Strain Tetrahedron	6, 8
Quadratic	1	C-0	3	2	Yes	Segment	Linear Strain Flange	15
	2	C-0	12	6	Yes	Triangle	Linear Strain Triangle	*
	2	C-0	8	4	No	Rectangle	Rectangular Membrane Element	10, 18
	3	C-0	30	10	Yes	Tetrahedron	Linear Strain Tetrahedron	14
Cubic	1	C-1	4	2	Yes	Segment	Simple Beam Element	
	2	C-0	18	3	Yes	Triangle	Quadratic Strain Triangle	*
	2	C-1	9	3	No	Triangle	Compatible Triang. Thin Plate, 3 nodes	23
	2	C-1	12	6	Yes	Triangle	Compatible Triang. Thin Plate, 6 nodes	**
	2	C-1	16	4	Yes	Rectangle	Compatible Rectangular Thin Plate	29
	3	C-0	24	8	No	Prism	Rectangular 3-D prism	10

Table 2 (Con't)

Displacement Function Order	Dim.	Comp. Type	Fundam. degrees of freedom (local system)	No. of distinct Nodes	Complete Polynomial?	Domain	Description	Ref.	
Quintic	1	C-1	6	2	No	Segment	Refined Beam Element	**	
	2	C-1	36	4	No	Rectangle	Refined Compatible Rectangular Thin Plate	29	
	3	C-1	18	3	No	Triangle	Refined Compatible Triangular Thick Plate	**	
	* In this report								
	** To be published in the Plate Bending report.								

Some of the most important and successful compatible finite elements constructed with polynomial displacement expansions are listed in Table 2. It should be noted that when a k -th dimensional element is used in the space ξ_s ($s > k$), complete compatibility may be lost, especially for $C-q$ ($q \geq 1$) elements. For instance, flat thin plate elements used to approximate shell structures.

I-2 GENERAL INTERPOLATION FORMULAE FOR FINITE ELEMENTS

I.2.1 The General Concept of Interpolation

Throughout this paragraph the vector symbol $\mathbf{x} = (x_1, \dots, x_s)$ denotes a point in a bounded, simply connected domain D of the Euclidean space ξ_s .

Let \mathcal{V} be a m -dimensional vector space of functions $f(\mathbf{x})$ defined and differentiable in D , and spanned by a basis $\boldsymbol{\varphi}^T = \langle \varphi_1(\mathbf{x}), \dots, \varphi_m(\mathbf{x}) \rangle$. By definition, any $f(\mathbf{x}) \in \mathcal{V}$ can be expressed as follows:

$$f(\mathbf{x}) = a_1 \varphi_1 + a_2 \varphi_2 + \dots + a_m \varphi_m = a_i \varphi_i(\mathbf{x}) = \mathbf{a}^T \boldsymbol{\varphi}(\mathbf{x}) \quad (\text{I-5})$$

where $\mathbf{a}^T = \langle a_1 \ a_2 \ , \dots \ , a_m \rangle$

are the generalized coordinates of $f(\mathbf{x})$ in the basis $\boldsymbol{\varphi}$. Consider now a configuration (N) of " m " distinct points of D

$$(N): (x_1 \ x_2, \dots, x_m)$$

at which $f(\mathbf{x})$ takes on the values $f_i = f(x_i)$ represented by a vector

$$\mathbf{f}^T = \langle f_1 \ f_2 \ , \dots \ , f_m \rangle \quad (\text{I-6})$$

Let $\varphi_{rs} = \varphi_r(\mathbf{x}_s)$ and \mathbf{A} be the $(m \times m)$ matrix $[\varphi_{rs}]$. If

$$\det \mathbf{A} \neq 0 \quad (I-7)$$

we can solve for

$$\mathbf{a} = \mathbf{A}^{-1} \mathbf{f} \quad (I-8)$$

In such a case the configuration or set (N) will be called a "nodal point system" in D for the space \mathcal{V} , and (I-6) the "nodal point vector".

We now construct a sequence of "m" functions $\phi_r(\mathbf{x})$:

$$\begin{aligned} \phi_r(\mathbf{x}) &= \frac{1}{f_r} (a_1 \varphi_1 + a_2 \varphi_2 + \dots + a_m \varphi_m) = \frac{1}{f_r} a_i \varphi_i(\mathbf{x}) \\ &= \frac{1}{f_r} \mathbf{a}^T \boldsymbol{\varphi}(\mathbf{x}) = \frac{1}{f_r} \mathbf{f}^T (\mathbf{A}^{-1})^T \boldsymbol{\varphi}(\mathbf{x}) \quad r = 1, 2, \dots, m \end{aligned} \quad (I-9)$$

which satisfy $[\phi_{rs}] = \mathbf{I}$, i.e., $\phi_r(\mathbf{x}_s) = \delta_{rs}$ (Kronecker delta)

Then $\langle \phi_1(\mathbf{x}), \dots, \phi_m(\mathbf{x}) \rangle$ is an orthonormal basis for \mathcal{V} in the nodal point system (N); such a basis is unique if condition (I-7) is satisfied. Functions $\phi_i(\mathbf{x})$ will be called "interpolating functions" or "shape functions".

Expression (I-5) becomes

$$f(\mathbf{x}) = f_1 \phi_1 + \dots + f_m \phi_m = f_i \phi_i(\mathbf{x}) = \mathbf{f}^T \boldsymbol{\phi}(\mathbf{x}) \quad (I-10)$$

and will be called the interpolation formula for $f(\mathbf{x})$ with respect to (N);

$\boldsymbol{\phi}$ is the "interpolating vector."

We can extend the class of nodal point systems if we select only "r" sample values of $f(\mathbf{x})$ at a nodal system $(N)_1$ plus $(m-r)$ partial derivatives

of $f(\mathbf{x})$ at $(N)_2$; this presupposes sufficient differentiability of the functions $f \in \mathcal{V}$. Since $f(\mathbf{x})$ must be uniquely determined with all constants of integration, not all combinations are possible; not only condition (I-7) must hold, but if "q" is the highest order of the derivatives considered, each coefficient of the multidimensional Taylor expansion of $f(\mathbf{x})$ up to the q-th order must be determined by the choice of the nodal point vector (I-6).

Frequently, both the value of the function and of certain derivatives are specified at the same points, i.e., $(N)_1$ and $(N)_2$ overlap. In such a case the number of different nodal points may be much less than "m", the dimension of the function space \mathcal{V} . This reduces the connectivity and increases the efficiency of the automatic solution.

I.2.2 Interpolation for Vector and Matrix Functions

The interpolation formula (I-10) may be extended immediately to vector and matrix functions of \mathbf{x} in D . Let

$$\begin{aligned} \tilde{\mathbf{f}}(\mathbf{x}) &= \langle f^1(\mathbf{x}) \dots f^q(\mathbf{x}) \rangle \\ \tilde{\mathbf{F}}(\mathbf{x}) &= \begin{bmatrix} f^{r1}(\mathbf{x}) \dots f^{r9}(\mathbf{x}) \\ \vdots \\ f^{r1}(\mathbf{x}) \dots f^{r9}(\mathbf{x}) \end{bmatrix} \end{aligned} \quad (\text{I-11})$$

where all $f^i(\mathbf{x})$ or $f^{ij}(\mathbf{x}) \in \mathcal{V}$. The nodal point system (N) is common to all component functions; their nodal point values are denoted by

$$f_n^i = f^i(\mathbf{x}_n) \qquad f_n^{ij} = f^{ij}(\mathbf{x}_n)$$

Then (I-10) in component notation is

$$f^i(x) = \phi_k(x) f_k^i \quad f^{ij}(x) = \phi_k(x) f_k^{ij} \quad (\text{I-12})$$

The expression of Equations (I-12) in matrix form depends on the structure selected for the nodal point values. As an example let us consider a vector function of 2 components having a 3 nodal point system:

$$\tilde{\mathbf{f}}(\mathbf{x}) = \begin{Bmatrix} f^1 \\ f^2 \end{Bmatrix} = \begin{bmatrix} \phi_1 f_1^1 + \phi_2 f_2^1 + \phi_3 f_3^1 \\ \phi_1 f_1^2 + \phi_2 f_2^2 + \phi_3 f_3^2 \end{bmatrix}$$

If we chose a nodal point matrix $\mathbf{F} = [f_n^i]$ (2 x 3):

$$\tilde{\mathbf{f}}(\mathbf{x}) = \langle \phi_1 \ \phi_2 \ \phi_3 \rangle : \begin{bmatrix} f_1^1 & f_2^1 & f_3^1 \\ f_1^2 & f_2^2 & f_3^2 \end{bmatrix} = \phi^T : \mathbf{F} \quad (\text{I-13a})$$

If instead we have a nodal point vector \mathbf{f} (6 x 1):

$$\begin{aligned} \mathbf{f}(\mathbf{x}) &= \begin{bmatrix} \phi_1 & \cdot & \phi_2 & \cdot & \phi_3 & \cdot \\ \cdot & \phi_1 & \cdot & \phi_2 & \cdot & \phi_3 \end{bmatrix} \begin{Bmatrix} f_1^1 \\ f_1^2 \\ f_2^1 \\ f_2^2 \\ f_3^1 \\ f_3^2 \end{Bmatrix} \\ &= [\bar{\Phi}_1 \ \bar{\Phi}_2 \ \bar{\Phi}_3] \begin{Bmatrix} f_1 \\ f_2 \\ f_3 \end{Bmatrix} = \bar{\Phi} \mathbf{f} \end{aligned} \quad (\text{I-13b})$$

where

$$\bar{\Phi}_i = \begin{bmatrix} \phi_i & \cdot \\ \cdot & \phi_i \end{bmatrix} \quad \mathbf{f}_i = \begin{Bmatrix} f_i^1 \\ f_i^2 \end{Bmatrix}$$

In general we shall use the symbol ϕ for a vector of interpolating or shape functions and Φ for a matrix of such terms; they will be referred to as "interpolation vector" and "interpolation matrix" for brevity.

The tilde on top of a vector or matrix function is used to distinguish it from the vector or matrix of their nodal values.

1.3 COORDINATE SYSTEMS FOR PLANE TRIANGLES

1.3.1 Cartesian and Triangular Coordinates

A plane triangle 1-2-3 lies on the x-y plane of a global cartesian frame (x,y,z), the coordinates of the corners being (x_i, y_i) , $i = 1, 2, 3$ (Fig. 1.1). Global dimensions, parallel to x and y, are denoted by a_i and b_i (Fig. 1.2).

Three local cartesian systems (s_i, n_i) , $i = 1, 2, 3$, are defined with the s_i axes along the sides, in counterclockwise cyclic sense and with origin at the corners (Fig. 1.1); n_i axes are directed as inward normal of the corresponding sides. Intrinsic dimensions: side lengths l_i , heights h_i and opposite corner projections d_i , may be regarded as coordinates of the corners in the local systems; their subscript is always related to the opposite corner number (Fig. 1.3).

The position of any internal point P may be specified either by its global coordinates or by any pair of local coordinates. A third and very useful system is defined as follows: let A_1 , A_2 and A_3 be the areas of the three subtriangles subtended by P and the corners, the index designating as usual the opposite corner number (Fig. 1.4). The three triangular coordinates

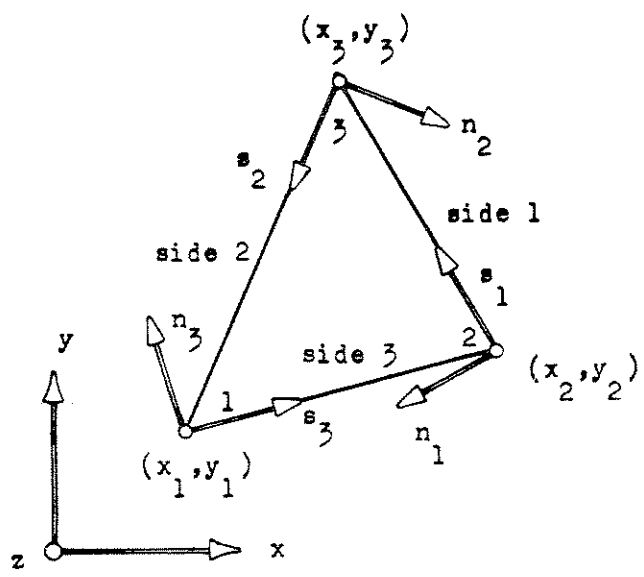


Fig. 1.1 - Local and Global Cartesian Systems.

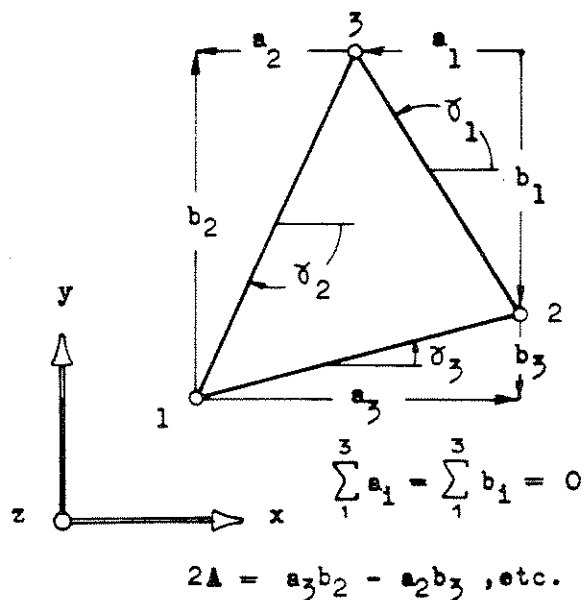


Fig. 1.2 - Global Dimensions and Side Angles.

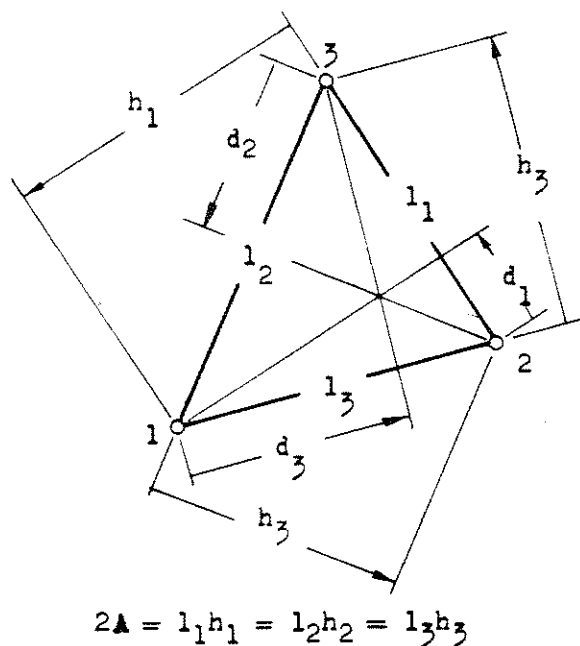


Fig. 1.3 - Intrinsic Dimensions.

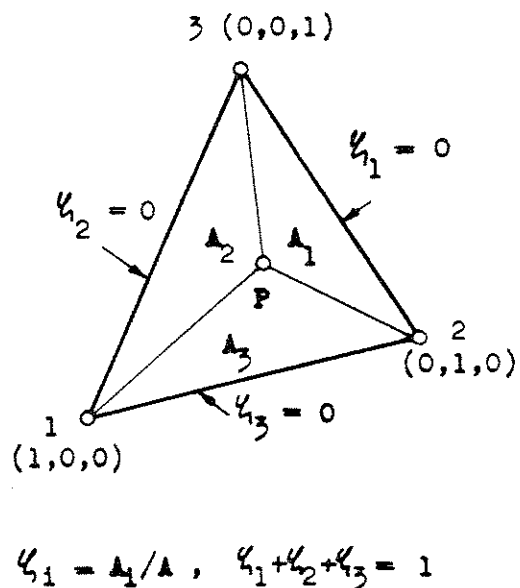


Fig. 1.4 - Triangular or Natural Coordinates.

of P are

$$\begin{aligned} \zeta_1 &= A_1/A & \zeta_2 &= A_2/A & \zeta_3 &= A_3/A \\ \zeta_1 + \zeta_2 + \zeta_3 &= 1 \end{aligned} \quad (1-14)$$

where $A = A_1 + A_2 + A_3$ is the total area of the triangle. The symbol ζ_i will designate the set $(\zeta_1, \zeta_2, \zeta_3)$; the vector symbol ζ refers to the set ζ_i as a (3×1) vector, i.e.,

$$\zeta^T = \langle \zeta_1, \zeta_2, \zeta_3 \rangle$$

Finally, the symbol ζ_B will denote the triangular coordinates of a point on the sides. Thus a function $f(x,y)$ expressed in triangular coordinates, may be written as $f(\zeta_1, \zeta_2, \zeta_3)$, $f(\zeta_i)$ or $f(\zeta)$; $f(\zeta_B)$ is a function defined on the boundary.

The triangular coordinates of all images of a point P under all linear transformations mapping one triangle onto another, remain invariant. Thus we see that the set ζ_i is dimensionless, homogeneous and intrinsic (i.e., independent of the position of the external reference system and of the shape of the element).

Equations $\zeta_i = \text{constant}$ represent lines parallel to the corresponding sides. The equations of the side "j" is $\zeta_j = 0$. The three corners have coordinates $(1,0,0)$, $(0,1,0)$ and $(0,0,1)$; the three midpoints of the sides $(1/2,1/2,0)$, $(0,1/2,1/2)$ and $(1/2,0,1/2)$; the centroid $(1/3,1/3,1/3)$ and so on.

The derivation of element properties is greatly simplified when all area functions are expressed by interpolation formulas in triangular coordinates,

i.e., $f(x,y) \Rightarrow f(\zeta_i)$. Relations between the different coordinate systems are given in I.3.2. Also, for brevity, partial derivatives of a function $f(\zeta_i)$ in the directions of the above defined cartesian systems will be referred to as follows:

with respect to s_i axes: "side derivatives"
 with respect to n_i axes: "normal derivatives"
 with respect to x,y axes: "global derivatives".

I.3.2 Relations Between Coordinate Systems

In this paragraph, indices "j" and "k" will denote the 1st and 2nd cyclic permutations of "i", i.e.,

$$\text{for } i = 1,2,3, \quad j = 2,3,1, \quad k = 3,1,2$$

(a) Between global and local coordinate systems:

$$\begin{Bmatrix} s_i \\ n_i \end{Bmatrix} = \begin{bmatrix} \cos \delta_i & \sin \delta_i \\ -\sin \delta_i & \cos \delta_i \end{bmatrix} \begin{Bmatrix} x-x_k \\ y-y_k \end{Bmatrix} = \frac{1}{l_i} \begin{bmatrix} a_i & -b_i \\ b_i & a_i \end{bmatrix} \begin{Bmatrix} x-x_k \\ y-y_k \end{Bmatrix} \quad (\text{I-15a})$$

$$\begin{Bmatrix} x \\ y \end{Bmatrix} = \frac{1}{l_i} \begin{bmatrix} a_i & b_i \\ -b_i & a_i \end{bmatrix} \begin{Bmatrix} s_i \\ n_i \end{Bmatrix} + \begin{Bmatrix} x_k \\ y_k \end{Bmatrix} \quad (\text{I-15b})$$

hence

$$\begin{aligned} \frac{\partial x}{\partial s_i} &= \frac{\partial y}{\partial n_i} = \frac{a_i}{l_i} & \frac{\partial x}{\partial n_i} &= -\frac{\partial y}{\partial s_i} = \frac{b_i}{l_i} \\ \frac{\partial s_i}{\partial x} &= \frac{\partial n_i}{\partial y} = \frac{a_i}{l_i} & \frac{\partial s_i}{\partial y} &= -\frac{\partial n_i}{\partial x} = \frac{b_i}{l_i} \end{aligned} \quad (\text{I-16})$$

(b) Between global and triangular coordinates:

$$\begin{Bmatrix} 1 \\ x \\ y \end{Bmatrix} = \begin{bmatrix} 1 & 1 & 1 \\ x_1 & x_2 & x_3 \\ y_1 & y_2 & y_3 \end{bmatrix} \begin{Bmatrix} \zeta_1 \\ \zeta_2 \\ \zeta_3 \end{Bmatrix} \quad (\text{I-17a})$$

$$\begin{Bmatrix} \zeta_1 \\ \zeta_2 \\ \zeta_3 \end{Bmatrix} = \frac{1}{2A} \begin{bmatrix} x_2 y_3 - x_3 y_2 & y_2 - y_3 & x_3 - x_2 \\ x_3 y_1 - x_1 y_3 & y_3 - y_1 & x_1 - x_3 \\ x_1 y_2 - x_2 y_1 & y_1 - y_2 & x_2 - x_1 \end{bmatrix} \begin{Bmatrix} 1 \\ x \\ y \end{Bmatrix} \quad (\text{I-17b})$$

$$= \frac{1}{2A} \begin{bmatrix} 2A_{23} & b_1 & a_1 \\ 2A_{31} & b_2 & a_2 \\ 2A_{12} & b_3 & a_3 \end{bmatrix} \begin{Bmatrix} 1 \\ x \\ y \end{Bmatrix}$$

where $2A = a_j b_i - a_i b_j$ and A_{ij} is the area subtended by corners i, j and the origin of coordinates. Note that $2A \zeta_i = 2A_{jk} + b_i x + a_i y = 0$ is the equation of side i .

Hence

$$\begin{aligned} \frac{\partial \zeta_i}{\partial x} &= \frac{b_i}{2A} & \frac{\partial \zeta_i}{\partial y} &= \frac{a_i}{2A} \\ \frac{\partial x}{\partial \zeta_i} &= x_i & \frac{\partial y}{\partial \zeta_i} &= y_i \end{aligned} \quad (\text{I-18})$$

(c) Between local and triangular coordinates

$$\begin{Bmatrix} 1 \\ s_i \\ n_i \end{Bmatrix} = \begin{bmatrix} 1 & 1 & 1 \\ \cdot & l_i & d_i \\ \cdot & \cdot & h_i \end{bmatrix} \begin{Bmatrix} \zeta_k \\ \zeta_i \\ \zeta_j \end{Bmatrix} \quad (\text{I-19a})$$

$$\begin{Bmatrix} \zeta_j \\ \zeta_k \\ \zeta_i \end{Bmatrix} = \frac{1}{2A} \begin{bmatrix} 2A & -h_i & d_i - l_i \\ \cdot & h_i & -d_i \\ \cdot & \cdot & l_i \end{bmatrix} \begin{Bmatrix} 1 \\ s_i \\ n_i \end{Bmatrix} \quad (\text{I-19b})$$

where $2A = l_i h_i$ (no sum).

Hence

$$\begin{bmatrix} \frac{\partial \zeta_1}{\partial s_1} & \frac{\partial \zeta_1}{\partial s_2} & \frac{\partial \zeta_1}{\partial s_3} \\ \frac{\partial \zeta_2}{\partial s_1} & \frac{\partial \zeta_2}{\partial s_2} & \frac{\partial \zeta_2}{\partial s_3} \\ \frac{\partial \zeta_3}{\partial s_1} & \frac{\partial \zeta_3}{\partial s_2} & \frac{\partial \zeta_3}{\partial s_3} \end{bmatrix} = \frac{1}{2A} \begin{bmatrix} 0 & h_2 & -h_3 \\ -h_1 & 0 & h_3 \\ h_1 & -h_2 & 0 \end{bmatrix} = \begin{bmatrix} 0 & \frac{1}{l_2} & -\frac{1}{l_3} \\ -\frac{1}{l_1} & 0 & \frac{1}{l_3} \\ \frac{1}{l_1} & -\frac{1}{l_2} & 0 \end{bmatrix}$$

$$\begin{bmatrix} \frac{\partial \zeta_1}{\partial n_1} & \frac{\partial \zeta_1}{\partial n_2} & \frac{\partial \zeta_1}{\partial n_3} \\ \frac{\partial \zeta_2}{\partial n_1} & \frac{\partial \zeta_2}{\partial n_2} & \frac{\partial \zeta_2}{\partial n_3} \\ \frac{\partial \zeta_3}{\partial n_1} & \frac{\partial \zeta_3}{\partial n_2} & \frac{\partial \zeta_3}{\partial n_3} \end{bmatrix} = \frac{1}{2A} \begin{bmatrix} l_1 & -d_2 & d_3 - l_3 \\ d_1 - l_1 & l_2 & -d_3 \\ -d_1 & d_2 - l_2 & l_3 \end{bmatrix} \quad (\text{I-20})$$

The derivatives of a function $f(\zeta_1, \zeta_2, \zeta_3)$ with respect to local or global cartesian axes can be obtained immediately by the chain rule and formulae (I-18) and (I-20):

$$\frac{\partial f}{\partial s_i} = \frac{1}{l_i} \left(\frac{\partial f}{\partial \zeta_k} - \frac{\partial f}{\partial \zeta_j} \right) \quad (\text{I-21})$$

$$\frac{\partial f}{\partial n_i} = \frac{1}{2A} \left(\frac{\partial f}{\partial \zeta_i} l_i + \frac{\partial f}{\partial \zeta_j} (d_i - l_i) - \frac{\partial f}{\partial \zeta_k} d_i \right) \quad (\text{no sum})$$

$$\frac{\partial f}{\partial x} = \frac{b_m}{2A} \frac{\partial f_m}{\partial \zeta_m} = \frac{1}{2A} \left(\frac{\partial f}{\partial \zeta_1} b_1 + \frac{\partial f}{\partial \zeta_2} b_2 + \frac{\partial f}{\partial \zeta_3} b_3 \right) \quad (\text{I-22})$$

$$\frac{\partial f}{\partial y} = \frac{a_m}{2A} \frac{\partial f_m}{\partial \zeta_m} = \frac{1}{2A} \left(\frac{\partial f}{\partial \zeta_1} a_1 + \frac{\partial f}{\partial \zeta_2} a_2 + \frac{\partial f}{\partial \zeta_3} a_3 \right)$$

Similarly higher derivatives may be constructed, for instance

$$\frac{\partial^2 f}{\partial x \partial y} = \frac{a_m b_n}{4A^2} \frac{\partial^2 f}{\partial \xi_m \partial \xi_n}$$

I.4 POLYNOMIAL INTERPOLATION FOR PLANE TRIANGLES

I.4.1 Polynomial Expressions in Triangular Coordinates

The domain D of I.2.1 is here the flat triangle 1-2-3 of I.3.1 (Fig. 1.1). A complete polynomial space P_n in two dimensions is spanned by the coordinate functions

$$\{\varphi_i\} = \langle 1 \quad x \quad y \quad x^2 \quad xy \dots y^n \rangle \quad (I-23)$$

and has dimension $m = (n+2)(n+1)/2$. Any polynomial $P_n(x,y)$ of order "n" may also be expressed as a polynomial $P_s(\xi_i)$, $s \geq n$, in triangular coordinates using Equation (I-17₂); such representation is not unique, since each term may contain arbitrary factors $(\xi_1 + \xi_2 + \xi_3)^q = 1$. When all such factors have been removed, $P_s(\xi_i) \equiv P_n(\xi_i)$ has degree "n" and will be called irreducible. There are

$$r = (n+3)(n+2)(n+1)/6$$

different monomial terms in a general $P_n(\xi_i)$, but only "m" are independent and the rest, i.e., $(r-m) = (n+2)(n+1)n/6$ terms, are linear combinations thereof.

For rectangular regions, cartesian systems, after division by the side lengths if necessary, provide natural coordinates (a natural system is one in which the element boundaries are zero coordinate lines); the

interpolation formulas for corner nodal point systems are the well-known Lagrange and Hermite polynomials. They have been used, for instance, by Melosh [10] for three-dimensional elements; by Bogner, Fox and Schmidt [27] for membrane and plate elements and by Pestel [30] for the dynamic analysis of beams. Similarly, for triangular elements, the interpolation functions (I-10) assume particularly simple form when expressed in triangular coordinates; they usually can be constructed by inspection rather than by the general method (I-9) which yields the orthonormal system from a known basis like (I-23). The tedious process of inverting the transformation matrix \mathbf{A} is then avoided.

I.4.2 Determination of Complete Polynomials from Boundary Conditions

The most important properties concerning determination of complete polynomials in triangular coordinates are:

(a) For $n \geq 3$, a complete irreducible polynomial $P_n(\zeta_i)$ cannot be uniquely specified by its boundary values. In effect, we may add arbitrary terms

$$\zeta_1^{m_1} \zeta_2^{m_2} \zeta_3^{m_3} \quad \text{with } m_i \geq 1, i=1,2,3 \quad (\text{I-24})$$

belonging to the subspace $(\mathcal{P}-0)_n$ of all polynomials of order $\leq n$ vanishing on the sides. There are $(n-2)(n-1)n/6$ of such terms, but not all independent; for instance if $n=4$ we have four terms

$$(\mathcal{P}-0)_4 : \zeta_1 \zeta_2 \zeta_3, \zeta_1^2 \zeta_2 \zeta_3, \zeta_1 \zeta_2^2 \zeta_3, \zeta_1 \zeta_2 \zeta_3^2$$

but only three are independent since $\zeta_1^2 \zeta_2 \zeta_3 + \zeta_1 \zeta_2^2 \zeta_3 + \zeta_1 \zeta_2 \zeta_3^2 = \zeta_1 \zeta_2 \zeta_3$.

(b) For $n \geq 6$, a complete irreducible polynomial $P_n(\zeta_i)$ cannot be uniquely determined from the values of P_n and the normal gradient

$\partial P_n / \partial n$ on the boundary. For we may add arbitrary terms

$$\zeta_1^{m_1} \zeta_2^{m_2} \zeta_3^{m_3} \quad \text{with } m_i \geq 2, i=1,2,3 \quad (I-25)$$

belonging to the subspace $(\mathcal{P}-1)_n$ of all polynomials of order $\leq n$ whose values and all derivatives are zero on the sides. There are $(n-5)(n-4)(n-3)/6$ of such terms, but not all independent. Evidently $(\mathcal{P}-1)_n \in (\mathcal{P}-0)_n$.

Similarly we may define subspaces $(\mathcal{P}-q)_n$ contained in all previous ones. Their importance lies in the fact that their members do not affect compatibility requirements for C-q triangular elements, i.e., they are natural additional modes.

Thus terms $\in (\mathcal{P}-0)$ may be used for plane stress elements; they can be specified at internal nodal points, or, if they do not belong to $(\mathcal{P}-1)$ (some $m_i = 1$), by normal derivatives on the boundary.

Terms $\in (\mathcal{P}-1)$ might be employed for thin plate elements; they can be specified at internal nodes, or by "r-th" order normal gradients on the boundary ($r \geq 2$), provided they do not belong to the class $(\mathcal{P}-r)$.

I.4.3 List of Interpolation Formulae for Complete Polynomials of the First Three Orders

I.4.3.1 Linear Interpolation (n=1, m=3).

The logical choice is to take the corners 1,2,3 for the nodal point system (N_1) of Fig. 1.5. Then

$$\begin{aligned} f(\zeta_1, \zeta_2, \zeta_3) &= f(\zeta_i) = f_1 \zeta_1 + f_2 \zeta_2 + f_3 \zeta_3 \\ &= \langle f_1 \ f_2 \ f_3 \rangle \begin{Bmatrix} \zeta_1 \\ \zeta_2 \\ \zeta_3 \end{Bmatrix} = \mathbf{f}^T \boldsymbol{\zeta} = \boldsymbol{\zeta}^T \mathbf{f} \end{aligned} \quad (\text{I-26})$$

i.e., $\phi_i = \zeta_i$, $i=1,2,3$; these interpolating functions are sometimes called "pyramid functions", e.g., by Synge [31], because of their shape.

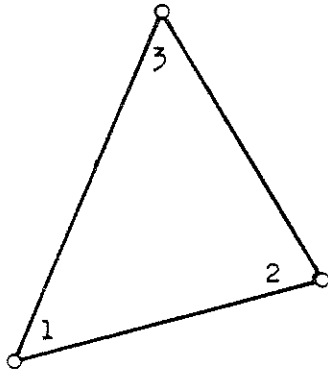
I.4.3.2 Quadratic Interpolation (n=2, m=6)

The best choice is to take corners 1,2,3 and midpoints 4,5,6 to form the nodal system (N_2) depicted in Fig. 1.6. Then

$$f(\zeta_i) = \langle f_1 \ f_2 \ f_3 \ f_4 \ f_5 \ f_6 \rangle \begin{Bmatrix} \zeta_1(2\zeta_1-1) \\ \zeta_2(2\zeta_2-1) \\ \zeta_3(2\zeta_3-1) \\ 4\zeta_1\zeta_2 \\ 4\zeta_2\zeta_3 \\ 4\zeta_3\zeta_1 \end{Bmatrix} = \mathbf{f}^T \boldsymbol{\phi}_{(2)} \quad (\text{I-27})$$

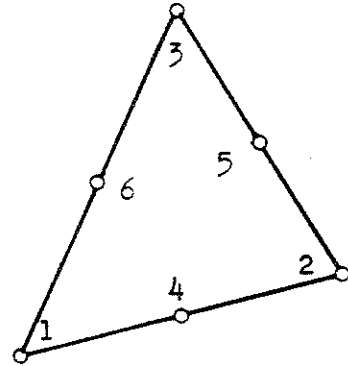
i.e.,

$$\left. \begin{aligned} \phi_i &= \zeta_i(2\zeta_i-1) \\ \phi_{i+3} &= 4\zeta_i\zeta_j \end{aligned} \right\} \begin{array}{l} i = 1, 2, 3 \\ j = 2, 3, 1 \end{array}$$



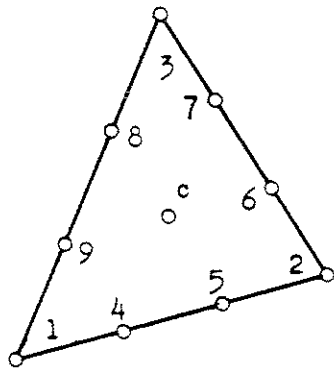
$f_i, i = 1, 2, 3$

Fig. 1.5 - Linear Interpolation.
Nodal Point System (N_1).



$f_i, i = 1, 2, 3, 4, 5, 6$

Fig. 1.6 - Quadratic Interpolation.
Nodal Point System (N_2).



$f_i, i = 1, 2, \dots, 9, c$

Fig. 1.7 - Cubic Interpolation.
Nodal Point System (N_3^*).

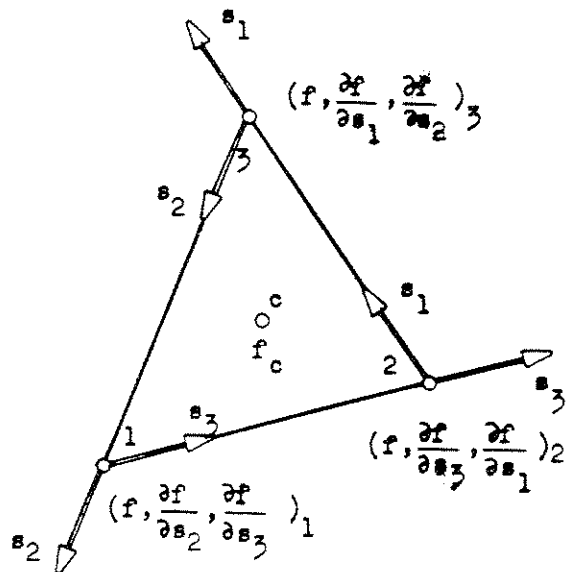


Fig. 1.8 - Cubic Interpolation.
Nodal Point System (\bar{N}_3).

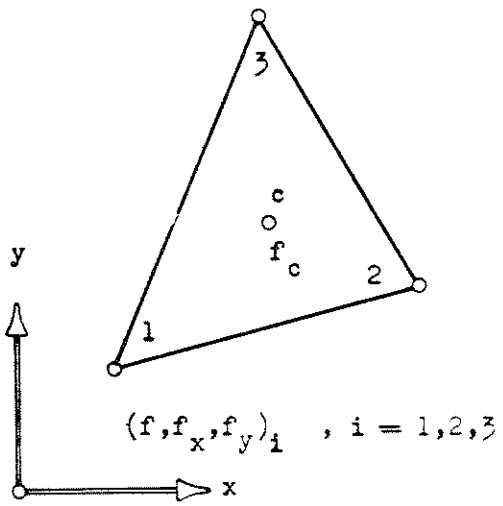


Fig. 1.9 - Cubic Interpolation.
Nodal Point System (N_3) .

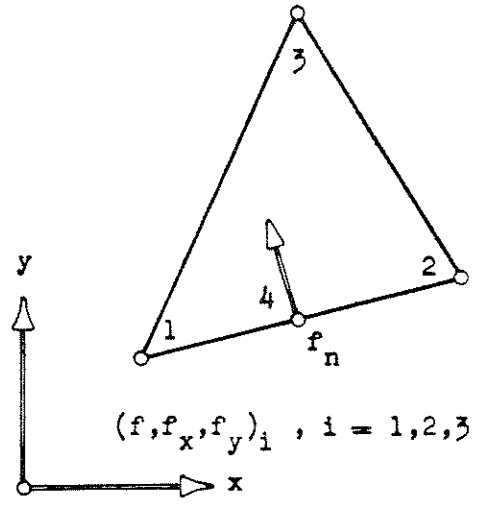


Fig. 1.10 - Cubic Interpolation.
Nodal Point System $(N_3)_p$.

It would also be possible to select the corner values and three corner side derivatives, one at each, in cyclic order. However, this system lacks the complete symmetry of (N_2) .

1.4.3.3 Cubic Interpolation (n=3, m=10)

Here we find the first member of the $(\mathcal{P}-0)$ class: the term $\zeta_1 \zeta_2 \zeta_3$ which vanishes identically on the sides. Several choices of nodal systems are possible; the most important ones are described below.

(a) First Choice: system (N_3^*) of Fig. 1.7.

This system consists of 10 nodal points; corners 1,2,3, third points of the sides 4,5,...,9 and centroid c (Fig. 1.7). The nodal point vector is

$$\mathbf{f}^T = \langle f_1 \ f_2 \ f_3 \ f_4 \ f_5 \ f_6 \ f_7 \ f_8 \ f_9 \ f_c \rangle$$

then

$$f(\zeta_i) = \mathbf{f}^T \boldsymbol{\phi}_{(3)}^* \quad (I-28)$$

with

$$\boldsymbol{\phi}_{(3)} = \frac{1}{2} \left\{ \begin{array}{l} \zeta_1 (3\zeta_1 - 1) (3\zeta_1 - 2) \\ \zeta_2 (3\zeta_2 - 1) (3\zeta_2 - 2) \\ \zeta_3 (3\zeta_3 - 1) (3\zeta_3 - 2) \\ 9\zeta_1 \zeta_2 (3\zeta_1 - 1) \\ 9\zeta_1 \zeta_2 (3\zeta_2 - 1) \\ 9\zeta_2 \zeta_3 (3\zeta_2 - 1) \\ 9\zeta_2 \zeta_3 (3\zeta_3 - 1) \\ 9\zeta_3 \zeta_1 (3\zeta_3 - 1) \\ 9\zeta_3 \zeta_1 (3\zeta_1 - 1) \\ 54 \zeta_1 \zeta_2 \zeta_3 \end{array} \right\}$$

(b) Second Choice: Nodal System (\bar{N}_3) of Fig. 1.8.

This second system has only four distinct nodal points; the 3 corners, at which we specify the value of f and both side derivatives, plus the centroid (Fig. 1.8). The nodal point vector is arranged as follows:

$$\mathbf{f}^T = \langle f_1 \ f_{21} \ f_{31} \ f_2 \ f_{32} \ f_{12} \ f_3 \ f_{13} \ f_{23} \ f_c \rangle$$

where we put $f_{ik} = \left(\frac{\partial f}{\partial S_i} \right)_k$

The interpolation formula is

$$f(\zeta_i) = \mathbf{f}^T \bar{\Phi}_{(3)} \quad (I-29)$$

where

$$\bar{\Phi}_{(3)} = \left\{ \begin{array}{l} \zeta_1^2 (\zeta_1 + 3\zeta_2 + 3\zeta_3) - 7\zeta_1 \zeta_2 \zeta_3 \\ \quad - \zeta_2 (\zeta_3 \zeta_1^2 - \zeta_1 \zeta_2 \zeta_3) \\ \quad \quad \zeta_3 (\zeta_1^2 \zeta_2 - \zeta_1 \zeta_2 \zeta_3) \\ \zeta_2^2 (\zeta_2 + 3\zeta_3 + 3\zeta_1) - 7\zeta_1 \zeta_2 \zeta_3 \\ \quad - \zeta_3 (\zeta_1 \zeta_2^2 - \zeta_1 \zeta_2 \zeta_3) \\ \quad \quad \zeta_1 (\zeta_2^2 \zeta_3 - \zeta_1 \zeta_2 \zeta_3) \\ \zeta_3^2 (\zeta_3 + 3\zeta_1 + 3\zeta_2) - 7\zeta_1 \zeta_2 \zeta_3 \\ \quad - \zeta_1 (\zeta_2 \zeta_3^2 - \zeta_1 \zeta_2 \zeta_3) \\ \quad \quad \zeta_2 (\zeta_3^2 \zeta_1 - \zeta_1 \zeta_2 \zeta_3) \\ \quad \quad \quad 27\zeta_1 \zeta_2 \zeta_3 \end{array} \right.$$

Note the corrections introduced by terms $\zeta_1 \zeta_2 \zeta_3$ so that all functions ϕ_1 to ϕ_9 vanish at c.

This formula and (I-28) are related through the transformation matrix

$$\begin{Bmatrix} f_1 \\ f_2 \\ f_3 \\ f_4 \\ f_5 \\ f_6 \end{Bmatrix} = \frac{1}{27} \begin{bmatrix} 20 & \cdot & 4l_3 & 7 & -2l_3 & \cdot & \cdot & \cdot & \cdot \\ 7 & \cdot & 2l_3 & 20 & -4l_3 & \cdot & \cdot & \cdot & \cdot \\ \cdot & \cdot & \cdot & 20 & \cdot & 4l_1 & 7 & -2l_1 & \cdot \\ \cdot & \cdot & \cdot & 7 & \cdot & 2l_1 & 20 & -4l_1 & \cdot \\ 7 & -2l_2 & \cdot & \cdot & \cdot & \cdot & 20 & \cdot & 4l_2 \\ 20 & -4l_2 & \cdot & \cdot & \cdot & \cdot & 7 & \cdot & 2l_2 \end{bmatrix} \begin{Bmatrix} f_1 \\ f_{21} \\ f_{31} \\ f_2 \\ f_{22} \\ f_{12} \\ f_3 \\ f_{13} \\ f_{23} \end{Bmatrix} \quad (\text{I-30})$$

(c) Third Choice: Nodal System (N_3) of Fig. 1.9.

This system is similar to the previous one, but the derivatives at the three corners are taken with respect to the global directions (x,y). The nodal point vector is

$$\mathbf{f}^T = \langle f_1 \quad f_{x1} \quad f_{y1} \quad f_2 \quad f_{x2} \quad f_{y2} \quad f_3 \quad f_{x3} \quad f_{y3} \quad f_c \rangle$$

where $f_{xk} = (f_x)_k$ $f_{yk} = (f_y)_k$

Then

$$f(\zeta_i) = \mathbf{f}^T \boldsymbol{\phi}_{(3)} \quad (\text{I-31})$$

with

$$\Phi_{(3)} = \begin{Bmatrix} \zeta_1^2(\zeta_1 + 3\zeta_2 + 3\zeta_3) - 7\zeta_1\zeta_2\zeta_3 \\ \zeta_1^2(a_3\zeta_2 - a_2\zeta_3) + (a_2 - a_3)\zeta_1\zeta_2\zeta_3 \\ \zeta_1^2(b_2\zeta_3 - b_3\zeta_2) + (b_3 - b_2)\zeta_1\zeta_2\zeta_3 \\ \zeta_2^2(\zeta_2 + 3\zeta_3 + 3\zeta_1) - 7\zeta_1\zeta_2\zeta_3 \\ \zeta_2^2(a_1\zeta_3 - a_3\zeta_1) + (a_3 - a_1)\zeta_1\zeta_2\zeta_3 \\ \zeta_2^2(b_3\zeta_1 - b_1\zeta_3) + (b_1 - b_3)\zeta_1\zeta_2\zeta_3 \\ \zeta_3^2(\zeta_3 + 3\zeta_1 + 3\zeta_2) - 7\zeta_1\zeta_2\zeta_3 \\ \zeta_3^2(a_2\zeta_1 - a_1\zeta_2) + (a_1 - a_2)\zeta_1\zeta_2\zeta_3 \\ \zeta_3^2(b_1\zeta_2 - b_2\zeta_1) + (b_2 - b_1)\zeta_1\zeta_2\zeta_3 \\ 27\zeta_1\zeta_2\zeta_3 \end{Bmatrix}$$

This interpolation formula can be immediately obtained from Equation (I-29) using (I-18). It is used in the derivation of the stiffness of the quadratically varying strain triangle (III.3).

(d) Fourth Choice: Nodal System $(N_3)_p$ of Fig. 1.10.

Again we have four nodal points: the 3 corners at which the value of f and the global derivatives are specified ($\partial f / \partial y$ has been changed of sign) plus the normal derivative at midpoint 4 (Fig. 1.10). The nodal values are ordered as follows:

$$\mathbf{f}^T = \langle f_1 \quad -f_{y1} \quad f_{x1} \quad f_2 \quad -f_{y2} \quad f_{x2} \quad f_3 \quad -f_{y3} \quad f_{x3} \quad f_{n4} \rangle$$

Then

$$f(\zeta_i) = \mathbf{f}^T \Phi_{(3)p} \quad (\text{I-32})$$

with

$$\Phi_{(3)P} = \left[\begin{array}{l} \zeta_1^2 (\zeta_1 + 3\zeta_2 + 3\zeta_3) + 6\mu_3 \zeta_1 \zeta_2 \zeta_3 \\ \zeta_1^2 (b_3 \zeta_2 - b_2 \zeta_3) + (b_3 \mu_3 - b_1) \zeta_1 \zeta_2 \zeta_3 \\ \zeta_1^2 (a_3 \zeta_2 - a_2 \zeta_3) + (a_3 \mu_3 - a_1) \zeta_1 \zeta_2 \zeta_3 \\ \zeta_2^2 (\zeta_2 + 3\zeta_3 + 3\zeta_1) + 6\lambda_3 \zeta_1 \zeta_2 \zeta_3 \\ \zeta_2^2 (b_1 \zeta_3 - b_3 \zeta_1) + (b_2 - b_3 \lambda_3) \zeta_1 \zeta_2 \zeta_3 \\ \zeta_2^2 (a_1 \zeta_3 - a_3 \zeta_1) + (a_2 - a_3 \lambda_3) \zeta_1 \zeta_2 \zeta_3 \\ \zeta_3^2 (\zeta_3 + 3\zeta_1 + 3\zeta_2) \\ \zeta_3^2 (b_2 \zeta_1 - b_1 \zeta_2) \\ \zeta_3^2 (a_2 \zeta_1 - a_1 \zeta_2) \\ + \mu_3 \zeta_1 \zeta_2 \zeta_3 \end{array} \right]$$

where $\lambda_3 = d_3/l_3$, $\mu_3 = 1 - \lambda_3$.

This formula is fundamental for the construction of compatible thin plate triangular elements. If we make $f(\zeta_1) = w(\zeta_1) =$ transversal deflection (positive downwards), the above selected global derivatives

$$-w_y = \theta_x \quad w_x = \theta_y$$

are the rotations about the in-plane axes.

I.5 AREA INTEGRATION OF FUNCTIONS IN TRIANGULAR COORDINATES

I.5.1 Formulas for Polynomial Expressions

In the derivation of stiffness matrices for flat triangular elements, area integrals of polynomial terms in triangular coordinates are frequently required. Their values are independent of the shape of the triangle and may be expressed as a fraction of the area

$$I(m_i, m_j, m_k) = \int_A \zeta_i^{m_i} \zeta_j^{m_j} \zeta_k^{m_k} dA = \alpha A \quad (I-33)$$

where indices i, j, k represent any permutation of $1, 2, 3$. The value of the coefficient α may be found in Table 3 for orders $n = m_i + m_j + m_k = 1$ to 6 .

Some numerical vectors and matrices which appear frequently as area integrals of interpolation vectors and their products, are listed below for the lowest polynomial orders:

$$L_1 = \frac{1}{A} \int_A \zeta^T dA = \frac{1}{3} \langle 1 \quad 1 \quad 1 \rangle$$

$$L_2 = \frac{1}{A} \int_A \phi_{(2)}^T dA = \frac{1}{3} \langle 0 \quad 0 \quad 0 \quad 1 \quad 1 \quad 1 \rangle$$

$$L_3^* = \frac{1}{A} \int_A \phi_{(3)}^{*T} dA = \frac{1}{120} \langle 4 \quad 4 \quad 4 \quad 9 \quad 9 \quad 9 \quad 9 \quad 9 \quad 9 \quad 54 \rangle$$

$$L_3 = \frac{1}{A} \int_A \phi_{(3)}^T dA = \frac{1}{60} \langle 11 \quad 2(a_3 - a_2) \quad 2(b_2 - b_3) \quad 11 \quad 2(a_1 - a_3)$$

$$2(b_3 - b_1) \quad 11 \quad 2(a_2 - a_1) \quad 2(b_1 - b_2) \quad 27 \rangle$$

$$L_{11} = \frac{1}{A} \int_A \zeta_i \zeta_j^T dA = \frac{1}{12} \begin{bmatrix} 2 & 1 & 1 \\ 1 & 2 & 1 \\ 1 & 1 & 2 \end{bmatrix}$$

$$L_{12} = \frac{1}{A} \int_A \zeta_i \phi_{(2)}^T dA = \frac{1}{60} \begin{bmatrix} 2 & -1 & -1 & 8 & 4 & 8 \\ -1 & 2 & -1 & 8 & 8 & 4 \\ -1 & -1 & 2 & 4 & 8 & 8 \end{bmatrix}$$

$$L_{22} = \frac{1}{A} \int_A \phi_{(2)} \phi_{(2)}^T dA = \frac{1}{180} \begin{pmatrix} 6 & -1 & -1 & 0 & -4 & 0 \\ -1 & 6 & -1 & 0 & 0 & -4 \\ -1 & -1 & 6 & -4 & 0 & 0 \\ 0 & 0 & -4 & 32 & 16 & 16 \\ -4 & 0 & 0 & 16 & 32 & 16 \\ 0 & -4 & 0 & 16 & 16 & 32 \end{pmatrix}$$

$$L_{33}^* = \frac{1}{A} \int_A \phi_{(3)}^* \phi_{(3)}^* dA =$$

$$= \frac{1}{20160} \begin{pmatrix} 228 & 33 & 33 & 54 & 0 & 81 & 81 & 0 & 54 & 108 \\ 33 & 228 & 33 & 0 & 54 & 54 & 0 & 81 & 81 & 108 \\ 33 & 33 & 228 & 81 & 81 & 0 & 54 & 54 & 0 & 108 \\ 54 & 0 & 81 & 1620 & -567 & -405 & -162 & -405 & 810 & 486 \\ 0 & 54 & 81 & -567 & 1620 & 810 & -405 & -162 & -405 & 486 \\ 81 & 54 & 0 & -405 & 810 & 1620 & -567 & -405 & -162 & 486 \\ 81 & 0 & 54 & -162 & -405 & -567 & 1620 & 810 & -405 & 486 \\ 0 & 81 & 54 & -405 & -162 & -405 & 810 & 1620 & -567 & 486 \\ 54 & 81 & 0 & 810 & -405 & -162 & -405 & -567 & 1620 & 486 \\ 108 & 108 & 108 & 486 & 486 & 486 & 486 & 486 & 486 & 5832 \end{pmatrix}$$

Table 3. Area Integrals $\propto A = \int_A \psi_i^{m_i} \psi_j^{m_j} \psi_k^{m_k} dA$
of Polynomial Terms in Triangular Coordinates.

Order $n=m_i+m_j+m_k$	m_i	m_j	m_k	$M \propto$	Factor M
1	1	0	0	1	3
2	2	0	0	2	12
	1	1	0	1	
3	3	0	0	6	60
	2	1	0	2	
	1	1	1	1	
4	4	0	0	12	180
	3	1	0	3	
	2	2	0	2	
	2	1	1	1	
5	5	0	0	60	1260
	4	1	0	12	
	3	2	0	6	
	3	1	1	3	
	2	2	1	2	
6	6	0	0	180	5040
	5	1	0	30	
	4	2	0	12	
	3	3	0	9	
	4	1	1	6	
	3	2	1	3	
	2	2	2	2	

I.5.2 Numerical Integration

For some elements, such as axisymmetric triangular rings [6], the integration of functions other than polynomials over the area of the triangle is required. If a closed form expression cannot be obtained or if such explicit form is complicated or prone to cancellation error, numerical integration is the best procedure. We consider here Gauss-type expressions:

$$\frac{1}{A} \int_A f(\zeta_1, \zeta_2, \zeta_3) dA = \sum_{k=1}^N w_k f(\zeta_k) + R \quad (\text{I-34})$$

where ζ_k are the triangular coordinates of the integration points P_k ($k=1, 2, \dots, N$). Formulas for the first five orders, taken from Hammer and Stroud [32], are given in Table 4. They are of the symmetric type, i.e., all images of P_k under all affine transformations of the triangle onto itself are also integration points with the same weight w_k . If $R = O(h^r)$ is the remainder, h being a characteristic dimension of the triangle, the formula is exact for all polynomials of order up to $(r-1)$.

Table 4. Numerical Integration Formulas for Triangles

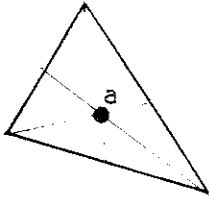
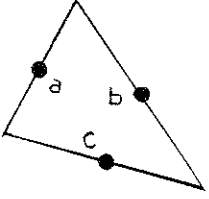
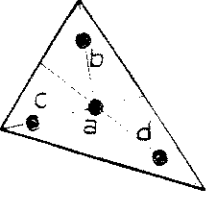
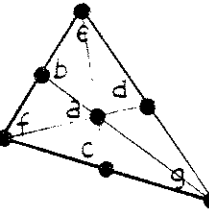
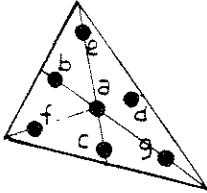
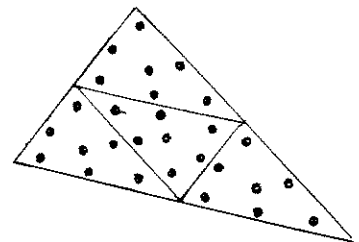
No.	Order	Fig.	Rem.	Pnts	Triangular Coordinates	Weights w_k
1	Linear		$R=O(h^2)$	a	1/3, 1/3, 1/3	1
2	Quadratic		$R=O(h^3)$	a b c	1/2, 1/2, 0 0, 1/2, 1/2 1/2, 0, 1/2	1/3 1/3 1/3
3	Cubic		$R=O(h^4)$	a b c d	1/3, 1/3, 1/3 11/15, 2/15, 11/15 2/15, 11/15, 2/15 2/15, 2/15, 11/15	-27/48 25/48
4	Cubic		$R=O(h^4)$	a b c d e f g	1/3, 1/3, 1/3 1/2, 1/2, 0 0, 1/2, 1/2 1/2, 0, 1/2 1, 0, 0 0, 1, 1 0, 0, 1	27/60 8/60 3/60

Table 4 (Con't)

No.	Order	Fig.	Rem.	Pnts	Triangular Coordinates	Weights w_k
5	Quintic		$R=O(h^6)$	a	1/3, 1/3, 1/3	0.225
				b	$\alpha_1, \beta_1, \beta_1$	
				c	$\beta_1, \alpha_1, \beta_1$	0.13239415
				d	$\beta_1, \beta_2, \beta_2$	
				e	$\alpha_2, \beta_2, \beta_2$	0.12593918
				f	$\beta_2, \alpha_2, \beta_2$	
				g	$\beta_2, \beta_2, \alpha_2$	
				with		
				$\alpha_1 = 0.05961587$		
				$\beta_1 = 0.47014206$		
				$\alpha_2 = 0.79742699$		
				$\beta_2 = 0.10128651$		

Notes:

- 1) Use of the cubic formula (3) is not recommended since the negative weight may cause severe cancellation error.
- 2) When the function $f(\zeta_i)$ is unbounded on a certain portion of the boundary (for instance, on the symmetry axis for axisymmetric ring elements) an expression like (5) with only internal integration points should be used.
- 3) To improve the accuracy, we may subdivide the triangle and integrate over each subregion. For example, joining the midpoints and using the quintic formula (5) for each portion (see Fig.) we may reduce the error approximately $2^6 = 64$ times. Programming is simplified by the fact that each subtriangle has the same area; therefore all weights are merely divided by 4.



II. DERIVATION OF CONVENTIONAL STIFFNESS MATRICES
FOR PLANE ELEMENTS

II.1 BASES FOR THE CONSTRUCTION OF STIFFNESS MATRICES

II.1.1 The Conventional Ritz Technique and the Finite Element Method

(1) In the conventional Ritz method, successive approximations are obtained by expanding the class

$$\Omega_n : \langle \varphi_1 \varphi_2 \varphi_3 \dots \varphi_n \rangle \quad (\text{II-1})$$

of trial displacement functions over the entire structure.

The set Ω_∞ is said to be relatively complete with respect to the class of continuous functions satisfying the kinematic boundary conditions, if both the displacement field and all displacement gradients entering into the governing variational problem can be uniformly approximated by members of the class (II-1) as $n \rightarrow \infty$.

It can easily be shown that the strain energy U_n converges monotonically to its true value $U^* \geq U_n$ as $n \rightarrow \infty$ if the set Ω_∞ is relatively complete [34]. However, the uniform convergence of the sequence of displacement solutions has been proved only for certain types of functionals; moreover, their gradients may not converge even if the displacement sequence does [33].

(2) The previous technique is obviously restricted to simple shapes and not adequate for automatic programming. In the finite element method we apply the Ritz procedure to each element of the discretized structure. We may try to improve the solution by the following procedures:

- (a) Decreasing the mesh size by repeated subdivision;
- (b) Expanding the class Ω of displacement functions for

each element; this may be done

(b.1) introducing fundamental modes;

(b.2) introducing additional modes;

(c) Improving the geometry of the element.

Sufficient conditions for convergence of the strain energy and influence coefficients using method (a) of repeated subdivision are simpler to meet (see II.1.2) and we are not faced with the difficulties of the conventional Ritz procedure.

The second method (b) leads to the development of refined elements; the best results are obtained by injecting fundamental degrees of freedom which improve both interface and internal displacement patterns. The use of additional modes is discussed in II.1.3.

Consistently refined elements guarantee a faster convergence and better results for coarse networks. This technique shares some of the characteristics of the conventional Ritz procedure; however, for large "n" the derivation becomes increasingly complex and in general the actual geometry of the structure can be approximated only by (a) or (c). Therefore in practice we select a certain "n" and further improvements are done by subdivision. For each type of problem there seems to be a practical balance between the work necessary to derive and assemble the stiffness matrix and the work involved in the solution of the equilibrium equations in order to attain a certain accuracy level.

Procedure (c) has not been systematically explored yet. It is evident that, to fully exploit the possibilities of a higher order displacement field,

the element should be allowed to be bounded by arbitrary surfaces or lines of degree equal to the order of the displacement expansion; for example a six nodal point plane or curved triangle bounded by plane or space parabolas. This procedure would permit a very accurate representation of the actual geometry (a shortcoming of coarse networks of highly refined elements) and be a powerful tool for analyzing problems involving finite displacements and strains.

II.1.2 Selection of Displacement Functions

The key to the derivation of a deformation-consistent stiffness matrix is the selection of a displacement field satisfying the following requirements:

- (1) Internal and interface compatibility as defined in I.1.3;
- (2) Displacement functions must depend linearly on nodal displacements;
- (3) Rigid body displacement states must be included;
- (4) Uniform strain states must be included;
- (5) Displacement field must be spatially isotropic, i.e., intrinsically related to the element and independent of the external frame of reference.

Requirement (1) bounds the strain energy of the discretized structure \mathcal{S} considered continuous; if no geometric approximations are involved, we also get bounds for the influence coefficients of the actual structure \mathcal{S}^* . A monotonic behavior results if the mesh is subdivided into elements of the same type so that all previous displacement states are contained in the new ones (Melosh [10]).

Requirement (2) is automatically satisfied by using interpolation formulas of the type (I-10).

Requirement (3) is necessary to include the conditions of global static equilibrium; otherwise self-straining would result from rigid body motions [12].

Requirement (4) is a necessary condition for the convergence to the actual strain field; otherwise the missing strain states cannot be attained (and actually disappear) as the mesh size is reduced. The work "strain" is to be interpreted here as "displacement gradients entering into the formulation of the internal energy"; for instance, curvatures in pure bending elements.

Requirement (5) insures that the resulting generalized force-displacement relations (and therefore the solution of the problem) are objective, i.e., independent of the position of the external reference system. This condition is even more important in the step-by-step solution of geometrically nonlinear problems. The invariance condition may be expressed as

$$\mathbf{T}^T f(\mathbf{K}) \mathbf{T} = f(\mathbf{T}^T \mathbf{K} \mathbf{T}) \quad (\text{II-2})$$

where the transformation matrix \mathbf{T} represents a Galilean motion of the external frame and f is any invariant function of \mathbf{K} . Stiffness matrices satisfying (II-2) will be called objective or invariant.

A natural coordinate system is one having the element interfaces as coordinate surfaces; therefore it is intrinsically related to the element. An example of this is provided by the triangular coordinates defined in I.3.1 for a plane triangle. The invariance condition is automatically fulfilled if

the displacements are represented by isotropic functions in a natural coordinate system.

In the case of polynomial displacement functions, it is desirable to use complete polynomials (I-23) which possess the following properties:

- (i) Invariance is automatically satisfied since any complete polynomial is isotropic;
- (ii) Rigid body displacement and uniform strain states are included if the degree is at least $(q+1)$ for a C- q element;
- (iii) The solution does not depend on the choice of the fundamental nodal system, since no constraints have been imposed on the polynomial class (I-4).

The simplest C-0 elements satisfying requirements (1) through (5) are the so-called "topologically simplexes" [38], or, in short, "simplex" elements of constant strain and complete linear displacement field: bar, triangle, tetrahedron (Fig. 2.1). A n -th dimensional simplex has $(n+1)$ fundamental nodal points (corners).

When using incomplete polynomial expansions in natural coordinates, it is not immediately evident whether we are including all necessary rigid body displacement and uniform strain states. A simple and general way to control such requirements consists of restraining the nodal displacements in such a way that the displacement field becomes a simpler one satisfying all conditions, like a complete polynomial or the corresponding simplex in the case of a triangle or tetrahedron. For instance, for the 4 nodal point plane

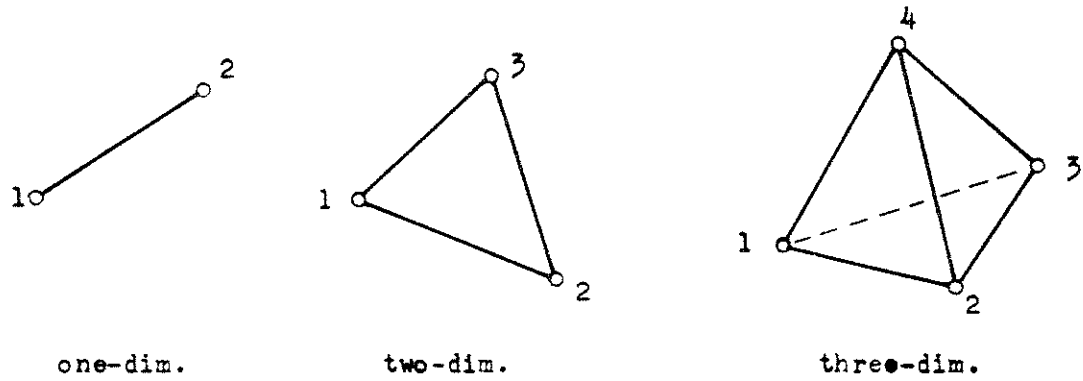
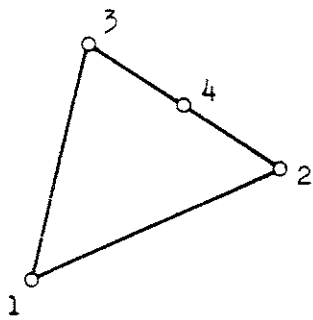
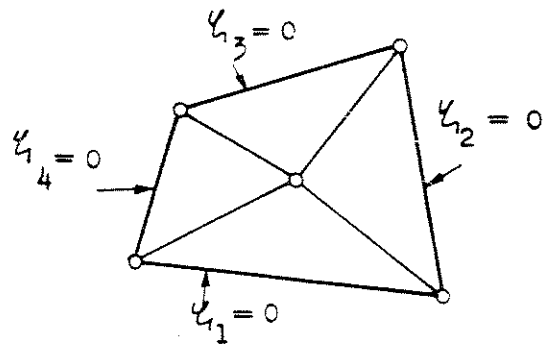


Fig. 2.1 - Simplex Elements.

Fig. 2.2 - Plane Triangle
with 4 Nodal Points.Fig. 2.3 - Plane Quadrilateral
formed with 4 Simplex Elements.

triangle shown in Fig. 2.2, we try for the u -component the interpolation formula

$$u(\xi_i) = \langle \xi_1, \xi_2(2\xi_3-1), \xi_3(2\xi_2-1), 4\xi_2\xi_3 \rangle \begin{Bmatrix} u_1 \\ u_2 \\ u_3 \\ u_4 \end{Bmatrix}$$

which satisfies compatibility. Setting $u_4 = (u_2+u_3)/2$ we get

$$u(\xi_i) = \langle \xi_1, \xi_2, \xi_3 \rangle \begin{Bmatrix} u_1 \\ u_2 \\ u_3 \end{Bmatrix}$$

the linear field of the constant strain triangle (see III.1.1). Therefore the assumed displacement field satisfies all conditions.

II.1.3 Introduction of Additional Modes

It has been proposed [35,36] to improve existing stiffness matrices in a systematic way by including additional and independent deformation modes not affecting compatibility (see I.1.3). We thereby have expanded the class of coordinate functions

$$\Omega = \Omega_1 + \Omega_2 \quad (\text{II-3})$$

and generated complete load-displacement relations of the form

$$\begin{bmatrix} \mathbf{K}_{11} & \mathbf{K}_{12} \\ \mathbf{K}_{12}^T & \mathbf{K}_{22} \end{bmatrix} \begin{Bmatrix} \mathbf{r}_1 \\ \mathbf{r}_2 \end{Bmatrix} = \begin{Bmatrix} \mathbf{R}_1 \\ \mathbf{R}_2 \end{Bmatrix} \quad (\text{II-4a})$$

where

- \mathbf{K}_{11} : stiffness associated with fundamental modes Ω_1
- \mathbf{K}_{22} : stiffness associated with additional modes Ω_2
- \mathbf{K}_{12} : coupling stiffness.

r_1 and r_2 are the nodal vectors (I-1) and R_1 and R_2 the associated generalized forces. Since the rigid body displacement states must be included in Ω_1 by requirement (3) of II.1.2 and the additional shapes are independent, K_{22} is nonsingular and we may eliminate r_2 to get

$$\begin{aligned} K &= K_{11} - K_{12} K_{22}^{-1} K_{12}^T \\ R &= R_1 - K_{12}^{-1} K_{12}^T R_2 \end{aligned} \quad (\text{II-4b})$$

as condensed stiffness matrix and condensed generalized force vector, respectively.

For plane triangular (C-q) elements we may use, for instance, members of the polynomial class (\mathcal{P} -q) defined in I.4.2.

This technique may be considered as a conventional Ritz procedure applied to the element considered as a structure subjected to the constraints imposed by the fundamental deformation modes as kinematic boundary conditions. If the class $(\Omega_2)_\infty$ is relatively complete with respect to this problem, we get in the limit the exact solution of the element subjected to fundamental boundary constraints and loaded with generalized nodal forces associated with the fundamental degrees of freedom. The effect of the Ω_2 modes is to improve the satisfaction of the internal microscopic equilibrium equations.

The inclusion of a few additional modes has proved useful in the following cases:

- (i) to complete a polynomial displacement field of a certain order; for example in the QST element developed in III.3;
- (ii) to include desirable physical deformation characteristics; for instance, the spar stiffness developed by De Veubeke [15];

- (iii) to minimize the effect of incomplete compatibility for certain elements (generalized stiffness method of Jones [37]); although these are not exactly additional modes in the sense of I.1.4.

Otherwise the inclusion of a large number of these functions has little advantages in practice for the following reasons:

- (a) The formation of matrices and load vectors of Equation (II-4a) plus the condensation process (II-4b) is complicated and time-consuming; moreover, for many structural types, numerical sensitivity and round-off errors may offset the advantage of having a slightly more flexible element;
- (b) When the actual geometry is only approximated by the assembly of elements, the inclusion of these higher order deformation modes may be detrimental to the solution. This occurs when the "true" solution of the discretized structure under nodal loads is quite different from the true solution for the actual structure; in general the "exact" solution under concentrated nodal forces displays undesirable stress singularities. The example of the conical shell element developed with Bessel functions is suggestive [39].
- (c) No improvement is possible for simplex elements of constant strain (Fig. 2.1), since the internal equilibrium equations are satisfied by the fundamental linear displacement modes; in this case $\mathbf{K}_{12} = \mathbf{0}$. Nevertheless it is possible to try to "improve"

elements formed by a combination of simplexes; for instance the plane quadrilateral assembled with four constant strain triangles (Fig. 2.3) may be given additional modes of the type

$$\sum_{m_k} \alpha_{m_1 m_2 m_3 m_4} \zeta_1^{m_1} \zeta_2^{m_2} \zeta_3^{m_3} \zeta_4^{m_4} \quad (m_k \geq 1)$$

where $\zeta_k = 0$ are the equations of the four sides in a natural coordinate system; here the equilibrium equations are violated on the internal interfaces. The practical value of this technique is open to question; it seems much more convenient to directly combine refined elements, constraining the displacement variation along the external sides. For example, we may assemble 4 nodal point triangles (Fig. 2.2) or four 5 nodal point triangles to form 4 nodal point quadrilaterals; this technique is well suited for automatic computation. A quantitative evaluation of the efficiency of different combinations is presented in Appendix II.

II.2 GENERAL DERIVATION OF CONVENTIONAL STIFFNESS MATRICES

II.2.1 Validity

The procedure described hereafter is valid for small strains and rotations (linearized form of the strain-displacement equations) and yields the conventional stiffness matrix. The case of finite displacements is treated in IV.3 and IV.4.

Although the derivation is carried out specifically for plane stress and plane strain triangular elements, it can be obviously applied to any (C-0) element for which interpolation formulae, preferably in terms of natural coordinates, can be constructed. Bending (C-1) elements present some particular problems, not discussed in this report.

Notation: a tilde on top of a vector or matrix function (I-11) is used when necessary to indicate that it is a function of the coordinates, in contrast to the plain symbol which represents the array of their nodal values. No distinction is necessary for:

shape functions ϕ_i (nodal values are indicated with other symbols);
 scalar functions (nodal vectors are written as bold face characters).

II.2.2 Displacement Functions

For PS problems, the complete displacement field is specified by the two components $u(x,y)$ and $v(x,y)$ in the global directions. Therefore we select two n-th order polynomials specified by

$$s \leq m = (n+2)(n+1)/2$$

nodal values at a nodal system $(N_u) = (N_v) \equiv (N_r)$; the equal sign being valid for a complete polynomial. The displacement components are then specified in triangular coordinates by the interpolation formulas

$$\begin{aligned} u(\zeta_i) &= \phi_{u_i} u_i = \Phi_u^T u \\ v(\zeta_i) &= \phi_{v_i} v_i = \Phi_v^T v \end{aligned} \tag{II-5}$$

where \mathbf{u} and \mathbf{v} are the nodal displacement vectors for $u(\zeta_i)$ and $v(\zeta_i)$ respectively. For symmetry $\phi_u = \phi_v = \phi$, i.e.,

$$\tilde{\mathbf{r}}(\zeta_i) = \begin{Bmatrix} u(\zeta_i) \\ v(\zeta_i) \end{Bmatrix} = \begin{bmatrix} \phi^T & \cdot \\ \cdot & \phi^T \end{bmatrix} \begin{Bmatrix} \mathbf{u} \\ \mathbf{v} \end{Bmatrix} = \Psi \mathbf{r} \quad (\text{II-6})$$

\mathbf{r} is the total displacement vector of $2s$ components.

These functions must satisfy requirements listed in II.1.2.

II.2.3 Strain-Displacement Relations

The linearized strain-displacement relations are:

$$\begin{aligned} \epsilon_x(\zeta_i) &= \frac{\partial u(\zeta_i)}{\partial x} = \phi_x^T \mathbf{u} \\ \epsilon_y(\zeta_i) &= \frac{\partial v(\zeta_i)}{\partial y} = \phi_y^T \mathbf{v} \\ \delta_{xy}(\zeta_i) &= \frac{\partial v(\zeta_i)}{\partial x} + \frac{\partial u(\zeta_i)}{\partial y} = \phi_y^T \mathbf{u} + \phi_x^T \mathbf{v} \end{aligned} \quad (\text{II-7})$$

where the vectors ϕ_x and ϕ_y are composed by the derivatives of the shape functions with respect to the global axes. From (I-22)

$$\frac{\partial \phi_i}{\partial x} = \frac{1}{2A} \frac{\partial \phi_i}{\partial \zeta_k} b_k \quad \frac{\partial \phi_i}{\partial y} = \frac{1}{2A} \frac{\partial \phi_i}{\partial \zeta_k} a_k \quad (\text{II-8})$$

We write (II-7) in matrix form as

$$\tilde{\epsilon}(\zeta_i) = \begin{Bmatrix} \epsilon_x(\zeta_i) \\ \epsilon_y(\zeta_i) \\ \delta_{xy}(\zeta_i) \end{Bmatrix} = \begin{bmatrix} \phi_x & \cdot \\ \cdot & \phi_y \\ \phi_y & \phi_x \end{bmatrix} \begin{Bmatrix} \mathbf{u} \\ \mathbf{v} \end{Bmatrix} = \tilde{\mathbf{B}} \mathbf{r} \quad (\text{II-9})$$

where $\tilde{\mathbf{B}}(\zeta_i)$ is the $(3 \times 2s)$ strain-nodal displacement matrix.

II.2.4 Constitutive Law

II.2.4.1 Linear Elastic Material

The two-dimensional constitutive law may be written in matrix form as follows (see Appendix I; 6 and 7):

$$\begin{Bmatrix} \sigma_x \\ \sigma_y \\ \tau_{xy} \end{Bmatrix} = \begin{bmatrix} c_{11} & c_{12} & c_{13} \\ c_{21} & c_{22} & c_{23} \\ c_{31} & c_{32} & c_{33} \end{bmatrix} \begin{Bmatrix} \epsilon_x \\ \epsilon_y \\ \gamma_{xy} \end{Bmatrix} \quad (\text{II-10})$$

or

$$\tilde{\sigma}(\xi_i) = \tilde{\mathbf{C}}(\xi_i) \tilde{\epsilon}(\xi_i) \quad (\text{II-11})$$

where the matrix $\tilde{\mathbf{C}}$ is symmetric, i.e., we consider only materials with a strain energy function (Green-elastic or hyperelastic).

Isotropic materials are characterized by two constants (E and ν);

$$\tilde{\mathbf{C}} = E_r \begin{bmatrix} \kappa & \nu & \cdot \\ \nu & \kappa & \cdot \\ \cdot & \cdot & \lambda \end{bmatrix} \quad (\text{II-12})$$

where

$$\begin{aligned} \text{for plane stress } \kappa &= 1, \quad \lambda = (1-\nu)/2, \quad E_r = E/(1-\nu^2) \\ \text{for plane strain } \kappa &= 1-\nu, \quad \lambda = 0.5-\nu, \quad E_r = E/((1+\nu)(1-2\nu)) \end{aligned} \quad (\text{II-13})$$

The case of anisotropic and in particular orthotropic materials, is treated in detail in Appendix I.

II.2.4.2 Nonlinear Elastic Material

The constitutive law may be written either in "secant" form

$$\tilde{\sigma}(\xi_i) = \tilde{C}^*(\xi_i, \tilde{\epsilon}) \tilde{\epsilon}(\xi_i) \quad (\text{II-14})$$

or in incremental ("tangent") form

$$d\tilde{\sigma}(\xi_i) = \tilde{C}(\xi_i, \tilde{\epsilon}) d\tilde{\epsilon}(\xi_i) \quad (\text{II-15})$$

The first expression is used in the solution by iteration, the second one in the step-by-step procedure (cf. IV.1). In any case, the only difference from the linear case lies in the fact that \tilde{C} is also a function of the strain state and the problem is formally trivial. However, in the case of large strains (rubberlike materials) the conventional stiffness must be corrected as explained in IV.1.2.

II.2.4.3 General Nonlinear Material

In general, in the incremental law (II-15), $\tilde{C}(\xi_i)$ becomes a differential or integral (functional) operator, a function of the past history and the present configuration. The case of elasto-plastic material is treated in IV.2.

II.2.5 Generalized Force-Displacement Relations

The external loads acting on the element are denoted by

$$\tilde{\mathbf{p}}^T(\xi_i) = \langle p_x(\xi_i) \quad p_y(\xi_i) \rangle \quad : \text{ surface tractions per unit length}$$

specified on the region B_p of the boundary;

$$\tilde{\mathbf{f}}^T(\xi_i) = \langle f_x(\xi_i) \quad f_y(\xi_i) \rangle \quad : \text{ body forces per unit volume.}$$

The total potential energy is

$$V = U - P = \frac{1}{2} W_i - W_e \quad (\text{II-16})$$

where U : strain energy calculated from the strain field associated with the displacement field;

P : potential energy of prescribed loads;

W_e, W_i : external and internal work.

Using (II-6), (II-9) and (II-10) we may write:

$$\begin{aligned} V &= \frac{1}{2} \int_D \tilde{\boldsymbol{\epsilon}}^T \tilde{\boldsymbol{\sigma}} dV - \int_{B_p} \tilde{\mathbf{p}}^T(\tilde{\mathbf{r}})_{B_p} dS - \int_D \tilde{\mathbf{f}}^T \tilde{\mathbf{r}} dV \\ &= \frac{1}{2} \mathbf{r}^T \int_D \tilde{\mathbf{B}}^T \tilde{\mathbf{C}} \tilde{\mathbf{B}} dV \mathbf{r} - \int_{B_p} \mathbf{p}^T(\boldsymbol{\Psi})_{B_p} dS \mathbf{r} - \int_D \tilde{\mathbf{f}}^T \boldsymbol{\Psi} dV \mathbf{r} \\ &= \frac{1}{2} \mathbf{r}^T \mathbf{K} \mathbf{r} - \mathbf{R}_p^T \mathbf{r} - \mathbf{R}_f^T \mathbf{r} = \frac{1}{2} \mathbf{R}^T \mathbf{r} - \mathbf{S}^T \mathbf{r} \end{aligned} \quad (\text{II-17})$$

where \mathbf{K} is the $(2s \times 2s)$ stiffness matrix;

$\mathbf{R} = \mathbf{K} \mathbf{r}$ are the generalized nodal forces (internal reactions) associated with the nodal displacements \mathbf{r} ;

$\mathbf{R}_p, \mathbf{R}_f$ are generalized force vectors kinematically equivalent to the prescribed surface and body forces respectively (i.e., they produce the same W_e). $\mathbf{S} = \mathbf{R}_p + \mathbf{R}_f$ are the total applied generalized forces.

Setting the first variation of V to zero (minimum potential energy principle)

$$\delta V = 0$$

we obtain the generalized force-displacement relations (macroscopic equilibrium equations):

$$\mathbf{K} \mathbf{r} = \mathbf{R}_p + \mathbf{R}_f = \mathbf{S} \quad (\text{II-18})$$

or

$$\mathbf{R} = \mathbf{S}$$

Then at the equilibrium position, $W_i = W_e$.

Writing the element of volume as $dV = h \, dA$, we have the following expression for the element stiffness matrix of a slice:

$$\mathbf{K} = \int_A \tilde{\mathbf{B}}^T(\zeta_i) \tilde{\mathbf{C}}(\zeta_i) \tilde{\mathbf{B}}(\zeta_i) h(\zeta_i) \, dA \quad (\text{II-19})$$

In practice, the generation of \mathbf{K} by direct integration of Equation (II-19) is unnecessarily cumbersome, especially for refined elements ($n \geq 2$). A more elegant procedure, which reduces to integration of a cyclically symmetric matrix of polynomial terms in triangular coordinates, is described in II.3.

II.3 PRACTICAL CONSTRUCTION OF STIFFNESS MATRICES

II.3.1 Selection of Nodal System for Element Functions

II.3.1.1 Strains

The strain components vary as $(n-1)$ -th order polynomials. We select a nodal point system (N_ϵ) which specifies completely their variation through the corresponding interpolation formula. We need

$$m_\epsilon = (n+1)n/2$$

values for each strain component. Let

$$\boldsymbol{\epsilon}^T = \langle \boldsymbol{\epsilon}_x^T \quad \boldsymbol{\epsilon}_y^T \quad \gamma_{xy}^T \rangle \quad (\text{II-20})$$

be the $(3m_\epsilon \times 1)$ vector of nodal strains, composed by three $(m_\epsilon \times 1)$ subvectors

$$\boldsymbol{\epsilon}_x = \langle \epsilon_{x_1} \quad \epsilon_{x_2} \quad \dots \quad \epsilon_{x_{m_\epsilon}} \rangle, \text{ etc}$$

Then

$$\boldsymbol{\epsilon} = \begin{Bmatrix} \boldsymbol{\epsilon}_x \\ \boldsymbol{\epsilon}_y \\ \gamma_{xy} \end{Bmatrix} = \begin{bmatrix} \mathbf{U} & \mathbf{V} \\ \mathbf{V} & \mathbf{U} \end{bmatrix} \begin{Bmatrix} \mathbf{u} \\ \mathbf{v} \end{Bmatrix} = \mathbf{B} \mathbf{r} \quad (\text{II-21})$$

where \mathbf{U} and \mathbf{V} are $(m_\epsilon \times S)$ submatrices obtained by evaluating ϕ_x and ϕ_y of (II-9) at (N_ϵ) . Hence \mathbf{B} , the $(3m_\epsilon \times 2S)$ nodal strain-displacement matrix, is $\tilde{\mathbf{B}}(\xi_1)$ evaluated at (N_ϵ) .

We note en passant that \mathbf{U} and \mathbf{V} are used after solving for nodal displacements to obtain nodal strains and stresses.

II.3.1.2 Constitutive Law

We suppose now that the variation of the matrix $\tilde{\mathbf{C}}(\xi_1)$ inside the element may be approximated by a n_c -th order polynomial law. A new nodal system (N_c) having

$$m_c = (n_c + 2)(n_c + 1) / 2$$

points is selected.

We denote by

$$\mathbf{C}_{(1)} \quad \mathbf{C}_{(2)} \quad \dots \quad \mathbf{C}_{(m_C)}$$

the stress-strain matrices obtained by evaluating $\tilde{\mathbf{C}}(\xi_i)$ at (N_C) and by

$$\mathbf{C}^T = \left[\mathbf{C}_{(1)} \quad \mathbf{C}_{(2)} \quad \dots \quad \mathbf{C}_{(m_C)} \right] \quad (\text{II-22})$$

the nodal stress-strain matrix; their components may also be ordered as a nodal vector.

II.3.1.3 Stresses

Stress components will vary as $(n+1+n_C)$ -th order polynomials; these cannot be complete (unless $n_C=0$) since they are constrained by (II-10), however for simplicity we treat them as such and select a nodal system (N_σ) with

$$m_\sigma = (n+n_C+1)(n+n_C)/2$$

points and define

$$\boldsymbol{\sigma}^T = \langle \sigma_x^T \quad \sigma_y^T \quad \tau_{xy}^T \rangle \quad (\text{II-23})$$

with

$$\sigma_x^T = \langle \sigma_{x_1} \quad \sigma_{x_2} \quad \dots \quad \sigma_{x_{m_\sigma}} \rangle \quad \text{etc}$$

as the $(3m_\sigma \times 1)$ vector of nodal stresses at (N_σ) .

II.3.1.4 Thickness

For a plane strain slice element ($h=1$) or a plane stress element of constant thickness, h may be taken outside the integral (II-19). Otherwise we proceed as for $\tilde{\mathbf{C}}$ and define a n_h -th order polynomial variation

specified by m_h values at a nodal system (N_h); the nodal thickness vector being

$$\mathbf{h}^T = \langle h_1 \ h_2 \ \dots \ h_{m_h} \rangle \quad (\text{II-24})$$

All these nodal systems are summarized in Table 5.

II.3.2 Stiffness Matrix

The interpolation formulas for strains, constitutive law, stresses and thickness with respect to the nodal systems defined in II.3.1 may be written

$$\begin{aligned} \check{\epsilon}(\xi_i) &= \Phi_{\epsilon}^T(\xi_i) \epsilon \\ \check{\mathbf{C}}(\xi_i) &= \Phi_{\mathbf{C}}^T(\xi_i) : \mathbf{C} \\ \check{\sigma}(\xi_i) &= \Phi_{\sigma}^T(\xi_i) \sigma \\ h(\xi_i) &= \Phi_h^T(\xi_i) h \end{aligned} \quad (\text{II-25})$$

Evaluating $\check{\epsilon}$ and $\check{\mathbf{C}}$ at (N_{σ}) we have

$$\begin{aligned} \epsilon_{\sigma} &= \Lambda \epsilon \quad (\Lambda \equiv \Phi_{\epsilon}^T \text{ at } (N_{\sigma})) \\ \mathbf{C}_{\sigma} &\equiv \check{\mathbf{C}}(\xi_i) \text{ at } (N_{\sigma}) \end{aligned} \quad (\text{II-26})$$

and the nodal stress vector is related to the nodal strain vector through

$$\sigma = \mathbf{C}_{\sigma} \epsilon_{\sigma} = \mathbf{C}_{\sigma} \Lambda \epsilon \quad (\text{II-27})$$

The strain energy integral may be expressed as follows:

$$U = \frac{1}{2} \epsilon^T \int_A \Phi_{\epsilon} \Phi_h^T h \Phi_{\sigma}^T dA \sigma = \frac{1}{2} \epsilon^T \int_A \Phi_{\epsilon} \Phi_h^T h \Phi_{\sigma}^T dA \mathbf{C}_{\sigma} \Lambda \epsilon$$

$$\text{or} \quad U = \frac{1}{2} \epsilon^T \mathbf{Q} \mathbf{D} \epsilon = \frac{1}{2} \epsilon^T \mathbf{N} \epsilon \quad (\text{II-28})$$

where

$$\left\{ \begin{array}{l} \mathbf{Q} = \int_A \Phi_{\epsilon} \Phi_h^T h \Phi_{\sigma}^T dA \\ \mathbf{D} = \mathbf{C}_{\sigma} \Lambda \end{array} \right.$$

Table 5. Nodal Systems for Element Functions

Variable	Polynomial Law Order	Nodal System	No. of nodal values per comp.	Total No. of nodal values
Displacements $\tilde{\mathbf{r}}$	n	(N_r)	$s \leq m$	$2s$
Strains $\tilde{\mathbf{e}}$	$n_e = n - 1$	(N_e)	m_e	$3m_e$
Material Law $\tilde{\mathbf{C}}$	n_c	(N_c)	m_c	$9m_c$
Stresses $\tilde{\mathbf{\sigma}}$	$n_\sigma = n + n_c - 1$	(N_σ)	m_σ	$3m_\sigma$
Thickness h	n_h	(N_h)	m_h	m_h
Density ρ	n_ρ	(N_ρ)	m_ρ	m_ρ
Surface Load $\tilde{\mathbf{p}}$	n_p	(N_p)	m_p	$2m_p$
Body Force $\tilde{\mathbf{f}}$	n_f	(N_f)	m_f	$2m_f$
Temperature θ	n_θ	(N_θ)	m_θ	m_θ
Thermal coeff. $\tilde{\alpha}$	n_α	(N_α)	m_α	$3m_\alpha$

Notes:

- (a) Each m_k is related to n_k by $m_k = (n_k + 2)(n_k + 1)/2$ (complete polynomial in two variables) except for surface load p , for which $m_p = n_p + 1$ (one variable)
- (b) Corresponding interpolation formulas are designated by the vector symbol Φ for scalar functions or single components, by the matrix symbol Φ for vector and matrix functions, with the corresponding subscripts.

and $\mathbf{N} = \mathbf{QD}$ is the stiffness matrix in terms of the nodal strains considered as generalized coordinates.

To get the stiffness in terms of nodal displacements, we make use of the transformation (II-21)

$$\mathbf{K} = \mathbf{B}^T \mathbf{Q} \mathbf{D} \mathbf{B} = \mathbf{B}^T \mathbf{N} \mathbf{B} \quad (\text{II-29})$$

which is the best way to assemble \mathbf{K} in automatic computation. This relation may be interpreted as the following chain of matrix operations:

- (a) Nodal strains at (N_ϵ) from nodal displacements at (N_r):

$$\boldsymbol{\epsilon} = \mathbf{B} \mathbf{r} \quad (\text{II-30a})$$

- (b) Nodal stresses at (N_σ) from nodal strains at (N_ϵ):

$$\boldsymbol{\sigma} = \mathbf{D} \boldsymbol{\epsilon} \quad (\text{II-30b})$$

- (c) Nodal forces at (N_r) from nodal stresses at (N_σ):

$$\mathbf{R} = \mathbf{B}^T \mathbf{Q} \boldsymbol{\sigma} \quad (\text{II-30c})$$

Thus the work is reduced to the computation of \mathbf{B} , \mathbf{D} and \mathbf{Q} :

- (i) \mathbf{B} is integrated by the submatrices \mathbf{U} and \mathbf{V} of Equation (II-21)

which are computed by replacing the triangular coordinates of the nodal strain system (N_σ) into ϕ_x and ϕ_y of Equation (II-9).

- (ii) \mathbf{D} is generated by the multiplication of \mathbf{C}_σ and \mathbf{A} , two constant matrices obtained by evaluating the constitutive law $\mathbf{C}(\xi_i)$ and the interpolation matrix $\mathbf{\Phi}_\epsilon$ for strains at the nodal stress system (N_σ). Since the vector $\boldsymbol{\epsilon}_\sigma$ has the form (II-20) the matrix

\mathbf{C}_σ has the following structure

$$\mathbf{C}_\sigma = \begin{bmatrix} \mathbf{C}_{11} & \mathbf{C}_{12} & \mathbf{C}_{13} \\ & \mathbf{C}_{22} & \mathbf{C}_{23} \\ \text{symm.} & & \mathbf{C}_{33} \end{bmatrix} \quad (\text{II-31})$$

where each $(m_\sigma \times m_\sigma)$ block \mathbf{C}_{ij} is a diagonal matrix

$$\mathbf{C}_{ij} = \text{diag} \langle c_{ij}^{(1)} \ c_{ij}^{(2)} \ \dots \ c_{ij}^{(m_\sigma)} \rangle \quad (\text{II-32})$$

composed by the material coefficients c_{ij} evaluated at the " m_σ " points of the nodal system (N_σ) .

In elastic problems, the stress-strain law $\tilde{\mathbf{C}}$ is usually assumed to be constant inside the element; in such a case we may select $(N_\sigma) \equiv (N_\epsilon)$, $\mathbf{D} = \mathbf{C}$, and each block of Equation (II-31) becomes

$$\mathbf{C}_{ij} = c_{ij} \mathbf{I} \quad (\text{II-33})$$

\mathbf{I} being the identity matrix of order $m_\sigma = m_\epsilon$.

(iii) The formation of \mathbf{Q} may be simplified if we observe that $\bar{\Phi}_\epsilon$ and $\bar{\Phi}_\sigma$ have the structure

$$\bar{\Phi}_\epsilon = \begin{bmatrix} \phi_\epsilon & \cdot & \cdot \\ \cdot & \phi_\epsilon & \cdot \\ \cdot & \cdot & \phi_\epsilon \end{bmatrix} \quad \bar{\Phi}_\sigma = \begin{bmatrix} \phi_\sigma & \cdot & \cdot \\ \cdot & \phi_\sigma & \cdot \\ \cdot & \cdot & \phi_\sigma \end{bmatrix} \quad (\text{II-34})$$

where ϕ_ϵ and ϕ_σ are the interpolation vectors for a single strain and stress component. Furthermore, to make the integral dimensionless, we introduce a relative dimensionless thickness

$$\xi(\zeta_i) = h(\zeta_i) / h_r \quad (\text{II-35})$$

h_r being a reference thickness. The nodal vector of relative thicknesses and the corresponding interpolation vector are

$$\xi = h_r^{-1} \mathbf{h} \quad \phi_\xi \equiv \phi_h \quad (\text{II-36})$$

Therefore we may express \mathbf{Q} as a diagonal supermatrix

$$\mathbf{Q} = A h_r \begin{bmatrix} \bar{\mathbf{Q}} & \cdot & \cdot \\ \cdot & \bar{\mathbf{Q}} & \cdot \\ \cdot & \cdot & \bar{\mathbf{Q}} \end{bmatrix} \quad (\text{II-37})$$

where

$$\bar{\mathbf{Q}} = \frac{1}{A} \int_A \phi_\epsilon \phi_\xi^T \xi \phi_\sigma dA \quad (\text{II-38})$$

is a purely numerical ($m_\epsilon \times m_\sigma$) matrix which can be readily computed using Table 3. Moreover, it generally displays a high cyclic symmetry and only a few integrals need to be evaluated.

Notice that $\phi_\xi^T \xi$ enters in the integral (II-38) as a scalar multiplying all entries of $\phi_\epsilon \phi_\sigma^T$. If the thickness is constant, we have simply

$$\bar{\mathbf{Q}} = \frac{1}{A} \int_A \phi_\epsilon \phi_\sigma^T dA \quad (\text{II-39})$$

For the lowest polynomial orders such matrices (designated by \mathbf{L}_{ij}) have been tabulated in I.5.1.

Finally, if the stress-strain law $\tilde{\mathbf{C}}$ is constant, we may combine (II-33) with (II-37) immediately to express \mathbf{N} in the form

$$\mathbf{N} = \mathbf{Q} \mathbf{D} = \mathbf{Q} \mathbf{C}_0 = A h_r \begin{bmatrix} c_{11} \bar{\mathbf{Q}} & c_{12} \bar{\mathbf{Q}} & c_{13} \bar{\mathbf{Q}} \\ & c_{22} \bar{\mathbf{Q}} & c_{23} \bar{\mathbf{Q}} \\ & & c_{33} \bar{\mathbf{Q}} \end{bmatrix} \quad (\text{II-40})$$

II.4 PRACTICAL COMPUTATION OF CONSISTENT FORCE VECTORS AND MASS MATRICES

II.4.1 Surface Loads

An in-plane surface loading $\tilde{\mathbf{p}}(\zeta_B)$ acts on the portion B_p of the element boundary. The same process described in II.3 can be used to evaluate the equivalent generalized force vector R_p .

We suppose that $\tilde{\mathbf{p}}(\zeta_B)$ is already integrated through the thickness $h(\zeta_B)$ at B_p . Its variation law is assumed to be a n_p -th order polynomial in one variable, specified by

$$m_p = n_p + 1$$

sample values of p at a nodal system (N_p) so that

$$\tilde{\mathbf{p}}(\zeta_B) = \begin{Bmatrix} p_x(\zeta_B) \\ p_y(\zeta_B) \end{Bmatrix} = \begin{bmatrix} \Phi_p^T & \cdot \\ \cdot & \Phi_p^T \end{bmatrix} \begin{Bmatrix} p_x \\ p_y \end{Bmatrix} = \Phi_p^T \mathbf{p} \quad (\text{II-41})$$

where $\mathbf{p}^T = \langle p_x^T \ p_y^T \rangle$ is the nodal vector of sample loads.

The displacement of the boundary B_p depends only on nodal points located on the common element interface B_p^* which contains B_p . Hence

$$\tilde{\mathbf{r}}_B(\zeta_B) = \begin{Bmatrix} u(\zeta_B) \\ v(\zeta_B) \end{Bmatrix} = \begin{bmatrix} \Phi_B^T & \cdot \\ \cdot & \Phi_B^T \end{bmatrix} \begin{Bmatrix} u_B \\ v_B \end{Bmatrix} = \Phi_B^T \mathbf{r}_B \quad (\text{II-42})$$

where

$$\mathbf{r}_B^T = \langle \mathbf{u}_B^T \ \mathbf{v}_B^T \rangle \quad \text{include only those components of the nodal}$$

displacement \mathbf{r} which determine the displacement $\mathbf{r}_B(\zeta_B)$ of B_p ;

Φ_B is obtained from Φ of Equation (II-6) by extracting interpolating functions corresponding to \mathbf{u}_B and \mathbf{v}_B and evaluating them at B_p^* where they become functions of a single triangular coordinate.

From the expression (II-17) of the external work W_e , we immediately obtain

$$R_{Bp}^T = p^T \int_{B_p} \phi_p \phi_B^T ds \quad (\text{II-43})$$

or, if we define

$$P_B = \int_{B_p} \phi_p \phi_B^T ds \quad (\text{II-44})$$

then

$$R_{Bpx} = p_x^T P_B \quad R_{Bpy} = p_y^T P_B \quad (\text{II-45})$$

where R_B is the force vector associated to r_B . Only nodes on B_p^* receive loading.

As an example, suppose that \tilde{p} acts on the side 3 of a plane triangle (Fig. 2.4); the equation of the side is $\zeta_3 = 0$ or $\zeta_1 + \zeta_2 = 1$. If we express all functions of (II-44) in terms of ζ_1 , we obtain (since $ds = l_3 d\zeta_1$):

$$P_B = l_3 \int_0^1 \phi_p(\zeta_1) \phi_B^T(\zeta_1) d\zeta_1 \quad (\text{II-46})$$

and similarly for sides 2 and 3 by cyclic permutation of subindices.

Actual production programs are usually constructed to accept normal pressure and surface shear, which are most commonly specified in practice, and to transform them automatically to nodal forces in the global directions.

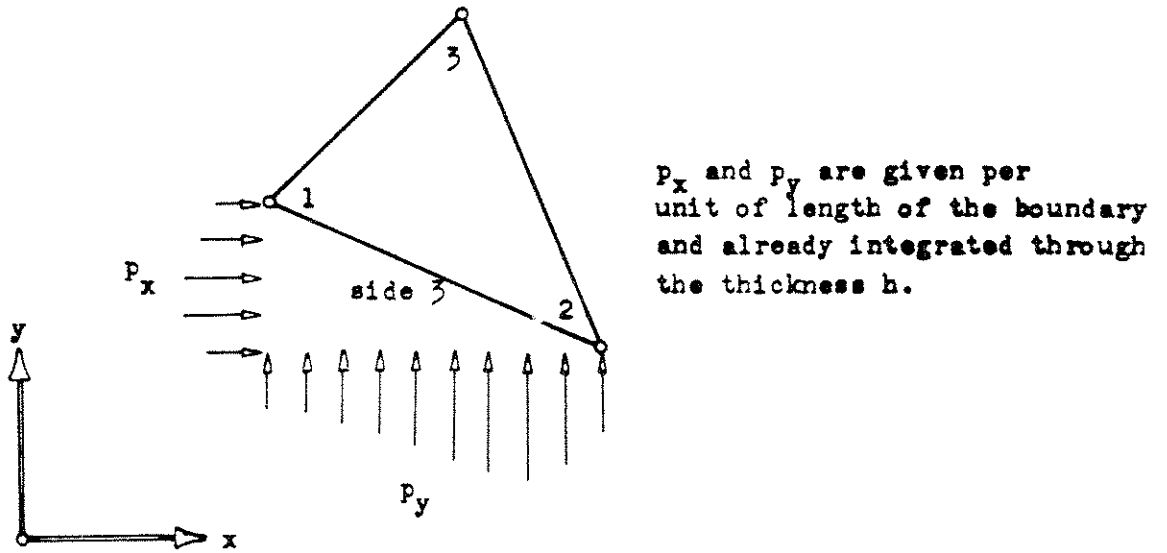


Fig. 2.4 - In-plane Distributed Loading on Plane Triangle.

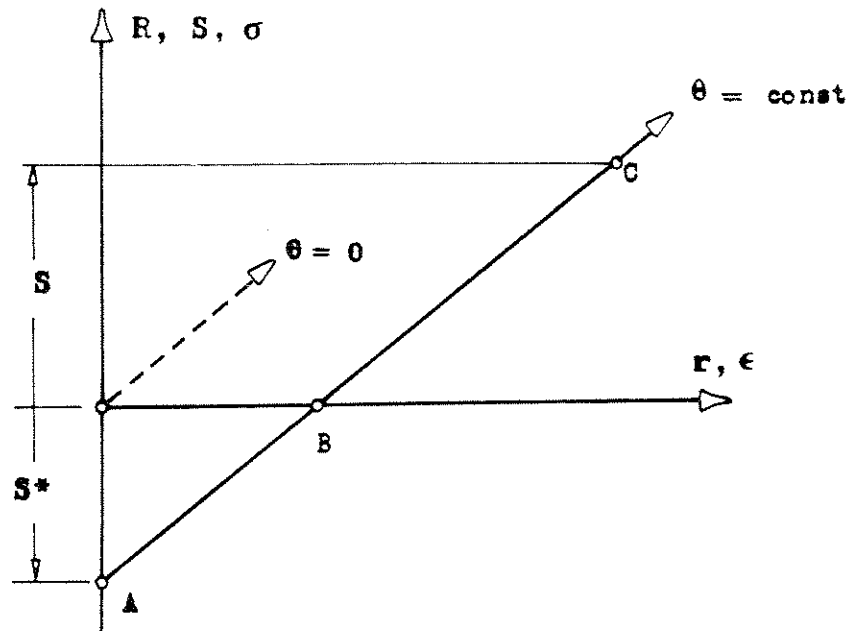


Fig. 2.5 - Solution of Thermoelastic Problems by the Initial Stress Method.

II.4.2 Body Forces

This case is simpler. We define a nodal system (N_f) , a nodal body force vector

$$\mathbf{f} = \langle \mathbf{f}_x^T \quad \mathbf{f}_y^T \rangle$$

of sample values of $\tilde{\mathbf{f}}(\xi_i)$, and the interpolation formulas

$$f_x(\xi_i) = \phi_f^T \mathbf{f}_x \quad f_y(\xi_{i1}) = \phi_f^T \mathbf{f}_y \quad (\text{II-47})$$

Equation (II-17) gives immediately

$$\begin{aligned} R_{fx}^T &= A h_r \mathbf{f}_x^T \mathbf{F} \\ R_{fy}^T &= A h_r \mathbf{f}_y^T \mathbf{F} \end{aligned} \quad (\text{II-48})$$

where

$$\mathbf{F} = \frac{1}{A} \int_A \phi_f \phi_\xi^T \xi \phi^T dA \quad (\text{II-49})$$

may be readily evaluated with help of Table 3. For constant thickness the integral

$$\mathbf{F} = \frac{1}{A} \int_A \phi_f \phi^T dA \quad (\text{II-50})$$

is of the same type of (II-39) and has been tabulated in I.5.1 for the lowest polynomial orders.

The most important body force (in static problems) is the gravity load. If the element is on a vertical plane and φ is the angle forced by the global x-axis and the vertical direction, we have

$$f_x = \rho \cos \varphi \quad f_y = \rho \sin \varphi$$

hence the variation law and interpolation formulas for $\tilde{\mathbf{f}}$ are those for the density ρ .

II.4.3 Consistent Mass Matrix

A similar technique is followed to set up the consistent mass matrix \mathbf{M} used in dynamic problems. Let $\dot{\tilde{\mathbf{r}}}$ be the in-plane velocity; then the kinetic energy of the element is

$$2T = \int_V \dot{\tilde{\mathbf{r}}} \dot{\tilde{\mathbf{r}}} dm = \dot{\tilde{\mathbf{r}}} \int_V \Psi \rho \Psi^T dV \dot{\tilde{\mathbf{r}}} = \dot{\tilde{\mathbf{r}}}^T \mathbf{M} \dot{\tilde{\mathbf{r}}} \quad (\text{II-51})$$

hence

$$\mathbf{M} = \int_V \Psi(\xi_i) \rho(\xi_i) \Psi^T(\xi_i) dV \quad (\text{II-52})$$

where $\rho(\xi_i)$ is the density. Again since $\Psi = \begin{bmatrix} \phi & \cdot \\ \cdot & \phi \end{bmatrix}$

the velocity components \dot{u} and \dot{v} are uncoupled. Let

$$\mathbf{M} = \begin{bmatrix} M_1 & \cdot \\ \cdot & M_1 \end{bmatrix} \quad (\text{II-53})$$

Then for a constant density ρ and substituting for $dV = h_r \phi_\xi^T \xi dA$

we get

$$M_1 = \rho h_r \int_A \phi \phi_\xi^T \xi \phi^T dA = A h_r \bar{M} \quad (\text{II-54})$$

with

$$\bar{M} = \frac{1}{A} \int_A \phi \phi_\xi^T \xi \phi^T dA \quad (\text{II-55})$$

For constant thickness the integrals

$$\bar{M} = \frac{1}{A} \int_A \phi \phi^T dA \quad (\text{II-56})$$

may be found in I.5.1 for the lowest orders.

II.5 THERMOELASTIC PROBLEMS

II.5.1 Solution by the Initial Stress Method

For uncoupled thermoelastic problems, in which the temperature field $\theta(\xi_i)$ is known a priori, the most effective automatic solution procedure is the method of restraint or initial stress, described in what follows:

(a) Every element of the idealized structure is considered to be completely restrained, i.e., both the displacement field and the elastic strain field vanish everywhere. From the constitutive law (A1-2b) we have then a field of "initial stresses" or "restraint stresses"

$$\tilde{\sigma}^*(\xi_i) = -\tilde{c}(\xi_i) \tilde{\alpha}(\xi_i) \theta(\xi_i) = -\mathbf{t}(\xi_i) \theta(\xi_i) \quad (\text{II-57})$$

the associated nodal forces \mathbf{S}^* being "initial loads" or "restraint forces". We are then at the point (A) of Fig. 2.5.

(b) We release the stress field $\tilde{\sigma}^*$ by applying a nodal force system $-\mathbf{S}^*$; the element moves to the equilibrium position of point (C) determined by

$$\mathbf{S} - \mathbf{S}^* = \mathbf{R} = \mathbf{K} \mathbf{r} \quad (\text{II-58})$$

where \mathbf{S} denotes as usual the applied (external) forces. If $\mathbf{S} = \mathbf{0}$, $\mathbf{K} \mathbf{r} = -\mathbf{S}^*$, i.e., the initial thermal loads are equilibrated by the internal forces (point(B) of Fig. 2.5).

After assembling the stiffness relations (II-58) for the entire structure, we solve for nodal displacements and compute stresses from the constitutive law (A1-2b).

II.5.2 Computation of Initial Thermal Loads

For simplicity, elastic and thermal coefficients are assumed to be constant inside the element. No essential difficulty is encountered if the material law is variable.

Let (N_θ) be a nodal system for the element temperature field and θ the corresponding nodal vector. The variation of temperature is given by $\theta(\xi_i) = \Phi_\theta^T \theta$ and the initial stresses, from Equation (II-57)

$$\tilde{\sigma}^* = -\mathbf{t} \Phi_\theta \theta \quad (\text{II-59})$$

Since \mathbf{t} is constant, we may take $(N_\theta) = (N_{\sigma^*})$, a nodal system for each prestress component; the variation of σ_x^* , σ_y^* and τ_{xy}^* is then specified by

$$\tilde{\sigma}^* = \begin{Bmatrix} \sigma_x^* \\ \sigma_y^* \\ \tau_{xy}^* \end{Bmatrix} = \begin{bmatrix} \Phi_\theta^T & & \\ & \Phi_\theta^T & \\ & & \Phi_\theta^T \end{bmatrix} \begin{Bmatrix} \sigma_x^* \\ \sigma_y^* \\ \tau_{xy}^* \end{Bmatrix} = \Phi_\theta^T \sigma^* \quad (\text{II-60})$$

The internal work stored at (B) is (see (A1-3))

$$\begin{aligned} W_i &= \int_V -\tilde{\mathbf{e}}^T \mathbf{t} \theta \, dV = \int_V \tilde{\mathbf{e}}^T \tilde{\boldsymbol{\sigma}}^* \, dV = \\ &= \mathbf{r}^T \mathbf{B}^T \int_A \tilde{\Phi}_\epsilon \tilde{\Phi}_h^T h \tilde{\Phi}_\theta^T \, dA \cdot \boldsymbol{\sigma}^* = \mathbf{r}^T \mathbf{S}^* \end{aligned}$$

Hence the associated nodal forces are

$$\mathbf{S}^* = \mathbf{B}^T \int_A \tilde{\Phi}_\epsilon \tilde{\Phi}_h^T h \tilde{\Phi}_\theta^T \, dA \boldsymbol{\sigma}^* = \mathbf{B}^T \mathbf{Q}^* \boldsymbol{\sigma}^* \quad (\text{II-62})$$

Proceeding as in (II.3.2) we may express the integral \mathbf{Q}^* as

$$\mathbf{Q}^* = A h_r \begin{bmatrix} \bar{\mathbf{Q}}^* & \cdot & \cdot \\ \cdot & \bar{\mathbf{Q}}^* & \cdot \\ \cdot & \cdot & \bar{\mathbf{Q}}^* \end{bmatrix} \quad (\text{II-63})$$

where

$$\bar{\mathbf{Q}}^* = \frac{1}{A} \int_A \Phi_\epsilon \Phi_\xi^T \xi \Phi_\theta^T \, dA \quad (\text{II-64})$$

Finally, using the block decomposition (II-21) for \mathbf{B} , we obtain for the x and y components of \mathbf{S}^*

$$\begin{aligned} \mathbf{S}_x^* &= A h_r (\mathbf{U}^T \bar{\mathbf{Q}}^* \boldsymbol{\sigma}_x^* + \mathbf{V}^T \bar{\mathbf{Q}}^* \boldsymbol{\tau}_{xy}^*) \\ \mathbf{S}_y^* &= A h_r (\mathbf{V}^T \bar{\mathbf{Q}}^* \boldsymbol{\sigma}_y^* + \mathbf{U}^T \bar{\mathbf{Q}}^* \boldsymbol{\tau}_{xy}^*) \end{aligned} \quad (\text{II-65})$$

If the material is thermoisotropic (A1-12) or (A1-15)

$$\boldsymbol{\sigma}_x^* = \boldsymbol{\sigma}_y^* = \frac{E\alpha}{\rho} \theta \quad \boldsymbol{\tau}_{xy}^* = 0 \quad (\text{II-66})$$

therefore

$$\begin{aligned} \mathbf{S}_x^* &= \frac{E A h_r \alpha}{\rho} \mathbf{U}^T \bar{\mathbf{Q}}^* \theta \\ \mathbf{S}_y^* &= \frac{E A h_r \alpha}{\rho} \mathbf{V}^T \bar{\mathbf{Q}}^* \theta \end{aligned} \quad (\text{II-67})$$

where

$$\mu = 1 - \nu \quad \text{for plane stress}$$

$$\mu = 1 - 2\nu \quad \text{for plane strain.}$$

If the temperature variation law is the same of the elastic stresses then we may take $(N_{\sigma^*}) \equiv (N_{\sigma}) \equiv (N_{\theta})$, hence $\Phi_{\theta} \equiv \Phi_{\sigma}$ and

$$\bar{Q}^* = \bar{Q} \quad (\text{II-68})$$

as given by Equation (II-38); no new evaluation of integrals is then necessary.

III. TRIANGULAR ELEMENT STIFFNESS MATRICES FOR LINEAR
PROBLEMS. POLYNOMIAL ORDERS $n = 1, 2$ and 3

III.1 THE CONSTANT STRAIN TRIANGULAR ELEMENT (CST)

III.1.1 Displacement and Strain Fields

This is the earliest example of a compatible two-dimensional displacement model, introduced by Turner, Clough, Martin and Topp [2].

The displacements u , v are linear functions of the coordinates. We select the 3 corners as nodal points, i.e., $(N_r) = (N_1)$ of Fig. 1.5; using the linear interpolation formula (I-26) we write

$$\begin{aligned} u(\xi_i) &= \langle \xi_1 \ \xi_2 \ \xi_3 \rangle \mathbf{u} = \xi_i^T \mathbf{u} \\ v(\xi_i) &= \langle \xi_1 \ \xi_2 \ \xi_3 \rangle \mathbf{v} = \xi_i^T \mathbf{v} \end{aligned} \quad (\text{III-1})$$

where

$$\mathbf{u}^T = \langle u_1 \ u_2 \ u_3 \rangle \quad \mathbf{v}^T = \langle v_1 \ v_2 \ v_3 \rangle$$

This element has six degrees of freedom. The strains are given by Equation (II-7):

$$\begin{aligned} \epsilon_x^T &= \xi_x^T \mathbf{u} = \frac{1}{2A} \langle b_1 \ b_2 \ b_3 \rangle \mathbf{u} \\ \epsilon_y^T &= \xi_y^T \mathbf{v} = \frac{1}{2A} \langle a_1 \ a_2 \ a_3 \rangle \mathbf{v} \\ \gamma_{xy}^T &= \xi_y^T \mathbf{u} + \xi_x^T \mathbf{v} = \frac{1}{2A} \langle a_1 \ a_2 \ a_3 \rangle \mathbf{u} + \frac{1}{2A} \langle b_1 \ b_2 \ b_3 \rangle \mathbf{v} \end{aligned}$$

Since the strains are constant, we can select as (N_ϵ) system any point of the triangle and Equation (II-21) reduces to

$$\boldsymbol{\epsilon} = \begin{Bmatrix} \epsilon_x \\ \epsilon_y \\ \gamma_{xy} \end{Bmatrix} = \frac{1}{2A} \begin{bmatrix} b_1 & b_2 & b_3 & \cdot & \cdot & \cdot \\ \cdot & \cdot & \cdot & a_1 & a_2 & a_3 \\ a_1 & a_2 & a_3 & b_1 & b_2 & b_3 \end{bmatrix} \begin{Bmatrix} \mathbf{u} \\ \mathbf{v} \end{Bmatrix} = \mathbf{B} \mathbf{r} \quad (\text{III-3})$$

III.1.2 Stiffness Matrix

The stress-strain law (II-10) is assumed constant inside the element:

$$\tilde{\sigma} \equiv \sigma = \tilde{C} \tilde{\epsilon} = C \epsilon \quad (\text{III-4})$$

The nodal point system (N_σ) \equiv (N_ϵ), i.e., any point of the triangle.

Therefore

$$\Lambda \equiv I \quad D = C_\sigma = C \quad (\text{III-5})$$

The shape function matrices reduce to $\Phi_\sigma \equiv \Phi_\epsilon \equiv I$ and Q is given by

$$Q = \int_A I \phi_h^T(\xi_i) h \, dA \quad (\text{III-6})$$

If the thickness h is constant, $\phi_h = 1$, $Q = AhI$ and the stiffness matrix is

$$K = \underset{(6 \times 6)}{B^T} Q D B = Ah \underset{(6 \times 6)}{B^T} C B =$$

$$= \frac{h}{4A} \begin{bmatrix} b_1 & \cdot & a_1 \\ b_2 & \cdot & a_2 \\ b_3 & \cdot & a_3 \\ \cdot & a_1 & b_1 \\ \cdot & a_2 & b_2 \\ \cdot & a_3 & b_3 \end{bmatrix} \begin{bmatrix} c_{11} & c_{12} & c_{13} \\ & c_{22} & c_{23} \\ \text{symm.} & & c_{33} \end{bmatrix} \begin{bmatrix} b_1 & b_2 & b_3 & \cdot & \cdot & \cdot \\ \cdot & \cdot & \cdot & a_1 & a_2 & a_3 \\ a_1 & a_2 & a_3 & b_1 & b_2 & b_3 \end{bmatrix} \quad (\text{III-7})$$

Since $2A = a_i b_j - a_j b_i$ is a homogeneous quadratic function of the dimensions a and b , the stiffness matrix is independent of the size of the element. This is valid for any PS stiffness matrix expressed solely in terms of in-plane nodal displacements (not gradients).

For any variation of thickness $h(\zeta_i)$, the stiffness matrix has the same form (III-7) if we replace h by its area average

$$h_m = \frac{1}{A} \int_A h(\zeta_i) dA \quad (\text{III-8})$$

III.1.3 Consistent Nodal Forces and Mass Matrix

It is easy to verify that the nodal loads $\mathbf{R} = \mathbf{K} \mathbf{r}$ are the static resultant of the internal stresses. Similarly, the kinematically equivalent nodal forces are simply the static resultant of the body or surface forces acting on the element. This property is a consequence of the linearity of the assumed displacement field and holds for any simplex element (Fig. 2.1).

For instance, a constant density ρ and thickness h gives three nodal loads equal to $\rho Ah/3$.

The consistent mass matrix for constant ρ and h follows from Equations (II-53), (II-54) and (II-56):

$$\mathbf{M}_1 = \rho h \int_A \boldsymbol{\psi} \boldsymbol{\psi}^T dA = \rho A h \mathbf{L}_{11} = \frac{1}{12} \rho A h \begin{bmatrix} 2 & 1 & 1 \\ 1 & 2 & 1 \\ 1 & 1 & 2 \end{bmatrix}$$

i.e.,

$$M = \frac{1}{12} \rho A h \begin{bmatrix} 2 & 1 & 1 & \cdot & \cdot & \cdot \\ 1 & 2 & 1 & \cdot & \cdot & \cdot \\ 1 & 1 & 2 & \cdot & \cdot & \cdot \\ \cdot & \cdot & \cdot & 2 & 1 & 1 \\ \cdot & \cdot & \cdot & 1 & 2 & 1 \\ \cdot & \cdot & \cdot & 1 & 1 & 2 \end{bmatrix} \quad (\text{III-9})$$

III.2 THE LINEARLY VARYING STRAIN TRIANGULAR ELEMENT (LST)

III.2.1 Motivation

The constant strain triangle of III.1 provides in general a reasonable displacement pattern, but the interpretation of element stresses is often difficult, especially in regions of high gradients. Different averaging procedures to obtain nodal point stresses have been proposed [17, 24], but the results are usually poor near boundaries, where extrapolation (not averaging) is required.

The linear strain triangle, proposed by De Veubeke [15], has been extensively tried and found to represent a significant improvement over CST meshes having similar or larger number of degrees of freedom; in particular, interface strain "jumps" are greatly reduced; nodal stresses obtained by simple averaging are extremely consistent and may be used with confidence.

III.2.2 Displacement Functions

In-plane displacements are assumed to be complete quadratic functions of the coordinates x, y . We select the nodal point system (N_2) of Fig. 1.6 for $u(x, y)$ and $v(x, y)$; i.e., three corners 1, 2, 3 plus the midpoints of the

sides 4,5,6. This element has then 12 kinematic degrees of freedom (Fig. 3.1).

Using the quadratic interpolation formula (I-27), we can write the components $u(\xi_i)$, $v(\xi_i)$ in triangular coordinates as follows:

$$\begin{aligned} u(\xi_i) &= \Phi_{(2)}^T(\xi_i) \mathbf{u} \\ v(\xi_i) &= \Phi_{(2)}^T(\xi_i) \mathbf{v} \end{aligned} \quad (\text{III-10})$$

where

$$\begin{aligned} \mathbf{u}^T &= \langle u_1 \ u_2 \ u_3 \ u_4 \ u_5 \ u_6 \rangle \\ \mathbf{v}^T &= \langle v_1 \ v_2 \ v_3 \ v_4 \ v_5 \ v_6 \rangle \\ \Phi_{(2)}^T &= \langle \xi_1(2\xi_1-1) \ \xi_2(2\xi_2-1) \ \xi_3(2\xi_3-1) \ 4\xi_1\xi_2 \ 4\xi_2\xi_3 \ 4\xi_3\xi_1 \rangle \end{aligned}$$

III.2.3 Strain-Displacement Relations

By differentiating the shape functions of (III-10) with respect to the global axes, we get the strain components:

$$\begin{aligned} \epsilon_x(\xi_i) &= \Phi_x^T \mathbf{u} \\ \epsilon_y(\xi_i) &= \Phi_y^T \mathbf{v} \\ \delta_{xy}(\xi_i) &= \Phi_y^T \mathbf{u} + \Phi_x^T \mathbf{v} \end{aligned} \quad (\text{III-11})$$

where

$$\Phi_x = \frac{\partial \Phi_{(2)}}{\partial x} = \frac{1}{2A} \begin{Bmatrix} (4\xi_1-1)b_1 \\ (4\xi_2-1)b_2 \\ (4\xi_3-1)b_3 \\ 4(\xi_2b_1 + \xi_1b_2) \\ 4(\xi_3b_2 + \xi_2b_3) \\ 4(\xi_1b_3 + \xi_3b_1) \end{Bmatrix} \quad \Phi_y = \frac{\partial \Phi_{(2)}}{\partial y} = \frac{1}{2A} \begin{Bmatrix} (4\xi_1-1)a_1 \\ (4\xi_2-1)a_2 \\ (4\xi_3-1)a_3 \\ 4(\xi_2a_1 + \xi_1a_2) \\ 4(\xi_3a_2 + \xi_2a_3) \\ 4(\xi_1a_3 + \xi_3a_1) \end{Bmatrix}$$

Since the strain components are linear functions of the coordinates, we select (N_1) as nodal strain system (Fig. 3.2). The nodal strain vector will be

$$\epsilon^T = \langle \epsilon_x^T \quad \epsilon_y^T \quad \delta_{xy}^T \rangle \quad (9 \times 1) \quad (\text{III-12})$$

with

$$\left. \begin{aligned} \epsilon_x^T &= \langle \epsilon_{x1} \quad \epsilon_{x2} \quad \epsilon_{x3} \rangle \\ \epsilon_y^T &= \langle \epsilon_{y1} \quad \epsilon_{y2} \quad \epsilon_{y3} \rangle \\ \delta_{xy}^T &= \langle \delta_{xy1} \quad \delta_{xy2} \quad \delta_{xy3} \rangle \end{aligned} \right\} \quad (3 \times 1 \text{ each})$$

Then the component variation is specified by linear interpolation

$$\epsilon_x(\zeta_{1r}) = \zeta_r^T \epsilon_x \quad \text{etc.} \quad (\text{III-13})$$

After evaluation of (III-11) at (N_ϵ) we obtain

$$\epsilon = \begin{Bmatrix} \epsilon_x \\ \epsilon_y \\ \delta_{xy} \end{Bmatrix} = \begin{bmatrix} U & \cdot \\ \cdot & V \\ V & U \end{bmatrix} \begin{Bmatrix} u \\ v \end{Bmatrix} = B r \quad (\text{III-14})$$

where U and V result from evaluation of ϕ_x and ϕ_y at the 3 corners:

$$U = \frac{1}{2A} \begin{bmatrix} 3b_1 & -b_2 & -b_3 & 4b_2 & \cdot & 4b_3 \\ -b_1 & 3b_2 & -b_3 & 4b_1 & 4b_3 & \cdot \\ -b_1 & -b_2 & 3b_3 & \cdot & 4b_2 & 4b_1 \end{bmatrix} \quad (\text{III-15})$$

$$V = \frac{1}{2A} \begin{bmatrix} 3a_1 & -a_2 & -a_3 & 4a_2 & \cdot & 4a_3 \\ -a_1 & 3a_2 & -a_3 & 4a_1 & 4a_3 & \cdot \\ -a_1 & -a_2 & 3a_3 & \cdot & 4a_2 & 4a_1 \end{bmatrix}$$

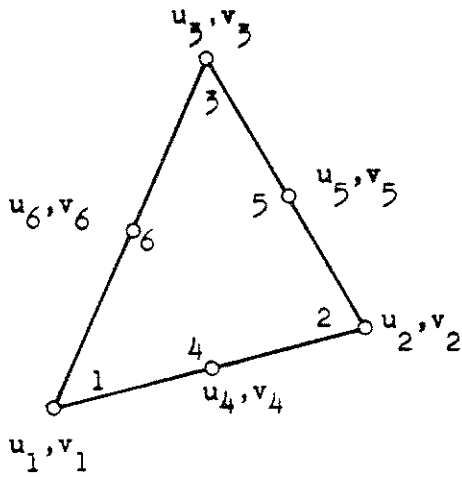


Fig. 3.1 - LST : Nodal System (N_r)
for displacements.

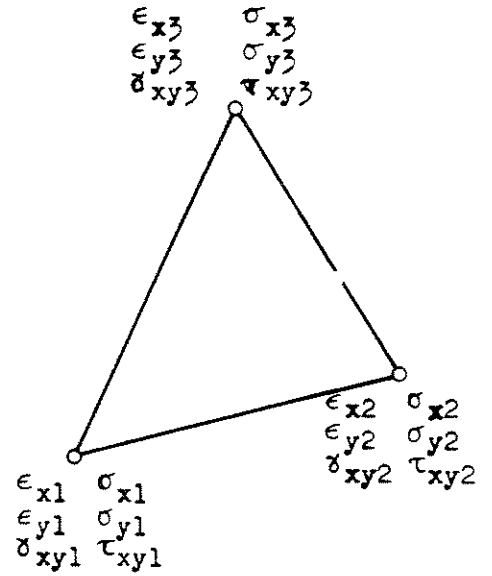


Fig. 3.2 - LST : Nodal Systems (N_ϵ)
and (N_σ) for strains and stresses.

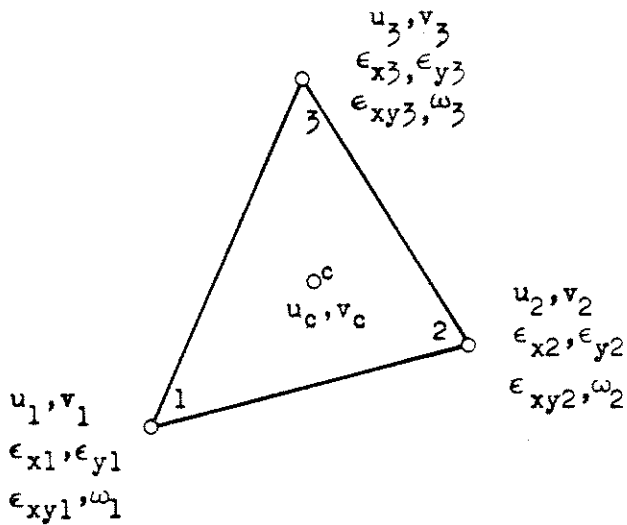


Fig. 3.3 - QST : Nodal System (N_r)
for displacements.

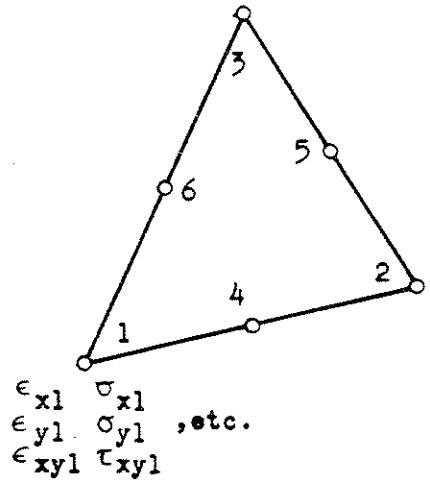


Fig. 3.4 - QST : Nodal Systems (N_ϵ)
and (N_σ) for strains and stresses.

The cyclic symmetry makes the automatic generation of \mathbf{U} and \mathbf{V} very simple.

III.2.4 Stress-Strain Law

As in III.2.2, the material is assumed to be homogeneous inside the element, i.e., the matrix $\tilde{\mathbf{C}}$ of Equation (II-10)

$$\tilde{\boldsymbol{\sigma}}(\xi_i) = \begin{Bmatrix} \sigma_x \\ \sigma_y \\ \tau_{xy} \end{Bmatrix} = \begin{bmatrix} c_{11} & c_{12} & c_{13} \\ & c_{22} & c_{23} \\ \text{symm.} & & c_{33} \end{bmatrix} \begin{Bmatrix} \epsilon_x \\ \epsilon_y \\ \gamma_{xy} \end{Bmatrix} = \mathbf{C} \tilde{\boldsymbol{\epsilon}}(\xi_i) \quad (\text{III-16})$$

does not depend on ξ_i . The stress components will also vary linearly and we select the same nodal system $(N_\sigma) = (N_\epsilon)$ of the strains (Fig. 3.2)

The nodal stress vector has the same structure of (III-12)

$$\boldsymbol{\sigma}^T = \langle \sigma_x^T \quad \sigma_y^T \quad \tau_{xy}^T \rangle \quad (\text{III-17})$$

with

$$\sigma_x^T = \langle \sigma_{x_1} \quad \sigma_{x_2} \quad \sigma_{x_3} \rangle, \text{ etc.}$$

The variation of the stress components is also given by linear interpolation formulas

$$\sigma_x(\xi_i) = \xi_i^T \sigma_x, \text{ etc} \quad (\text{III-18})$$

Since $(N_\sigma) \equiv (N_\epsilon)$ we have $\mathbf{A} = \mathbf{I}$ and the matrix \mathbf{D} is given by (II-33); it is a (9 x 9) matrix integrated by nine (3 x 3) blocks

$$\mathbf{D} = \begin{bmatrix} c_{11} \mathbf{I} & c_{12} \mathbf{I} & c_{13} \mathbf{I} \\ & c_{22} \mathbf{I} & c_{23} \mathbf{I} \\ \text{symm.} & & c_{33} \mathbf{I} \end{bmatrix} \quad (\text{III-19})$$

with

$$\mathbf{I} = \begin{bmatrix} 1 & \cdot & \cdot \\ \cdot & 1 & \cdot \\ \cdot & \cdot & 1 \end{bmatrix}$$

III.2.5 Strain Energy Integration

The interpolation matrices for stresses and strains, according to Equations (III-18) and (III-13) are

$$\Phi_\epsilon = \Phi_\sigma = \begin{bmatrix} \psi_1 & \cdot & \cdot \\ \cdot & \psi_2 & \cdot \\ \cdot & \cdot & \psi_3 \end{bmatrix} \quad (9 \times 3) \quad (\text{III-20})$$

As in (II-35) we define a reference thickness h_r and the relative dimensionless thickness

$$\xi(\psi_i) = h(\psi_i)/h_r \quad (\text{III-21})$$

the corresponding nodal vector and interpolation formula being $\xi = h_r^{-1} \mathbf{h}$ and $\phi_\xi \equiv \phi_h$ respectively. Then we use (II-37) and write \mathbf{Q} as

$$\mathbf{Q} = A h_r \begin{bmatrix} \bar{Q} & \cdot & \cdot \\ \cdot & \bar{Q} & \cdot \\ \cdot & \cdot & \bar{Q} \end{bmatrix} \quad (\text{III-22})$$

with

$$\bar{Q} = \frac{1}{A} \int_A \psi \phi_\xi^T \xi \psi^T dA \quad (\text{III-23})$$

(a) For constant thickness $h = h_r$ we have $\phi_\xi = 1$ and

$$\bar{Q} = \frac{1}{A} \int_A \psi \psi^T dA = \mathbf{L}_{11} = \frac{1}{12} \begin{bmatrix} 2 & 1 & 1 \\ 1 & 2 & 1 \\ 1 & 1 & 2 \end{bmatrix} \quad (\text{III-24})$$

or

$$\mathbf{Q} = \frac{Ah}{12} \begin{bmatrix} 2 & 1 & 1 & \cdot & \cdot & \cdot & \cdot & \cdot & \cdot \\ 1 & 2 & 1 & \cdot & \cdot & \cdot & \cdot & \cdot & \cdot \\ 1 & 1 & 2 & \cdot & \cdot & \cdot & \cdot & \cdot & \cdot \\ \cdot & \cdot & \cdot & 2 & 1 & 1 & \cdot & \cdot & \cdot \\ \cdot & \cdot & \cdot & 1 & 2 & 1 & \cdot & \cdot & \cdot \\ \cdot & \cdot & \cdot & 1 & 1 & 2 & \cdot & \cdot & \cdot \\ \cdot & \cdot & \cdot & \cdot & \cdot & \cdot & 2 & 1 & 1 \\ \cdot & \cdot & \cdot & \cdot & \cdot & \cdot & 1 & 2 & 1 \\ \cdot & \cdot & \cdot & \cdot & \cdot & \cdot & 1 & 1 & 2 \end{bmatrix}$$

(b) For plane stress element with linearly varying thickness, we take $(N_h) = (N_\xi) = (N_1)$, $\phi_\xi = \psi$:

$$\bar{\mathbf{Q}} = \frac{1}{A} \int_A \psi \psi^T \xi \psi^T dA$$

Using Table 3 we get immediately:

$$\bar{\mathbf{Q}} = \frac{1}{60} \begin{bmatrix} 6\xi_1 + 3\xi_2 + 3\xi_3 & 3\xi_1 + 3\xi_2 + \xi_3 & 3\xi_1 + \xi_2 + 3\xi_3 \\ & 3\xi_1 + 6\xi_2 + 3\xi_3 & \xi_1 + 3\xi_2 + 3\xi_3 \\ \text{symm.} & & 3\xi_1 + 3\xi_2 + 6\xi_3 \end{bmatrix} \quad (\text{III-25})$$

(c) For plane stress element with parabolically varying thickness, we take $(N_h) = (N_\xi) = (N_2)$, $\phi_\xi \equiv \phi_{(2)}$:

$$\bar{\mathbf{Q}} = \frac{1}{A} \int_A \psi \phi_{(2)} \xi \psi^T dA$$

and again using Table 3 we get

$$\bar{\mathbf{Q}} = \frac{1}{180} \begin{bmatrix} q_{11} & q_{12} & q_{13} \\ & q_{22} & q_{23} \\ \text{symm.} & & q_{33} \end{bmatrix} \quad (\text{III-26})$$

with

$$\begin{aligned}
 q_{11} &= 6 \xi_1 - 2 \xi_2 - 2 \xi_3 + 12 \xi_4 + 4 \xi_5 + 12 \xi_6 \\
 q_{22} &= -2 \xi_1 + 6 \xi_2 - 2 \xi_3 + 12 \xi_4 + 12 \xi_5 + 4 \xi_6 \\
 q_{33} &= -2 \xi_1 - 2 \xi_2 + 6 \xi_3 + 4 \xi_4 + 12 \xi_5 + 12 \xi_6 \\
 q_{12} &= - \xi_3 + 8 \xi_4 + 4 \xi_5 + 4 \xi_6 \\
 q_{23} &= -\xi_1 + 4 \xi_4 + 8 \xi_5 + 4 \xi_6 \\
 q_{31} &= - \xi_2 + 4 \xi_4 + 4 \xi_5 + 8 \xi_6
 \end{aligned}$$

It should be noticed that only 8 different integrals are needed to form q_{11} and q_{12} and the rest follows from cyclic permutations of the indices 1-2-3 and 4-5-6.

III.2.6 Stiffness Matrix

The (12x12) stiffness matrix is given, according to (II-29) by

$$K = B^T Q D B = B^T N B \quad (\text{III-27})$$

with

$$\begin{aligned}
 N = Q D &= A h_r \begin{bmatrix} \bar{Q} & \cdot & \cdot \\ \cdot & \bar{Q} & \cdot \\ \cdot & \cdot & \bar{Q} \end{bmatrix} \begin{bmatrix} C_{11} & C_{12} & C_{13} \\ & C_{22} & C_{23} \\ \text{symm.} & & C_{33} \end{bmatrix} \\
 &= A h_r \begin{bmatrix} N_{11} & N_{12} & N_{13} \\ & N_{22} & N_{23} \\ \text{symm.} & & N_{33} \end{bmatrix}
 \end{aligned}$$

where

$$N_{ij} = \bar{Q} C_{ij} = \bar{Q} c_{ij} I = c_{ij} \bar{Q}$$

Using (III-14) we write K in the partitioned form:

$$K = A h_r \begin{bmatrix} \mathbf{U}^T & \cdot & \mathbf{V}^T \\ \cdot & \mathbf{V}^T & \mathbf{U}^T \end{bmatrix} \begin{bmatrix} c_{11} \bar{Q} & c_{12} \bar{Q} & c_{13} \bar{Q} \\ & c_{22} \bar{Q} & c_{23} \bar{Q} \\ \text{symm.} & & c_{33} \bar{Q} \end{bmatrix} \begin{bmatrix} \mathbf{U} & \cdot \\ \cdot & \mathbf{V} \\ \mathbf{V} & \mathbf{U} \end{bmatrix} \quad (\text{III-28})$$

$$= \begin{bmatrix} K_{uu} & K_{uv} \\ K_{vu} & K_{vv} \end{bmatrix}$$

For the case of constant thickness h , this expression is given in detailed form on next page (upon using Equations (III-15) and (III-24)).

If we define the (6x6) matrices

$$M_{uu} = \mathbf{U}^T \bar{Q} \mathbf{U} \quad M_{uv} = \mathbf{U}^T \bar{Q} \mathbf{V} = M_{vu}^T \quad M_{vv} = \mathbf{V}^T \bar{Q} \mathbf{V}$$

then the (6x6) blocks of (III-28) can be expressed as

$$\begin{aligned} K_{uu} &= A h_r [c_{11} M_{uu} + c_{13} (M_{uv} + M_{vu}) + c_{33} M_{vv}] \\ K_{uv} &= A h_r [c_{12} M_{uv} + c_{13} M_{uu} + c_{23} M_{vv} + c_{33} M_{vu}] = K_{vu}^T \\ K_{vv} &= A h_r [c_{22} M_{vv} + c_{23} (M_{uv} + M_{vu}) + c_{33} M_{uu}] \end{aligned} \quad (\text{III-30})$$

For isotropic material (II.2.4.1):

$$\begin{aligned} c_{11} = c_{22} &= \kappa E_r & c_{12} &= \nu E_r & c_{33} &= \lambda E_r \\ c_{13} = c_{23} &= 0 \end{aligned}$$

Closed form expressions for each k_{ij} may be easily obtained; however the best way of assembling \mathbf{K} in the computer program is in the form (III-28) taking account of the zero blocks. To simplify the assembly of the complete stiffness matrix and the solution coding, the vector of nodal displacements is rearranged so as to have the two components (u,v) at each node together:

$$\begin{aligned} \mathbf{r}^T &= \langle \mathbf{r}_1^T \mathbf{r}_2^T \mathbf{r}_3^T \mathbf{r}_4^T \mathbf{r}_5^T \mathbf{r}_6^T \rangle \\ &= \langle u_1 \ v_1 \ u_2 \ v_2 \ u_3 \ v_3 \ u_4 \ v_4 \ u_5 \ v_5 \ u_6 \ v_6 \rangle \end{aligned}$$

This is achieved simply by addressing the products which originally corresponded to rows and columns number 1,2,3,...,12 to rows and columns 1,3,5,7,9,11,2,4,6,8,10,12 respectively. Then the stiffness matrix can be partitioned into thirty-six (2x2) blocks which are called "point stiffness submatrices." More details are given in the description of the computer program.

III.2.7 Kinematically Equivalent Force Vectors

III.2.7.1 Surface Loading

To fix the ideas, we assume that a general distributed in-plane load $\tilde{\mathbf{p}}(\zeta_B)$, already integrated through the boundary thickness, acts on the side 3 of the element.

We derive the formulas for the component $p_x(\zeta_B)$ which is given by the interpolation expression (II-41)

$$p_x(\zeta_B) = \Phi_F^T p_x \quad (\text{III-31})$$

The vector u_B of Equation (II-42) is $\langle u_1 \quad u_4 \quad u_2 \rangle$ which specifies the displacement of the side 3 by the interpolation formula

$$u(\xi_1) = \langle \xi_1(2\xi_1-1) \quad 4\xi_1(1-\xi_1) \quad (1-\xi_1)(1-2\xi_1) \rangle \begin{Bmatrix} u_1 \\ u_4 \\ u_2 \end{Bmatrix} = \Phi_B^T u_B \quad (\text{III-32})$$

obtained extracting ϕ_1, ϕ_4 and ϕ_2 from $\Phi_{(2)}$ and setting $\xi_3 = 0$ and $\xi_2 = 1 - \xi_1$.

Applying Equations (II-46) and (II-45) we get for the generalized nodal forces

$$\begin{aligned} R_{x_1} &= p_x^T l_3 \int_0^1 \Phi_p(\xi_1) \xi_1 (2\xi_1 - 1) d\xi_1 \\ R_{x_4} &= p_x^T l_3 \int_0^1 \Phi_p(\xi_1) \xi_1 (1 - \xi_1) d\xi_1 \\ R_{x_2} &= p_x^T l_3 \int_0^1 \Phi_p(\xi_1) (1 - \xi_1) (1 - 2\xi_1) d\xi_1 \end{aligned} \quad (\text{III-33})$$

We obtain similar expression for the R_y forces by replacing x by y in Equations (III-33). Expressions for the other two sides follow by cyclically permuting the indices 1-2-3 and 4-5-6.

Examples:

(a) Linear variation of p_x , defined by p_{x1} and p_{x2} :

$$p_x(\xi_1) = \langle \xi_1 \quad 1 - \xi_1 \rangle \begin{Bmatrix} p_{x1} \\ p_{x2} \end{Bmatrix} = \Phi_p^T p_x$$

Replacing into (III-33) we get

$$\begin{Bmatrix} R_{x_1} \\ R_{x_4} \\ R_{x_2} \end{Bmatrix} = \frac{l_3}{6} \begin{bmatrix} 1 & 0 \\ 2 & 2 \\ 0 & 1 \end{bmatrix} \begin{Bmatrix} p_{x1} \\ p_{x2} \end{Bmatrix} \quad (\text{III-34})$$

If $p_x = p = \text{constant}$, we find

$$R_{x_1} = R_{x_2} = p l_3 / 6 \quad R_{x_4} = 4 R_{x_1}$$

i.e., the midpoint force is 4 times the corner forces the coefficients are the same as in Simpson's rule of integration.

(b) Parabolic variation of p_x , defined by

$$p_x^T = \langle p_{x_1} \quad p_{x_4} \quad p_{x_2} \rangle$$

Then $\Phi_p \equiv \Phi_B$ of (III-32) and we get

$$\begin{Bmatrix} R_{x_1} \\ R_{x_4} \\ R_{x_2} \end{Bmatrix} = \frac{l_3}{30} \begin{bmatrix} 4 & 2 & -1 \\ 2 & 16 & 2 \\ -1 & 2 & 4 \end{bmatrix} \begin{Bmatrix} p_{x_1} \\ p_{x_4} \\ p_{x_2} \end{Bmatrix} \quad \text{(III-35)}$$

III.2.7.2 Gravity Forces

We assume that they act along the $-y$ axis and that the density ρ is constant over the element; the body force components are

$$f_x = 0 \quad f_y = -\rho$$

then (II-48), with $\Phi_f = 1$, $f_x = 0$ and $f_y = -\rho$ (scalar), gives

$$\begin{aligned} R_{f_x}^T &= 0 \\ R_{f_y}^T &= A h_r F \end{aligned} \quad \text{(III-36)}$$

with

$$F = \xi^T \int_A \Phi_\xi \Phi_{(z)} dA$$

(a) For a parabolic variation of thickness, we select $(N_h) \equiv (N_\xi) \equiv (N_2)$, i.e.,

$$\Phi_\xi = \Phi_{(z)} \quad \xi^T = \langle \xi_1 \quad \xi_2 \quad \xi_3 \quad \xi_4 \quad \xi_5 \quad \xi_6 \rangle$$

therefore

$$\mathbf{F} = \boldsymbol{\xi}^T \int_A \boldsymbol{\phi}_{(2)} \boldsymbol{\phi}_{(2)}^T dA = \boldsymbol{\xi}^T \mathbf{L}_{22}$$

$$\mathbf{R}_y^T = -\boldsymbol{\xi}^T \frac{A h r \rho}{180} \begin{bmatrix} 6 & -1 & -1 & 0 & -4 & 0 \\ -1 & 6 & -1 & 0 & 0 & -4 \\ -1 & -1 & 6 & -4 & 0 & 0 \\ 0 & 0 & -4 & 32 & 16 & 16 \\ -4 & 0 & 0 & 16 & 32 & 16 \\ 0 & -4 & 0 & 16 & 16 & 32 \end{bmatrix} \quad (\text{III-37})$$

(b) For linearly varying thickness $(N_h) \equiv (N_\xi) \equiv (N_1)$, i.e.,

$$\boldsymbol{\phi}_\xi = \boldsymbol{\zeta} \quad \boldsymbol{\xi}^T = \langle \xi_1 \quad \xi_2 \quad \xi_3 \rangle$$

$$\mathbf{F} = \boldsymbol{\xi}^T \int_A \boldsymbol{\zeta} \boldsymbol{\phi}_{(2)} dA = \boldsymbol{\xi}^T \mathbf{L}_{12}$$

$$\mathbf{R}_y^T = -\boldsymbol{\xi}^T \frac{A h r \rho}{60} \begin{bmatrix} 2 & -1 & -1 & 8 & 4 & 8 \\ -1 & 2 & -1 & 4 & 8 & 8 \\ -1 & -1 & 2 & 8 & 8 & 4 \end{bmatrix} \quad (\text{III-38})$$

(c) Finally, if $h = \text{constant}$

$$\mathbf{R}_y^T = -\rho A h \mathbf{L}_2 = -\rho A h \frac{1}{3} \langle 0 \ 0 \ 0 \ 1 \ 1 \ 1 \rangle \quad (\text{III-39})$$

i.e., three equal loads on the midpoints.

III.2.8 Consistent Mass Matrix

For constant density ρ and thickness, we get from (II-56)

$$\begin{aligned} \mathbf{M}_1 &= \rho h \int_A \boldsymbol{\Phi}_{(2)} \boldsymbol{\Phi}_{(2)}^T dA = \rho Ah \mathbf{L}_{22} \\ &= \frac{\rho Ah}{180} \begin{bmatrix} 6 & -1 & -1 & 0 & -4 & 0 \\ -1 & 6 & -1 & 0 & 0 & -4 \\ -1 & -1 & 6 & -4 & 0 & 0 \\ 0 & 0 & -4 & 32 & 16 & 16 \\ -4 & 0 & 0 & 16 & 32 & 16 \\ 0 & -4 & 0 & 16 & 16 & 32 \end{bmatrix} \end{aligned} \quad (\text{III-40})$$

and

$$\mathbf{M} = \begin{bmatrix} \mathbf{M}_1 & \cdot \\ \cdot & \mathbf{M}_1 \end{bmatrix}$$

We see that most of the mass is taken by the midpoints and that the coupling between them is similar to the corner mass coupling of the CST (III-9).

III.2.9 Restraint Thermal Forces

The temperature field $\theta(\xi_i)$ is assumed to be linear and defined by the 3 corner temperatures $\boldsymbol{\theta}^T = \langle \theta_1 \ \theta_2 \ \theta_3 \rangle$ so that

$$\theta(\xi_i) = \boldsymbol{\xi}^T \boldsymbol{\theta}$$

The material is assumed to be elastically and thermally isotropic, and homogeneous inside the element. The initial stress field (II-57) is then linear and given by (II-66)

$$\boldsymbol{\sigma}_x^* = \boldsymbol{\sigma}_y^* = \frac{E\alpha}{\rho} \boldsymbol{\theta} \quad \boldsymbol{\tau}_{xy}^* = \mathbf{0} \quad (\text{III-41})$$

where

$$\mu = \begin{cases} 1-\nu \\ 1-2\nu \end{cases} \text{ for plane } \begin{cases} \text{stress} \\ \text{strain} \end{cases}$$

The restraint nodal forces (initial loads) are given by (II-67); since the variation of temperature is the same as that of the elastic stresses, $\bar{Q}^* = \bar{Q}$ and

$$\begin{aligned} \mathbf{s}_x^* &= \frac{EA\alpha h_r}{\mu} \mathbf{U}^T \bar{Q} \boldsymbol{\theta} \\ \mathbf{s}_y^* &= \frac{EA\alpha h_r}{\mu} \mathbf{V}^T \bar{Q} \boldsymbol{\theta} \end{aligned} \quad (\text{III-42})$$

Replacing \mathbf{U} and \mathbf{V} by their expressions (III-15) and \bar{Q} by (III-24) we get for a constant thickness h :

$$\mathbf{s}_x^* = \frac{E\alpha h_r}{6\mu} \left\{ \begin{array}{l} b_1 \theta_1 \\ b_2 \theta_2 \\ b_3 \theta_3 \\ (2b_2 + b_1) \theta_1 + (b_2 + 2b_1) \theta_2 + (b_2 + b_1) \theta_3 \\ (b_3 + b_2) \theta_1 + (2b_3 + b_2) \theta_2 + (b_3 + 2b_2) \theta_3 \\ (b_1 + 2b_3) \theta_1 + (b_1 + b_3) \theta_2 + (2b_1 + b_3) \theta_3 \end{array} \right\} \quad (\text{III-43})$$

and similarly for \mathbf{s}_y^* replacing b_i 's for a_i 's.

III.3 THE QUADRATICALLY VARYING STRAIN TRIANGULAR ELEMENT (QST)

III.3.1 Displacement Functions

The in-plane displacement components are selected to be complete cubic polynomial functions of x, y ; we have then 20 degrees of freedom, 10 per component. We have seen in I.4.2 that it is impossible to specify uniquely a complete cubic polynomial from its boundary values because of the presence of the mode $\psi_1 \psi_2 \psi_3$ which vanishes on the sides. Hence there must be two additional modes, one per component.

We select the nodal system (N_3) of Fig. 1.9 for the displacements; it consists of the three corners 1,2,3 plus the centroid o (Fig. 3.3). The corresponding nodal displacements are naturally classified into two categories:

(a) 18 fundamental degrees of freedom: displacements and their global derivatives at the corners; these values specify boundary displacements uniquely:

(b) 2 additional degrees of freedom: centroid displacements, to be eliminated later by condensation.

The nodal displacement vector $\bar{\mathbf{r}}$ is arranged as follows:

$$\bar{\mathbf{r}} = \langle \bar{\mathbf{u}}^T \quad \bar{\mathbf{v}}^T \rangle \quad (\text{III-45})$$

$$\bar{\mathbf{u}}^T = \langle u_1 \quad u_{x_1} \quad u_{y_1} \quad u_2 \quad u_{x_2} \quad u_{y_2} \quad u_3 \quad u_{x_3} \quad u_{y_3} \quad u_0 \rangle$$

$$\bar{\mathbf{v}}^T = \langle v_1 \quad v_{x_1} \quad v_{y_1} \quad v_2 \quad v_{x_2} \quad v_{y_2} \quad v_3 \quad v_{x_3} \quad v_{y_3} \quad v_0 \rangle$$

(III-45a)

The bar on top is used to differentiate $\bar{\Gamma}$ from the final displacement vector Γ which has only 18 components and combinations of the cross derivatives.

Using the cubic interpolation formula $\Phi_{(3)}$ given by (I-31) we express u and v in triangular coordinates as

$$\begin{aligned} u(\xi_i) &= \Phi_{(3)}^T u \\ v(\xi_i) &= \Phi_{(3)}^T v \end{aligned} \quad (\text{III-46})$$

This displacement field satisfies all requirements listed in II.1.2. Moreover, since the polynomial is complete, it is the best single cubic displacement field for a slice triangular element.

Recently, Tocher and Hartz [40] have developed a third order plane stress element by using the cubic expansion of the 9-degree-of-freedom compatible triangular plate element [23] for both in-plane components. This element has the same 18 degrees of freedom of the QST and complete continuity of displacement gradients along the sides (the variation of $\partial u/\partial n$ and $\partial v/\partial n$ is constrained to be linear). This additional compatibility is not necessary for plane stress elements; besides of complicating the derivation, it stiffens the element by restraining its polynomial expansion.

III.3.2 Strain-Displacement Relations

To obtain the interpolation vectors Φ_x and Φ_y of Equation (II-7) we differentiate $\Phi_{(3)}$ with respect to the global axes.

$$\text{Let } \begin{cases} H_a = 2A \frac{\partial(\xi_1 \xi_2 \xi_3)}{\partial x} = \xi_1 \xi_2 b_3 + \xi_2 \xi_3 b_1 + \xi_3 \xi_1 b_2 \\ H_b = 2A \frac{\partial(\xi_1 \xi_2 \xi_3)}{\partial y} = \xi_1 \xi_2 a_3 + \xi_2 \xi_3 a_1 + \xi_3 \xi_1 a_2 \end{cases}$$

Then

$$\Phi_x = \frac{1}{2A} \left\{ \begin{array}{l} 6\zeta_1(1-\zeta_1)b_1 - 7Hb \\ 2\zeta_1 b_1(a_3\zeta_2 - a_2\zeta_3) + 2\zeta_1^2 A + (a_3 - a_2)Hb \\ 2\zeta_1 b_1(b_2\zeta_3 - b_3\zeta_2) + (b_3 - b_2)Hb \\ 6\zeta_2(1-\zeta_2)b_2 - 7Hb \\ 2\zeta_2 b_2(a_1\zeta_3 - a_3\zeta_1) + 2\zeta_2^2 A + (a_1 - a_3)Hb \\ 2\zeta_2 b_2(b_3\zeta_1 - b_1\zeta_3) + (b_1 - b_3)Hb \\ 6\zeta_3(1-\zeta_3)b_3 - 7Hb \\ 2\zeta_3 b_3(a_2\zeta_1 - a_1\zeta_2) + 2\zeta_3^2 A + (a_1 - a_2)Hb \\ 2\zeta_3 b_3(b_1\zeta_2 - b_2\zeta_1) + (b_2 - b_1)Hb \\ 27Hb \end{array} \right.$$

(III-47)

$$\Phi_y = \frac{1}{2A} \left\{ \begin{array}{l} 6\zeta_1(1-\zeta_1)a_1 - 7Ha \\ 2\zeta_1 a_1(a_3\zeta_2 - a_2\zeta_3) + (a_2 - a_3)Ha \\ 2\zeta_1 a_1(b_2\zeta_3 - b_3\zeta_2) + 2\zeta_1^2 A + (b_3 - b_2)Ha \\ 6\zeta_2(1-\zeta_2)a_2 - 7Ha \\ 2\zeta_2 a_2(a_1\zeta_3 - a_3\zeta_1) + (a_3 - a_1)Ha \\ 2\zeta_2 a_2(b_3\zeta_1 - b_1\zeta_3) + 2\zeta_2^2 A + (b_1 - b_3)Ha \\ 6\zeta_3(1-\zeta_3)a_3 - 7Ha \\ 2\zeta_3 a_3(a_2\zeta_1 - a_1\zeta_2) + (a_1 - a_2)Ha \\ 2\zeta_3 a_3(b_1\zeta_2 - b_2\zeta_1) + 2\zeta_3^2 A + (b_2 - b_1)Ha \\ 27Ha \end{array} \right.$$

Since the variation of the strain components is quadratic, we naturally select the nodal strain system $(N_\epsilon) = (N_2)$, i.e., corners 1,2,3 and mid-points 4,5,6 (Fig. 3.4). The nodal strain vector is arranged as usual

$$\epsilon^T = \langle \epsilon_x^T \quad \epsilon_y^T \quad \gamma_{xy}^T \rangle \quad (\text{III-48})$$

where

$$\epsilon_x^T = \langle \epsilon_{x_1} \quad \epsilon_{x_2} \quad \epsilon_{x_3} \quad \epsilon_{x_4} \quad \epsilon_{x_5} \quad \epsilon_{x_6} \rangle$$

Evaluating ϕ_x and ϕ_y at (N_2) we obtain the (6x10) submatrices **U** and **V** of (II-21) relating

$$\epsilon = \begin{Bmatrix} \epsilon_x \\ \epsilon_y \\ \gamma_{xy} \end{Bmatrix} = \begin{bmatrix} \mathbf{U} & \mathbf{V} \\ \mathbf{V} & \mathbf{U} \end{bmatrix} \begin{Bmatrix} \bar{u} \\ \bar{v} \end{Bmatrix} = \mathbf{B} \mathbf{r} \quad (\text{III-49})$$

U and **V** are given on next page. We see that the corner strains are directly given by the selected generalized nodal displacements and will be identical for all adjacent elements. Because of their quadratic variation, they will not, in general, match along the sides (except at the corners).

III.3.3 Strain Energy Integration

The constitutive law **C** is assumed constant inside the element. The stress components variation is also quadratic and we select $(N_\sigma) = (N_\epsilon) = (N_2)$. the stress vector σ has the same structure of the nodal strain vector (III-48).

The interpolation vectors for strains and stresses are $\phi_\epsilon = \phi_\sigma = \phi_{(2)}$; assuming also a constant thickness we get from Equation (II-39)

$$\begin{aligned}
& \frac{1}{8A} \begin{bmatrix} \cdot & 8A & \cdot & \cdot & \cdot & \cdot & \cdot & \cdot & \cdot & \cdot \\ \cdot & \cdot & \cdot & 8A & \cdot & \cdot & \cdot & \cdot & \cdot & \cdot \\ \cdot & \cdot & \cdot & \cdot & \cdot & 8A & \cdot & \cdot & \cdot & \cdot \\ 6b_1-7b_3 & (b_1-2b_3)a_3 & (2b_3-b_1)b_3 & 6b_2-7b_3 & (2b_3-b_2)a_3 & (b_2-2b_3)b_3 & -7b_3 & (a_1-a_2)b_3 & (b_2-b_1)b_3 & 27b_3 \\ -7b_1 & (a_2-a_3)b_1 & (b_3-b_2)b_1 & 6b_2-7b_1 & (b_2-2b_1)a_1 & (2b_1-b_2)b_1 & 6b_3-7b_1 & (2b_1-b_3)a_1 & (b_3-2b_1)b_1 & 27b_1 \\ 6b_1-7b_2 & (2b_2-b_1)a_2 & (b_1-2b_2)b_2 & -7b_2 & (a_3-a_1)b_2 & (b_1-b_3)b_2 & 6b_3-7b_2 & (b_3-2b_2)a_2 & (2b_2-b_3)b_2 & 27b_2 \end{bmatrix} \\
& \frac{1}{8A} \begin{bmatrix} \cdot & \cdot & \cdot & \cdot & \cdot & \cdot & \cdot & \cdot & \cdot & \cdot \\ \cdot & \cdot & \cdot & \cdot & \cdot & \cdot & \cdot & \cdot & \cdot & \cdot \\ \cdot & \cdot & \cdot & \cdot & \cdot & \cdot & \cdot & \cdot & \cdot & \cdot \\ 6a_1-7a_3 & (a_1-2a_3)a_3 & (2a_3-a_1)b_3 & 6a_2-7a_3 & (2a_3-a_2)a_3 & (a_2-2a_3)b_3 & -7a_3 & (a_1-a_2)a_3 & (b_2-b_1)a_3 & 27a_3 \\ -7a_1 & (a_2-a_3)a_1 & (b_3-b_2)a_1 & 6a_2-7a_1 & (a_2-2a_1)a_1 & (2a_1-a_2)b_1 & 6a_3-7a_1 & (2a_1-a_3)a_1 & (a_3-2a_1)b_1 & 27a_1 \\ 6a_1-7a_2 & (2a_2-a_1)a_2 & (a_1-2a_2)b_2 & -7a_2 & (a_3-a_1)a_2 & (b_1-b_3)a_2 & 6a_3-7a_1 & (a_3-2a_2)a_2 & (2a_2-a_3)b_2 & 27a_2 \end{bmatrix}
\end{aligned}$$

(III-50)

$$\begin{aligned}
& \frac{1}{8A} \begin{bmatrix} \cdot & \cdot & \cdot & \cdot & \cdot & \cdot & \cdot & \cdot & \cdot & \cdot \\ \cdot & \cdot & \cdot & \cdot & \cdot & \cdot & \cdot & \cdot & \cdot & \cdot \\ \cdot & \cdot & \cdot & \cdot & \cdot & \cdot & \cdot & \cdot & \cdot & \cdot \\ 6a_1-7a_3 & (a_1-2a_3)a_3 & (2a_3-a_1)b_3 & 6a_2-7a_3 & (2a_3-a_2)a_3 & (a_2-2a_3)b_3 & -7a_3 & (a_1-a_2)a_3 & (b_2-b_1)a_3 & 27a_3 \\ -7a_1 & (a_2-a_3)a_1 & (b_3-b_2)a_1 & 6a_2-7a_1 & (a_2-2a_1)a_1 & (2a_1-a_2)b_1 & 6a_3-7a_1 & (2a_1-a_3)a_1 & (a_3-2a_1)b_1 & 27a_1 \\ 6a_1-7a_2 & (2a_2-a_1)a_2 & (a_1-2a_2)b_2 & -7a_2 & (a_3-a_1)a_2 & (b_1-b_3)a_2 & 6a_3-7a_1 & (a_3-2a_2)a_2 & (2a_2-a_3)b_2 & 27a_2 \end{bmatrix}
\end{aligned}$$

$$\bar{Q} = \frac{1}{A} \int_A \phi_{(2)} \phi_{(2)}^T dA = L_{22} = \frac{1}{180} \begin{bmatrix} 6 & -1 & -1 & 0 & -4 & 0 \\ & 6 & -1 & 0 & 0 & -4 \\ & & 6 & -4 & 0 & 0 \\ & & & 32 & 16 & 16 \\ \text{symm.} & & & & 32 & 16 \\ & & & & & 32 \end{bmatrix} \quad (\text{III-51})$$

and $N = Q D = Q C$ is given by Equation (II-40):

$$N = Ah \begin{bmatrix} c_{11} \bar{Q} & c_{12} \bar{Q} & c_{13} \bar{Q} \\ & c_{22} \bar{Q} & c_{23} \bar{Q} \\ \text{symm.} & & c_{33} \bar{Q} \end{bmatrix} \quad (\text{III-52})$$

III.3.4 Stiffness Matrix

The (20x20) stiffness matrix \bar{K} associated with \bar{F} follows from Equation (II-29)

$$\begin{aligned} K &= Ah \begin{bmatrix} U^T & \cdot & V^T \\ \cdot & V^T & U^T \end{bmatrix} \begin{bmatrix} c_{11} \bar{Q} & c_{12} \bar{Q} & c_{13} \bar{Q} \\ & c_{22} \bar{Q} & c_{23} \bar{Q} \\ \text{symm.} & & c_{33} \bar{Q} \end{bmatrix} \begin{bmatrix} U & \cdot \\ \cdot & V \\ V & U \end{bmatrix} \\ &\quad (20 \times 18) \qquad (18 \times 18) \qquad (18 \times 20) \\ &= \begin{bmatrix} K_{uu} & | & K_{uv} \\ \hline K_{uv}^T & | & K_{vv} \end{bmatrix} \\ &\quad (20 \times 20) \end{aligned} \quad (\text{III-53})$$

These four (10x10) blocks may be expanded as in Equations (III-30).

Now we modify the structure of the nodal displacement vector as follows:

(a) Cross derivatives of u and v are combined to form

$$(v_x + u_x)/2 : \text{ shear strain component } \epsilon_{xy} = \frac{1}{2} \gamma_{xy}$$

$$(v_x - u_x)/2 : \text{ average in-plane rotation } \omega_{xy} = \omega$$

These two quantities have now a direct physical meaning in the small displacement theory.

(b) Move the centroid displacements u_0 and v_0 to the bottom of the vector to facilitate their elimination.

The complete new arrangement is denoted by \mathbf{r}^* :

$$\mathbf{r}^* = \langle \mathbf{r}_1^T; \mathbf{r}_0^T \rangle = \langle \mathbf{r}_1^T; \mathbf{r}_2^T; \mathbf{r}_3^T; \mathbf{r}_0^T \rangle \quad (\text{III-54})$$

where

$$\left\{ \begin{array}{l} \mathbf{r}_1^T = \langle u_1, v_1, \epsilon_{x1}, \epsilon_{y1}, \epsilon_{xy1}, \omega_1 \rangle \\ \mathbf{r}_0^T = \langle u_0, v_0 \rangle \\ \text{(similarly for } \mathbf{r}_2 \text{ and } \mathbf{r}_3 \text{)} \end{array} \right.$$

The (20x20) stiffness matrix \mathbf{K}^* associated to \mathbf{r}^* may be partitioned as follows

$$\mathbf{K}^* = \left[\begin{array}{c|c} \mathbf{K}_{11} & \mathbf{K}_{10} \\ \hline \mathbf{K}_{10}^T & \mathbf{K}_{00} \end{array} \right] \begin{array}{l} 18 \text{ rows} \\ 2 \text{ rows} \end{array} \quad (\text{III-55})$$

and the elimination of \bar{r}_0 by the condensation procedure (II.1.3) provides the final (18x18) condensed matrix \mathbf{K}

$$\mathbf{K} = \mathbf{K}_{11} - \mathbf{K}_{10} \mathbf{K}_{00}^{-1} \mathbf{K}_{10}^T \quad (\text{III-56})$$

associated with the 18 fundamental degrees of freedom specified in \mathbf{r} .

Since the transformation for the cross derivatives is

$$\begin{Bmatrix} u_y \\ v_x \end{Bmatrix} = \begin{bmatrix} 1 & -1 \\ 1 & 1 \end{bmatrix} \begin{Bmatrix} \epsilon_{xy} \\ \omega \end{Bmatrix} \quad (\text{III-57})$$

in automatic computation the matrix \mathbf{K}^* can be formed directly from $\bar{\mathbf{K}}$, by addressing and combining its rows and columns in the following manner:

Rows and Columns of					
\mathbf{K}^*	$\bar{\mathbf{K}}$	\mathbf{K}^*	$\bar{\mathbf{K}}$	\mathbf{K}^*	$\bar{\mathbf{K}}$
1	1	7	4	13	7
2	11	8	14	14	17
3	2	9	5	15	8
4	13	10	16	16	19
5	12+3	11	15+6	17	18+9
6	12-3	12	15-6	18	18-9
				19	10
				20	20

The final condensation (III-56) may be performed by symmetric Gauss elimination, starting at the bottom of \mathbf{K}^* and reducing columns 20 and 19; the final \mathbf{K} is then the (18x18) top principal minor. The same reduction can be performed on the load vector. The automatic procedure to condense and recover internal displacements is described in detail in Appendix III for the LST quadrilateral.

III.3.5 Kinematically Equivalent Force Vectors

III.3.5.1 Surface Loading

We again assume that a general distributed load $p(\zeta_B)$ acts on the side 3 of the triangle (Fig. 3.6) and focus our attention on the component $p_x(\zeta_B)$ given by the interpolation formula

$$p_x(\zeta_1) = \Phi_p^T(\zeta_1) \mathbf{p}_x \quad (\text{III-58})$$

To simplify the derivation, we write the displacement $u(\zeta_1)$ of side 3 in terms of

$$\bar{\mathbf{u}}_B^T = \langle u_1 \ u_{x1} \ u_{y1} \ u_x \ u_{x2} \ u_{y2} \rangle$$

extracted from the subvector $\bar{\mathbf{u}}$ of Equation (III-45a). On using the expression (I-31) for $\Phi_{(3)}$ and evaluating the corresponding shape functions on side 3 ($\zeta_3 = 0$, $\zeta_2 = 1 - \zeta_1$), we get

$$u(\zeta_1) = \bar{\mathbf{u}}_B^T \begin{Bmatrix} \zeta_1^2 (3-2\zeta_1) \\ \zeta_1^2 (1-\zeta_1) a_3 \\ -\zeta_1^2 (1-\zeta_1) b_3 \\ (1-\zeta_1)^2 (1+2\zeta_1) \\ -(1-\zeta_1)^2 \zeta_1 a_3 \\ (1-\zeta_1)^2 \zeta_1 b_3 \end{Bmatrix} \quad (\text{III-59})$$

Using Equations (II-46) and (II-45), we get for the generalized forces $\bar{\mathbf{R}}_{uB}$ associated to $\bar{\mathbf{u}}_B$:

$$\begin{aligned} \bar{R}_{pu_1} &= \mathbf{p}_x^T l_3 \int_0^1 \phi_p(\zeta_1) \zeta_1^2 (3-2\zeta_1) d\zeta_1 \\ \bar{R}_{pux_1} &= \mathbf{p}_x^T l_3 a_3 \int_0^1 \phi_p(\zeta_1) \zeta_1^2 (1-\zeta_1) d\zeta_1 = -\frac{a_3}{b_3} R_{puy_1} \\ \bar{R}_{puy_1} &= -\mathbf{p}_x^T l_3 b_3 \int_0^1 \phi_p(\zeta_1) \zeta_1^2 (1-\zeta_1) d\zeta_1 \\ \bar{R}_{pu_2} &= \mathbf{p}_x^T l_3 \int_0^1 \phi_p(\zeta_1) (1-\zeta_1)^2 (1+2\zeta_1) d\zeta_1 \\ \bar{R}_{pux_2} &= -\mathbf{p}_x^T l_3 a_3 \int_0^1 \phi_p(\zeta_1) (1-\zeta_1)^2 \zeta_1 d\zeta_1 = -\frac{a_3}{b_3} R_{puy_2} \\ \bar{R}_{puy_2} &= \mathbf{p}_x^T l_3 b_3 \int_0^1 \phi_p(\zeta_1) (1-\zeta_1)^2 \zeta_1 d\zeta_1 \end{aligned} \quad (\text{III-60})$$

Obviously \bar{R}_{ux} and \bar{R}_{uy} are linearly dependent since the cubic side displacement depends only on four parameters (corner displacements and side derivatives).

We proceed similarly for the components $p_y(\zeta_1)$. Formulas for the other two sides follow from cyclic permutation.

The final nodal forces associated to r , are for corner 1 :

$$\begin{Bmatrix} R_{pu_1} \\ R_{pv_1} \\ R_{pex_1} \\ R_{pey_1} \\ R_{pex_{y_1}} \\ R_{pw_1} \end{Bmatrix} = \begin{Bmatrix} \bar{R}_{pu_1} \\ \bar{R}_{pv_1} \\ \bar{R}_{pux} \\ \bar{R}_{pvy} \\ \bar{R}_{pvx} + \bar{R}_{puy} \\ \bar{R}_{pvx} - \bar{R}_{puy} \end{Bmatrix} \quad (\text{III-61})$$

where for the forces associated with the cross derivatives we have used the transpose of (III-57). No condensation is necessary since the centroid loads are zero.

Example: linear variation of p_x , defined by

$$p_x(\zeta_1) = \zeta_1 p_{x_1} + (1 - \zeta_1) p_{x_2}$$

Replacing into (III-58) we get immediately

$$\begin{Bmatrix} \bar{R}_{pu_1} \\ \bar{R}_{pux_1} \\ \bar{R}_{puy_1} \\ \bar{R}_{pu_2} \\ \bar{R}_{pux_2} \\ \bar{R}_{puy_2} \end{Bmatrix} = \frac{l_3}{60} \begin{bmatrix} 21 & 9 \\ 3a_3 & 2a_3 \\ -3b_3 & -2b_3 \\ 9 & 21 \\ -2a_3 & -3a_3 \\ 2b_3 & 3b_3 \end{bmatrix} \begin{Bmatrix} p_{x_1} \\ p_{x_2} \end{Bmatrix} \quad (\text{III-62})$$

For an uniform load $p_{x1} = p_{x2} = p$:

$$\begin{aligned}\bar{R}_{p u_1} &= \bar{R}_{p v_1} = p l_3 / 2 \\ \bar{R}_{p u x_1} &= -\bar{R}_{p u x_2} = p a_3 l_3 / 12 \\ \bar{R}_{p u y_1} &= -\bar{R}_{p u y_2} = p b_3 l_3 / 12\end{aligned}\tag{III-63}$$

A concentrated in-plane corner moment M_ω may be input directly as the generalized force R_ω associated with ω .

III.3.5.2 Gravity Forces

We assume that they act along the -Y direction and that both the density and the thickness h are constant. Therefore

$$f_x = 0, \quad f_y = -\rho \quad \phi_\xi = 1$$

and Equation (II-48) gives for the generalized forces \bar{R}_f associated with \bar{r}

$$\begin{aligned}\bar{R}_{f x}^T &= 0 \\ \bar{R}_{f y}^T &= -\rho A h F\end{aligned}\tag{III-64}$$

with

$$\begin{aligned}F &= \frac{1}{A} \int_A \phi_{(3)} dA = L_3 = \\ &= \frac{1}{60} \langle 11 \quad 2(a_3 - a_2) \quad 2(b_2 - b_3) \quad 11 \quad 2(a_1 - a_3) \quad 2(b_3 - b_1) \quad 11 \quad 2(a_2 - a_1) \quad 2(b_1 - b_2) \quad 27 \rangle\end{aligned}$$

To obtain the final nodal force vector R_f associated with r , we must

$$(1) \text{ form } \begin{aligned} R_{fexy}^* &= \bar{R}_{fvx} + \bar{R}_{fuy} \\ R_{f\omega}^* &= \bar{R}_{fvx} - \bar{R}_{fuy} \end{aligned}$$

at each corner, and rearrange R^* according to the structure of r^* ;

(2) eliminate the centroid loads $R_{fox}^* = 0$, $R_{foy}^* = -27 \rho Ah / 60 = -0,45 \rho Ah$ by the condensation process (II-4b)

$$R_f = R_f^* - K_{00}^{-1} K_{10}^T R_{fo}^*$$

using submatrices (III-56).

III.3.6 Possibilities of the QST

The cubic element introduced here has not been applied yet to the analysis of two-dimensional problems, but in the author's opinion it will represent probably the last stage in the development of refined PS elements since higher order expansions become unnecessarily complex. Its fundamental advantages seems to be:

(a) It can take relatively high strain gradients with a coarse subdivision and solve exactly or nearly exactly many practical problems like bending under linearly varying moments;

(b) It may be combined naturally with bending elements like beams, thin plates, etc., which use cubic expansions, for instance to construct a flat element for shell analysis. The inclusion of the rotational

degree of freedom is especially important for the analysis of shell surfaces intersecting at a finite angle;

(c) The displacement gradients are continuous at the corners and obtained directly from the solution of the equilibrium equations; the strain discontinuity along the edges is not likely to be very large;

(d) In-plane concentrated moments can be incorporated directly as generalized forces;

(e) The choice of the corners solely as nodal points simplifies the coding and reduces the total number of equations and the connectivity (band width) for the assembled structure. The following figures are significant:

Consider a single connected plane network of E elements. For $E \rightarrow \infty$ the total number of corner points tends asymptotically to $0.5 E$ and the number of midpoints to $1.5 E$. Therefore the total number of equations is approximately (in a large mesh)

1.0 E for CST mesh

4.0 E for LST mesh

3.0 E for QST mesh

so that the number of unknowns is actually less for the QST than for the LST with the same subdivision, despite the fact that in the first case we have a cubic displacement expansion instead of a quadratic one. However, this advantage is reduced if four triangles are combined to form arbitrary quadrilaterals by condensation of the internal nodal points (see Appendix II).

For a large mesh of E quadrilaterals, we have approximately E corner points and $2E$ midpoints and the figures are now

2.0 E for CST

6.0 E for LST

6.0 E for QST

The connectivity of the LST mesh has been reduced, but the QST has still the advantage of a more refined expansion for the same number of equations to solve.

Certain disadvantages of the cubic element are

(a) The derivation for a straight side triangle does not permit such a close approximation to the actual geometry of the body (in case of curved boundaries) as that obtained with the CST for a similar number of degrees of freedom. In this respect, the QST is not worse than the LST;

(b) Specification of boundary conditions associated with displacement gradients requires a more careful examination of the problem;

(c) Strain-type generalized displacements (ϵ_x , ϵ_y and ϵ_{xy}) transform as second-order tensors; therefore coordinate transformations in plane (for skew B.C's) or in space (for shell elements) are complicated.

IV. ANALYSIS OF NONLINEAR PROBLEMS

IV.1 GENERAL FORMULATION

IV.1.1 Classification of Nonlinear Effects

Nonlinear relations between kinematic and mechanical variables arise naturally from two sources:

1. Nonlinear constitutive relations; this will be referred to as material or physical nonlinearity. The constitutive or material law (tensorial equation connecting kinematic and static field variables) may have the following structure:

(a) Differential law: instant values of the constitutive variables and possibly their objective time rates of any order are related through a differential operator. If at most first order rates are involved, we have a direct incremental relation. Examples are provided by the theories of nonlinear elasticity, hypoelasticity, elastoplasticity, viscoplasticity and viscoelastic models.

(b) Integral or functional law: the constitutive equation includes the effect of the past history as well as the present configuration (actually (a) is contained as a limiting case). General viscoelastic materials belong to this class; in particular linear and nonlinear Boltzmann-Volterra solids, simple materials, etc. The mathematical structure of the material law is obviously reflected in the discretized representation of the structure. In case (a), incremental load-displacement equations can be established in terms of the field variables

and their rates at the present configuration; physical path-dependence in plasticity is accounted for by keeping track of a set of parameters affecting the incremental equation. On the other hand, for materials of type (b), "stiffness relations" become functional operators of the present and all previous configurations; however, if we accept the principle of fading memory [41], only a certain number of past solutions need to be retained in order to attain a certain accuracy level in the numerical solution [42].

2. Finite change in geometry; this effect will be called geometric nonlinearity and appears at two levels:

(a) The use of actual measures of deformation to account for finite strains and rotations introduce nonlinear terms in the strain-displacement equations.

(b) Equilibrium equations and boundary conditions must be formulated in the deformed geometry.

IV.1.2 Solution Procedures

The general structural problem may be stated as follows:

The values of the field variables at the initial or reference state Γ_0 are known. We seek the solution at a "final" state Γ_f for which certain parameters (loads, displacements) are specified. The problem is assumed to be well-posed in the sense of a continuous and bounded dependence of the space of genuine solutions on the initial state.

A fundamental question is whether the final solution depends on the path $\Gamma_0 \rightarrow \Gamma_f$. If so (nonconservative systems), the history of the

applied parameters must also be supplied. Path-dependence is related to geometric and material characteristics; possible cases are:

(a) Elastic material: linear or nonlinear elasticity for small or finite deformations is characterized by a unique dependence of the static variables on the total displacement field (the converse is not true in general). Hence, finite strain tensors, defined from the difference of the initial and final displacement configurations, are meaningful measures of deformation.

(b) Nonconservative material, infinitesimal deformations: the final stress state is path-dependent, but since no distinction needs to be made between material and spatial coordinates, the total infinitesimal strain tensor is uniquely defined by the total displacement field.

(c) Nonconservative materials, finite deformations: here even the final strain field obtained by path-integration of the incremental strains is generally path-dependent [43] since the resulting differential system is non-holonomic except in special cases (ex: one-dimensional problems). This point has seldom been stressed. The definition of a "total" finite strain from the total displacement field has no meaning; the only natural measure is provided by path-integration.

Two methods of analysis have been currently employed for the analysis of nonlinear problems:

(1) Direct iteration procedure: the final state is determined by iterative solution of a system of nonlinear equations. Any of the well-known techniques for solving this type of equations may be used, for instance, Newton's method.

(2) Step-by-step or incremental procedure; the final configuration is reached after a certain number of linearized steps more or less evenly distributed between \square_0 and \square_f . In the displacement formulation, this method is equivalent to the numerical integration of a system of nonlinear differential (or integro-differential) equations.

Combinations of (1) and (2), i.e., step-iteration, may be considered as well.

The direct iterative technique has obvious limitations. In the first place, convergence is usually expected only on physical grounds; the process may diverge or converge to a different solution. Secondly, it should not be applied to path-dependent (nonconservative) systems, and definitely not in the case (c) mentioned above. However, sometimes we may use an "equivalent" conservative stress-strain law and analyze the problem as a nonlinear elastic case. Example: the deformation theory of plasticity (Hencky), for increasing proportional loading and small deformations. Or important parameters may be path-independent, such as the limit load of a perfectly plastic structure.

The incremental procedure is completely general and provides a description of intermediate states, but it is usually more time-consuming.

The iteration process, whenever applicable, should be preferred when one or a few states are of interest. Nothing more will be said about iteration, since a special formulation is required for each problem. For some applications we refer to References [17] and [44].

IV.1.3 Variational Formulation of the Incremental Method

We consider here the general formulation of the step-by-step displacement solution of structural problems including both physical and geometric non-linearity.

The finite region or "element" D is considered at an arbitrary state Γ in the solution path (Fig. 4.1), where Γ is a position parameter. Such configuration may be regarded as an initial or "undeformed" stressed state, with complete independence of the past history (which might only enter through the constitutive law).

The element D is referred to a local spatial curvilinear system x^i ($i=1,2,3$); in addition, common or global systems X^i should be used to assemble for the complete discretized structure.

An incremental position is denoted by $\Gamma_{\Delta} = \Gamma + \Delta\Gamma$. The contravariant initial stress tensor τ^{ij} at Γ becomes

$$\bar{\tau}^{ij} = \tau^{ij} + \Delta\bar{\tau}^{ij} \quad \text{at } \Gamma_{\Delta} \quad (\text{IV-1})$$

where $\bar{\tau}^{ij}$ are components referred to the rotated (convected) local frames \bar{x}^i at each point of D , and measured per unit of "undeformed" area at Γ . The body force field F^i and surface tractions T^i become

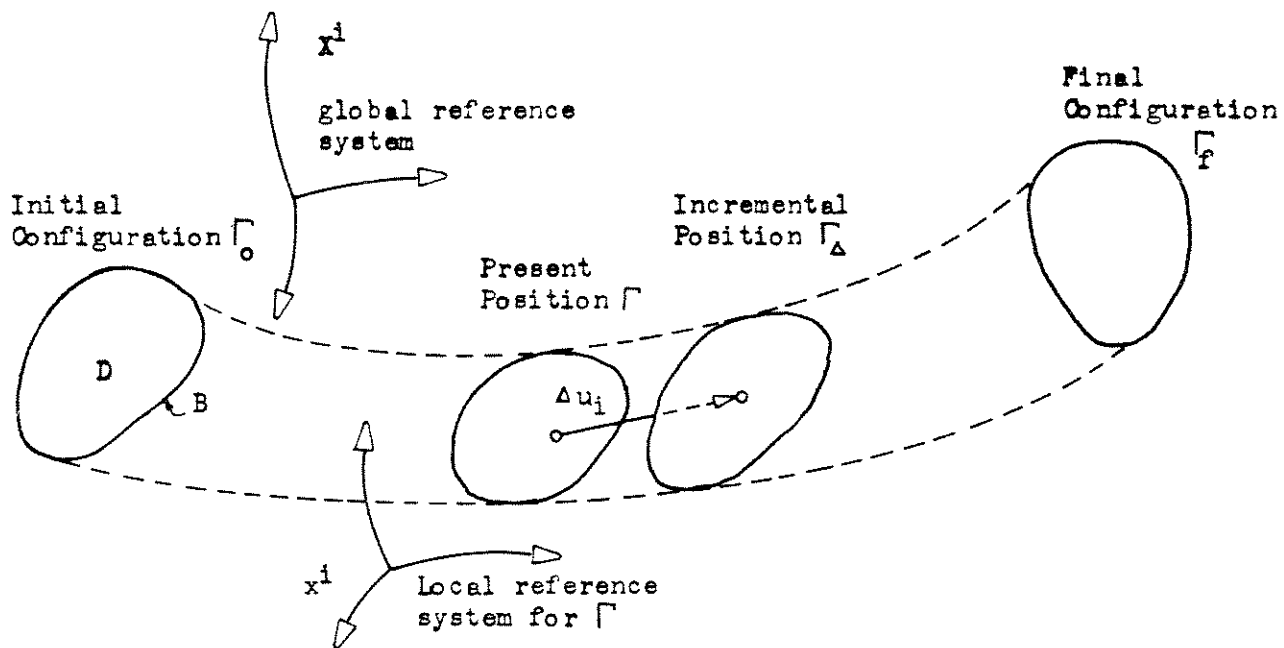


Fig. 4.1 - Incremental or Step-by-step Procedure.

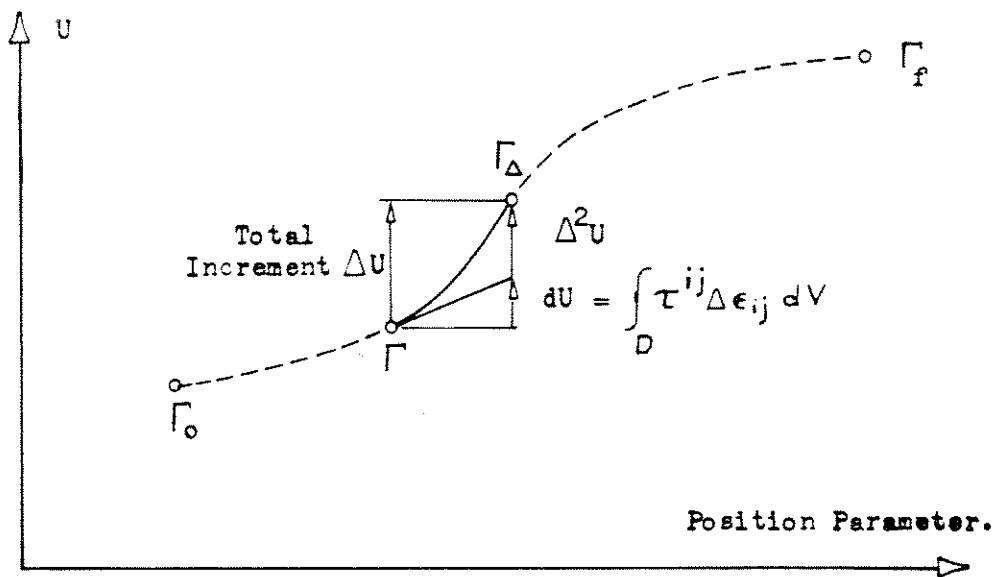


Fig. 4.2 - Meaning of Strain Energy Increments..

$F^i + \Delta \bar{F}^i$ and $T^i + \Delta \bar{T}^i$ at Γ_Δ , also referred to rotated axes and measured per unit of area and volume at Γ .

The incremental displacement field is Δu_i . Since the x^i system is a Lagrangian frame for Γ_Δ , the incremental Cauchy covariant strain tensor ΔE_{ij} is given by (a comma denotes covariant differentiation with respect to x^i):

$$2\Delta E_{ij} = (\Delta u_{i,j} + \Delta u_{j,i}) + \Delta u_{,i}^k \Delta u_{k,j} = 2(\Delta \epsilon_{ij} + \Delta \eta_{ij}) \quad (\text{IV-2})$$

where

$$\begin{aligned} \Delta \epsilon_{ij} &= \frac{1}{2} (\Delta u_{i,j} + \Delta u_{j,i}) \\ \Delta \eta_{ij} &= \frac{1}{2} \Delta u_{,i}^k \Delta u_{k,j} \end{aligned}$$

are the infinitesimal or linear incremental strain tensor, and the quadratic incremental strain tensor, respectively.

We seek a variational formulation in terms of incremental displacements as primary variables which enables us to construct discretized load-displacement relations at Γ . To this end, we make use of the principle of virtual displacements at $\Gamma_\Delta = \Gamma + \Delta \Gamma$. Since the stress field (IV-1) is conjugate of the strain field (IV-2), we may write

$$\int_D (\tau^{ij} + \Delta \bar{\tau}^{ij}) \delta(\Delta E_{ij}) dV = \int_D (F^i + \Delta \bar{F}^i) \delta u_i dV + \int_{E_T} (T^i + \Delta \bar{T}^i) \delta (u_i) dS \quad (\text{IV-3})$$

where all integrals are referred to the "undeformed" position Γ and the virtual variation of the incremental strain field (IV-2) is

$$\delta(\Delta E_{ij}) = \delta(\Delta \epsilon_{ij}) + \delta(\Delta \eta_{ij}) \quad (\text{IV-4})$$

with

$$2\delta(\Delta\epsilon_{ij}) = \delta(\Delta u_{i,j}) + \delta(\Delta u_{j,i}) \quad (\text{IV-5a})$$

$$2\delta(\Delta\eta_{ij}) = \Delta u_{,i}^k \delta(\Delta u_{k,j}) + \Delta u_{k,j} \delta(\Delta u_{,i}^k) \quad (\text{IV-5b})$$

The virtual displacement expression at Γ is (here $\delta(\Delta\eta_{ij})$ vanishes because of (IV-5b)):

$$\int_D \tau^{ij} \delta(\Delta\epsilon_{ij}) dV = \int_D F^i \delta(\Delta u_k) dV + \int_{B_T} T^i \delta(\Delta u_i) dS \quad (\text{IV-6})$$

Equation (IV-6) is merely the statement of the equilibrium of the initial stress field τ^{ij} with the applied body and surface forces. The virtual displacement field in Equations (IV-3) and (IV-6) may be the same, since they are referred to the same state. Therefore subtracting we get

$$\begin{aligned} & \int_D [\tau^{ij} \delta(\Delta\eta_{ij}) + \Delta\bar{\tau}^{ij} \delta(\Delta\epsilon_{ij}) + \Delta\bar{\tau}^{ij} \delta(\Delta\eta_{ij})] dV \\ = & \int_D \Delta F^i \delta(\Delta u_i) dV + \int_{B_T} \Delta T^i \delta(u_i)_{B_T} dV \end{aligned} \quad (\text{IV-7})$$

Now we introduce the incremental material law in the symbolic form

$$\Delta\bar{\tau}^{ij} = C^{ijkl} \Delta\epsilon_{kl} \quad (\text{IV-8})$$

where C^{ijkl} are in general functional operators including the effect of the past history. The second term of the left side of Equation (IV-7) becomes (since $C^{ijkl} = C^{klij}$)

$$\Delta\bar{\tau}^{ij} \delta(\Delta\epsilon_{ij}) = \Delta\epsilon_{kl} C^{ijkl} \delta(\Delta\epsilon_{ij}) = \frac{1}{2} \delta(\Delta\bar{\tau}^{ij} \Delta\epsilon_{ij})$$

and the last term is of the third order in the incremental displacements Δu_i .

Consequently, Equation (IV-7) becomes an exact differential in the second order terms. Let

$$\frac{1}{2} \Delta^2 U = \int_D [\tau^{ij} \Delta \eta_{ij} + \frac{1}{2} \Delta \epsilon_{kl} C^{ijkl} \Delta \epsilon_{ij}] dV + O(\Delta u_i \Delta u_j \Delta u_k) \quad (IV-8a)$$

$$\frac{1}{2} \Delta^2 P = \int_D \Delta \bar{F}^i \Delta u_i dV + \int_{B_T} \Delta \bar{T}^i (\Delta u_i)_{B_T} dS \quad (IV-8b)$$

$$I = \frac{1}{2} \Delta^2 (U - P) = \frac{1}{2} \Delta^2 V \quad (IV-8c)$$

Then the incremental variational principle may be stated as

$$\delta I = 0 \quad \text{at} \quad \bar{\Gamma} \quad (IV-9)$$

for all kinematically admissible incremental displacement fields. A similar principle was obtained by Biot [45] in 1934 for a linear medium under initial stress.

It is important to realize that the total strain energy increment ΔU from $\bar{\Gamma}$ to $\bar{\Gamma} + \Delta \bar{\Gamma}$ is actually (Fig. 4.2)

$$\Delta U = U_{\bar{\Gamma} + \Delta \bar{\Gamma}} - U_{\bar{\Gamma}} = dU + \frac{1}{2} \Delta^2 U = dU + \frac{1}{2} d^2 U + \frac{1}{6} \Delta^3 U = \dots$$

where

$$dU = \int_D \tau^{ij} d\epsilon_{ij} dV$$

represents the work of the existing stress state on the linear (infinitesimal) incremental strain tensor, which is of first order in the incremental displacements and only zero for an initial unstressed state. This term equilibrates the work of the existing applied forces F^i , T^i and does not affect the

incremental relations.

For a linear elastic material and infinitesimal strains, U becomes a quadratic function in the u_i . When referred to the initial unstressed state ($\tau^{ij} = 0$, $\Delta u_i = u_i$, $\Delta \epsilon_{ij} = \epsilon_{ij}$).

$$U = \Delta U = \frac{1}{2} \Delta^2 U = \frac{1}{2} \int_D \epsilon_{kl} C^{ijkl} \epsilon_{ij} dV$$

and we recover the usual minimum potential energy principle as used in II.2.5.

Since the incremented stress tensor $\bar{\tau}^{ij}$ defined by (IV-1) is referred to unit of initial area and rotated axes, in order to perform the next step it is necessary to recover the actual stress tensor τ^{ij} at \square_{Δ} , whose components are referred to the local Lagrangean system x^i and measured per unit of "deformed" area. To the first order

$$\tau^{ij} = \bar{\tau}^{ij} (1 - \Delta \epsilon_{kk}) + \frac{1}{2} \bar{\tau}^{ik} (\Delta \epsilon_{jk} + 2 \Delta \omega_{jk}) + \frac{1}{2} \bar{\tau}^{jk} (\Delta \epsilon_{ik} + 2 \Delta \omega_{ik}) \quad (IV-10)$$

where

$$2 \Delta \omega_{ij} = \Delta u_{i,j} - \Delta u_{j,i}$$

are components of the incremental infinitesimal rotation tensor. In Equation (IV-10) all products of $\Delta \epsilon_{ij}$ and $\Delta \omega_{ij}$ have been neglected.

For instance, in the case of plane stress ($\tau^{i3} = 0$, ($i = 1, 2, 3$), $\Delta \epsilon_{i3} = \Delta \epsilon_{23} = 0$, $\Delta \omega = \Delta \omega_{12}$, $\Delta \omega_{13} = \Delta \omega_{23} = 0$)

$$\begin{Bmatrix} \tau^{11} \\ \tau^{22} \\ \tau^{12} \end{Bmatrix} = \begin{bmatrix} 1 - \Delta \epsilon_{22} - \Delta \epsilon_{33} & 0 & \Delta \epsilon_{12} + 2 \Delta \omega \\ 0 & 1 - \Delta \epsilon_{11} - \Delta \epsilon_{33} & \Delta \epsilon_{12} - 2 \Delta \omega \\ \frac{1}{2} (\Delta \epsilon_{12} - 2 \Delta \omega) & \frac{1}{2} (\Delta \epsilon_{12} - 2 \Delta \omega) & 1 - \frac{\Delta \epsilon_{11} + \Delta \epsilon_{22}}{2} - \Delta \epsilon_{33} \end{bmatrix} \begin{Bmatrix} \bar{\tau}^{11} \\ \bar{\tau}^{22} \\ \bar{\tau}^{12} \end{Bmatrix} \quad (IV-11)$$

Similar transformations hold for body forces and surface tractions; for instance

$$\bar{T}^1 \doteq \bar{T}^{-1}(1 - \Delta\epsilon_{22} - \Delta\epsilon_{33}) + \bar{T}^2 \Delta\omega_{12} + \bar{T}^3 \Delta\omega_{13} \quad (\text{IV-12})$$

If the load increment is specified with respect to a fixed system of axes, an iterative process is necessary to restore equilibrium within each incremental step.

IV.1.4 Instantaneous Stiffness Matrix

The incremental displacement field is now constrained to be expressed in terms of a finite number of incremental covariant nodal displacements Δr_i by

$$\Delta u_k = \phi_{ik} \Delta r_i \quad \Delta u^k = \phi_i^k \Delta r_i \quad (\text{IV-13})$$

where ϕ_{ik} and ϕ_i^k are interpolating functions. The strain components are

$$\begin{aligned} \Delta\epsilon_{kl} &= \frac{1}{2} (\phi_{ik,l} + \phi_{il,k}) \Delta r_i \\ \Delta\eta_{kl} &= \frac{1}{2} \Delta r_i \phi_{i,k}^n \phi_{nj,l} \Delta r_j \end{aligned}$$

and replacing into Equation (IV-8a) we obtain for $\Delta^2 U$

$$\begin{aligned} \frac{1}{2} \Delta^2 U &= \frac{1}{2} \Delta r_i \int_D [\tau^{kl} \phi_{i,k}^n \phi_{nj,l} + \frac{1}{2} (\phi_{ik,l} + \phi_{il,k}) C^{klmn} (\phi_{jm,n} + \phi_{jn,m})] dV \\ &\cdot \Delta r_j + O(\Delta r^3) = \frac{1}{2} \Delta r_i K_{ij} \Delta r_j + O(\Delta r^3) \end{aligned} \quad (\text{IV-14})$$

where K_{ij} are the elements of the incremental or "instantaneous" stiffness matrix \mathbf{K} at Γ , since

$$K_{ij} = \frac{\partial(\Delta^2 U)}{\partial(\Delta r_i) \partial(\Delta r_j)} \Bigg|_{\substack{\Delta r_i=0 \\ \Delta r_j=0}} = \frac{\partial(d^2 U)}{\partial(dr_i) \partial(dr_j)}$$

Equation (IV-14) shows that the stiffness matrix splits naturally into

$$K = K_G + K_C \quad (IV-15)$$

where

$$K_{Gij} = \int_D \phi_{i,k}^n \tau^{kl} \phi_{nj,l} dV \quad (IV-16a)$$

$$2 K_{Cij} = \int_D (\phi_{ik,l} + \phi_{il,k}) C^{klmn} (\phi_{jm,n} + \phi_{jn,m}) dV \quad (IV-16b)$$

The first part is the so-called "geometric stiffness" or "initial stress stiffness matrix". The second part is the conventional stiffness, which takes account of the incremental stress-strain law at Γ .

Only the linear terms in the strain-displacement relations (IV-1) are needed to generate K_C , the work on the quadratic terms being of third order.

Conversely, only the quadratic terms $\Delta \eta_{ij}$ are required to assemble the geometric stiffness K_G , since the work of the initial stress field on the linear strain tensor is of first order. If the strain-displacement relations are linear, $K_G = 0$, regardless of material nonlinearity.

The components of the incremental nodal force vector ΔR associated with the Δr_i 's follow from the expression (IV-10b) for the second increment of the external work:

$$\Delta R_i = \int_D \Delta F^k \phi_{ki} dV + \int_{B_T} \Delta T^k (\phi_{ki})_{B_T} dS \quad (IV-17)$$

Finally, these relations must be transformed to a common or global system X^i (usually cartesian), before assembling for the complete structure in the usual way.

Therefore, the general formulation of the step-by-step displacement method leads naturally (in the limit $\Delta \rightarrow d$) to the matrix system of differential equations

$$dR = (K_C + K_G) dr \quad (IV-18)$$

of the first order in the generalized forces and displacements. If the constitutive law is of functional type, Equation (IV-18) becomes an integro-differential system, material kernels being contained in K_C .

We can see clearly how the different nonlinear effects enter into (IV-17):

- (a) Physical nonlinearity affects only K_C ;
- (b) Nonlinear strain-displacement terms affect only K_G ;
- (c) Change in geometry and boundary conditions affects dR , K_C and K_G , which must be evaluated taking account of the actual geometry at each step.

The uncoupling of effects (a) and (b) is a great advantage of the incremental method, since digital computer programs originally restricted to small displacements may be corrected to include the effect of geometric nonlinearity without changing the basic sequence of operations.

In most engineering problems dealing with finite change in geometry, extensional strains are small (although displacements and rotations may be large), and the local distortion of the element may be ignored. This assumption greatly simplifies the computation procedure, since otherwise the element type and assumed Rayleigh-Ritz displacement shapes have to be changed in general after the first step; only the nodal point coordinates in the global system need to be actualized. For problems involving large elastic strains (rubber elasticity) or large plastic distortions (metal forming), simplex elements (Fig. 2.1) with linear displacement fields are convenient, since the element type does not change.

Thermal nonlinear effects may be included by the procedure followed in II.5 for linear elastic materials, setting up a vector of incremental initial loads. This technique has been used extensively by Argyris [8,14].

IV.1.5 Numerical Integration Schemes

The step-by-step integration of the system (IV-18) can be performed only using high-speed digital computers; even so, time and storage limitations usually confine the treatment to moderately fine discretizations.

We shall consider here differential material laws for which (IV-17) are differential equations. The simplest method of integration is Euler's rule, a direct translation of the incremental procedure. The "n-th" step is

$$\begin{aligned} \mathbf{K}_{(n)} \Delta \mathbf{r}_{(n)} &= \Delta \mathbf{R}_{(n)} \\ \mathbf{r}_{(n+1)} &= \mathbf{r}_{(n)} + \Delta \mathbf{r}_{(n)} \end{aligned} \tag{IV-19}$$

The propagated error is of the first order in $\Delta \mathbf{r}$, provided the proper values of \mathbf{K}^{-1} are bounded. The midpoint rule

$$\begin{aligned} \mathbf{K}_{(n)} \Delta \bar{\mathbf{r}}_{(n)} &= \Delta \mathbf{R}_{(n)} \\ \mathbf{r}_{(n+1/2)} &= \mathbf{r}_{(n)} + \Delta \bar{\mathbf{r}}_{(n)}/2 \rightarrow \mathbf{K}_{(n+1/2)} \\ \mathbf{K}_{(n+1/2)} \Delta \mathbf{r}_{(n)} &= \Delta \mathbf{R}_{(n)} \\ \mathbf{r}_{(n+1)} &= \mathbf{r}_{(n)} + \Delta \mathbf{r}_{(n)} \end{aligned} \quad (\text{IV-20})$$

requires two evaluations per step, but is of second order. Higher order one-step methods are provided by Runge-Kutta formulas, but they are in general very cumbersome to code.

For problems with smooth load-displacement curves, integration and predictor-corrector methods may be employed; they require storage of several past solutions and special starting procedures. These techniques are not adequate for plasticity analysis in which sharp "breaks" may be expected, but are well suited for differential visco-elasticity, and of course, essential for integro-differential systems.

IV.2 ANALYSIS OF ELASTOPLASTIC PROBLEMS

IV.2.1 Scope

Plastic behavior is an important type of material or physical non-linearity. The constitutive law is of incremental type and relates stresses, strains and first strain rates.

The step-by-step method is naturally suited to follow an elastoplastic process. The theory necessary to generate the conventional incremental stiffness matrix is summarily presented and then a special but important yield

criterion (Von Mises) is considered in detail and applied to two-dimensional problems.

For simplicity the presentation is restricted to isotropic material and isothermal processes. The treatment of anisotropic elastoplasticity and thermal effects do not present in principle other difficulty than the ensuing algebraic complexity of the formulation; the real problem is to obtain enough experimental data to adequately characterize the material behavior in the numerical analysis.

IV.2.2 Summary of Fundamental Constitutive Relations of Elastoplasticity

This summary, with some notation changes, follows the classical work of Hill [46]. The present configuration of the element is considered as an initial stressed state; if the effect of finite deformations is included, the instantaneous conventional stiffness must be corrected as explained in IV.1.4.

Stress and strain increments are used instead of stress and strain rates. The use of rates ($\dot{\epsilon}$, $\dot{\tau}$, \dot{r} , \dot{s}) simplifies the notation, but obscures the meaning of the classical plasticity theory, which is essentially time-independent. The derivation is carried out in rectangular cartesian coordinates; only lower indices are then used for the different tensors.

IV.2.2.1 Stresses, Stress Deviator and Invariants

Total stress components will be denoted by τ_{ij} , stress increments by $d\tau_{ij}$. The components of the deviatoric stress tensor are defined by

$$s_{ij} = \tau_{ij} - \frac{1}{3} \delta_{ij} \tau_{kk} = \tau_{ij} - \delta_{ij} \tau \quad (\text{IV-21})$$

where $\tau = \tau_{kk}/3$ is the mean stress. Principal stresses are τ_1, τ_2 and τ_3 ; principal deviatoric stresses s_1, s_2 and s_3 .

The three invariants of the deviatoric stress tensor are

$$J_1 = s_{kk} = s_1 + s_2 + s_3 = 0$$

$$J_2 = -(s_1 s_2 + s_2 s_3 + s_3 s_1) = s_1^2 + s_2^2 + s_3^2 = \frac{1}{2} s_{ij} s_{ij}$$

$$J_3 = s_1 s_2 s_3 = \frac{1}{3} s_{ij} s_{jk} s_{ki}$$

IV.2.2.2 Incremental Strains

We consider here only the infinitesimal stress tensor which suffices to generate the conventional stiffness. The total strain increment is

$$de_{ij} = \frac{1}{2} (du_{i,j} + du_{j,i}) = de_{ij}^e + de_{ij}^p \quad (\text{IV-22})$$

where $de_{ij}^e =$ elastic strain increment;

$de_{ij}^p =$ plastic strain increment.

The incompressibility of the plastic distortion is expressed by

$$de_{kk} = 0 \quad (\text{IV-23})$$

Elastic and plastic work increment per unit of volume are

$$dW_e = \tau_{ij} de_{ij}^e \quad dW_p = \tau_{ij} de_{ij}^p \quad (\text{IV-24})$$

IV.2.2.3 Elastic Constitutive Equations

For a general anisotropic material, Equation (A1-1) of Appendix I may be written in incremental form:

$$de_{ij}^e = S_{ijkl} d\tau_{kl}$$

For isotropic material

$$d\epsilon_{ij}^e = \frac{ds_{ij}}{2G} + (1-2\nu)\delta_{ij} \frac{d\tau}{E} \quad (\text{IV-25})$$

IV.2.2.4 Yield Condition

The general equation of the yield surface is

$$f(\tau_{ij}, \epsilon_{ij}^p, \kappa) = 0 \quad (\text{IV-26})$$

where κ is a hardening parameter. We shall consider herein only the case of isotropic hardening (no Bauschinger effect) of an isotropic material. For this, Equation (IV-26) specializes to

$$f(J_2, J_3) = \kappa \quad (\text{IV-27})$$

where f does not depend upon the stress-strain history, which only enters through the parameter κ (strain-hardening or work-hardening effect). Both sides have dimension of stress.

A neutral stress change (stress point moving on a plane tangent to $f - \kappa = 0$) is defined as

$$df = \frac{\partial f}{\partial J_2} dJ_2 + \frac{\partial f}{\partial J_3} dJ_3 = 0 \quad (\text{IV-28})$$

since κ does not depend upon J_2 or J_3 . The condition that $d\epsilon_{ij}^p = 0$ for a neutral change may be satisfied if

$$d\epsilon_{ij}^p = G_{ij} df \quad (\text{IV-29})$$

where G_{ij} is a symmetric tensor, function of the state of stress and possibly of the previous strain history, but not of the stress increments (rates).

The incompressibility condition (IV-24) requires that $G_{kk} = \text{trace}(G) = 0$.

Moreover, the principal axes of $d\epsilon_{ij}^p$ should coincide with the principal stress axes; these conditions are met if

$$G_{ij} = h \frac{\partial g}{\partial \tau_{ij}} \quad (\text{IV-30})$$

where h and g are scalar functions of the invariants J_2 and J_3 and possibly of the strain history. Thence

$$d\epsilon_{ij}^p = h \frac{\partial g}{\partial \tau_{ij}} df = h \left(\frac{\partial g}{\partial J_2} s_{ij} + \frac{\partial g}{\partial J_3} t_{ij} \right) df \quad (\text{IV-31})$$

with $t_{ij} = s_{ik}s_{kj} - \frac{2}{3}\delta_{ij}J_2$.

IV.2.2.5 Hardening Law

In order to express mathematically the hardening properties of the material, we shall adopt the "work-hardening hypothesis", which is extremely suitable for generating the constitutive equations in matrix form. It states that the parameter K in Equation (IV-27) depends only on the total plastic work W_p dissipated along the structure path from the annealed state, i.e.,

$$f(J_2, J_3) = K = F(W_p) \quad (\text{IV-32})$$

where (neglecting elastic compressibility)

$$W_p = \int_{\text{path}} dW_p = \int_{\text{path}} \tau_{ij} d\epsilon_{ij}^p \quad (\text{IV-33})$$

upon which (IV-31) becomes

$$d\epsilon_{ij}^p = h F' \frac{\partial g}{\partial \tau_{ij}} \tau_{kl} d\epsilon_{kl}^p \quad (\text{IV-34})$$

$F' = dF/dw_p$ is the tangent to the $\kappa = F(w_p)$ curve, a characteristic of the material which can be obtained from a simple tension test (Fig. 4.3).

Upon multiplying (IV-34) by τ_{ij} and adding, we get

$$\tau_{ij} d\epsilon_{ij}^p = n F' \tau_{ij} \frac{\partial g}{\partial \tau_{ij}} (\tau_{kl} d\epsilon_{kl}^p) = n F' g \tau_{kl} d\epsilon_{kl}^p$$

from Euler's theorem for homogeneous functions, n being the degree of g . Thus $n F' g h = 1$ and (IV-34) reduces to

$$d\epsilon_{ij}^p = \frac{1}{ng} \frac{\partial g}{\partial \tau_{ij}} \frac{df}{F'} \quad (\text{IV-35})$$

which gives the incremental plastic strain components, provided $df \geq 0$.

If $df < 0$, $d\epsilon_{ij}^p = 0$ and we use only the elasticity equations (IV-26).

By total differentiation of the yield condition (IV-27) we also obtain

$$\frac{\partial f}{\partial \tau_{ij}} d\tau_{ij} = \frac{\partial \kappa}{\partial \epsilon_{ij}^p} d\epsilon_{ij}^p = p_{ij} d\epsilon_{ij}^p \quad (\text{IV-36})$$

and if the hardening law is of the form (IV-32):

$$\frac{\partial f}{\partial \tau_{ij}} d\tau_{ij} = F' \tau_{ij} d\epsilon_{ij}^p, \text{ i.e. } p_{ij} = F' \tau_{ij} \quad (\text{IV-37})$$

IV.2.2.6 Flow Rule

If $g \equiv \alpha f$ in Equation (IV-35):

$$d\epsilon_{ij}^p = \frac{\alpha df}{nf F'} \frac{\partial f}{\partial \tau_{ij}} = d\lambda \frac{\partial f}{\partial \tau_{ij}} \quad (\text{IV-38})$$

where

$$d\lambda = \frac{\alpha df}{nf F'} = \frac{\alpha}{nf F'} \frac{\partial f}{\partial \tau_{ij}} d\tau_{ij} = \frac{\alpha}{nf F'} p_{ij} d\epsilon_{ij}^p \quad (\text{IV-39})$$

is a scalar of proportionality.

IV.2.2.7 Von Mises Yield Criterion

This yield condition has the simplest analytic form; however it has been shown to be an excellent approximation for many metals. The yield surface is assumed to be a cylinder of radius $\bar{\sigma}$, uniformly expanding:

$$\bar{\sigma}^2 = 3J_2 = \frac{3}{2} s_{ij} s_{ij} = 3\kappa^2 \quad (\text{IV-40})$$

where $\bar{\sigma}$ is called the equivalent stress. The yield surface equation is

$$\frac{1}{3} \bar{\sigma}^2 = \kappa^2 = F^2(W_p) \quad \text{or} \quad \frac{\bar{\sigma}}{\sqrt{3}} = F(W_p) \quad (\text{IV-41})$$

If $\sigma_Y = Y = F(0)$ is the initial yield stress in simple tension or compression, then $Y/\sqrt{3}$ is the initial yield stress in simple shear.

IV.2.2.8 Prandtl-Reuss Equations

Assuming $g = J_2$, $\partial g / \partial \tau_{ij} = s_{ij}$, $n = 2$, Equation (IV-35)

becomes

$$d\epsilon_{ij}^P = \frac{s_{ij}}{2J_2} \frac{df}{F'} \quad (\text{IV-42})$$

If we combine this equation with Von Mises yield criterion (IV-41), we obtain for the incremental plastic strain

$$d\epsilon_{ij}^P = \frac{3s_{ij}}{2\bar{\sigma}^2} \frac{d\bar{\sigma}}{F'} \quad (\text{IV-43})$$

but this form of the constitutive equation is not very convenient, since it becomes 0/0 for a perfectly plastic material ($F'=0$)

IV.2.3 Matrix Expressions of Incremental Relations for Three-Dimensional Continua

IV.2.3.1 Arbitrary Yield Criterion

We derive here general three-dimensional constitutive relations for an isotropic material. As usual, we arrange stress and strain components as (6x1) vectors:

$$\begin{aligned}\tau^T &= \langle \tau_{11} \quad \tau_{22} \quad \tau_{33} \quad \tau_{12} \quad \tau_{23} \quad \tau_{31} \rangle \\ \epsilon^T &= \langle \epsilon_{11} \quad \epsilon_{22} \quad \epsilon_{33} \quad 2\epsilon_{12} \quad 2\epsilon_{23} \quad 2\epsilon_{31} \rangle\end{aligned}$$

The incremental elastic equation (IV-26), when inverted, reads

$$d\tau = C_e d\epsilon^e \quad (\text{IV-44})$$

where, for isotropic and compressible ($\nu \neq 1/2$) material

$$C_e = \frac{E}{(1-2\nu)(1+\nu)} \begin{bmatrix} 1-\nu & \nu & \nu & \cdot & \cdot & \cdot \\ \nu & 1-\nu & \nu & \cdot & \cdot & \cdot \\ \nu & \nu & 1-\nu & \cdot & \cdot & \cdot \\ \cdot & \cdot & \cdot & 0.5-\nu & \cdot & \cdot \\ \cdot & \cdot & \cdot & \cdot & 0.5-\nu & \cdot \\ \cdot & \cdot & \cdot & \cdot & \cdot & 0.5-\nu \end{bmatrix}$$

Instead of the hardening equation (IV-32) it is more convenient (to avoid irrational expressions) to work with the square of both sides:

$$f^2(J_2, J_3) = \kappa^2 = F^2(W_p) = H(W_p) \quad (\text{IV-45})$$

and (IV-37) becomes

$$\frac{\partial f^2}{\partial \tau_{ij}} d\tau_{ij} = \frac{\partial \kappa^2}{\partial \epsilon_{ij}^p} d\epsilon_{ij}^p = H' \tau_{ij} d\epsilon_{ij}^p \quad (\text{IV-46})$$

with $H' = 2FF' = dK^2/dW_p$.

Introduce now the (6x1) vectors

$$\begin{aligned} \mathbf{q}^T &= \langle q_{11} \quad q_{22} \quad q_{33} \quad 2q_{12} \quad 2q_{23} \quad 2q_{31} \rangle \\ \mathbf{p}^T &= \langle p_{11} \quad p_{22} \quad p_{33} \quad p_{12} \quad p_{23} \quad p_{31} \rangle \end{aligned} \quad (\text{IV-47})$$

with

$$q_{ij} = \frac{\partial f^2}{\partial \tau_{ij}} \quad p_{ij} = \frac{\partial K^2}{\partial \epsilon_{ij}^p}$$

The flow rule (IV-38) in matrix form is

$$d\epsilon^p = \mathbf{q} d\lambda \quad (\text{IV-48})$$

and (IV-46) becomes

$$\mathbf{q}^T d\boldsymbol{\tau} = \mathbf{p}^T d\epsilon^p \quad (\text{IV-49})$$

On combining (IV-44), (IV-45) and (IV-46), we get for $d\lambda$

$$d\lambda (\mathbf{p}^T \mathbf{q} + \mathbf{q}^T \mathbf{C}_e \mathbf{q}) = \mathbf{q}^T \mathbf{C}_e d\boldsymbol{\epsilon} \quad (\text{IV-50})$$

Define $1/\psi = \mathbf{p}^T \mathbf{q} + \mathbf{q}^T \mathbf{C}_e \mathbf{q}$, a scalar. Then

$$d\lambda = \psi \mathbf{q}^T \mathbf{C}_e d\boldsymbol{\epsilon} \quad (\text{IV-51})$$

and the incremental plastic strain vector, again using the flow rule (IV-48)

$$d\epsilon^p = \psi \mathbf{q} \mathbf{q}^T \mathbf{C}_e d\boldsymbol{\epsilon} = \boldsymbol{\Omega} d\boldsymbol{\epsilon} \quad (\text{IV-52})$$

The incremental relation between stress increment and total strain increment follows from the elasticity equation (IV-44)

$$d\boldsymbol{\tau} = \mathbf{C}_e (d\boldsymbol{\epsilon} - d\epsilon^p) = \mathbf{C} d\boldsymbol{\epsilon} \quad (\text{IV-53})$$

where

$$\mathbf{C} = \mathbf{C}_e (\mathbf{I} - \psi \mathbf{q} \mathbf{q}^T \mathbf{C}_e) = \mathbf{C}_e (\mathbf{I} - \mathbf{\Omega}) \quad (\text{IV-54})$$

is the instantaneous stress-strain matrix sought.

IV.2.3.2 Von Mises Yield Criterion

The direct computation of \mathbf{C} is carried out in detail for this important case. Since

$$f^2 = J_2 = K^2 = H(W_p), \quad \frac{\partial f^2}{\partial \tau_{ij}} = s_{ij}$$

we have

$$\begin{aligned} \mathbf{q}^T &= \langle s_{11} \ s_{22} \ s_{33} \ 2s_{12} \ 2s_{23} \ 2s_{31} \rangle \\ \mathbf{p}^T &= H' \boldsymbol{\tau} \end{aligned} \quad (\text{IV-55})$$

Carrying out operations we obtain for an isotropic material

$$\mathbf{p}^T \mathbf{q} = \frac{2}{3} H' \bar{\sigma}^2 \quad \mathbf{q}^T \mathbf{C}_e \mathbf{q} = \frac{2}{3} \frac{E \bar{\sigma}^2}{1 + \nu} \quad (\text{IV-56})$$

where $\bar{\sigma}^2 = 3 J_2$. Therefore

$$\psi = \frac{3}{2 \bar{\sigma}^2} \frac{1}{H' + \frac{E}{1 + \nu}}$$

and

$$\mathbf{\Omega} = \psi \mathbf{q} \mathbf{q}^T \mathbf{C}_e = \beta \begin{bmatrix} s_{11} s_{11} & s_{11} s_{22} & s_{11} s_{33} & s_{11} s_{12} & s_{11} s_{23} & s_{11} s_{31} \\ & s_{22} s_{22} & s_{22} s_{33} & s_{22} s_{12} & s_{22} s_{23} & s_{22} s_{31} \\ & & s_{33} s_{33} & s_{33} s_{12} & s_{33} s_{23} & s_{33} s_{31} \\ & & & 2s_{12} s_{12} & 2s_{12} s_{23} & 2s_{12} s_{31} \\ & & & & 2s_{23} s_{23} & 2s_{23} s_{31} \\ & & & & & 2s_{31} s_{31} \end{bmatrix} \quad (\text{IV-57})$$

where
$$\beta = \frac{\psi E}{1+\nu} = \frac{3}{2\bar{\sigma}^2 \left[1 + \frac{H'}{E}(1+\nu)\right]}$$
 provided $dW_p > 0$

otherwise $\beta = 0$ if $dW_p \leq 0$ (elastic loading or unloading).

IV.2.4 Incremental Relations for Plane Stress and Plane Strain (Von Mises Criterion)

The plane of symmetry is $(x_1, x_2) = (x, y)$. We eliminate $\tau_{13} = \tau_{23} = \epsilon_{13} = \epsilon_{23} = 0$, and consider only (4×1) vectors

$$\boldsymbol{\tau}^T = \langle \tau_{11} \quad \tau_{22} \quad \tau_{12} \quad \tau_{33} \rangle$$

$$\boldsymbol{\epsilon}^T = \langle \epsilon_{11} \quad \epsilon_{22} \quad 2\epsilon_{12} \quad \epsilon_{33} \rangle$$

For plane stress ($\tau_{33} = 0, \epsilon_{33} \neq 0$)

$$\mathbf{C}_e = \frac{E}{1-\nu^2} \begin{bmatrix} 1 & \nu & \cdot & \cdot \\ \nu & 1 & \cdot & \cdot \\ \cdot & \cdot & \frac{1-\nu}{2} & \cdot \\ \cdot & \cdot & \cdot & \cdot \end{bmatrix} \quad (\text{IV-58})$$

For plane strain ($\epsilon_{33} = 0, \tau_{33} \neq 0$)

$$\mathbf{C}_e = \frac{E}{(1+\nu)(1-2\nu)} \begin{bmatrix} 1-\nu & \nu & \cdot & \nu \\ \nu & 1-\nu & \cdot & \cdot \\ \cdot & \cdot & 0.5-\nu & \cdot \\ \nu & \cdot & \cdot & 1-\nu \end{bmatrix} \quad (\text{IV-59})$$

Also

$$\mathbf{q}^T = \langle s_{11} \quad s_{22} \quad 2s_{12} \quad s_{33} \rangle$$

$$\mathbf{p}^T = H' \langle \tau_{11} \quad \tau_{22} \quad \tau_{12} \quad \tau_{33} \rangle \quad (\text{IV-60})$$

$$\mathbf{p}^T \mathbf{q} = \frac{2}{3} H' \bar{\sigma}^2$$

as for the three-dimensional body. However, the expression for $\mathbf{q}^T \mathbf{C}_e \mathbf{q}$ is more complicated in the case of plane stress

$$\mathbf{q}^T \mathbf{C}_e \mathbf{q} = \frac{E}{1-\nu^2} \left[\frac{5-4\nu}{9} (\tau_{11}^2 + \tau_{22}^2) + \frac{2}{9} (5\nu-4) \tau_{11} \tau_{22} + 2(1-\nu) \tau_{12}^2 \right]$$

than for plane strain, where we have again

$$\mathbf{q}^T \mathbf{C}_e \mathbf{q} = 2E \bar{\sigma}^2 / 3(1+\nu)$$

For plane stress, the plastic strain-total strain matrix is

$$\mathbf{\Omega} = \psi \mathbf{q} \mathbf{q}^T \mathbf{C}_e = \beta \begin{bmatrix} s_{11}(s_{11} + \nu s_{22}) & s_{11}(s_{22} + \nu s_{11}) & (1-\nu) s_{11} s_{12} & \cdot \\ s_{22}(s_{11} + \nu s_{22}) & s_{22}(s_{22} + \nu s_{11}) & (1-\nu) s_{22} s_{12} & \cdot \\ 2s_{12}(s_{11} + \nu s_{22}) & 2s_{12}(s_{22} + \nu s_{11}) & 2(1-\nu) s_{12} s_{12} & \cdot \\ \cdot & \cdot & \cdot & \cdot \end{bmatrix} \quad (\text{IV-61})$$

(not symmetric)

with

$$1/\beta = \alpha_1 \bar{\sigma}^2 + \alpha_2 (\tau_{11}^2 + \tau_{22}^2) + \alpha_3 \tau_{11} \tau_{22} + \alpha_4 \tau_{12}^2$$

and

$$\alpha_1 = \frac{2}{3} (1-\nu^2) \frac{H'}{E} \quad \alpha_2 = \frac{5-4\nu}{9} \quad \alpha_3 = \frac{2(5\nu-4)}{9}$$

$$\alpha_4 = 2(1-\nu) \quad \bar{\sigma}^2 = \tau_{11}^2 + \tau_{22}^2 + 3\tau_{12}^2 - \tau_{11} \tau_{22}$$

Therefore we can delete the last row and column and work only with (3x1) vectors $\boldsymbol{\sigma}^T = \langle \sigma_x \sigma_y \tau_{xy} \rangle$ and $\boldsymbol{\epsilon}^T = \langle \epsilon_x \epsilon_y \gamma_{xy} \rangle$. The strain in the $x_3=z$ direction is provided by

$$d\epsilon_{33} = d\epsilon_z = d\epsilon_z^e + d\epsilon_z^p = -\frac{\nu}{1-\nu} (d\epsilon_x^e + d\epsilon_y^e) - (d\epsilon_x^p + d\epsilon_y^p)$$

For plane strain, we have an expression very similar to (IV-57):

$$\mathbf{\Omega} = \psi \mathbf{q} \mathbf{q}^T \mathbf{C}_e = \beta \begin{bmatrix} s_{11} s_{11} & s_{11} s_{22} & s_{11} s_{12} & s_{11} s_{33} \\ & s_{22} s_{22} & s_{22} s_{12} & s_{22} s_{33} \\ & & 2s_{12} s_{12} & s_{12} s_{33} \\ & & & s_{33} s_{33} \end{bmatrix} \quad (\text{IV-62})$$

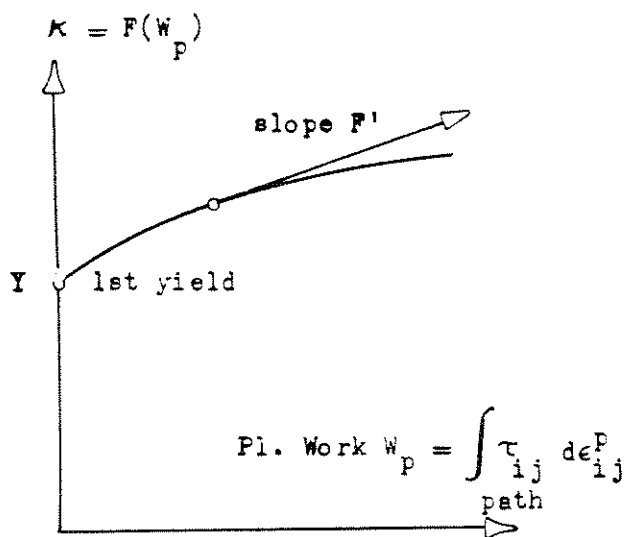


Fig. 4.3 - Work-Hardening Law.

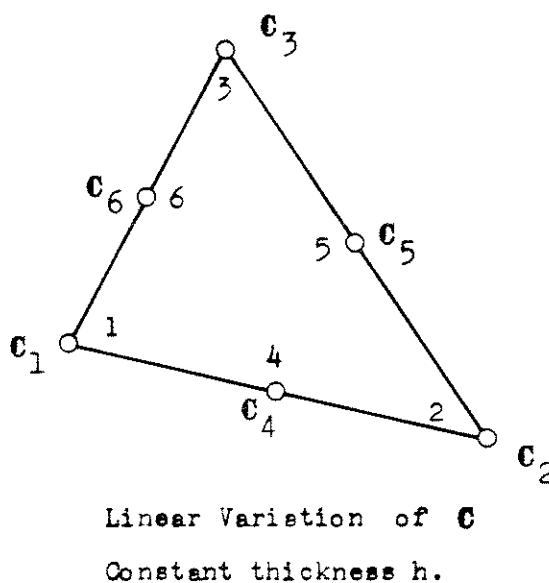


Fig. 4.4 - Element LST-P1

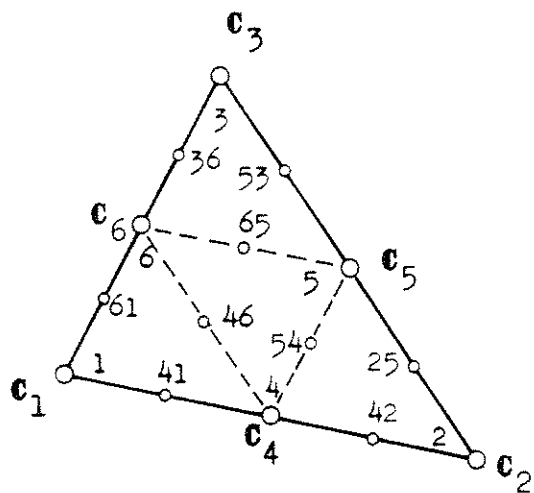


Fig. 4.5 - Element LST-P2.

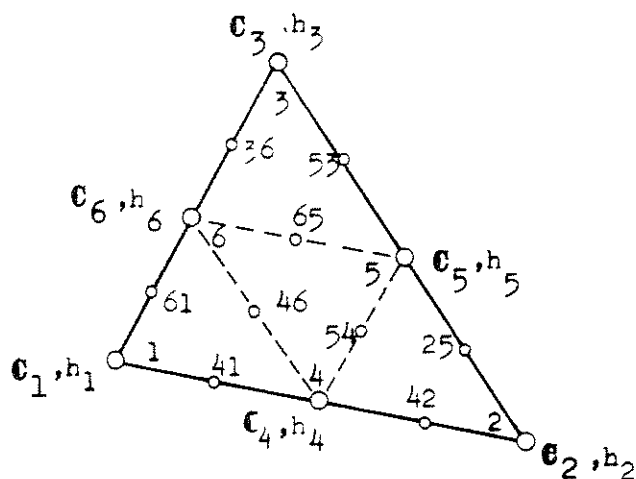


Fig. 4.6 - Element LST-P3.

with

$$\beta = \frac{3}{2\sigma^2} \frac{1}{1 + \frac{H'(1+\nu)}{E}}$$

The stress $\tau_{33} = \sigma_z$ must be retained, but the last column of \mathbf{C} can be deleted since $\epsilon_{33} = \epsilon_z = 0$.

IV.2.5 LST Plane Stress Elements for Elastoplastic Analysis

IV.2.5.1 General Remarks

Up to the present time, most displacement analysis of two or three-dimensional physically nonlinear structures have been carried out with help of simplex elements of constant strain. Since the material remains homogeneous inside such models, the integration necessary to construct the stiffness matrix is trivial.

When dealing with variable strain elements, material properties will vary as soon as the elastic range is exceeded, regardless of the assumptions made for the annealed state. Thus a new approximation is introduced when the variation of the material law (IV-53) is constrained by some type of interpolation function.

If a neat elastic-plastic boundary may be defined and the material is perfectly plastic, a more exact procedure may be attempted: the integration is carried out over two separated subregions in the case of partial plasticity. However, for two or three-dimensional elements, this technique complicates the programming and restricts the generality of the hardening law.

In spite of a more complicated derivation, the improvement obtained by using the linear strain triangle is even greater than for the elastic case.

The assumption of constant strain is more critical in the plasticity problem: a CST "yields" at once, introducing unwanted perturbations in the solution process [47].

The use of the work-hardening hypothesis (IV-32) permits a very simple formulation and programming of any type of plastic behavior, including elastic-perfectly plastic or even work-softening. The strain-hardening formulation employed by Argyris [14], - equivalent to the former one if Von Mises criterion (IV-41) is employed - needs some recasting in order to handle the limiting case of perfect plasticity.

Three types of LST elements are presented in the next paragraphs; the incremental material law (IV-8) is assumed given at a certain nodal system. Therefore, they may be employed for any type of material nonlinearity (they are not restricted to plasticity problems).

IV.2.5.2 LST-P1 Element

We are concerned here with the linear strain triangle described in detail in III.2 for the linear elastic case. The total incremental strain is constrained to vary linearly. For the nodal strain vector we select as usual

$$d\epsilon^T = \langle d\epsilon_x^T \quad d\epsilon_y^T \quad d\delta_{xy}^T \rangle \quad (IV-63)$$

where

$$d\epsilon_x^T = \langle d\epsilon_{x_1} \quad d\epsilon_{x_2} \quad d\epsilon_{x_3} \rangle, \text{ etc}$$

We assume that the current stress-strain law (IV-8) varies linearly over the element (in the sense that each component of the material tensor is a linear function of the coordinates x,y); and therefore determined by its corner values,

where each C_{ij} is a (6x3) submatrix of the form

$$C_{ij} = \frac{1}{4} \begin{bmatrix} 4c_{ij}^1 & \cdot & \cdot \\ \cdot & 4c_{ij}^2 & \cdot \\ \cdot & \cdot & 4c_{ij}^3 \\ c_{ij}^1 + c_{ij}^2 & c_{ij}^1 + c_{ij}^2 & \cdot \\ \cdot & c_{ij}^2 + c_{ij}^3 & c_{ij}^2 + c_{ij}^3 \\ c_{ij}^3 + c_{ij}^1 & \cdot & c_{ij}^3 + c_{ij}^1 \end{bmatrix} \quad (\text{IV-66})$$

c_{ij}^k designates the incremental coefficient c_{ij} at corner k . The integration for the strain energy is trivial when the thickness h is assumed constant.

Since

$$\bar{Q} = \frac{1}{A} \int_A \psi \Phi_{(2)} dA = L_{12} \quad (\text{IV-67})$$

where L_{12} has been tabulated in I.5.1:

$$L_{12} = \frac{1}{60} \begin{bmatrix} 2 & -1 & -1 & 8 & 4 & 8 \\ -1 & 2 & -1 & 8 & 8 & 4 \\ -1 & -1 & 2 & 4 & 8 & 8 \end{bmatrix}$$

The stiffness matrix in terms of nodal strains is, according to

Equation (II-28):

$$N = QD = Ah \begin{bmatrix} N_{11} & N_{12} & N_{13} \\ & N_{22} & N_{23} \\ \text{Symm.} & & N_{33} \end{bmatrix} \quad (\text{IV-68})$$

(9x9)

i.e., $(N_C) = (N_1)$ (Fig. 4.4).

The incremental stress components vary as second order functions; we select $(N_\sigma) = (N_2)$, i.e., corners 1-2-3 plus midpoints 4-5-6. The incremental nodal stress vector is

$$d\sigma^T = \langle d\sigma_x^T \ d\sigma_y^T \ d\tau_{xy}^T \rangle \quad (\text{IV-64})$$

where

$$d\sigma_x^T = \langle d\sigma_{x_1} \ d\sigma_{x_2} \ d\sigma_{x_3} \ d\sigma_{x_4} \ d\sigma_{x_5} \ d\sigma_{x_6} \rangle \quad \text{etc}$$

Now we must evaluate \tilde{C} and $d\tilde{\epsilon}$ at (N_σ) . From their assumed linear variation we have for Equation (II-26)

$$\Lambda = \begin{bmatrix} 1 & \cdot & \cdot \\ \cdot & 1 & \cdot \\ \cdot & \cdot & 1 \\ 1/2 & 1/2 & \cdot \\ \cdot & 1/2 & 1/2 \\ 1/2 & \cdot & 1/2 \end{bmatrix}$$

and C_σ has the structure indicated in Equation (II-31). Therefore, the incremental stress-strain law at (N_σ) is

$$d\sigma = C_\sigma \Lambda d\epsilon = D d\epsilon$$

with

$$D = \begin{bmatrix} C_{11} & C_{12} & C_{13} \\ & C_{22} & C_{23} \\ \text{symm.} & & C_{33} \end{bmatrix} \quad (\text{IV-65})$$

with

$$\mathbf{N}_{ij} = \frac{1}{10} \begin{bmatrix} 6c_{ij}^1 + 2c_{ij}^2 + 2c_{ij}^3 & 2c_{ij}^1 + 2c_{ij}^2 + c_{ij}^3 & 2c_{ij}^1 + c_{ij}^2 + 2c_{ij}^3 \\ & 2c_{ij}^1 + 6c_{ij}^2 + 2c_{ij}^3 & c_{ij}^1 + 2c_{ij}^2 + 2c_{ij}^3 \\ & \text{symm.} & 2c_{ij}^1 + 2c_{ij}^2 + 6c_{ij}^3 \end{bmatrix} \quad (\text{IV-69})$$

We see that \mathbf{N}_{ij} has the same structure as in the elastic element with linearly varying thickness (III-26)

Finally, the incremental stiffness in terms of nodal displacements is

$$\mathbf{K} = Ah \begin{bmatrix} \mathbf{U}^T & \mathbf{0} & \mathbf{V}^T \\ \mathbf{0} & \mathbf{V}^T & \mathbf{U}^T \end{bmatrix} \begin{bmatrix} \mathbf{N}_{11} & \mathbf{N}_{12} & \mathbf{N}_{13} \\ & \mathbf{N}_{22} & \mathbf{N}_{23} \\ \text{symm} & & \mathbf{N}_{33} \end{bmatrix} \begin{bmatrix} \mathbf{U} & \mathbf{0} \\ \mathbf{0} & \mathbf{V} \\ \mathbf{V} & \mathbf{U} \end{bmatrix} \quad (\text{IV-70})$$

where \mathbf{U} and \mathbf{V} are given by (III-15). For the finite displacement analysis, they must be computed taking account of the actual dimensions a_i , b_i .

IV.2.5.3 LST-P2 Element

To account for a more realistic variation of material properties over the element, especially for the case of partial plasticity, we now consider and record the constitutive law at corners and midpoints.

The element is subdivided into 4 subtriangles whose corners are numbered in the following cyclic order (Fig. 4.5):

$$1-4-6; \quad 2-5-4; \quad 3-6-5; \quad 4-5-6$$

Inside each subregion the entries of the stress-strain matrix \mathbf{C} are assumed to vary linearly. This should lead to a closer representation of the actual behavior in the case of the usual hardening laws than a parabolic

variation over the entire element. Therefore this element is made up of four LST-Pl constrained by the linear strain variation over their assembly.

For each subelement we define a nodal vector of incremental corner strains:

$$d\epsilon_{(k)}^T = \langle d\epsilon_{x(k)}^T \quad d\epsilon_{y(k)}^T \quad d\gamma_{xy(k)}^T \rangle$$

(k = subelement no. = 1,2,3,4.)

each $d\epsilon_{ij(k)}$ being a (3x1) vector such as

$$d\epsilon_{x(k)}^T = \langle d\epsilon_{x_1} \quad d\epsilon_{x_2} \quad d\epsilon_{x_3} \rangle, \text{ etc}$$

For the incremental stresses $d\sigma_{ij}$ of quadratic variation over each subelement, we select

$$d\sigma_{(k)}^T = \langle d\sigma_x^T \quad d\sigma_y^T \quad d\tau_{xy}^T \rangle$$

as the (18x1) vector of stresses at corners and midpoints of the k-th subtriangle; for instance, $d\sigma_{x(3)}$ contains the values of $d\sigma_x$ at 3,6,5,36,65,53 (see Fig. 4.5).

The internal work increment for each subelement is given by

$$\frac{1}{2} \Delta^2 U_{(k)} = d\epsilon_{(k)}^T Q d\sigma_{(k)} \quad (\text{IV-71})$$

with

$$Q = A_S h \begin{bmatrix} \bar{Q} & \cdot & \cdot \\ \cdot & \bar{Q} & \cdot \\ \cdot & \cdot & \bar{Q} \end{bmatrix}$$

where \bar{Q} is the numerical matrix (IV-67) and $A_S = A/4$ is the area of each subtriangle.

The incremental strain vectors $d\epsilon_{(k)}$ for each subelement can be related to the vector $d\epsilon$ of corner strains (IV-63) by imposing the linear constraint:

$$d\epsilon_{(k)} = M_{(k)} d\epsilon \quad (\text{IV-72})$$

where

$$M_{(1)} = \begin{bmatrix} 1 & \cdot & \cdot \\ 1/2 & 1/2 & \cdot \\ 1/2 & \cdot & 1/2 \end{bmatrix} \quad \cdot \quad \cdot \quad \cdot \quad \cdot \quad M_{(4)} = \begin{bmatrix} 1/2 & 1/2 & \cdot \\ \cdot & 1/2 & 1/2 \\ 1/2 & \cdot & 1/2 \end{bmatrix}$$

Next, we relate $d\sigma_{(k)}$ to $d\epsilon_{(k)}$ for each subelement through the material law. As for the LST-P1, we obtain again Equation (IV-65):

$$d\sigma_{(k)} = \begin{bmatrix} C_{11(k)} & C_{12(k)} & C_{13(k)} \\ & C_{22(k)} & C_{23(k)} \\ \text{symm.} & & C_{33(k)} \end{bmatrix} d\epsilon_{(k)} \quad (\text{IV-73})$$

where each $C_{ij(k)}$ is a (6x3) submatrix of the type (for $k = 1$)

$$C_{ij(1)} = \frac{1}{4} \begin{bmatrix} 4c_{ij}^1 & \cdot & \cdot \\ \cdot & 4c_{ij}^2 & \cdot \\ \cdot & \cdot & 4c_{ij}^3 \\ c_{ij}^1 + c_{ij}^4 & c_{ij}^1 + c_{ij}^4 & \cdot \\ \cdot & c_{ij}^4 + c_{ij}^6 & c_{ij}^4 + c_{ij}^6 \\ c_{ij}^6 + c_{ij}^1 & \cdot & c_{ij}^6 + c_{ij}^1 \end{bmatrix}$$

For $k = 2, 3, 4$, replace 1-4-6 by 2-5-4, 3-6-5 and 4-5-6.

Finally let

$$\mathbf{N}_{ij(k)} = \mathbf{M}_{(k)}^T \bar{\mathbf{Q}} \mathbf{C}_{ij(k)} \mathbf{M}_{(k)} \quad (\text{IV-74})$$

Then the instantaneous stiffness for subelement (k) in terms of the nodal strains $d\epsilon$ is

$$\mathbf{N}_{(k)} = A_s h \begin{bmatrix} N_{11(k)} & N_{12(k)} & N_{13(k)} \\ & N_{22(k)} & N_{23(k)} \\ \text{symm.} & & N_{33(k)} \end{bmatrix}$$

The complete \mathbf{N} is simply $\mathbf{N}_{(1)} + \mathbf{N}_{(2)} + \mathbf{N}_{(3)} + \mathbf{N}_{(4)}$. Upon substituting (IV-72) and (IV-73) into (IV-74) and adding, we get the following expression for each block \mathbf{N}_{ij}

$$\mathbf{N}_{ij} = \frac{1}{160} \begin{bmatrix} n_{11}^{ij} & n_{12}^{ij} & n_{13}^{ij} \\ & n_{22}^{ij} & n_{23}^{ij} \\ \text{symm.} & & n_{33}^{ij} \end{bmatrix} \quad (\text{IV-75})$$

where $n_{kl}^{ij} = \alpha_{kl}^p C_{ij}^p$ (sum over $p=1,2,3,4,5,6$).

Numerical weights α_{kl}^p are given in the following table:

		Corners			Midpoints		
k	l	p=1	p=2	p=3	p=4	p=5	p=6
1	1	46	2	2	50	10	50
2	2	2	46	2	50	50	10
3	3	2	2	46	10	50	50
1	2	7	7	1	35	15	15
1	3	7	1	7	15	15	35
2	3	1	7	7	15	35	15

We see that the properties at the midpoints have greater weight on the individual element strain energy. If they are the average of the corner properties, i.e., $c_{ij}^4 = (c_{ij}^1 + c_{ij}^2)/2$, etc., we recover the form (IV-69) for the LST-P1 element.

The stiffness matrix in terms of nodal displacements follows now from (IV-70).

IV.2.5.4 LST-P3 Element

For problems involving moderate or large plastic deformations, it is desirable to account for the actual deformed geometry at each step. This can be done by keeping track of the coordinates and thicknesses at the nodal points (the sides are still assumed to remain straight when performing area integrations).

We assume a parabolic variation of thickness $h(\zeta_i)$ determined by its values at the corners and midpoints (Fig. 4.6). This variation is finite, but small in the sense that $\partial h / \partial s \ll 1$, where s is any in-plane direction; therefore the state of plane stress is approximately preserved. As usual, we define a reduced thickness $\xi = h(\zeta_i) / h_r$ and nodal thickness vectors:

$$\begin{aligned} \xi^T &= \langle \xi_1 \ \xi_2 \ \xi_3 \ \xi_4 \ \xi_5 \ \xi_6 \rangle \\ \xi_{(i)} &= \langle \xi_1 \ \xi_4 \ \xi_6 \ \xi_{14} \ \xi_{46} \ \xi_{61} \rangle, \text{ etc} \end{aligned} \quad (\text{IV-76})$$

The variation of the material law $C(\zeta_i)$ is the same as for the LST-P2 element. For each subtriangle "k"

$$\bar{Q}_{(k)} = \frac{1}{A} \int_A \zeta \phi_{(2)}^T \xi_{(k)} \phi_{(2)}^T dA = \sum_{i=1}^6 \xi_{ik} \rho_i^T \quad (\text{IV-77})$$

where

$$\begin{aligned} \rho_1^T &= \frac{1}{5040} \begin{bmatrix} 30 & -4 & -4 & 12 & -4 & 12 \\ 6 & -4 & 1 & -8 & -12 & -4 \\ 6 & 1 & -4 & -4 & -12 & 8 \end{bmatrix} \\ \rho_2^T &= \frac{1}{5040} \begin{bmatrix} -4 & 6 & 1 & -8 & -4 & -12 \\ -4 & 30 & -4 & 12 & 12 & -4 \\ 1 & 6 & -4 & -4 & -8 & -12 \end{bmatrix} \\ \rho_3^T &= \frac{1}{5040} \begin{bmatrix} -4 & 1 & 6 & -12 & -4 & -8 \\ 1 & -4 & 6 & -12 & -8 & -4 \\ -4 & -4 & 30 & 4 & 12 & 12 \end{bmatrix} \\ \rho_4^T &= \frac{1}{5040} \begin{bmatrix} 12 & -8 & -12 & 96 & 32 & 48 \\ -8 & 12 & -12 & 96 & 48 & 32 \\ -4 & -4 & -4 & 32 & 32 & 32 \end{bmatrix} \\ \rho_5^T &= \frac{1}{5040} \begin{bmatrix} -4 & -4 & -4 & 32 & 32 & 32 \\ -12 & 12 & -8 & 48 & 96 & 32 \\ -12 & -8 & 12 & 32 & 96 & 48 \end{bmatrix} \\ \rho_6^T &= \frac{1}{5040} \begin{bmatrix} 12 & -12 & -8 & 48 & 32 & 96 \\ -4 & -4 & -4 & 32 & 32 & 32 \\ -8 & -12 & 12 & 32 & 48 & 96 \end{bmatrix} \end{aligned}$$

Only 12 different integrals need to be computed using Table 3; the matrices are completed by cyclic symmetry.

Thicknesses at auxiliary points are eliminated by using the quadratic interpolation formula over each subelement to get

$$\xi_{(k)} = T_k \xi \quad (\text{IV-78})$$

where

$$T_1 = \frac{1}{8} \begin{bmatrix} 8 & . & . & . & . & . \\ . & . & . & 8 & . & . \\ . & . & . & . & . & 8 \\ 3 & -1 & . & 6 & . & 8 \\ . & -1 & -1 & 4 & 2 & 4 \\ 3 & . & -1 & . & . & 6 \end{bmatrix}$$

$$\begin{aligned}
 \mathbf{T}_2 &= \frac{1}{8} \begin{bmatrix} \cdot & 8 & \cdot & \cdot & \cdot & \cdot \\ \cdot & \cdot & \cdot & \cdot & 8 & \cdot \\ \cdot & \cdot & \cdot & 8 & \cdot & \cdot \\ \cdot & 3 & -1 & \cdot & 6 & \cdot \\ -1 & \cdot & -1 & 4 & 4 & 2 \\ -1 & 3 & \cdot & 6 & \cdot & \cdot \end{bmatrix} \\
 \mathbf{T}_3 &= \frac{1}{8} \begin{bmatrix} \cdot & \cdot & 8 & \cdot & \cdot & \cdot \\ \cdot & \cdot & \cdot & \cdot & \cdot & 8 \\ \cdot & \cdot & \cdot & \cdot & 8 & \cdot \\ -1 & \cdot & 3 & \cdot & \cdot & 6 \\ -1 & -1 & \cdot & 2 & 4 & 4 \\ \cdot & -1 & 3 & \cdot & 6 & \cdot \end{bmatrix} \\
 \mathbf{T}_4 &= \frac{1}{8} \begin{bmatrix} \cdot & \cdot & \cdot & 8 & \cdot & \cdot \\ \cdot & \cdot & \cdot & \cdot & 8 & \cdot \\ \cdot & \cdot & \cdot & \cdot & \cdot & 8 \\ -1 & \cdot & -1 & 4 & 4 & 2 \\ -1 & -1 & \cdot & 2 & 4 & 4 \\ \cdot & -1 & -1 & 4 & 4 & 2 \end{bmatrix}
 \end{aligned}$$

Carrying out the condensation process as for the LST-P2 element, we find again for (IV-75):

$$n_{kl}^{ij} = \alpha_{kl}^P c_{ij}^P$$

but now

$$\alpha_{kl}^P = \beta_{kl}^{Pq} \xi_q \quad (\text{IV-79})$$

$$\text{over } \begin{cases} i, j, k, l = 1, 2, 3 \\ p, q = 1, 2, 3, 4, 5, 6 \end{cases}$$

The 324 weights β_{kl}^{Pq} were obtained from a small computer program and are listed as DATA statement for the array HPLARG in the stiffness subroutine of the plasticity plane stress program (Appendix IV).

IV.3 FINITE DEFORMATION ANALYSIS FOR ARBITRARY ELEMENTS

IV.3.1 Geometrically Nonlinear Problems

Technical publications concerned with the application of finite element methods to large deformation and stability problems are scarce. A survey of the work up to 1965 may be found in a paper by Martin [48]. A common characteristic of most derivations has been the lack of clarity motivated by the use of either pseudo-geometric procedures or unnecessarily awkward analytic computations, displaying a poor understanding of continuum mechanics. None of them, including [48], even mention that the incremented stress tensor is referred to the "initial" geometry and must be corrected to obtain the actual stresses.

The use of the incremental variational principle (IV-9) permits a concise and elegant formulation of the instantaneous geometry stiffness.

In general, the solution of the system (IV-17) requires step-by-step integration; however there are certain important exceptions:

(a) Large elastic deformations (rubberlike materials): instead of the "tangent" or instantaneous stiffness, we may construct, by means of an appropriate variational principle, a "secant" expression, function of the total displacement state. Physical and geometric nonlinearities will usually be coupled. The final equilibrium state in the deformed geometry is obtained by direct iteration.

(b) Large elastic rotations (slender structures: beams, plates, shells). As in (a), a direct iteration procedure may be employed. The computation is simplified if the distortion or change of geometry of the element in its local coordinate system is neglected.

(c) Static critical load. Consider a linear elastic structure subjected to a conservative and constant system of external loads whose amplitude is determined by a single parameter λ (proportional loading). Here U , P and $V = U - P$ are potentials, i.e., functions solely of the total displacement state \mathbf{r} measured from the initial reference configuration. Consider a virtual displacement $\delta \mathbf{r}$ from an equilibrium position. If no internal constraints are imposed, Trefftz's variational criterion of stability [49] is

$$\delta Q > 0, \quad \text{with} \quad 2Q = \delta^2 U = \delta \mathbf{r}^T \mathbf{K} \delta \mathbf{r}$$

At the critical value λ_{cr} , Q becomes positive semidefinite, i.e.,

$$\delta Q = \mathbf{K} \delta \mathbf{r} = (\mathbf{K}_C + \mathbf{K}_G(\lambda)) \delta \mathbf{r} = (\mathbf{K}_C + \lambda \bar{\mathbf{K}}_G) \delta \mathbf{r} = 0 \quad (\text{IV-80})$$

for some nontrivial buckling eigenmode $\delta \mathbf{r}$, and where \mathbf{K} , \mathbf{K}_C and \mathbf{K}_G are stiffness matrices for the complete discretized structure.

If displacements prior to the critical stage are neglected, \mathbf{K}_C and \mathbf{K}_G are constant and (IV-80) becomes a classical eigenvalue problem. Since $\delta \mathbf{r} = 0$ is also a solution, we have always a bifurcation of equilibrium (Fig. 4.7).

If the external forces are not constant, Trefftz's criterion still applies with $Q = V = U - P$.

For nonlinear elastic material, $\mathbf{K}_C = \mathbf{K}_C(\lambda)$ and (IV-80) must be solved by iteration or step-by-step methods. If change in geometry is considered, $\bar{\mathbf{K}}_G = \bar{\mathbf{K}}_G(\lambda)$, in such a case we may find also "asymptotic" instability ($\mathbf{r} \rightarrow \infty$ as $\lambda \rightarrow \lambda_{cr}$) or "snap-through" (no bifurcation or equilibrium), Fig. 4.7.

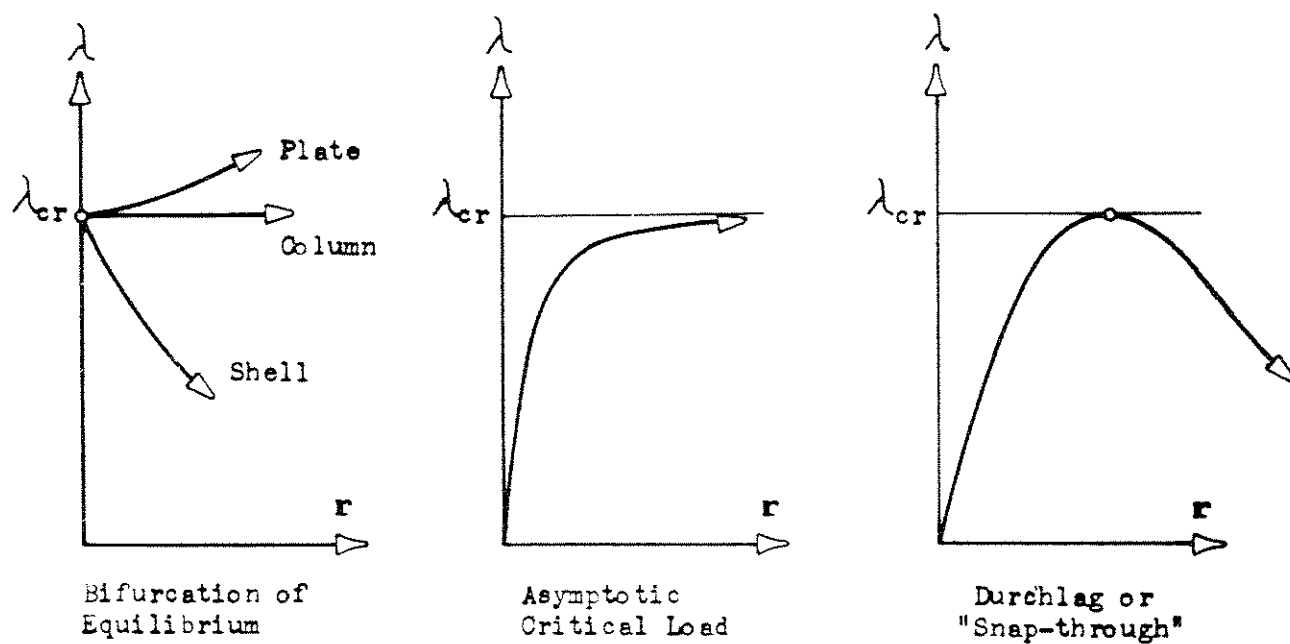


Fig. 4.7 - Elastic Critical Stages.

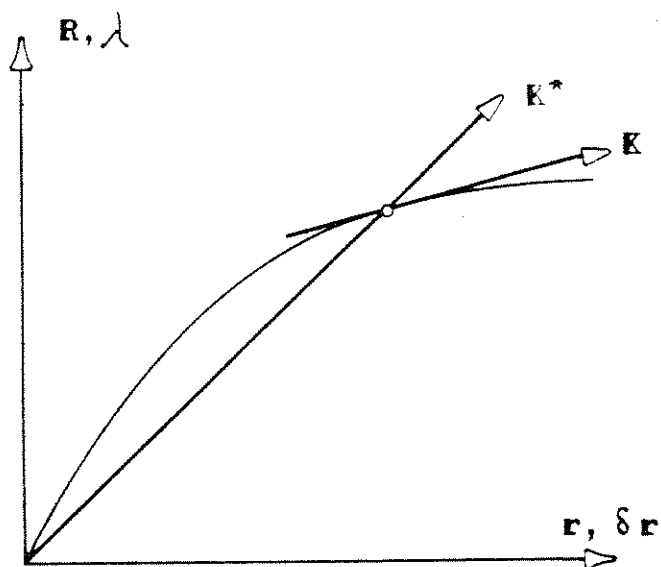


Fig. 4.8 - Secant and Tangent Stiffnesses.

The simplicity of Equation (IV-80) is due to the fact that \mathbf{K} is the instantaneous or tangent stiffness. If we use the "secant stiffness" \mathbf{K}^* (Fig. 4.8), the critical condition occurs for

$$\delta (\mathbf{K}^* \mathbf{r}) = \mathbf{K}^* \delta \mathbf{r} + \mathbf{r} \delta \mathbf{K}^* = 0 \quad (\text{IV-81})$$

only equivalent to (IV-80) for $\mathbf{r} = \mathbf{0}$ or $\mathbf{K}^* = \text{const.}$

For elastic material but nonconservative loading, the more general concept of dynamic stability must be employed [50].

Finally, for nonconservative material and general (multiparameter) loading, critical stages are path-dependent. An example (for one-parameter loading) is provided by Shanley's anelastic column analysis [51].

IV.3.2 Practical Generation of Geometric Stiffness Matrices

In all remaining paragraphs dealing with the finite deformation problem, symbols Δ or d for incremental strains or displacements are suppressed for brevity. The current configuration should be thought of as an initial or "undeformed" reference state.

The derivation will be carried out in rectangular cartesian coordinates; therefore, only lower indices are needed.

We must express the part of the incremental strain energy which generates \mathbf{K}_G , as a quadratic form in the nodal displacements:

$$\frac{1}{2} \Delta^2 U_G = \int_D \tau_{ij} \eta_{ij} dV = \frac{1}{2} \mathbf{r}^T \mathbf{K}_G \mathbf{r} \quad (\text{IV-82})$$

(where η_{ij} and \mathbf{r} stand for $\Delta\eta_{ij}$ and $\Delta\mathbf{r}$ as mentioned above). Let

$$\mathbf{r}^T = \langle \mathbf{u}_1^T \quad \mathbf{u}_2^T \quad \mathbf{u}_3^T \rangle \quad (\text{IV-83})$$

be the nodal component subvectors. For simplicity we assume that the variation of the component u_i is specified only by \mathbf{u}_i . By evaluation of the shape functions (IV-11) at the nodal displacement system we get interpolation formulas of the type

$$u_i(\zeta_n) = \Phi_i^T(\zeta_n) \mathbf{u}_i \quad (i=1,2,3) \quad (\text{IV-84})$$

where ζ_n is an intrinsic coordinate system $(\zeta_1, \zeta_2, \dots, \zeta_r)$ preferably a natural one, for the element. In Equation (IV-84) summation convention does not hold for vector or matrix symbols.

The quadratic terms of the finite strain tensor η_{ij} are

$$2\eta_{ij} = u_{k,i} u_{k,j} = \sum_{k=1}^3 \mathbf{u}_k^T \Phi_{k,i} \Phi_{k,j} \mathbf{u}_k \quad (\text{IV-85})$$

The variation of the initial stress state is specified by

$$\tau_{ij} = \Phi_{\tau_{ij}}^T \boldsymbol{\tau}_{ij} \quad (\text{IV-86})$$

where the $\Phi_{\tau_{ij}}$ may be different for each component $\boldsymbol{\tau}_{ij}$.

If we substitute into the integral (IV-82) we get for \mathbf{K}_G

$$\mathbf{K}_G = \begin{bmatrix} \mathbf{K}_{11} & \cdot & \cdot \\ \cdot & \mathbf{K}_{22} & \cdot \\ \cdot & \cdot & \mathbf{K}_{33} \end{bmatrix} \quad (\text{IV-87})$$

where

$$\mathbf{K}_{nn} = \sum_{i=1}^3 \sum_{j=1}^3 \int_D \Phi_{n,i} \Phi_{\tau_{ij}}^T \boldsymbol{\tau}_{ij} \Phi_{n,j} dV \quad (\text{IV-88})$$

This direct integration of the shape functions for displacement gradients is practical for simple cases; for instance the one-dimensional elements presented in IV.3.3. For refined two or three-dimensional elements it is more convenient to follow the procedure outlined in II.3 for the conventional stiffness. We select nodal point systems $(N_{u_{i,k}})$ for the displacement gradients, and to simplify

$$(N_{u_{i,1}}) = (N_{u_{i,2}}) = (N_{u_{i,3}}) \equiv (N_{\epsilon_i})$$

Therefore

$$\frac{\partial u_i}{\partial x_k} = \Phi_{\epsilon_i}^T u_{i,k} \quad (\text{IV-89})$$

and

$$u_{i,k} = U_{i,k} u_i$$

$U_{i,k}$ being the matrix of vectors $\Phi_{i,k}$ calculated at (N_{ϵ_i}) . Now each block of (IV-87) is

$$K_{nn} = \sum_{i=1}^3 \sum_{j=1}^3 U_{ni}^T \int_D \Phi_{\epsilon_i} \Phi_{\tau_{ij}}^T \tau_{ij} \Phi_{\epsilon_j}^T dV U_{nj} \quad (\text{IV-90})$$

Usually the shape functions are the same for all directions and we only need to evaluate one integral for all i, j . Here, as in Equation (IV-88), $\Phi_{\tau_{ij}}^T \tau_{ij}$ is a scalar multiplying all entries of the matrix $\Phi_{\epsilon_i} \Phi_{\epsilon_j}^T$.

For elements of constant strain and stress, the integrals of (IV-90) are simply $\tau_{ij} V$ (scalars).

For the frequent case of infinitesimal extensional strains but finite rotations, we might start from expressions for η_{ij} explicitly containing rotations and infinitesimal strains, i.e.,

$$\eta_{ij} = \frac{1}{2} (\epsilon_{ik} + \omega_{ik})(\epsilon_{jk} + \omega_{jk}) \quad (\text{IV-91})$$

and neglecting systematically certain terms like $\epsilon_{ik}\epsilon_{jk}$, $\epsilon_{ik}\omega_{jk}$, etc. However, it is more convenient and not more complicated (when working in natural coordinates), to carry out the exact derivation, neglecting terms only after examining the complete expression.

IV.3.3 Examples

The direct integration of Equation (IV-88) is applied to the derivation of the geometric stiffness of the two simplest (but important) one-dimensional elements.

IV.3.3.1 Stringer or Truss Member

Consider the prismatic truss element 1-2 of area A and length L in the present configuration \square , which may move on the x - y plane of a local cartesian system moving with the element (Fig. 4.9).

Let

$$\eta_2 = x/L \quad \eta_1 = 1 - \eta_2$$

be dimensionless natural coordinates of the stringer; then if

$$\mathbf{r}^T = \langle \mathbf{u}^T \quad \mathbf{v}^T \rangle$$

$$\mathbf{u}^T = \langle u_1 \quad u_2 \rangle$$

$$\mathbf{v}^T = \langle v_1 \quad v_2 \rangle$$

$$\eta^T = \langle \eta_1 \quad \eta_2 \rangle$$

$$\mathbf{u} = \eta^T \mathbf{u} \quad \mathbf{v} = \eta^T \mathbf{v}$$

Only the stress $\sigma_x = (P_2 - P_1)/A$ is present, hence (IV-82) becomes

$$\frac{1}{2} \Delta^2 U_G = \int \eta_{xx} \sigma_x dV = \frac{P_2 - P_1}{A} \eta_{xx}$$

but

$$\eta_{xx} = \frac{1}{2} \left(\frac{\partial u}{\partial x} \right)^2 + \frac{1}{2} \left(\frac{\partial v}{\partial x} \right)^2 = \frac{1}{2} \mathbf{u}^T \mathbf{a} \mathbf{a}^T \mathbf{u} + \frac{1}{2} \mathbf{v}^T \mathbf{a} \mathbf{a}^T \mathbf{v}$$

where

$$\mathbf{a} = \frac{1}{L} \langle 1 \quad -1 \rangle = \frac{\partial \psi}{\partial x}$$

so

$$\mathbf{K}_G = \frac{P}{L} \begin{bmatrix} 1 & -1 & \cdot & \cdot \\ -1 & 1 & \cdot & \cdot \\ \cdot & \cdot & 1 & -1 \\ \cdot & \cdot & -1 & 1 \end{bmatrix} \quad (\text{IV-91})$$

If we neglect the effect of the shortening and consider only the effect of the transversal displacement \mathbf{v} ,

$$\mathbf{K}_G = \frac{P}{L} \begin{bmatrix} \cdot & \cdot & \cdot & \cdot \\ \cdot & \cdot & \cdot & \cdot \\ \cdot & \cdot & 1 & -1 \\ \cdot & \cdot & -1 & 1 \end{bmatrix} \quad (\text{IV-92})$$

IV.3.3.2 Beam-Column

A prismatic beam-column element of symmetric cross-section is loaded on its (x-y) plane of symmetry. The element is assumed to be straight at the state \square so that axial force and bending effect are still uncoupled; however actual length L and cross section properties A and I should be used (Fig. 4.10).

We use the same natural coordinates $\xi_2 = x/L$, $\xi_1 = 1 - \xi_2$ of the stringer. Let

$$\mathbf{r}^T = \langle u_1 \quad u_2 \quad v_1 \quad v_2 \quad \theta_1 \quad \theta_2 \rangle$$

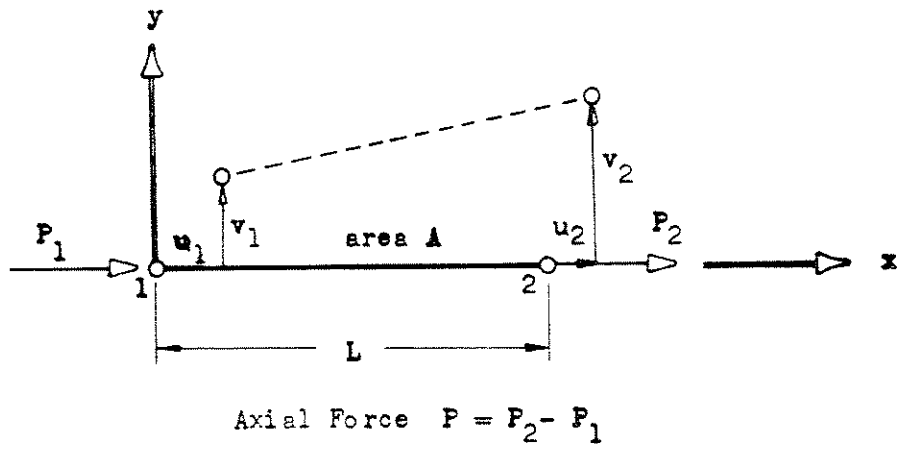


Fig. 4.9 - Stringer or Truss Member.

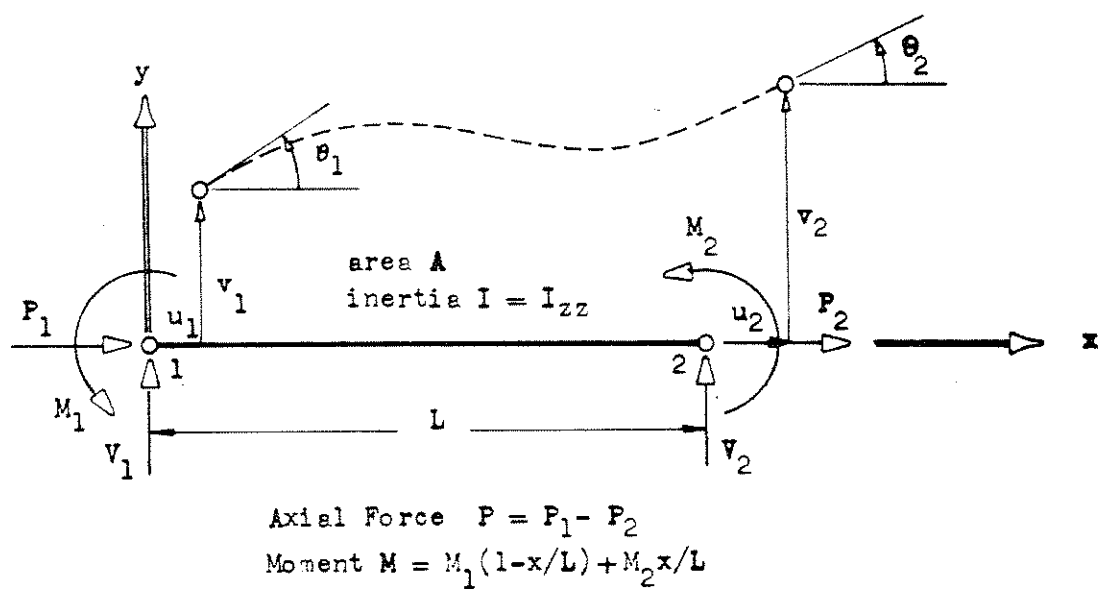


Fig. 4.10 - Beam - Column.

The incremental displacement field referred to the local (x-y) system is

$$v = \mathbf{r}^T \begin{Bmatrix} 0 \\ 0 \\ \zeta_1^2 (3-2\zeta_1) \\ \zeta_2^2 (3-2\zeta_2) \\ L \zeta_1^2 \zeta_2 \\ L \zeta_1 \zeta_2^2 \end{Bmatrix} = \mathbf{r}^T \boldsymbol{\phi}_v$$

$$u = u_1 \zeta_1 + u_2 \zeta_2 - y \frac{\partial v}{\partial x} = \mathbf{r}^T \begin{Bmatrix} \zeta_1 \\ \zeta_2 \\ 6y \zeta_1 (1-\zeta_1)/L \\ -6y \zeta_2 (1-\zeta_2)/L \\ y \zeta_1 (2-3\zeta_1) \\ y \zeta_2 (2-3\zeta_2) \end{Bmatrix} = \mathbf{r}^T \boldsymbol{\phi}_u$$

We neglect the work of the shear stresses and consider only the normal stress $\tau_{11} = \sigma_x$ on the quadratic strain η_{xx} :

$$\frac{1}{2} \Delta^2 U_G = \int_D \sigma_x \eta_{xx} dV$$

where, as for the stringer

$$\eta_{xx} = \frac{1}{2} \left(\frac{\partial u}{\partial x} \right)^2 + \frac{1}{2} \left(\frac{\partial v}{\partial x} \right)^2$$

and σ_x is assumed to be given by the engineer's theory of bending

$$\sigma_x = \frac{P}{A} + (M_1 \zeta_1 + M_2 \zeta_2) \frac{y}{I}$$

where $P = P_2 - P_1$ is the axial force. We split the geometric stiffness matrix as

$$K_G = K_{Gu} + K_{Gv}$$

with

$$K_{Gu} = \int \boldsymbol{\phi}_{ux} \sigma_x \boldsymbol{\phi}_{ux}^T dV$$

$$K_{Gv} = \int \boldsymbol{\phi}_{vx} \sigma_x \boldsymbol{\phi}_{vx}^T dV$$

K_{Gv} is associated with the large rotation about z , and K_{Gu} with the axial displacements (shortening plus bending distortion)

With

$$\phi_{vx} = \frac{\partial \phi_v}{\partial x} = \begin{Bmatrix} 0 \\ 0 \\ -6\zeta_1(1-\zeta_1)/L \\ 6\zeta_2(1-\zeta_2)/L \\ \zeta_1(3\zeta_1-2) \\ \zeta_2(3\zeta_2-2) \end{Bmatrix}$$

we obtain immediately the well-known result [48]

$$K_{Gv} = \frac{P}{30} \begin{bmatrix} \cdot & \cdot & \cdot & \cdot & \cdot & \cdot \\ \cdot & \cdot & \cdot & \cdot & \cdot & \cdot \\ \cdot & \cdot & 36/L & -36/L & 3 & 3 \\ \cdot & \cdot & -36/L & 36/L & -3 & -3 \\ \cdot & \cdot & 3 & -3 & 4L & L \\ \cdot & \cdot & 3 & -3 & L & 4L \end{bmatrix} \quad (\text{IV-93})$$

The bending stress $(M_1\zeta_1 + M_2\zeta_2)y/I$ do not contribute to the integral since $\int_A y dA = 0$.

To compute K_{Gu} we need

$$\phi_{ux} = \frac{\partial \phi_u}{\partial x} = \begin{Bmatrix} -1/L \\ +1/L \\ 6y(2\zeta_1-1)/L^2 \\ 6y(2\zeta_2-1)/L^2 \\ 2y(3\zeta_1-1)/L \\ -2y(3\zeta_2-1)/L \end{Bmatrix}$$

Then

$$K_{Gu} = K_{Gu}^{(P)} + K_{Gu}^{(M_1)} + K_{Gu}^{(M_2)}$$

where we have separated the contributions of the axial force P and of the end moments M_1 and M_2 . For $K_{Gu}^{(P)}$ we get

$$K_{Gu}^{(P)} = \frac{P}{A} \begin{bmatrix} A/L & -A/L & \cdot & \cdot & \cdot & \cdot \\ & A/L & \cdot & \cdot & \cdot & \cdot \\ & & 12I/L^3 & -12I/L^3 & -6I/L^2 & 6I/L^2 \\ & & & 12I/L^3 & -6I/L^2 & 6I/L^2 \\ \text{symm.} & & & & 4I/L & 2I/L \\ & & & & & 4I/L \end{bmatrix} \quad (\text{IV-94})$$

To simplify the expressions for $K_{Gu}^{(M_1)}$ and $K_{Gu}^{(M_2)}$ we suppose that

$$\int_A y^3 dA = 0$$

i.e., a doubly symmetric section. Then

$$K_{Gu}^{(M_1)} = \frac{M_1}{L^3} \begin{bmatrix} \cdot & \cdot & -1 & 1 & -L & \cdot \\ & \cdot & 1 & -1 & \cdot & L \\ & & \cdot & \cdot & \cdot & \cdot \\ \text{symm.} & & & \cdot & \cdot & \cdot \\ & & & & \cdot & \cdot \\ & & & & & \cdot \end{bmatrix} \quad (\text{IV-95})$$

and similarly for $K_{Gu}^{(M_2)}$. If $\int_A y^3 dA \neq 0$, the (4x4) elements of the right bottom corner do not vanish.

The contribution of K_{Gu} is usually ignored in buckling problems.

IV.4 GEOMETRIC STIFFNESS OF PLANE STRESS TRIANGULAR ELEMENTS

IV.4.1 General Derivation

The initial stress or geometric stiffness K_G of plane stress elements finds application in the problems of large deflection and stability of two-dimensional structures (slices, plates, shells) under predominantly in-plane action.

We consider the triangle 1-2-3 of Fig. 1.1 in the instantaneous or present configuration \square referred to a right handed cartesian frame x-y-z, the x-y plane determined by the 3 corners. This local cartesian system moves with the element and measures its actual geometry during a step-by-step solution.

To simplify the general derivation we make use of the following assumptions:

(a) the element type does not change; this implies that for refined displacement expansions (polynomial order ≥ 2):

element midsurface is approximately plane so that the coupling of bending and in-plane forces is neglected;

sides are assumed to remain straight so that all previously derived interpolation formulas hold; the error introduced is very small if the local distortion is negligible compared with the global displacements (see remarks at the end of II.1.1).

(b) incremental transverse displacements are function of x,y alone, i.e., $w = w(x,y)$.

The vector of nodal displacements is

$$\mathbf{r}^T = \langle \mathbf{u}^T \mathbf{v}^T \mathbf{w}^T \rangle \quad (\text{IV-96})$$

and the displacement functions in triangular coordinates

$$u(\xi_i) = \Phi^T \mathbf{u} \quad v(\xi_i) = \Phi^T \mathbf{v} \quad w(\xi_i) = \Phi^T \mathbf{w} \quad (\text{IV-97})$$

The displacement gradients are

$$\begin{Bmatrix} u_x(\xi_i) \\ v_x(\xi_i) \\ w_x(\xi_i) \end{Bmatrix} = \begin{bmatrix} \Phi_x^T & \cdot & \cdot \\ \cdot & \Phi_x^T & \cdot \\ \cdot & \cdot & \Phi_{wx}^T \end{bmatrix} \mathbf{r}$$

$$\begin{Bmatrix} u_y(\xi_i) \\ v_y(\xi_i) \\ w_y(\xi_i) \end{Bmatrix} = \begin{bmatrix} \Phi_y^T & \cdot & \cdot \\ \cdot & \Phi_y^T & \cdot \\ \cdot & \cdot & \Phi_{wy}^T \end{bmatrix} \mathbf{r} \quad (\text{IV-98})$$

$$u_z = v_z = w_z = 0$$

Proceeding as indicated in IV.3.2, we define nodal vectors for all displacement gradients

$$\mathbf{u}_x (= \mathbf{e}_x) , \mathbf{v}_x , \text{ etc}$$

so that

$$u_x(\xi_i) = \Phi^T \mathbf{u}_x , \text{ etc}$$

Evaluating ϕ_x , ϕ_y , ϕ_{wx} and ϕ_{wy} at the nodal systems of the displacement gradients, we get

$$\begin{Bmatrix} u_x \\ v_x \\ w_x \end{Bmatrix} = \begin{bmatrix} U & \cdot & \cdot \\ \cdot & U & \cdot \\ \cdot & \cdot & U_w \end{bmatrix} \mathbf{r}$$

$$\begin{Bmatrix} u_y \\ v_y \\ w_y \end{Bmatrix} = \begin{bmatrix} V & \cdot & \cdot \\ \cdot & V & \cdot \\ \cdot & \cdot & V_w \end{bmatrix} \mathbf{r}$$

(IV-99)

The components of the quadratic strain tensor working on the in-plane stresses are

$$2\eta_{xx} = u_x^T \phi_\epsilon \phi_\epsilon^T u_x + v_x^T \phi_\epsilon \phi_\epsilon^T v_x + w_x^T \phi_\epsilon \phi_\epsilon^T w_x$$

$$2\eta_{yy} = u_y^T \phi_\epsilon \phi_\epsilon^T u_y + v_y^T \phi_\epsilon \phi_\epsilon^T v_y + w_y^T \phi_\epsilon \phi_\epsilon^T w_y$$

(IV-100)

$$2\eta_{xy} = u_x^T \phi_\epsilon \phi_\epsilon^T u_y + u_y^T \phi_\epsilon \phi_\epsilon^T u_x + v_x^T \phi_\epsilon \phi_\epsilon^T v_y + v_y^T \phi_\epsilon \phi_\epsilon^T v_x + w_x^T \phi_\epsilon \phi_\epsilon^T w_y + w_y^T \phi_\epsilon \phi_\epsilon^T w_x$$

Initial stress components are represented by

$$\sigma_x(\zeta_i) = \phi_\sigma \sigma_x, \text{ etc}$$

(IV-101)

and the thickness variation by

$$h(\zeta_i) = h_r \Phi_{\xi}^T \xi \quad (\text{IV-102})$$

Introducing Equations (IV-100), (IV-101) and (IV-102) into the general expression (IV-90) for K_G , we may express again the final result in the following block form:

$$K_G = \begin{bmatrix} K_{Guu} & \cdot & \cdot \\ \cdot & K_{Gvv} & \cdot \\ \cdot & \cdot & K_{Gww} \end{bmatrix} \quad (\text{IV-103})$$

which reflects the decoupling (IV-97) of the displacement components and where

$$K_{Guu} = K_{Gvv} = A h_r \begin{bmatrix} \mathbf{U}^T & \mathbf{V}^T \end{bmatrix} \begin{bmatrix} \mathbf{J}_{xx} & \mathbf{J}_{xy} \\ \mathbf{J}_{xy}^T & \mathbf{J}_{yy} \end{bmatrix} \begin{bmatrix} \mathbf{U} \\ \mathbf{V} \end{bmatrix} \quad (\text{IV-104})$$

with

$$\mathbf{J}_{xx} = \frac{1}{A} \int_A \Phi_{\epsilon} \Phi_{\sigma}^T \sigma_x \Phi_{\xi}^T \xi \Phi_{\epsilon}^T dA \quad (\text{IV-105})$$

for \mathbf{J}_{yy} and \mathbf{J}_{xy} replace σ_x by σ_y and τ_{xy} , respectively; no new integrals need to be evaluated.

For the block K_{Gww} we have a similar expression, but with \mathbf{U}_w , \mathbf{V}_w and $\Phi_{\epsilon w}$ in (IV-104) and (IV-105).

If the transversal displacement law is the same of the in-plane components ($\Phi_w = \Phi$), the three blocks $K_{Guu} = K_{Gv} = K_{Gww}$ are identical.

Finally, if we consider only the geometric nonlinearity introduced by the transverse displacements (large rotations), we can delete the first two diagonal blocks and use

$$\mathbf{K}_G = \begin{bmatrix} \cdot & \cdot & \cdot \\ \cdot & \cdot & \cdot \\ \cdot & \cdot & \mathbf{K}_{G_{ww}} \end{bmatrix} \quad (\text{IV-106})$$

IV.4.2 Constant Strain Triangle

The initial stress field and all displacement gradients are constant over the element. For constant thickness we get

$$J_x = \sigma_x \quad J_y = \sigma_y \quad J_{xy} = \tau_{xy}$$

Using Equation (III-3) we find for each block of \mathbf{K}_G :

$$\mathbf{K}_{G_{uu}} = \mathbf{K}_{G_{vv}} = \mathbf{K}_{G_{ww}} = \frac{h}{4A} \begin{bmatrix} b_1 & a_1 \\ b_2 & a_2 \\ b_3 & a_3 \end{bmatrix} \begin{bmatrix} \sigma_x & \tau_{xy} \\ \tau_{xy} & \sigma_y \end{bmatrix} \begin{bmatrix} b_1 & b_2 & b_3 \\ a_1 & a_2 & a_3 \end{bmatrix} \quad (\text{IV-107})$$

For arbitrary thickness variation we can replace h by its area average (III-8) without error.

This simple derivation should be contrasted with the long analytic computation performed in [48], or the unnecessary appeal to geometric arguments, "natural" strains and loads, etc., in [18] and [14]. The confusion of material and spatial coordinates is deplorable.

IV.4.3 Linearly Varying Strain Triangle

The initial stress field is assumed to be linear and determined by the corner values, i.e., $\sigma_x = \psi_1^T \sigma_x$, etc. Then for a constant thickness, integrals (IV-105) for the in-plane blocks become

$$\begin{aligned} \mathbf{J}_{xx} &= \frac{1}{A} \int_A \psi_1 \psi_1^T \sigma_x \psi_1^T dA = \\ &= \frac{1}{60} \left\{ \begin{array}{l} \begin{bmatrix} 6 & 2 & 2 \\ 2 & 2 & 1 \\ 2 & 1 & 2 \end{bmatrix} \sigma_{x_1} + \begin{bmatrix} 2 & 2 & 1 \\ 2 & 6 & 2 \\ 1 & 2 & 2 \end{bmatrix} \sigma_{x_2} + \begin{bmatrix} 2 & 1 & 2 \\ 1 & 2 & 2 \\ 2 & 2 & 6 \end{bmatrix} \sigma_{x_3} \end{array} \right\} \end{aligned} \quad (\text{IV-108})$$

with similar expressions for \mathbf{J}_{yy} and \mathbf{J}_{xy} . Blocks \mathbf{K}_{Guu} and \mathbf{K}_{Gvv} are easily constructed from (IV-104) by using submatrices \mathbf{U} and \mathbf{V} given by Equations (III-15), where actual triangle dimensions should be employed.

If the variation of $w(\psi_i)$ is only linear, \mathbf{J}_{xxw} , \mathbf{J}_{yyw} and \mathbf{J}_{xyw} become scalars

$$\mathbf{J}_{xxw} = \frac{1}{A} \int_A \psi_1^T \sigma_x dA = \frac{1}{3} (\sigma_{x_1} + \sigma_{x_2} + \sigma_{x_3}), \text{ etc}$$

If the variation of w is parabolic, $\mathbf{K}_{Guu} = \mathbf{K}_{Gvv} = \mathbf{K}_{Gww}$.

Any other variation for stress components and thickness may be assumed. For instance, if the stress field is parabolic and determined by their corner and midpoint values, and the thickness is constant,

$$\begin{aligned} \mathbf{J}_{xx} &= \frac{1}{180} \left\{ \begin{array}{l} \begin{bmatrix} 6 & 0 & 0 \\ 0 & -2 & -1 \\ \cdot & -1 & -2 \end{bmatrix} \sigma_{x_1} + \begin{bmatrix} -2 & 0 & -1 \\ 0 & 6 & 0 \\ -1 & 0 & -2 \end{bmatrix} \sigma_{x_2} + \begin{bmatrix} -2 & -1 & 0 \\ -1 & -2 & 0 \\ 0 & 0 & 6 \end{bmatrix} \sigma_{x_3} \\ + \begin{bmatrix} 12 & 8 & 4 \\ 8 & 12 & 4 \\ 4 & 4 & 4 \end{bmatrix} \sigma_{x_4} + \begin{bmatrix} 4 & 4 & 4 \\ 4 & 12 & 8 \\ 4 & 8 & 12 \end{bmatrix} \sigma_{x_5} + \begin{bmatrix} 12 & 4 & 8 \\ 4 & 4 & 4 \\ 8 & 4 & 12 \end{bmatrix} \sigma_{x_6} \end{array} \right\} \end{aligned} \quad (\text{IV-109})$$

V. APPLICATION OF THE LINEAR STRAIN TRIANGLE

V.1 LINEAR ELASTIC PROBLEMS

V.1.1 Procedure

The following examples have been selected to illustrate the application of the linear strain triangle (LST) to some problems of linear elasticity. To simplify the comparison with analytic solutions, only isotropic material was considered.

All LST meshes were processed by a digital computer program using single six nodal point triangles as basic elements; the equilibrium equations were solved by a block S.O.R. iterative technique accelerated by group relaxation based on energy balance [17]. The internal stresses at the nodal points were averaged over all contributing elements having the same material properties.

A new and more efficient production program which makes use of an eight nodal point quadrilateral as basic block and a large capacity band solver for nodal displacements, is described in Appendix III; a fifth example analyzed with this program is presented there.

V.1.2 Cantilever Beam

A 4:1 cantilever beam is loaded with a parabolically varying end shear; the root is considered to be completely fixed. Four idealizations were considered (Fig. 5.1).

Meshes A-1 (CST) and B-1(LST) have 160 degrees of freedom each (after B.C.'s have been imposed) and thus directly comparable. Likewise meshes A-2 (CST) and B-2(LST), each with 576 degrees of freedom.

A comparison of end deflections and some internal stresses is presented in Fig. 5.2. For this problem, the elasticity solution coincides with the beam theory, except in the proximity of the built-in end where the full clamping condition constitutes a mixed problem of elasticity for which there is no closed form solution. The value given as theoretical end deflection

$$\delta_{th} = \frac{PL^3}{3EI} + \frac{4+5\nu}{2} \frac{PL}{EH} = 0.35583 \text{ in.}$$

is exact if the root section is free to warp but points A, B and A' (Fig. 5.1) are fixed. Therefore δ_{th} is an upper bound for the exact tip deflection δ_{ex} on the other hand, end deflections (direct influence coefficients) obtained from a compatible finite element analysis are lower bounds. An inspection of the values given by both LST meshes indicates that δ_{th} is very close to δ_{ex} and that their error is less than 1/2000 in any case. Normal stresses are predicted with a similar degree of accuracy when compared with the beam theory at a certain distance from the root. Both CST meshes are quite stiff; even the finer idealization yields an end deflection 5% below the correct value.

The variation of the shear stress τ_{xy} at a typical section away from the support is interesting: the element stresses for the fine CST mesh oscillate about the exact curve; the nodal point stresses obtained by Wilson's weighted averaging scheme [17] are significantly better at internal points, but a high residual stress is recorded at the boundary. The corresponding LST mesh produces a perfect fit of the parabola by straight lines.

Stress computer plots for the fine meshes are presented in Figs. 5.3 to 5.6. They were produced by linear interpolation of averaged corner nodal

stresses over a CST element; for a LST mesh each triangle is divided into four by joining the midpoints and the averaged nodal stresses at corners and midpoints (no longer the exact average of the adjoining corner values) taken as corner values for the subdivided mesh.

The LST mesh gives a better representation of the stress concentration at the root (Fig. 5.4) and less residual stress at boundary points (Fig. 5.5). It should be noted, however, that the performance of the CST is particularly poor for the simulation of bending deformation of slender structures.

V.1.3 Circular Hole in Tension Plate

This example was intended to test the performance of the higher order element for a problem of stress concentration due to geometry. The plate and load system are depicted in Fig. 5.7. Only a quadrant was analyzed; the four finite element idealizations (generated by a small computer program) are presented in Fig. 5.8. Both CST and LST meshes were employed.

Plots of σ_y / ρ at the symmetry section $y = 0$ for the four LST meshes are compared in Fig. 5.9 with Howland's analytic solution for a plate of finite width [53]. This solution should not be considered as extremely exact since it was evaluated numerically from a series of extremely poor convergence, especially away from the hole.

The comparison of stress concentration factors obtained with both types of elements (Fig. 5.10) indicates that the behavior of the CST is not so poor as in the first example; superior deformation characteristics of the LST are partially compensated by a better fitting of the curved boundary for the same

number of degrees of freedom. Consistently smaller CST concentration factors are caused by the fact that the value taken as boundary stress is actually representative of the stress at an internal point (within the edge elements).

Stress contour graphs for LST meshes No. 2 and No. 4 are presented in Figs. 5.11 and 5.12. If the latter is considered as exact, the stress patterns of mesh No. 2 may be regarded as sufficiently accurate for many practical purposes

V.1.4 Circular Disk Diametrically Loaded

This is a classical example of stress concentration caused by concentrated loads. The two LST idealizations for a quadrant of the disk are shown in Fig. 5.13. The quadrilateral subdivision was generated as a system of equally spaced bipolar coordinate curves, except near the poles (load points). Therefore the corner points lie on two orthogonal families of circles, which are also the isostatics for this problem.

Results of the analysis are presented in Figs. 5.14, 5.15 and 5.16 in the form of computer plots of stress contour lines for both meshes and for the exact solution applied to the nodal points of mesh No. 2.

The high degree of accuracy that may be attained for the stress patterns is evident. The most sensitive variation is that of the tensile principal stress σ_{\max} which is theoretically constant along the diameter $x = 0$ except at the load points, where infinite compressive stresses are necessary to restore equilibrium. This singularity is reflected in the instability of the contour lines for the elements near the load.

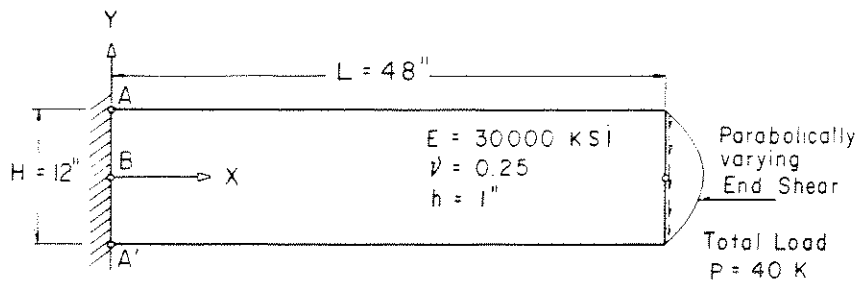
V.1.5 Buried Concrete Pipe

This example illustrates the versatility of application of the finite element method to problems with different materials, and the capability of the eight nodal point quadrilateral composed by four LST elements to simulate bending deformations. Fig. 5.17 shows the problem and the finite element idealization; since we are dealing with a plane strain problem, modified parameters E' and ν' were input for the plane stress program. Results for the concrete tube are presented in Fig. 5.18 and are self-explanatory. Stress contours of soil stresses were also printed by the program but not reproduced here.

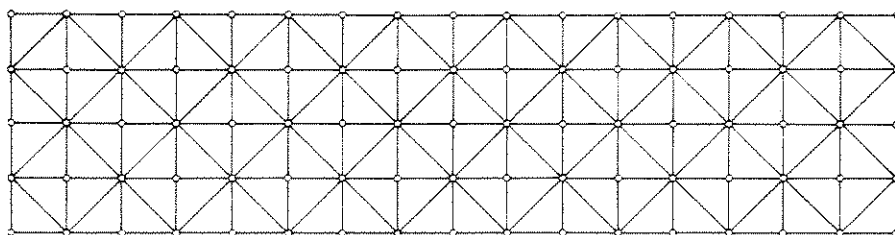
V.2 ELASTOPLASTIC PROBLEMS

V.2.1 Procedure

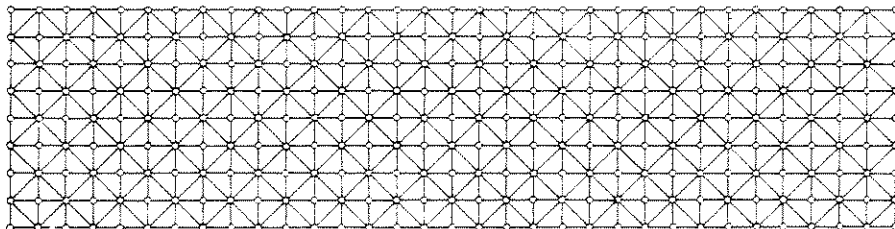
All examples were processed by the computer program for elastoplastic plane stress problems described in Appendix IV. The step-by-step analysis may be carried out considering either small (i.e., infinitesimal) or finite displacements. In the first case, the instantaneous stiffness consists only of the conventional part and is evaluated in the initial geometry. In the case of finite displacements, the geometric stiffness for a quadratic variation of initial stress (IV.4.4) is added, in-plane coordinates and thicknesses are actualized, and the incremented rotated stresses are transformed to actual (x-y) stresses after each step. The midpoint rule (IV.1.5) was used for the numerical solution; two displacement solutions are required at each step.



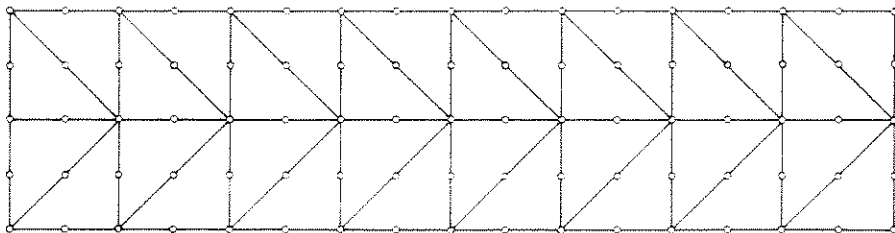
BEAM AND LOAD SYSTEM



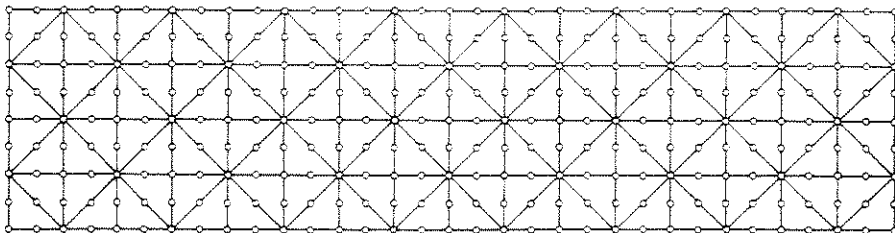
MESH A-1 - 128 CSTs



MESH A-2 - 512 CSTs



MESH B-1 - 32 LSTs



MESH B-2 - 128 LSTs

FIG. 5.1-CANTILEVER BEAM AND FINITE ELEMENT IDEALIZATIONS

DEFLECTION AND NORMAL STRESS			
Element	Mesh	Tip Deflection $\delta = v_C$	Stress σ_x at $X = 9", Y = 6"$
CST	A-1	0.30556	51.225
	A-2	0.34188	57.342
LST	B-1	0.35506	59.145
	B-2	0.35569	60.024
Beam Theory (upper bound for v_C)		0.35583	60.000

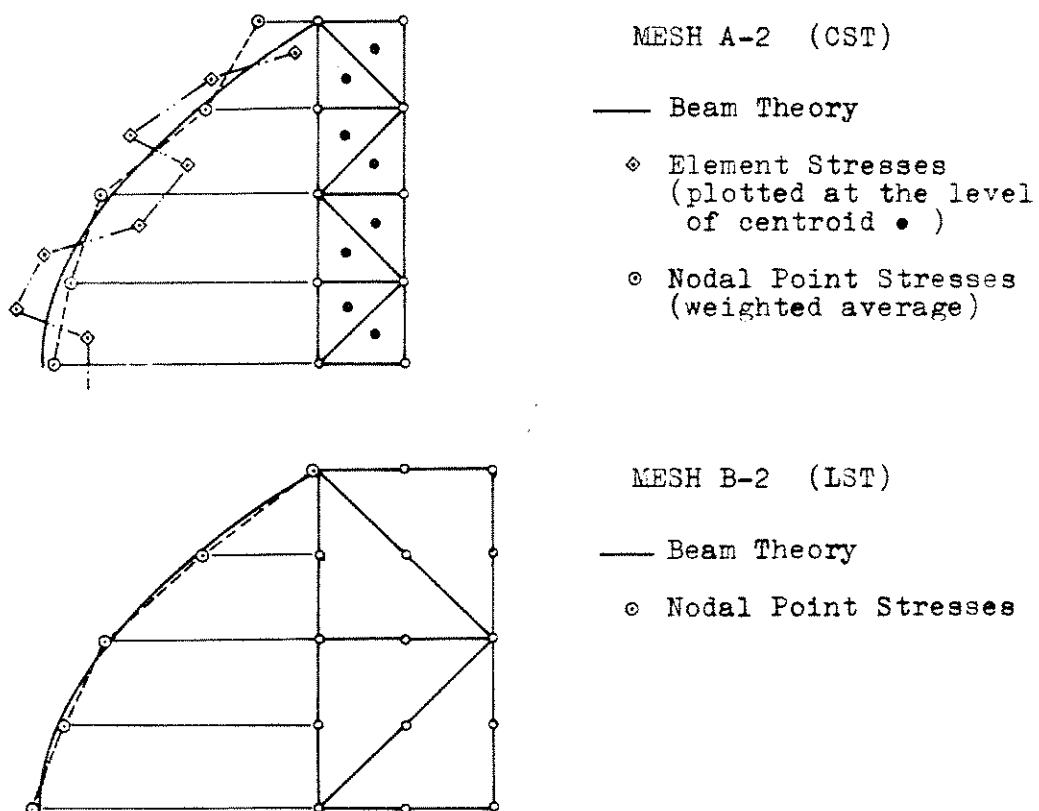
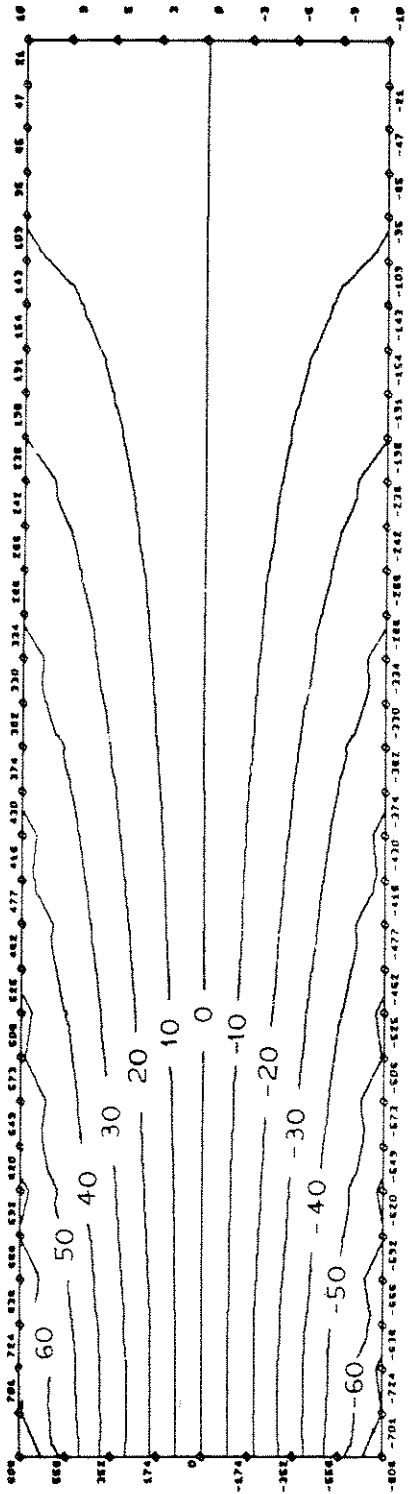
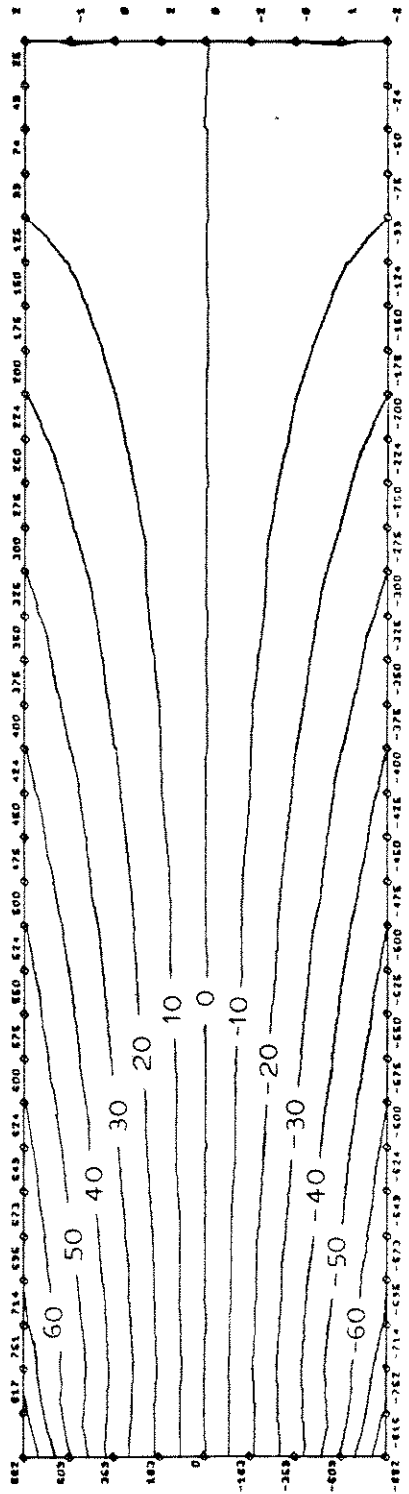
SHEAR STRESS VARIATION AT $X = 9"$ 

Fig. 5.2 - Cantilever Beam: Comparison between LST and CST Meshes.

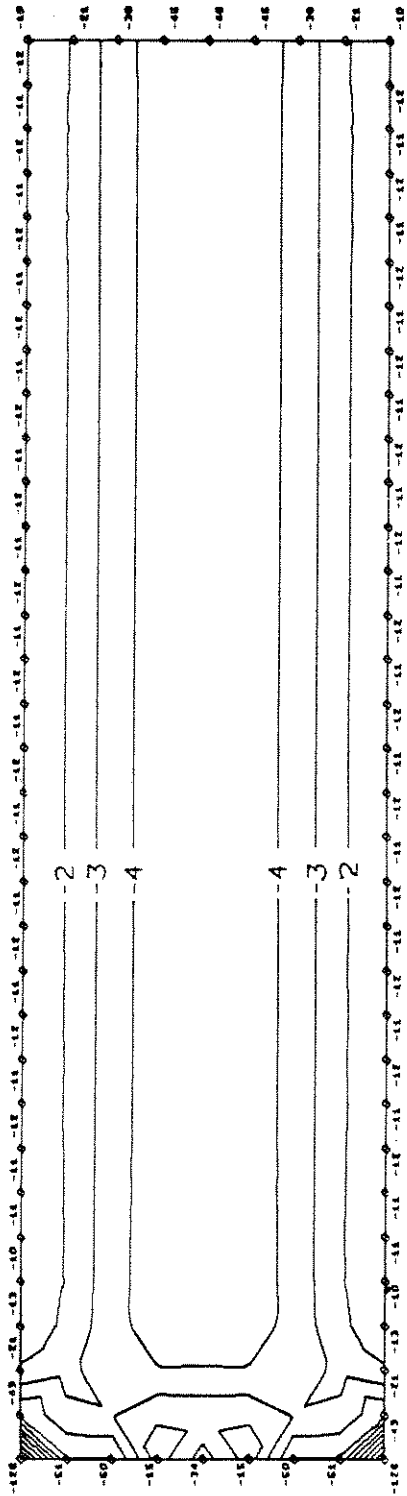


MESH A-2 CST

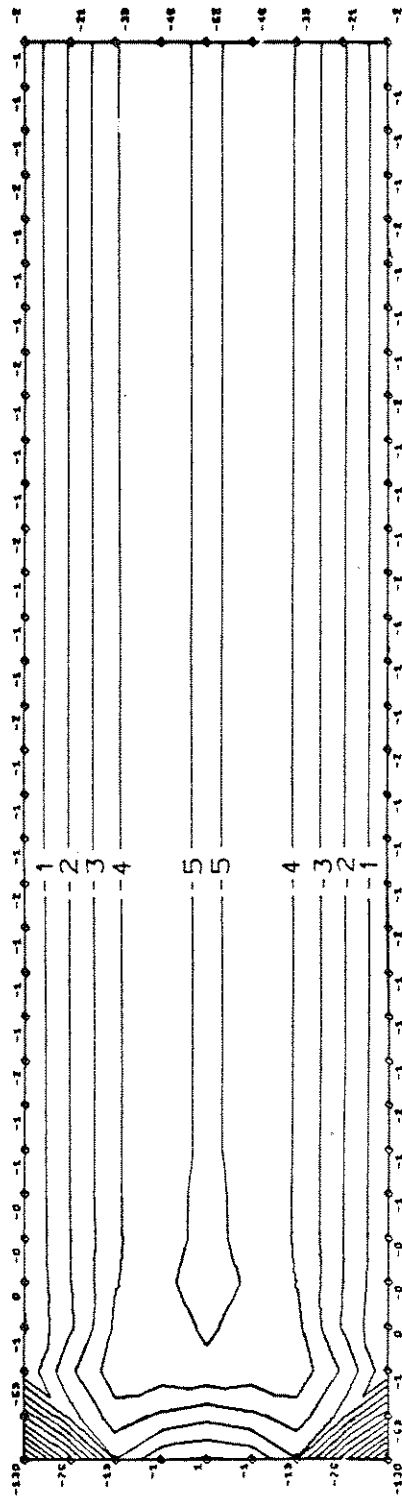


MESH B-2 LST

FIG 5.3 CANTILEVER BEAM - NORMAL STRESS σ_x

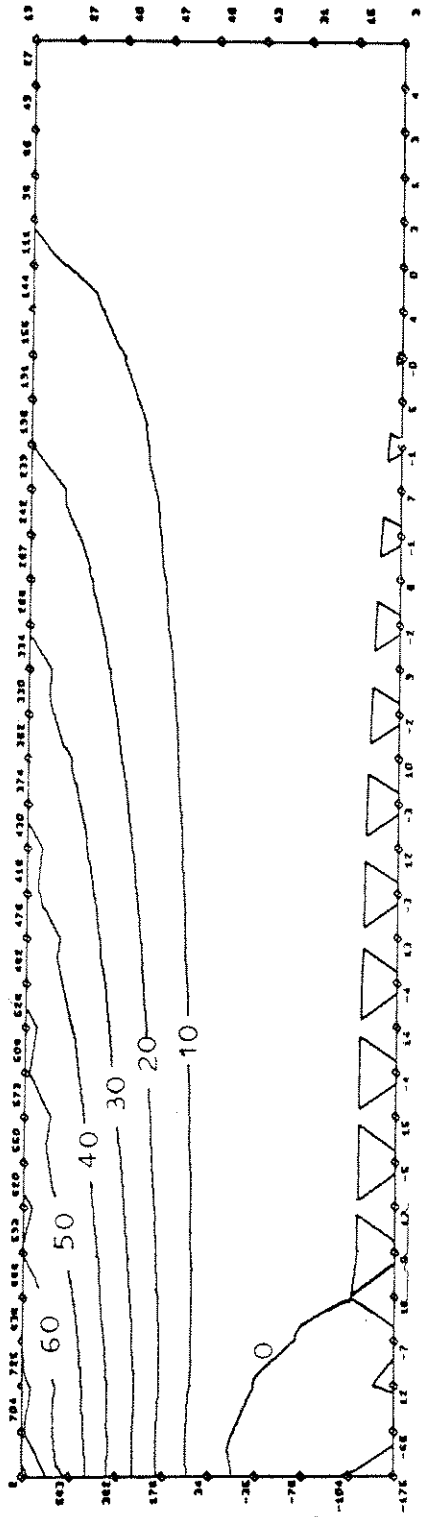


MESH A-2 CST

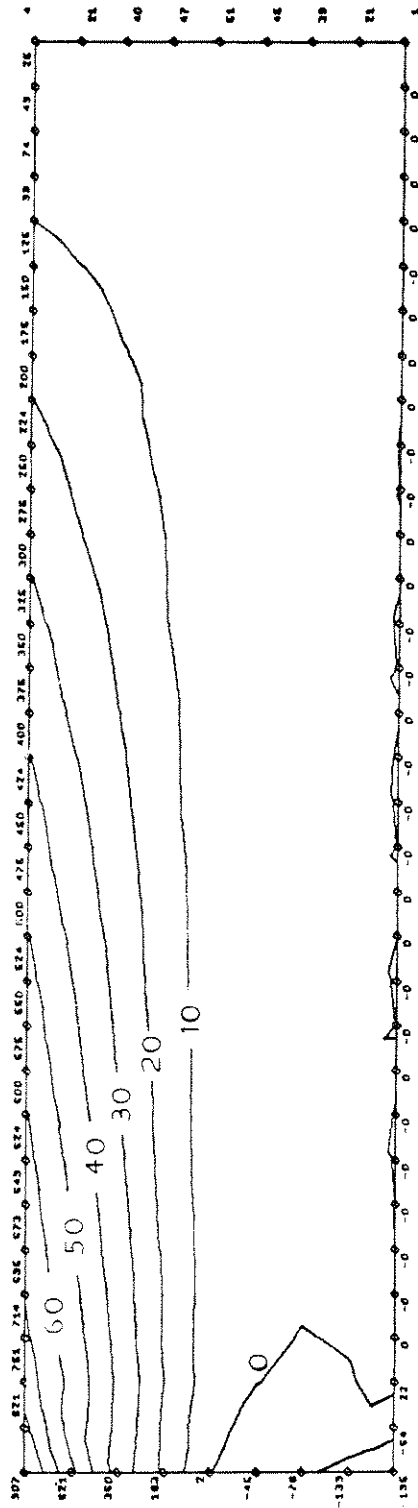


MESH B-2 LST

FIG 5.4 CANTILEVER BEAM - STRESS τ_{xy}

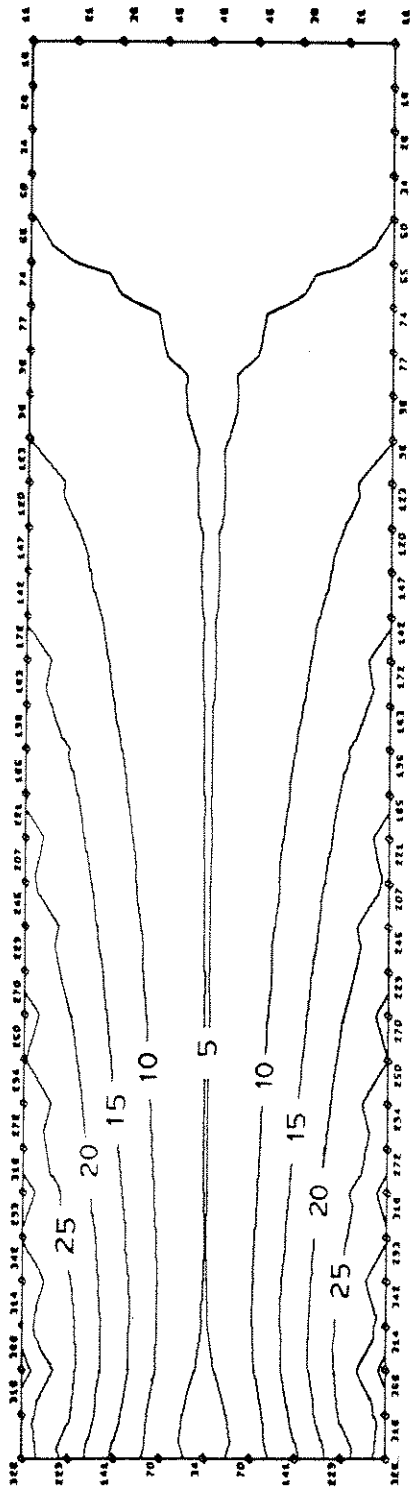


MESH A-2 CST

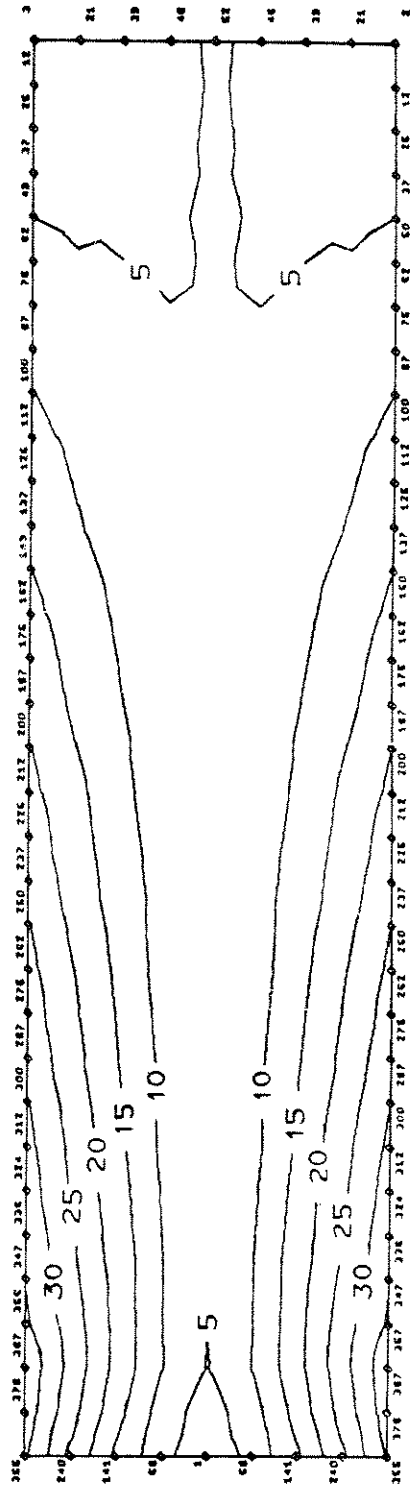


MESH B-2 LST

FIG 5.5 CANTILEVER BEAM - PRINCE. STRESS σ_{max} .



MESH A-2 CST



MESH B-2 LST

FIG 5.6 CANTILEVER BEAM - MAX. SHEAR τ_{max} .

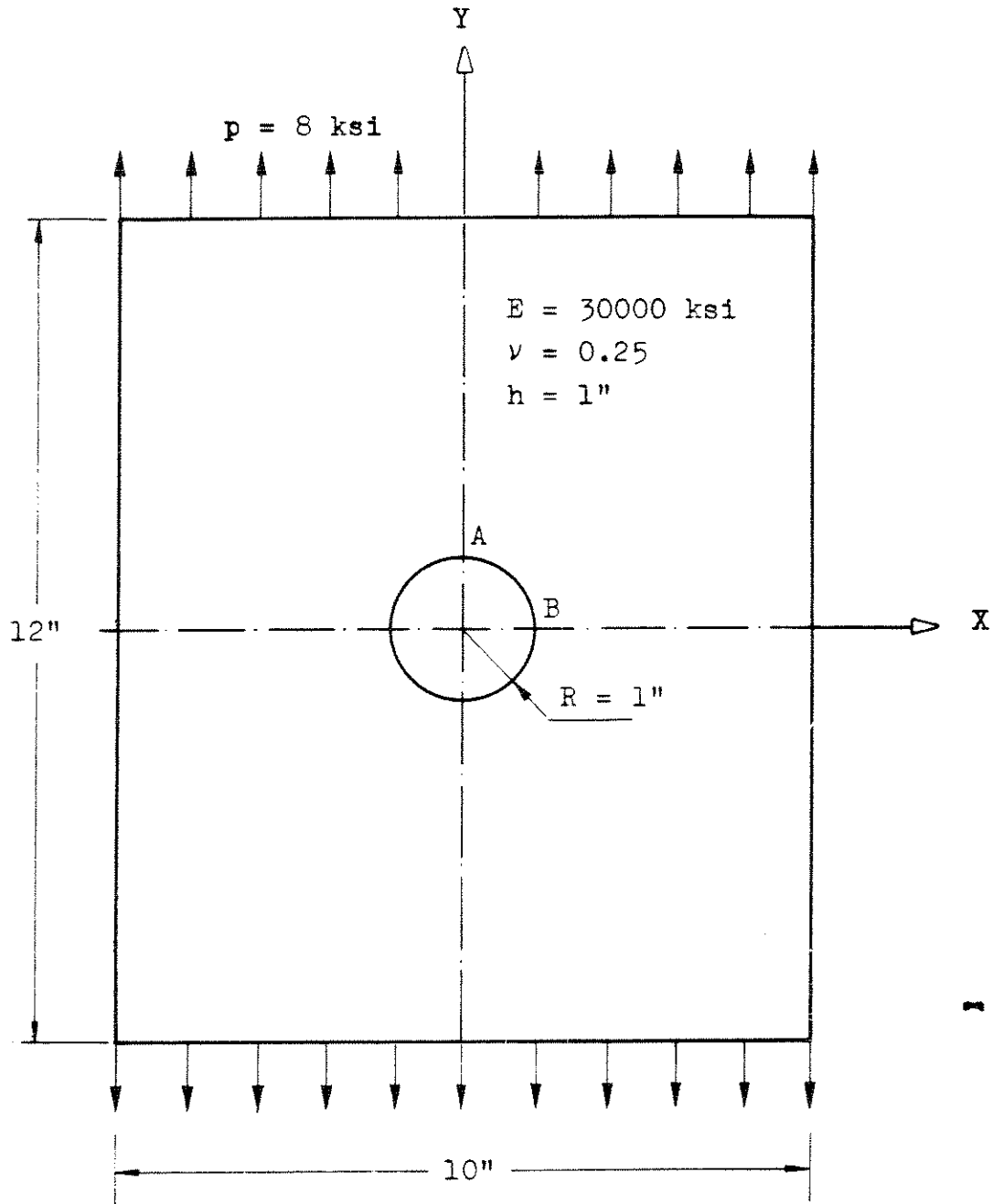
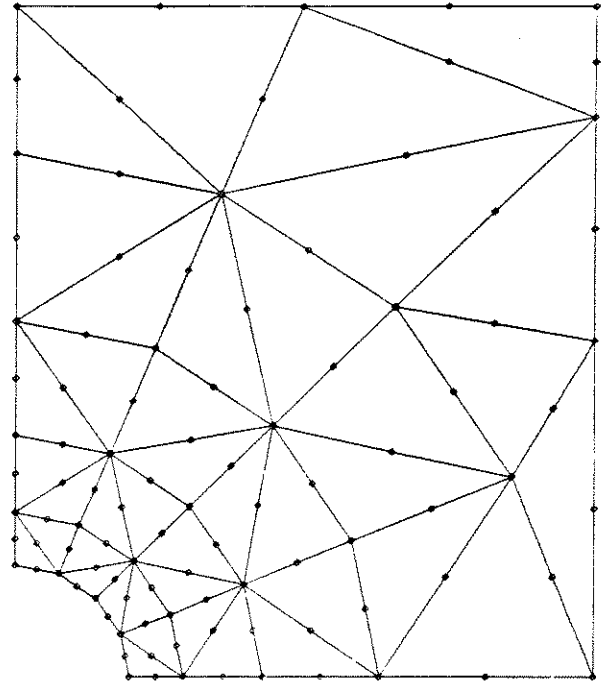
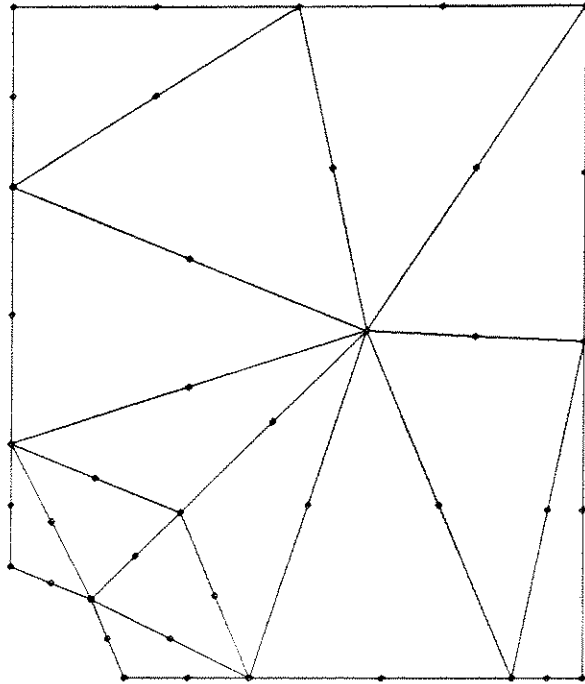


Fig. 5.7 - Plate with a Circular Hole under Uniaxial Tension.



MESH NO. 3

MESH NO. 4

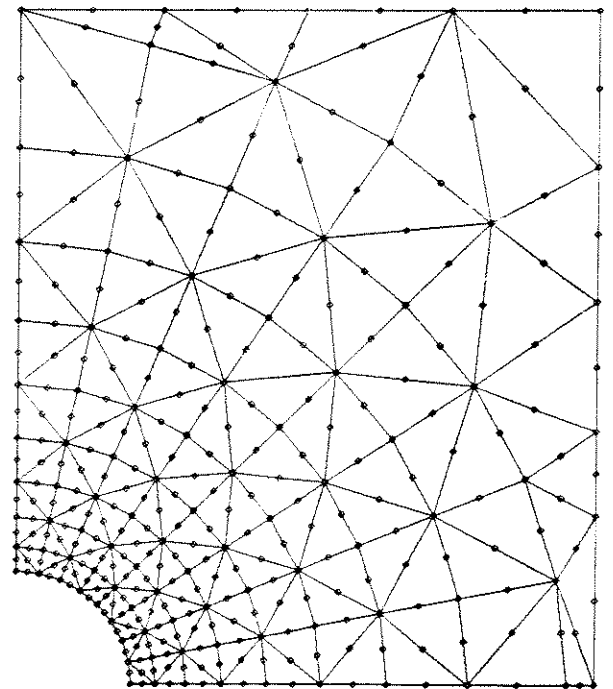
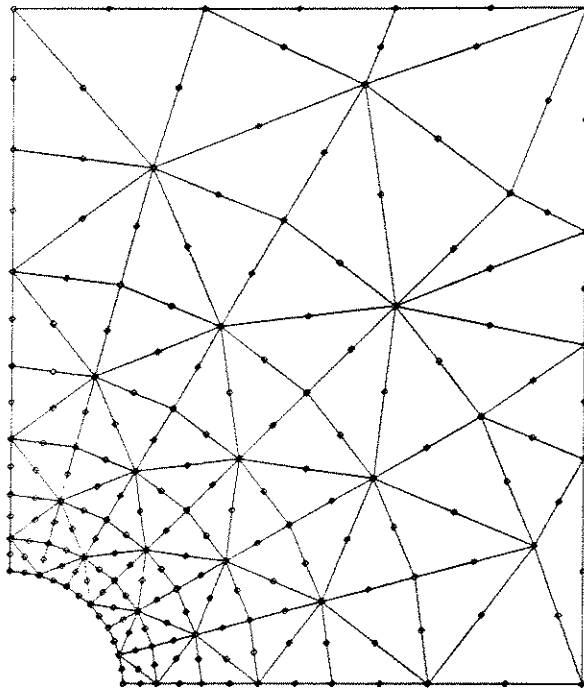


FIG. 5.8 - PLATE WITH CIRCULAR HOLE - FINITE ELEMENT IDEALIZATIONS

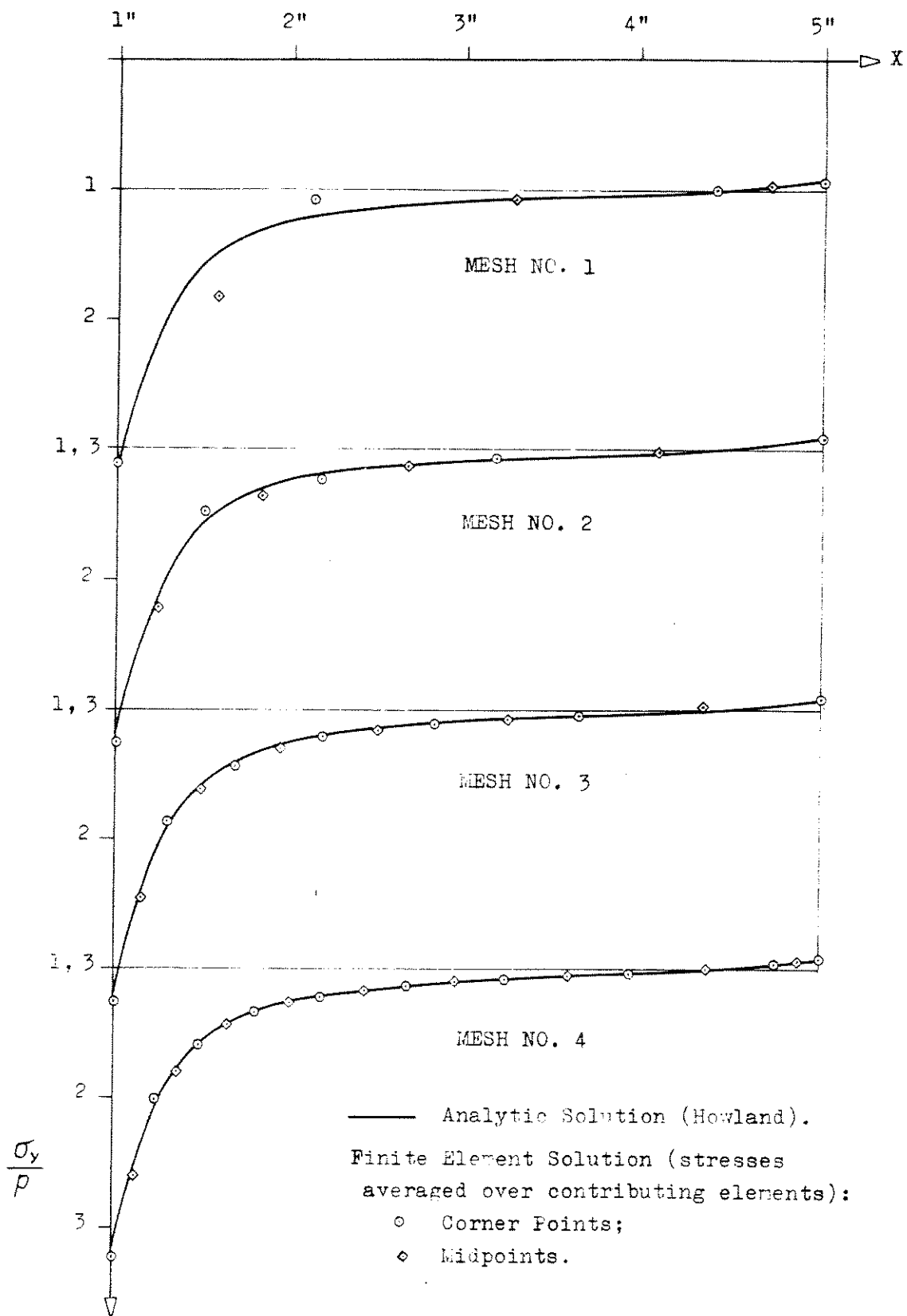
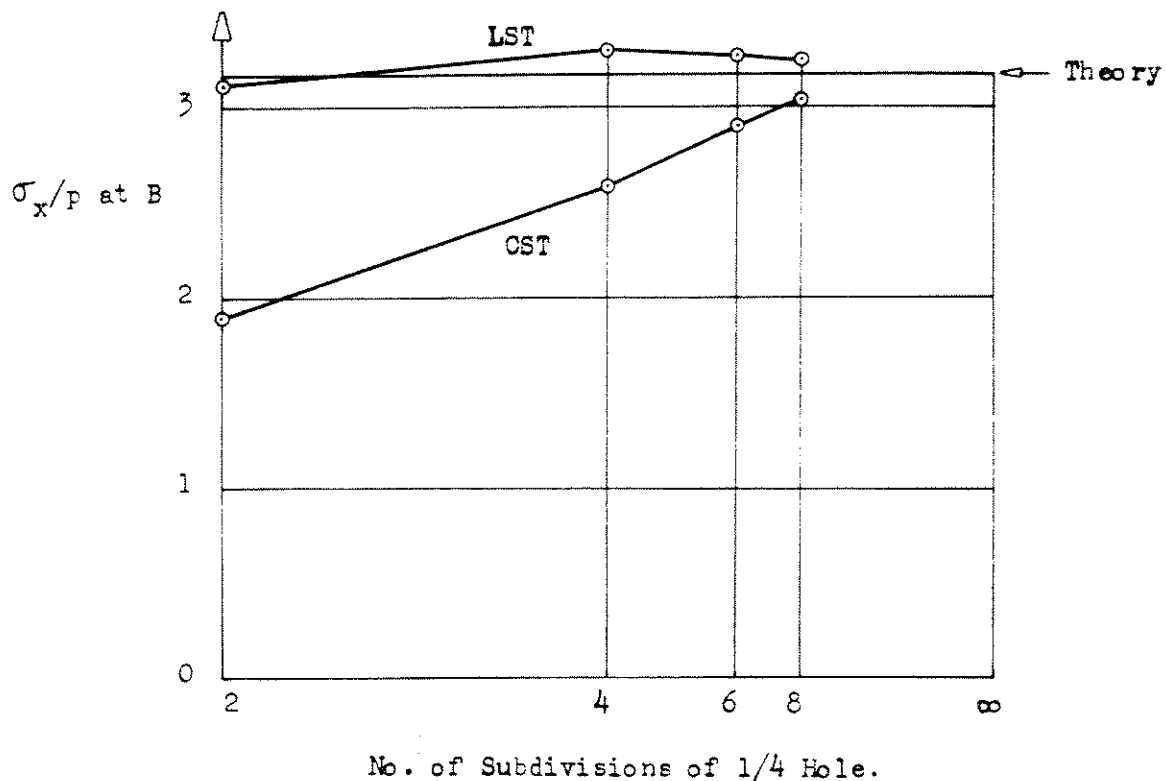
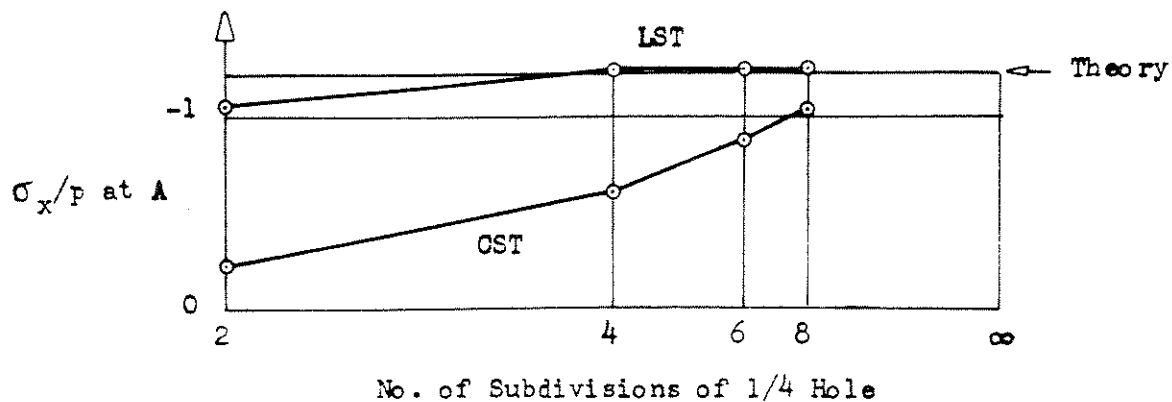


Fig. 5.9 - Plate with Circular Hole: Plots of σ_y/p at the Section $Y = 0$.



Note: for the same number of subdivisions, the LST mesh has approximately 3 times the number of degrees of freedom of the CST mesh.

Fig. 5.10 - Plate with Circular Hole: Comparison of LST and CST Stress Concentration Factors.

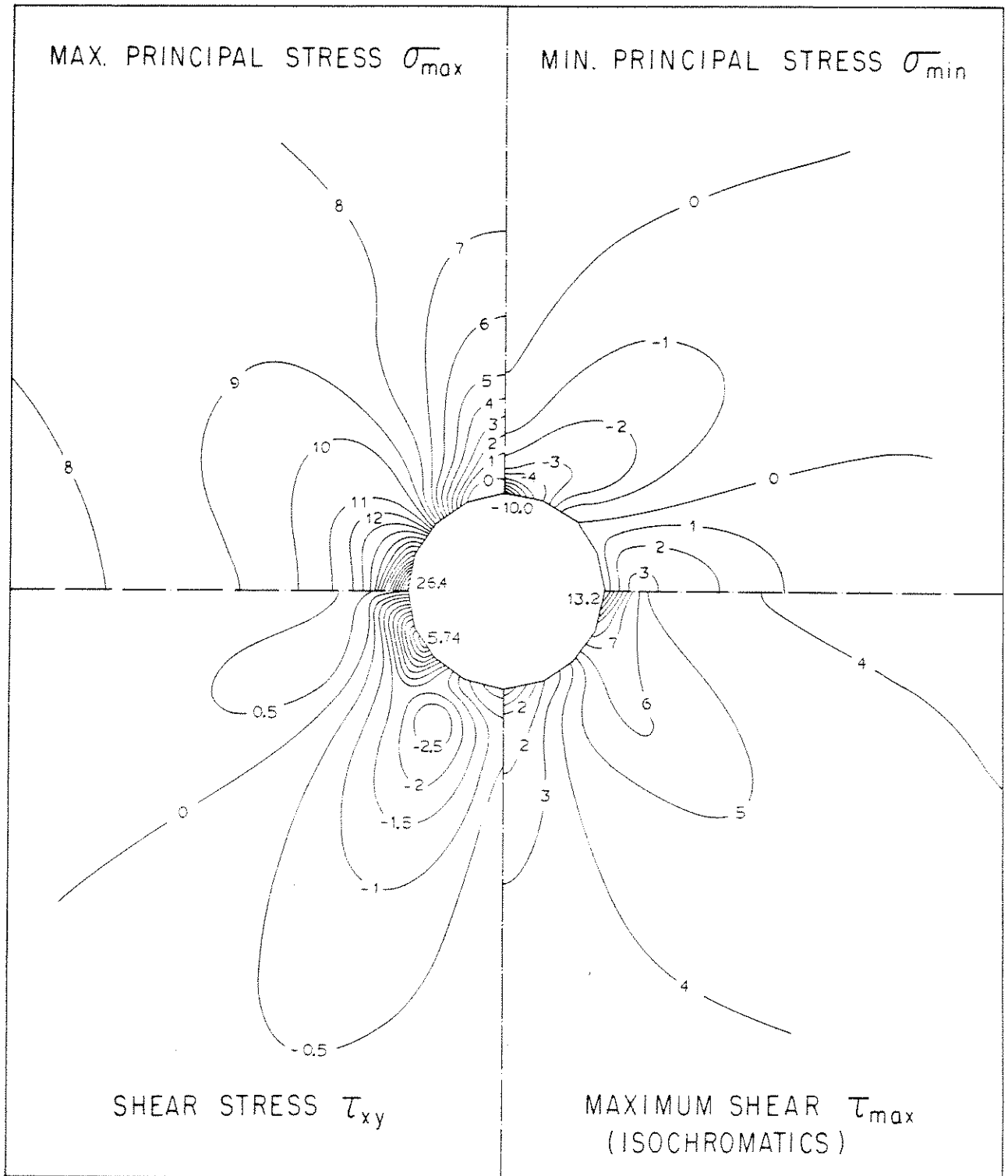


FIG. 5.11 - PLATE WITH CIRCULAR HOLE -
STRESS PATTERNS FOR MESH NO. 2

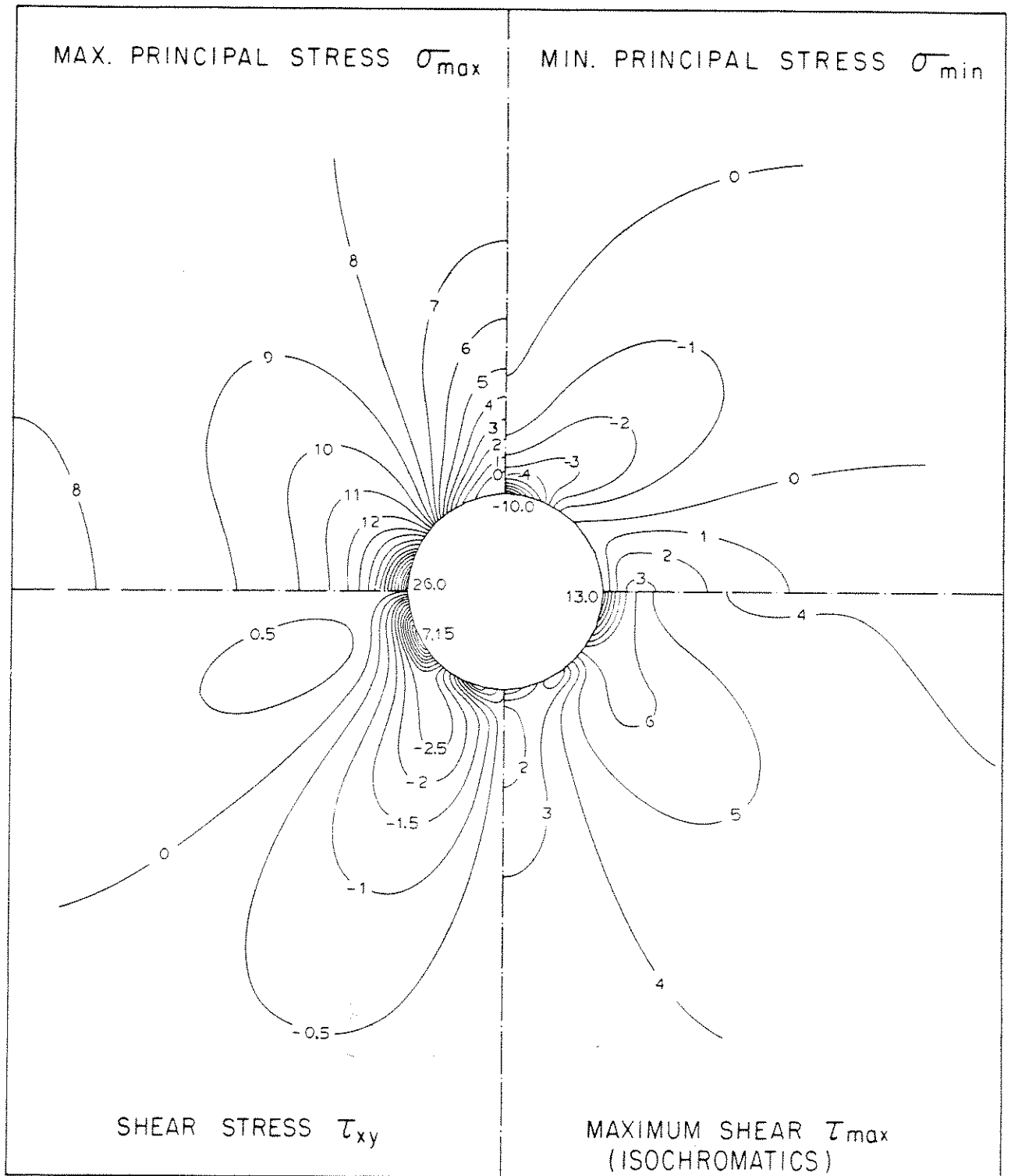


FIG. 5.12 - PLATE WITH CIRCULAR HOLE -
STRESS PATTERNS FOR MESH NO. 4

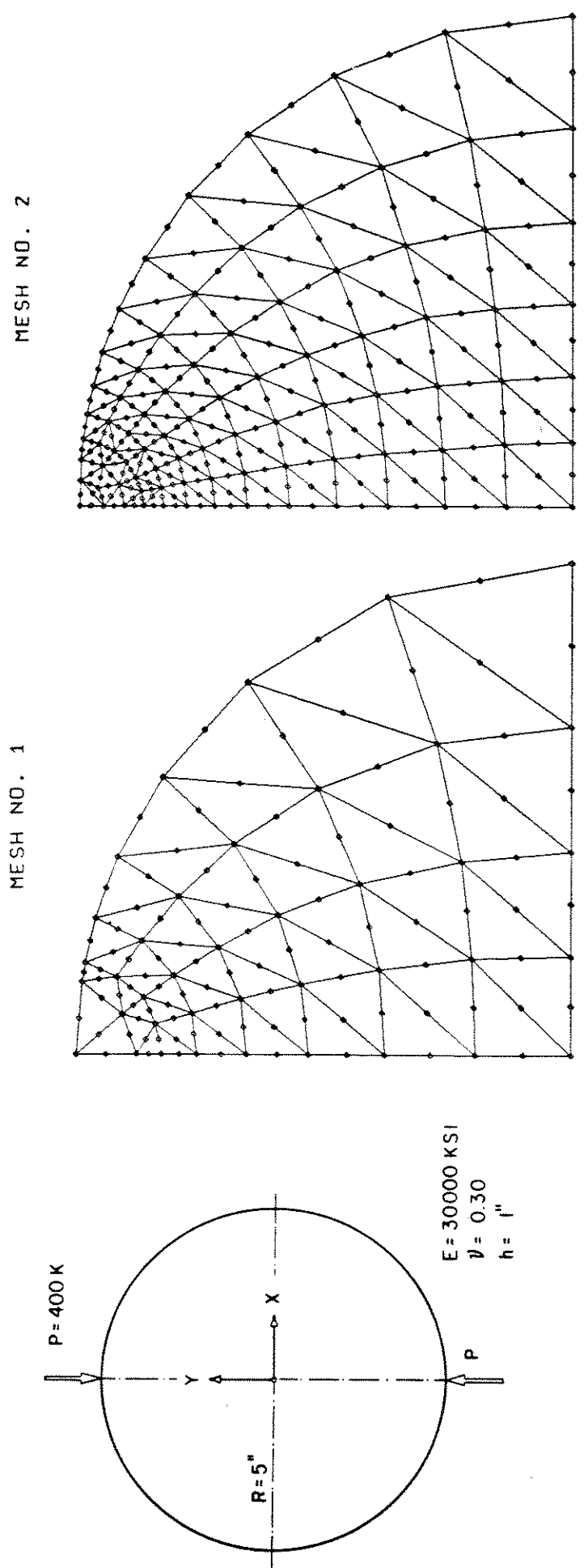
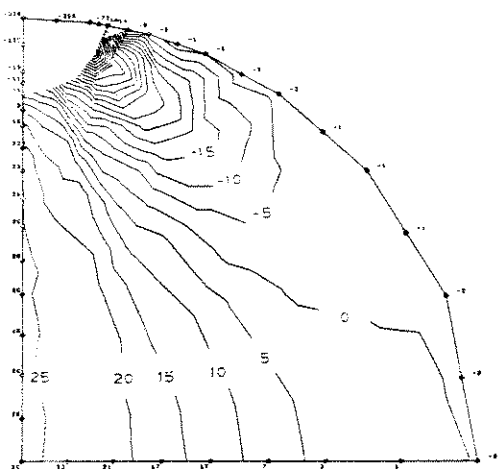
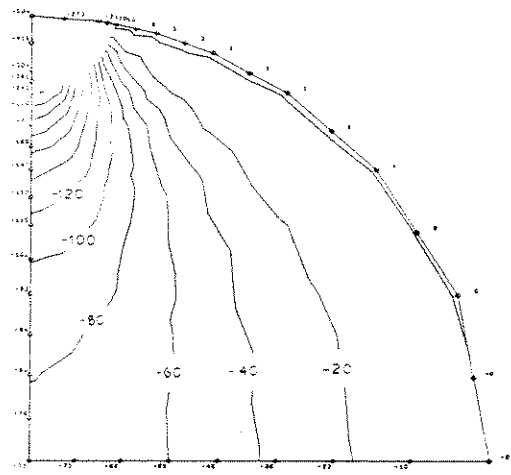


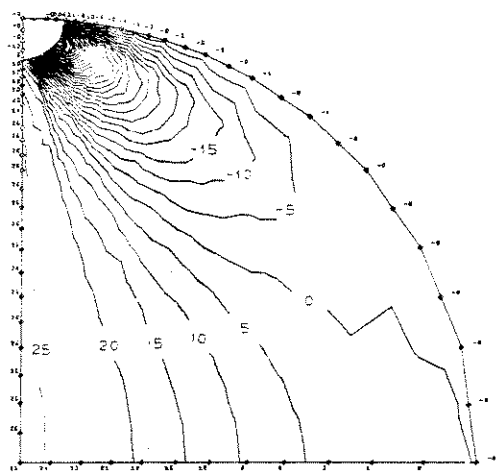
FIG. 5.13 CIRCULAR DISK AND FINITE ELEMENT IDEALIZATIONS



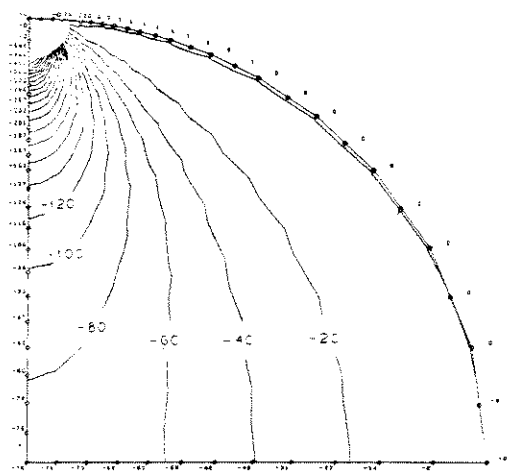
MESH 1



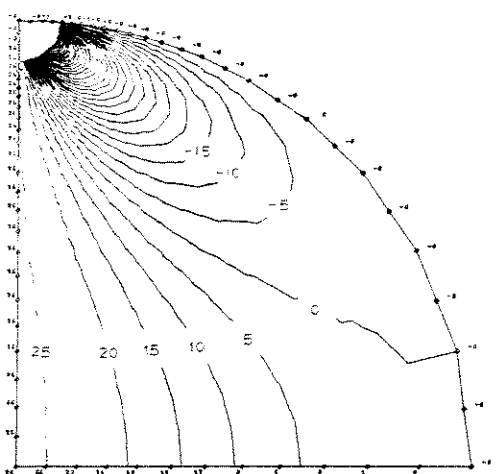
MESH 1



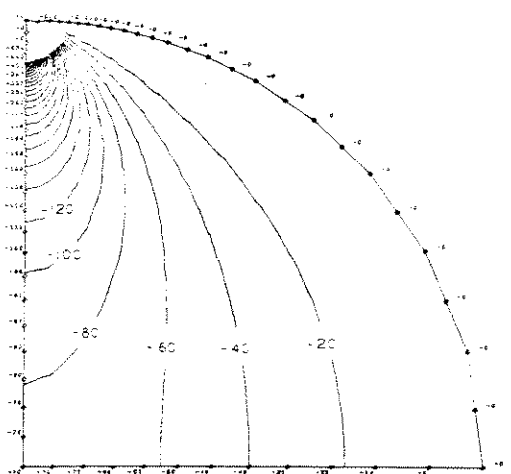
MESH 2



MESH 2



EXACT SOLUTION

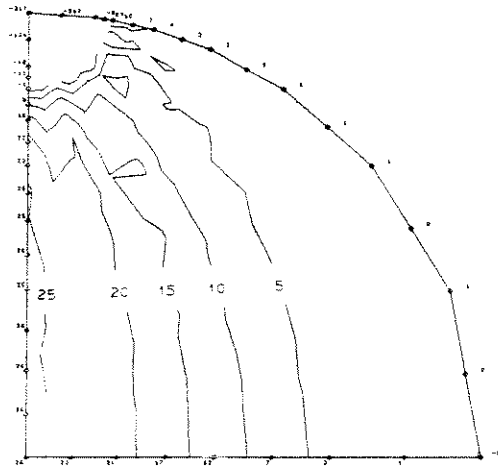


EXACT SOLUTION

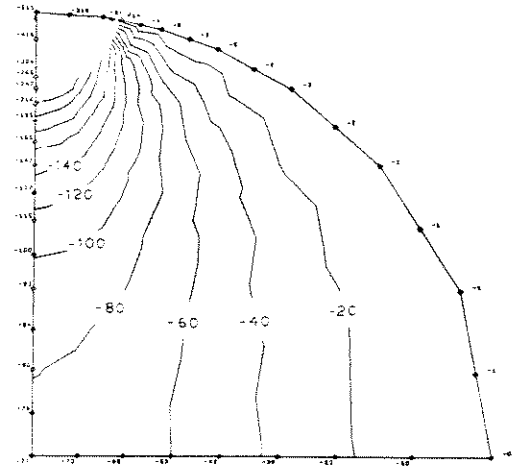
SIGMA XX

SIGMA YY

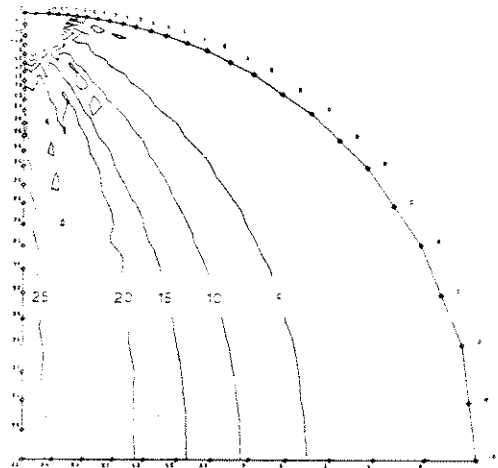
FIG. 5.14 - CIRCULAR DISK STRESS PATTERNS



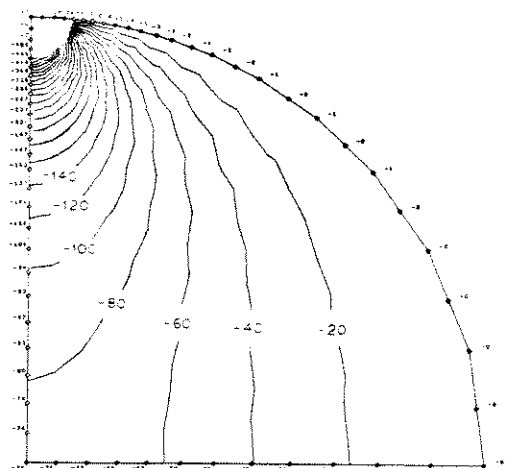
MESH 1



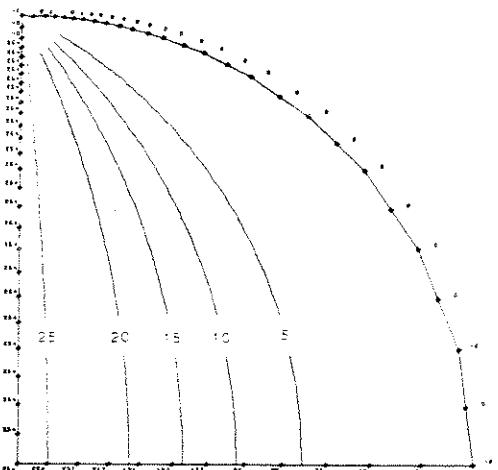
MESH 1



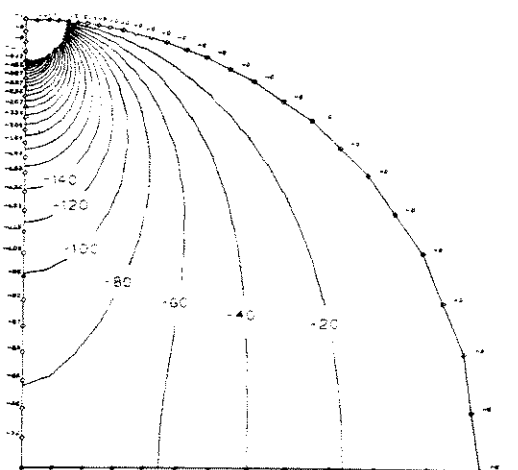
MESH 2



MESH 2



EXACT SOLUTION

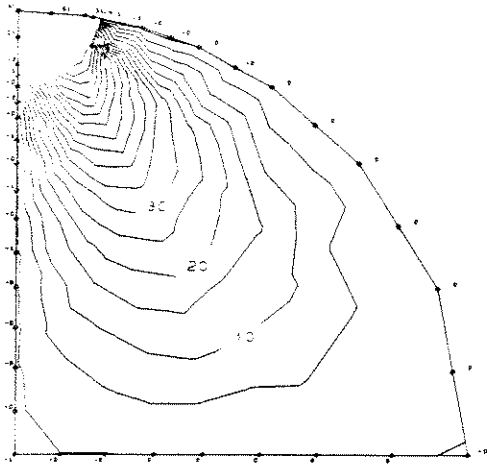


EXACT SOLUTION

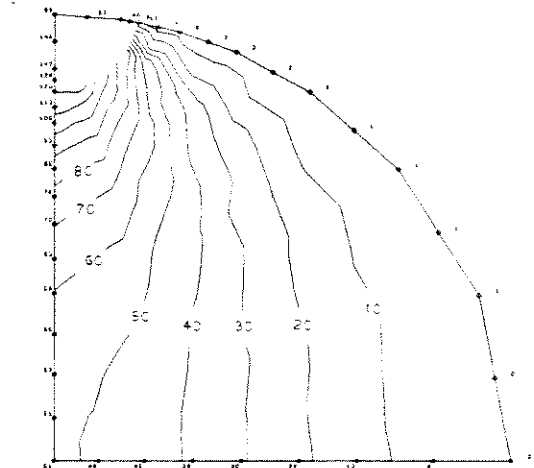
SIGMA MAX.

SIGMA MIN.

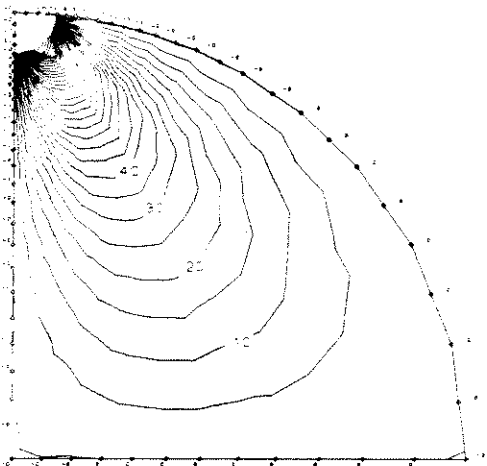
FIG. 5.15 - CIRCULAR DISK STRESS PATTERNS



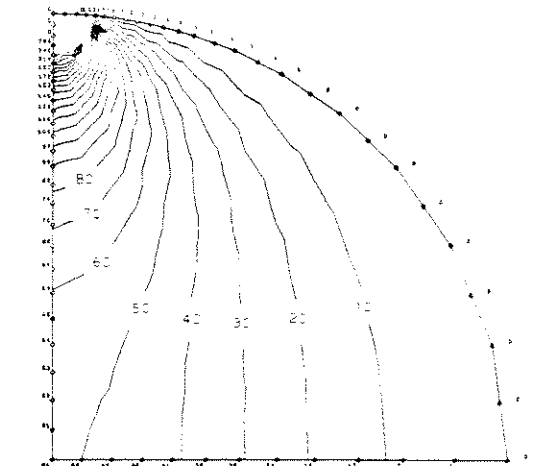
MESH 1



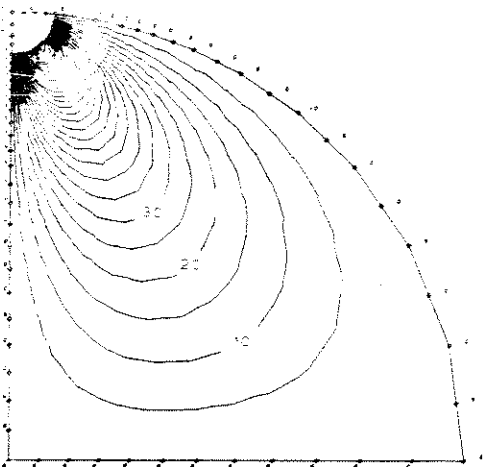
MESH 1



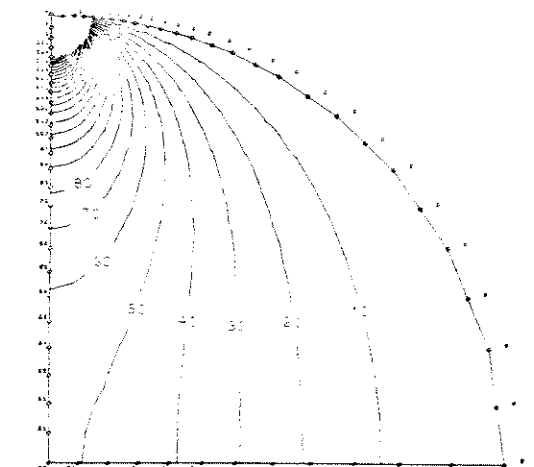
MESH 2



MESH 2



EXACT SOLUTION



EXACT SOLUTION

TAU XY

MAX SHEAR

FIG. 5.16 - CIRCULAR DISK STRESS PATTERNS

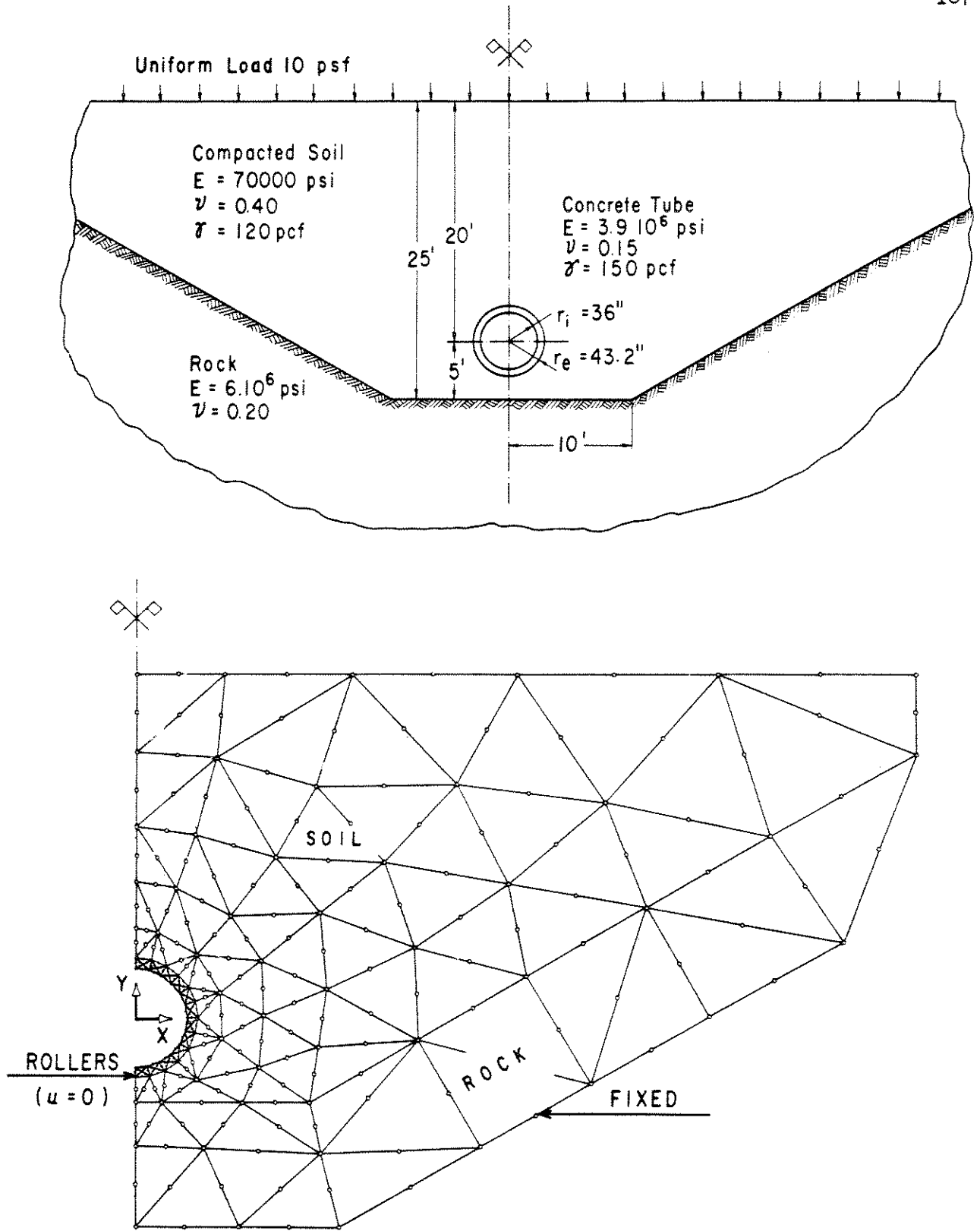
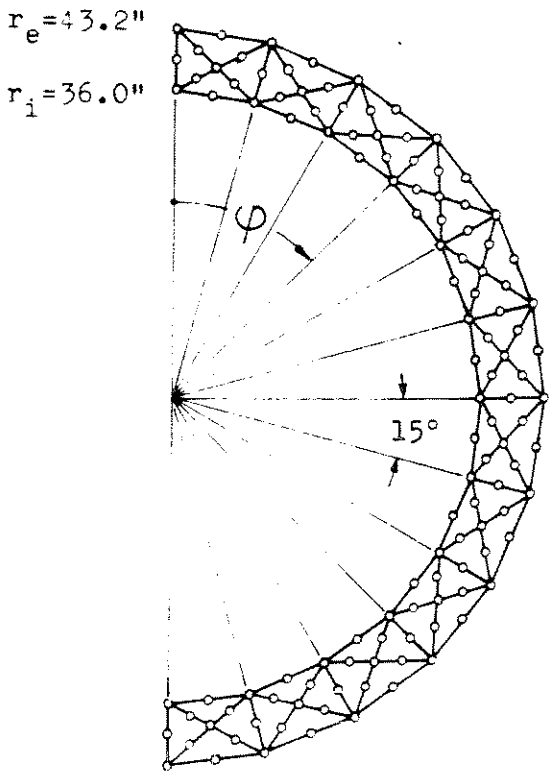
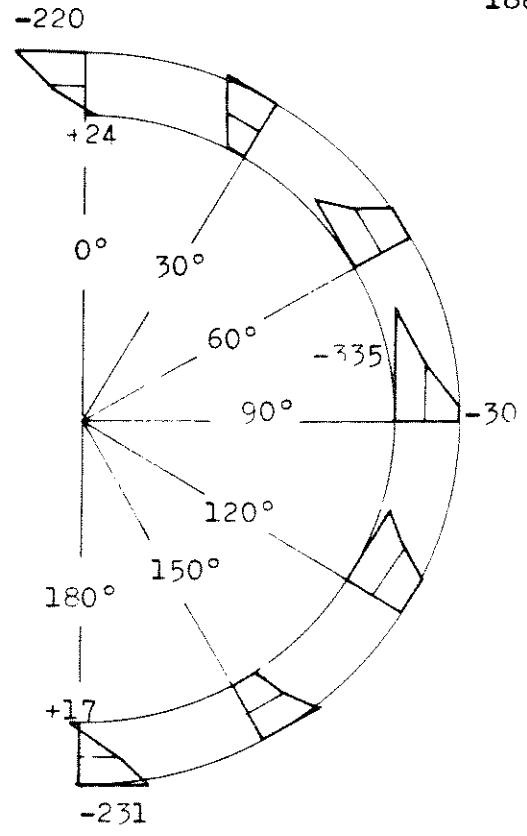


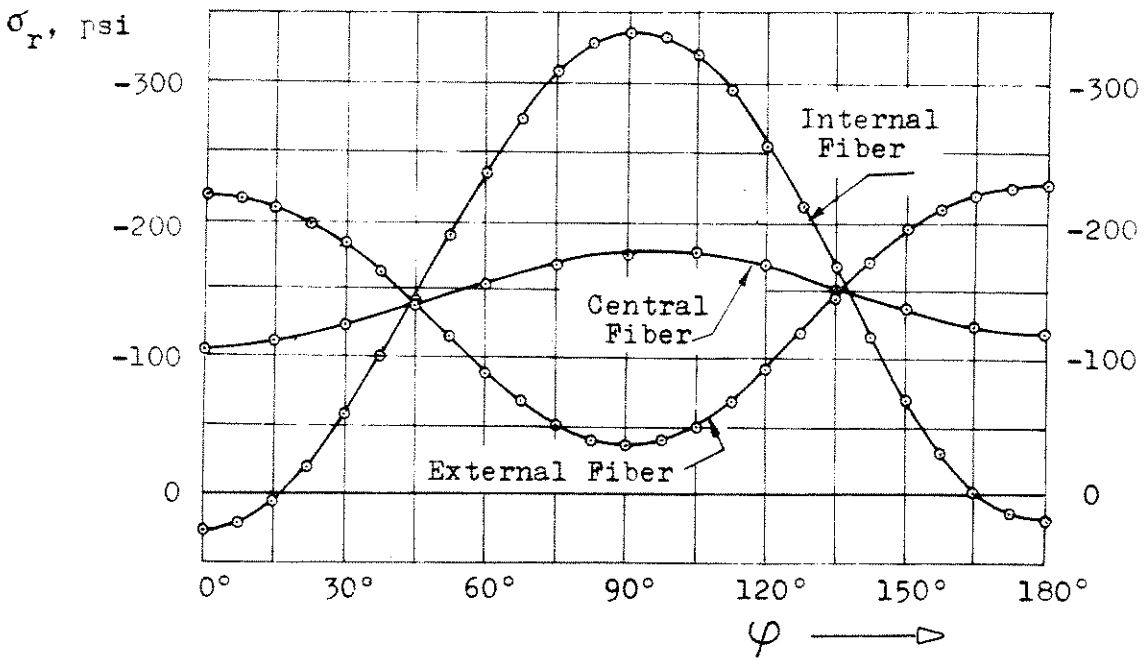
FIG. 5.17 BURIED CONCRETE PIPE AND FINITE ELEMENT IDEALIZATION



FINITE ELEMENT IDEALIZATION



NORMAL STRESSES AT SEVERAL SECTIONS



NORMAL STRESS VARIATION

Fig. 5.18 - Results for Buried Concrete Pipe

The purpose of this research program was merely to illustrate the adequacy of the finite element analysis based on the general incremental technique described in Chapter IV. Accordingly, to simplify coding and input data, Von Mises yield criterion and isotropic linear hardening were assumed. However, any yield or hardening criterion, temperature, strain-rate or stress-rate dependence may be easily incorporated for a production program capable of treating large systems. The basic organization of the solution procedure would be the same.

V.2.2 Plastic Hinge Formation (Small Displacements)

A two-dimensional analysis of the development of plastic regions in beams of narrow rectangular cross section (plane stress) was carried out for two cases:

- (a) End-loaded cantilever beam with completely fixed root (Fig. 5.19);
- (b) Simply supported beam under concentrated central load (Fig. 5.20);

An elastic-perfectly plastic material with a yield point of 10 ksi was assumed. In the first case, and because of the assumption of small displacements, the elastic neutral axis ($y = 0$) remains as such during plastic deformation, i.e., their points do not displace in the x -direction. This conclusion was numerically verified by running the complete beam with a coarse mesh. Consequently, only the upper portion was considered and the points of the neutral axis constrained to roll on lines $x = \text{constant}$ (Fig. 5.20). For the simply

supported beam no such simplification is possible since the lack of symmetry of the load requires the consideration of the entire cross section (Fig. 5.20).

Both cases were run by applying specified displacements at the load point; if the displacement at first yield is denoted by δ_y , the increments were

$$0.25 \delta_y \text{ up to } 4.0 \delta_y$$

$$0.50 \delta_y \text{ thereafter}$$

The maximum displacement of the load point was $8. \delta_y$ in both cases; the critical sections are by then completely plastified. After complete removal of the loads, the residual stresses were obtained.

A complete step (2 solutions) required 23 sec. in case (a) and 34 sec. for case (b) in an IBM 7094.

Stress contour lines for the critical regions were printed by the computer at several stages and are presented in Figs. 5.21 to 5.26.

The presence of shear and transversal stress produces interesting effects on the two-dimensional stress patterns. In case (a), the complete end fixity causes the critical section to develop at approximately 0.42 H from the built-in edge. In case (b), the wedge effect of the concentrated load can be clearly noticed by the formation of two plastic zones in the upper portion of the beam; in the intermediate (elastic) region we can observe a reversal of the transversal stress σ_y and a sudden drop of the normal stress σ_x , which becomes positive for large plastification; both regions finally merge near the neutral axis, but two small elastic cores remain.

Dimensionless load-displacement curves are shown in Fig. 5.27. The applied force P is referred to the so-called "ultimate load" P_u which would produce the "plastic moment" $M_p = \sigma_Y h H^2/4$ at the critical section ($x = 0.42 H$ for case (a), $x = 0$ for case (b)). Displacements δ at the load point are divided by the elastic displacement δ_{eu} which would take place for $P = P_u$. Strictly speaking, in case (b), yield would start at $x = 0$ as soon as the load P is applied; however, because of the finite element discretization, the first yield occurs at a finite P .

These load-displacement curves indicate that despite the assumption of zero hardening, the load continues to increase slowly even after the critical section is totally plastified, because of the continuous two-dimensional stress redistribution. This phenomenon is more pronounced in the case of the beam loaded at the center, which exceeds the theoretical ultimate load of the beam theory by at least 35%.

V.2.3 Plastic Buckling (Finite Displacements)

The 10:1 simply supported column shown in Fig. 5.28 was analyzed for instability in the plastic range (buckling in its x - y plane). The elastic critical stress is 100 ksi and the initial yield point 10 ksi. The hardening is linear, with a plastic modulus $E_p = E/100 = 100$ ksi. Since the average critical stress by the double-modulus theory is 3.6 ksi and by the tangent-modulus theory 1 ksi [52], the column must buckle as soon as the midsection is totally plastified, with a sharp decrease of the load.

The finite element idealization of the upper half is shown in Fig. 5.28. The displacement of the center point A of the simply supported edge

was applied by increments of

$$0.125 \delta_y \text{ up to } 2.00 \delta_y$$

$$0.250 \delta_y \text{ up to } 5.00 \delta_y$$

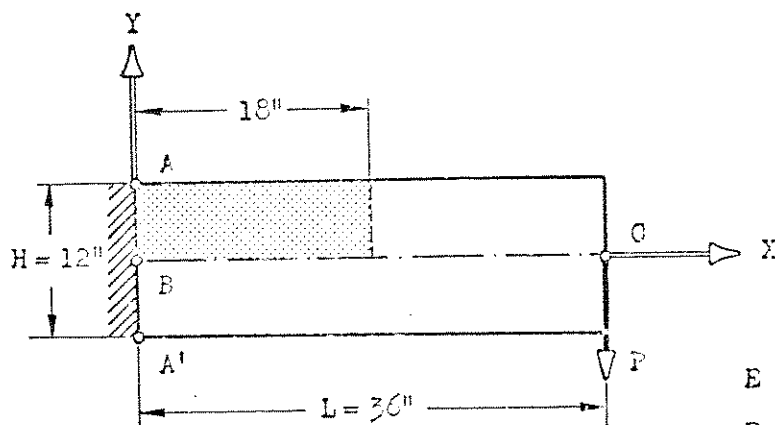
$$0.500 \delta_y \text{ thereafter}$$

where δ_y is the displacement of A at first yield. To avoid local yielding near the load, the thickness of the last four elements was doubled.

In order to achieve a smooth numerical behavior during buckling, the column was given an initial sinusoidal eccentricity of amplitude $e = 0.01''$, which represents 1/1200 of the total span and 1/30 of the radius of giration. The elastic normal stresses varied by $\pm 3.3\%$ with respect to the mean value.

Inestability took place as soon as the midsection was plastified. The convex side unloaded elastically; then the normal stress σ_x reversed to tension and finally yielding occurred again (Fig. 5.29). The process was stopped when the lateral deflection exceeded 5 in. (Fig. 5.30); at such stage the column behaves like a shallow arch and the two plastic regions are confined near the midsection; the rest of the column unloaded elastically under a continuously decreasing load.

A measure of the accuracy of the integration scheme is provided by the fact that the exact yield surface was never exceeded by more than 5% at any nodal point.



BEAM AND LOAD SYSTEM

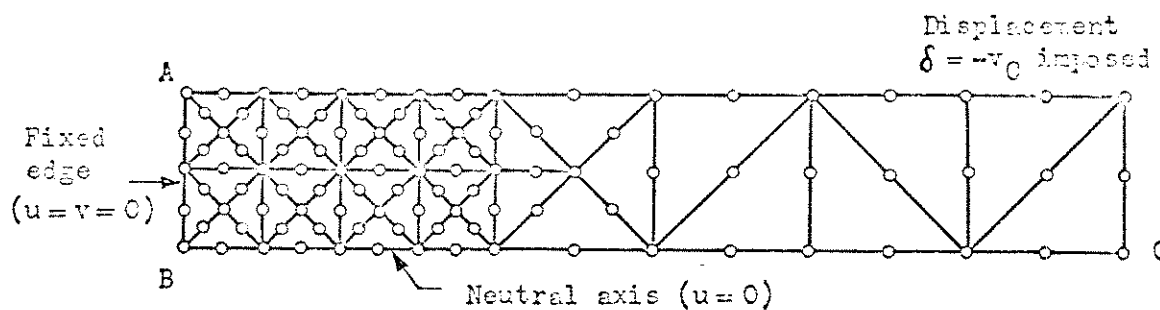
Shaded area is the region represented in Figs. 5.21 to 5.26.

$$E = 1000 \text{ ksi}$$

$$E_p = 0 \text{ (elastic-perfectly plastic)}$$

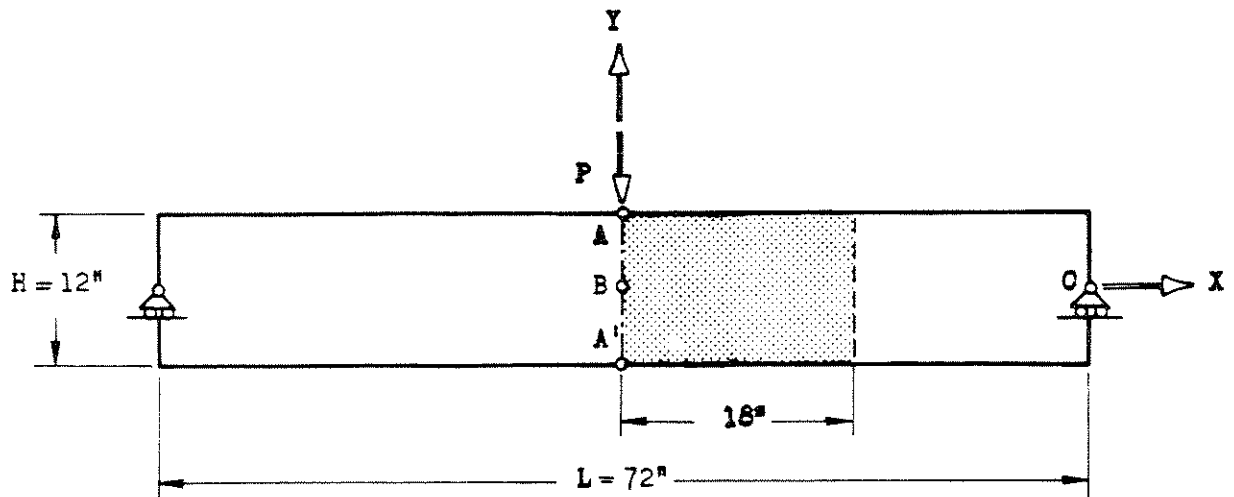
$$Y = 10 \text{ ksi}$$

$$\nu = 0,25$$



FINITE ELEMENT IDEALIZATION OF UPPER PORTION

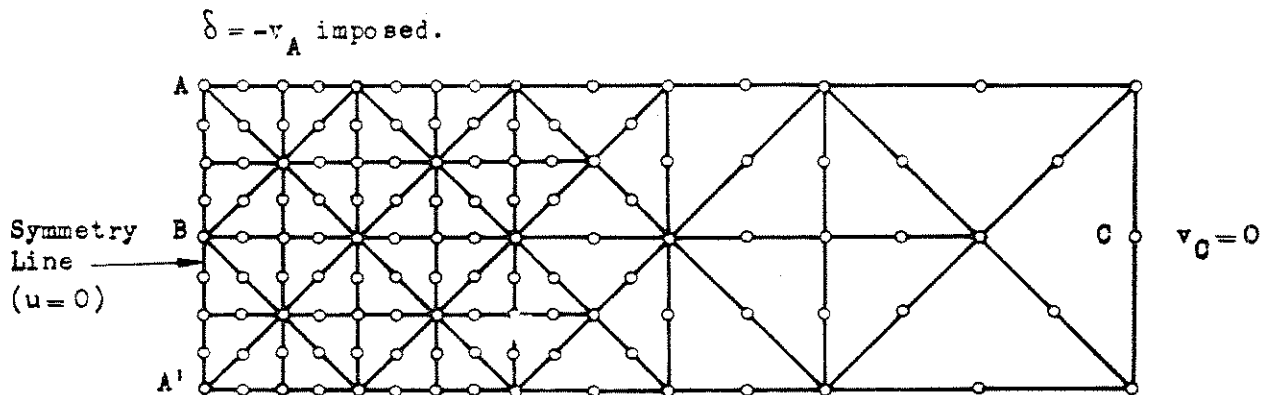
Fig. 5.19 - Plastic Hinge Formation: End-Loaded Cantilever Beam.



BEAM AND LOAD SYSTEM

Shaded area is the region represented in Figs. 5.21 to 5.26.

Same material properties of cantilever beam (Fig. 5.19).



FINITE ELEMENT IDEALIZATION OF RIGHT PORTION

Fig. 5.20 - Plastic Hinge Formation: Centrally-Loaded Simply Supported Beam.

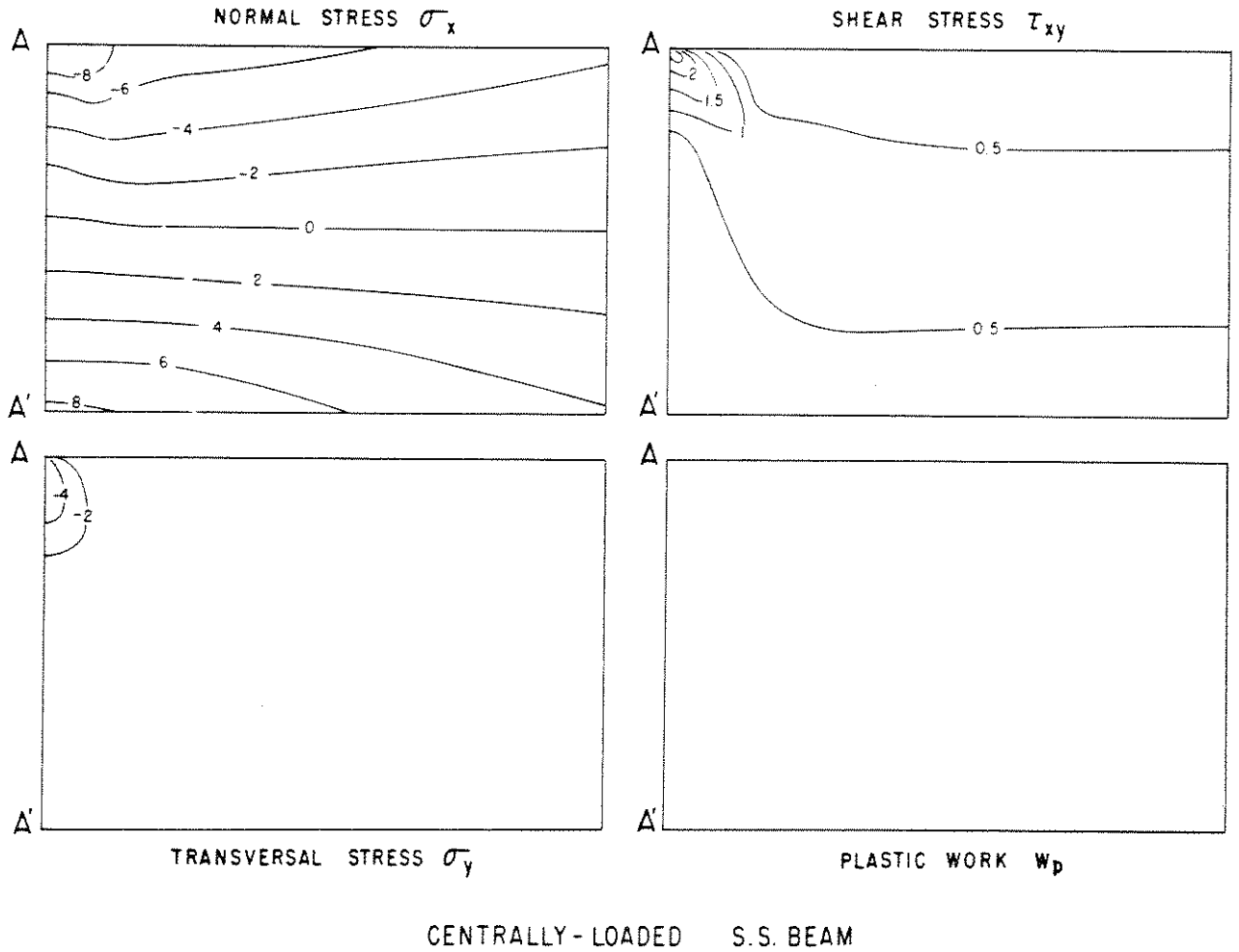
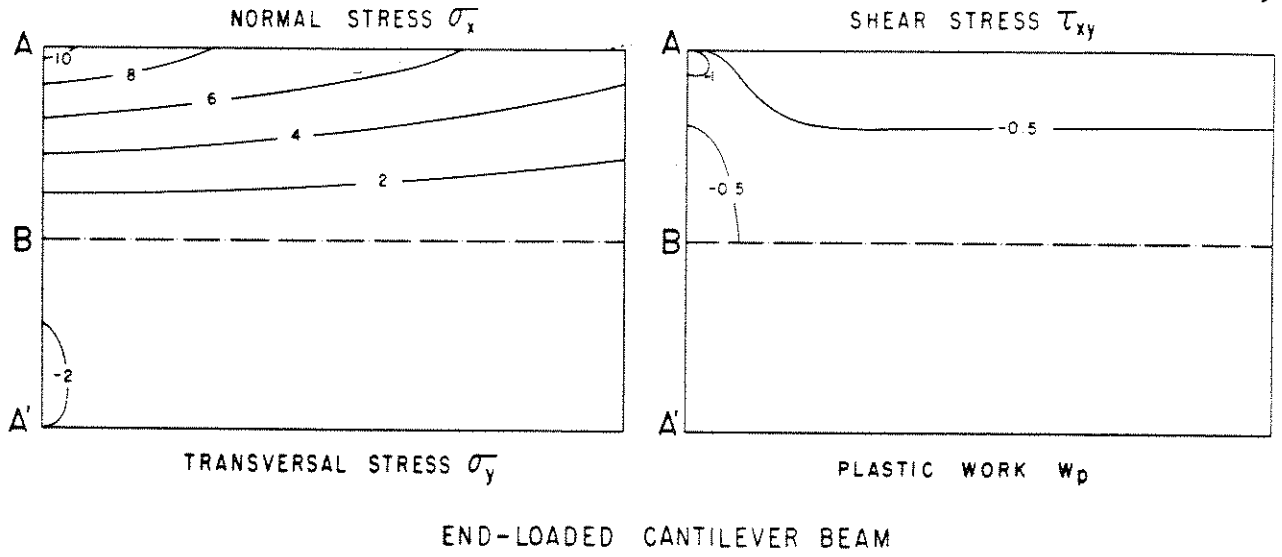
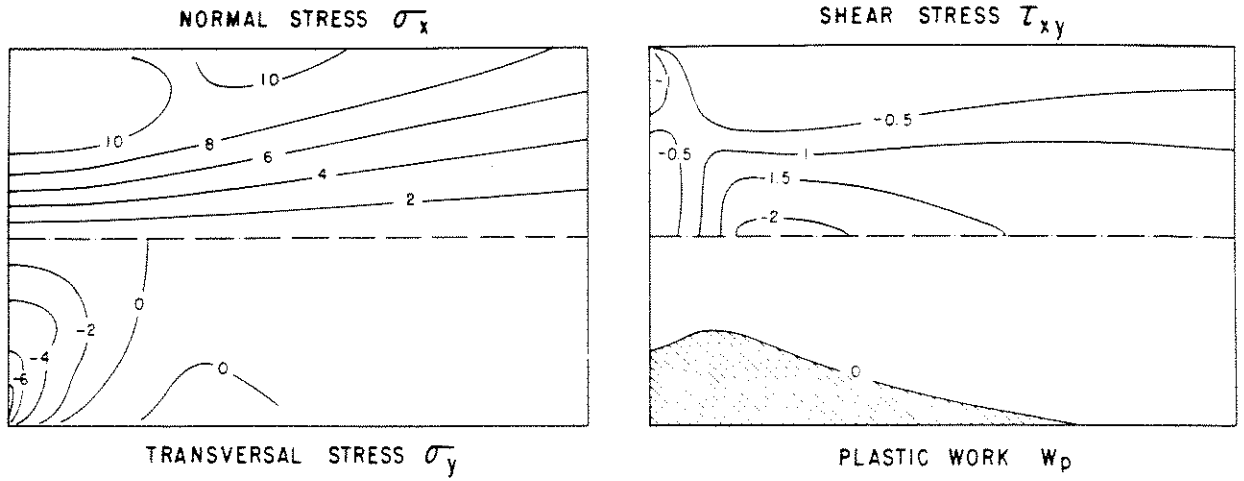
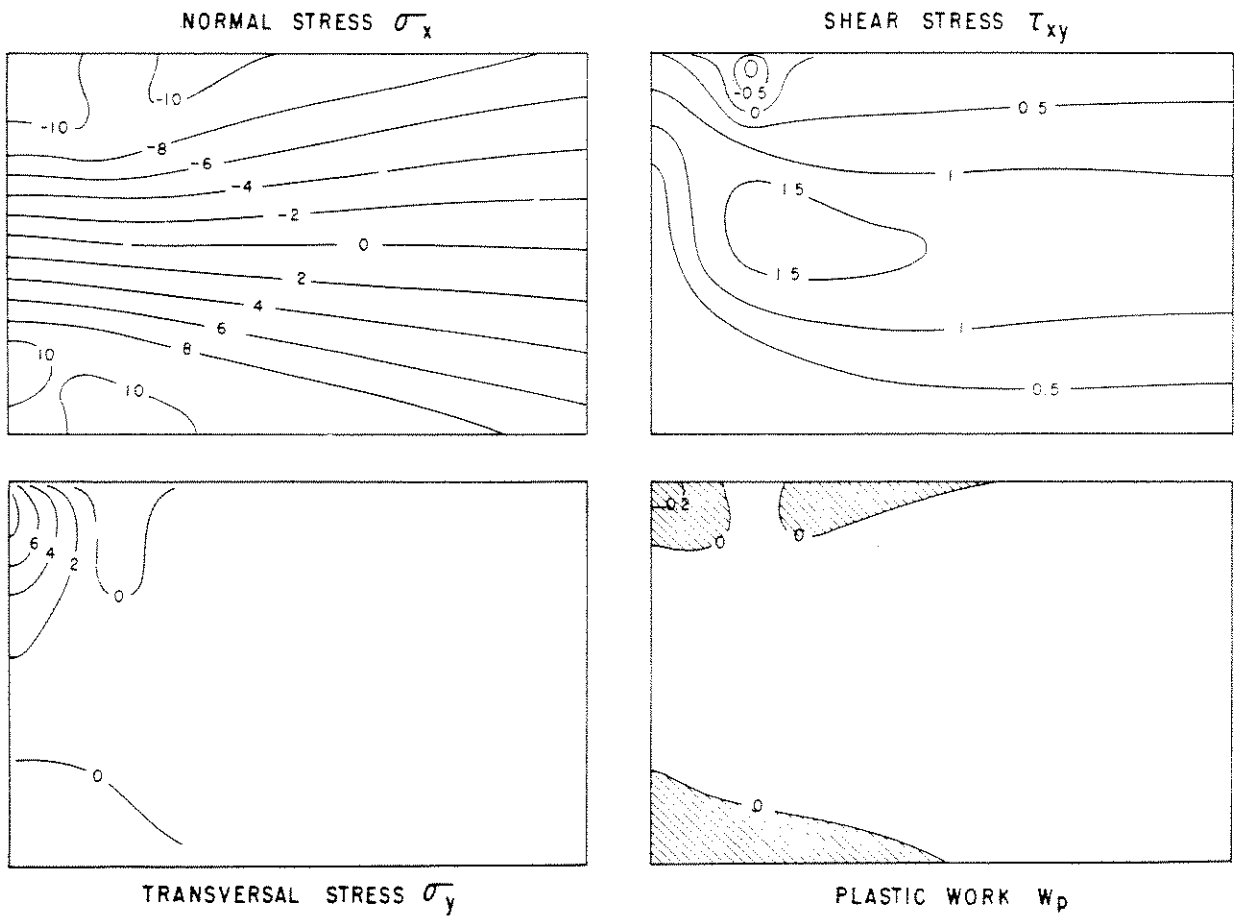


FIG. 5.21 PLASTIC HINGE FORMATION
 ELASTIC SOLUTION AT FIRST YIELD ($\delta/\delta_y=1$)



END-LOADED CANTILEVER BEAM



CENTRALLY-LOADED S.S. BEAM

FIG. 5.22 PLASTIC HINGE FORMATION

SOLUTION AT $\delta/\delta_y = 2.00$

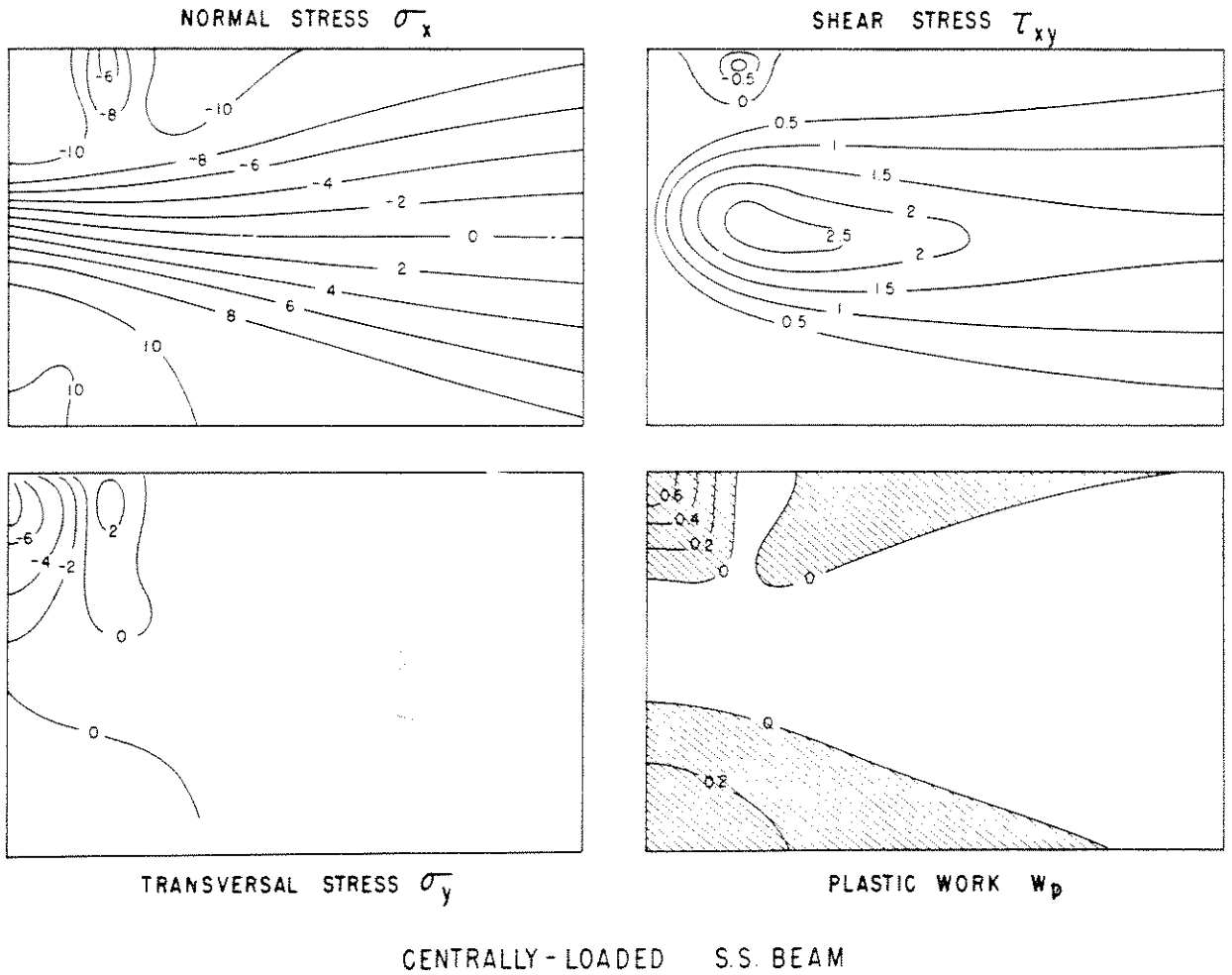
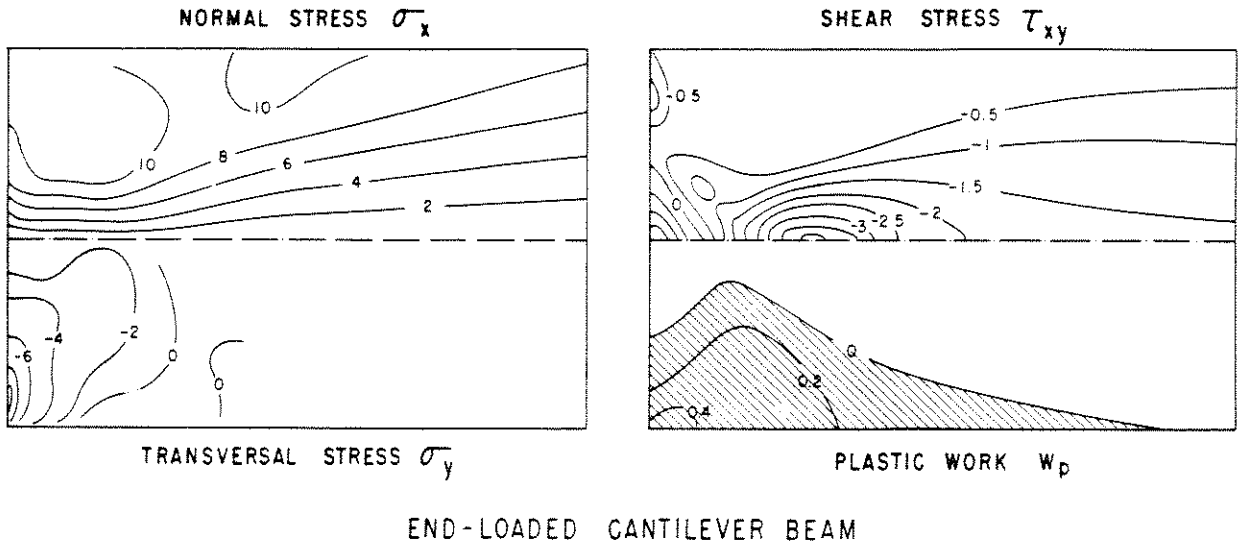


FIG. 5.23 PLASTIC HINGE FORMATION
SOLUTION AT $\delta/\delta_y = 3.25$

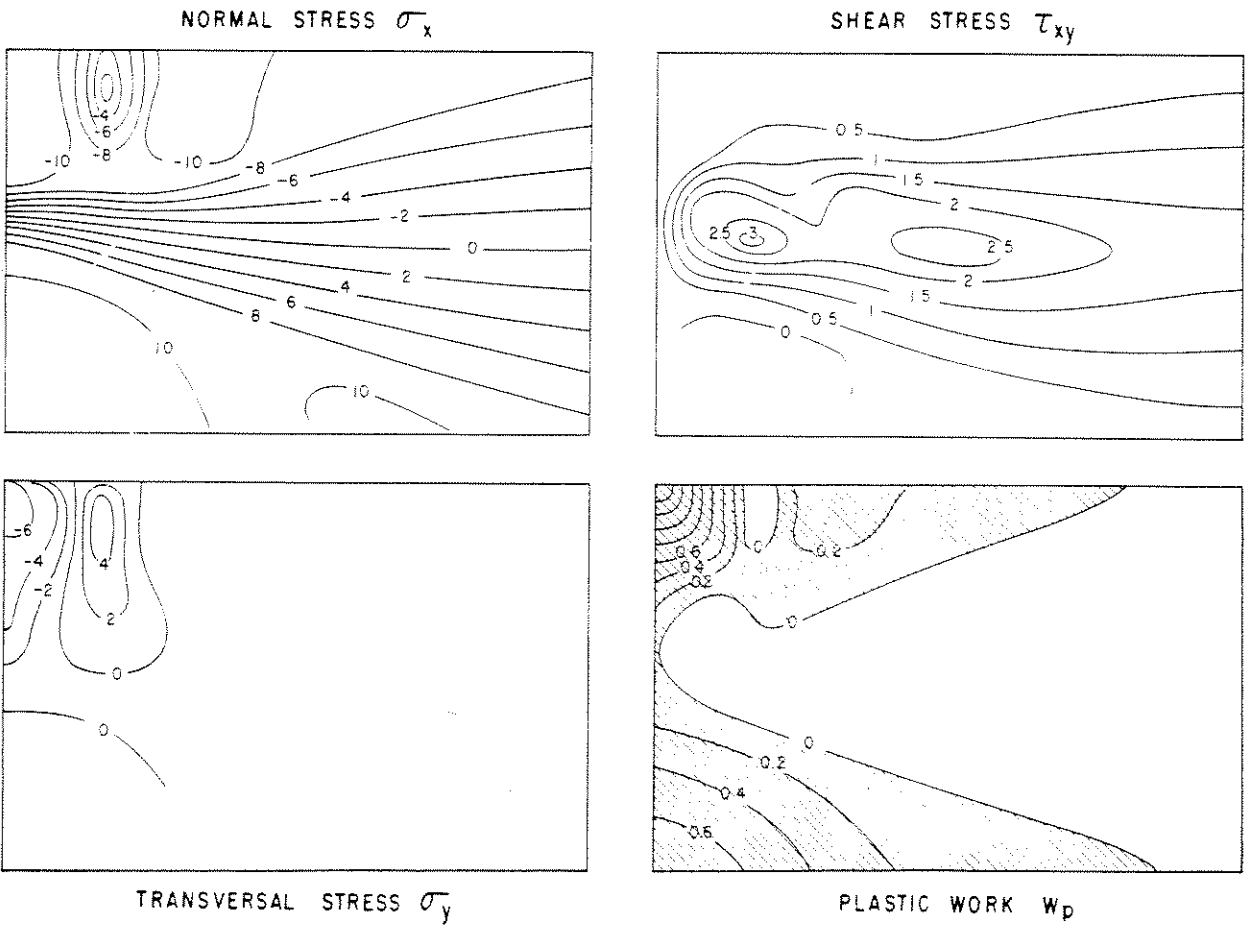
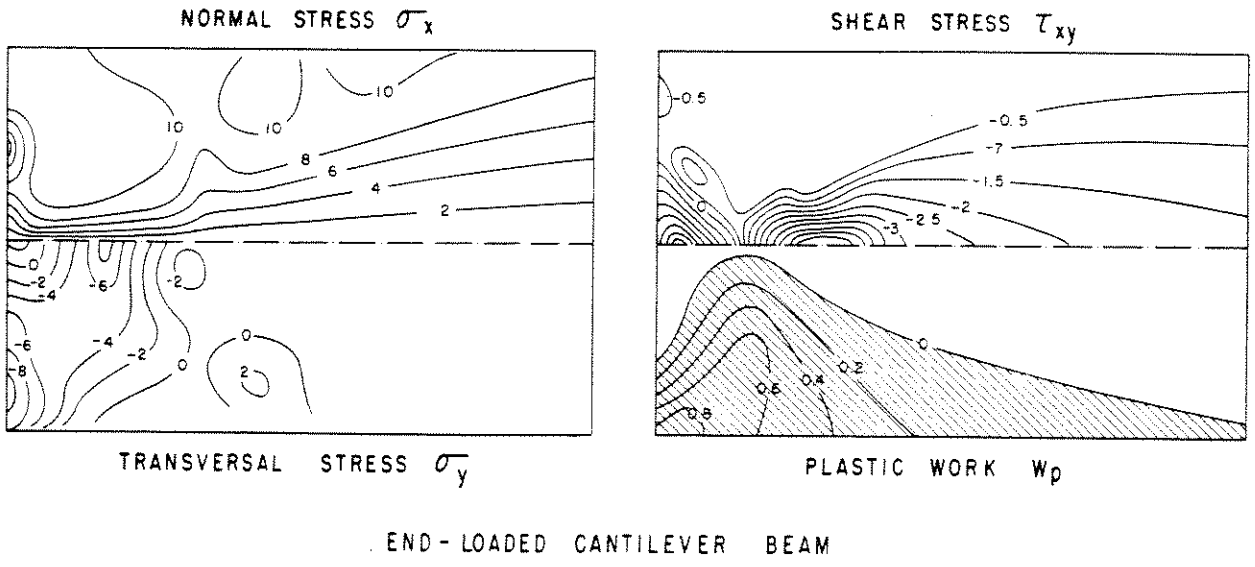


FIG. 5.24 PLASTIC HINGE FORMATION

SOLUTION AT $\delta/\delta_v = 5.00$

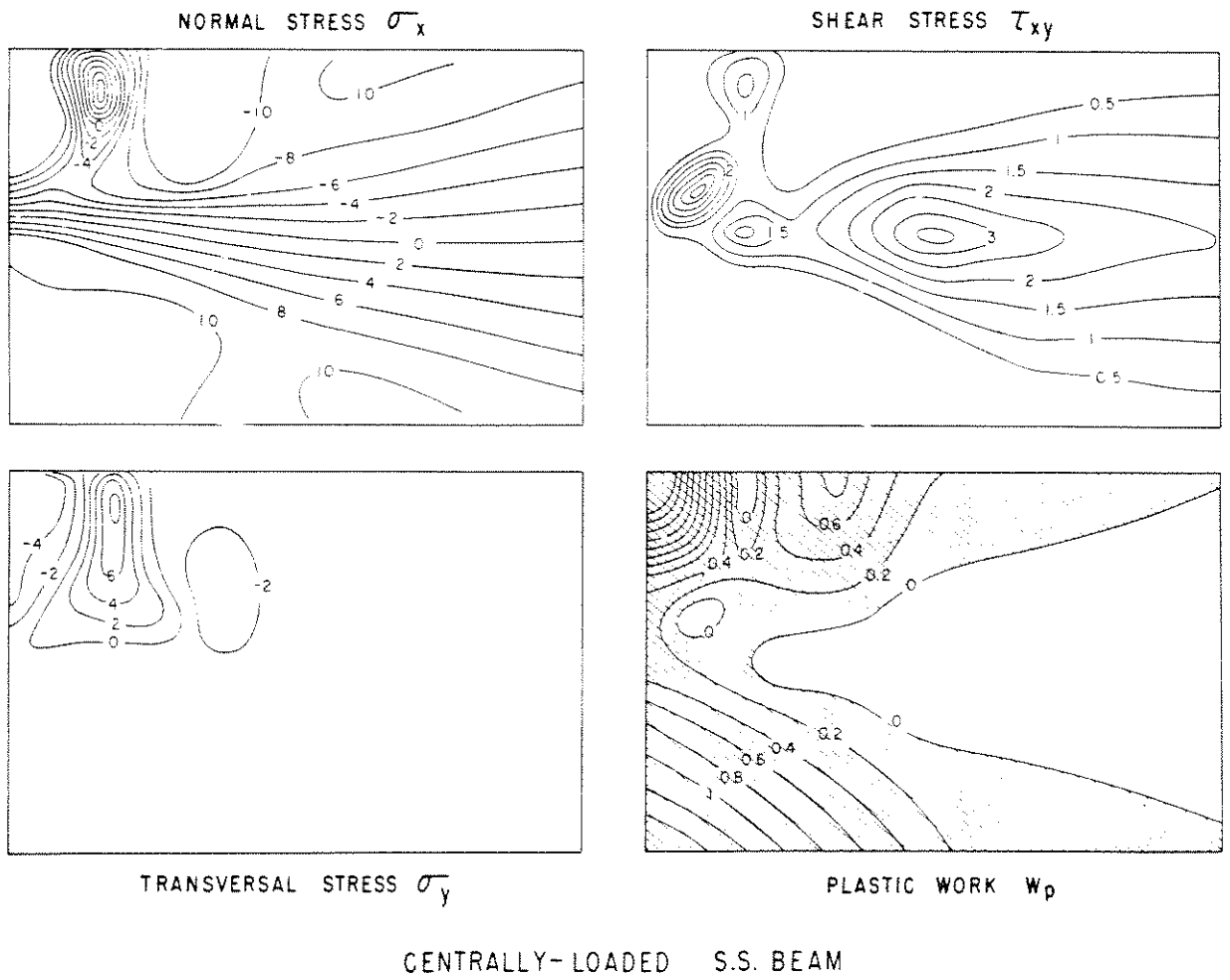
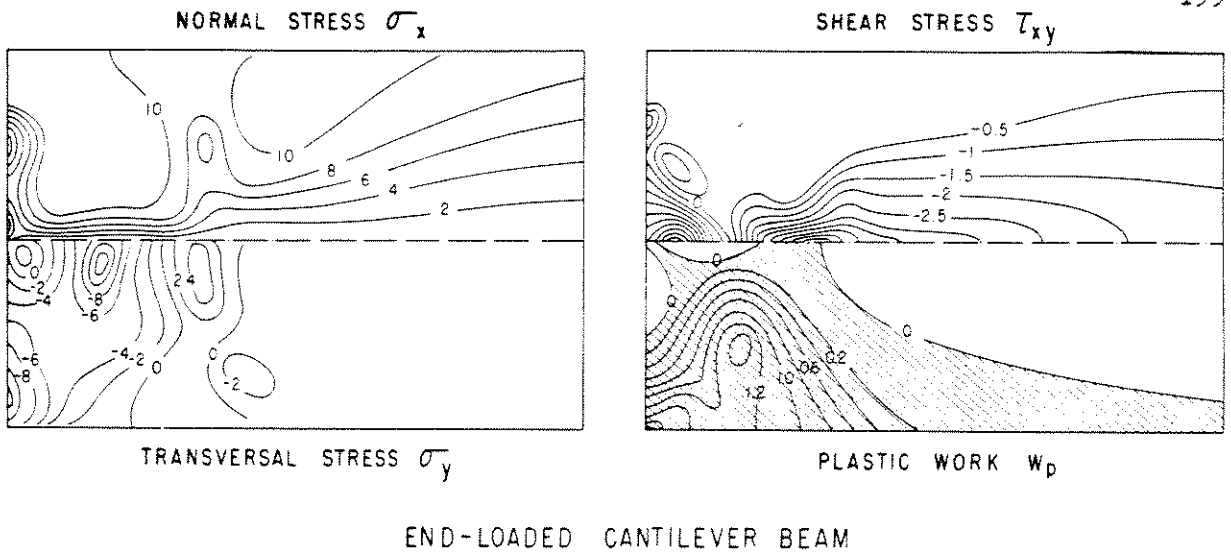


FIG. 5.25 PLASTIC HINGE FORMATION

SOLUTION AT $\delta/\delta_y = 8.00$

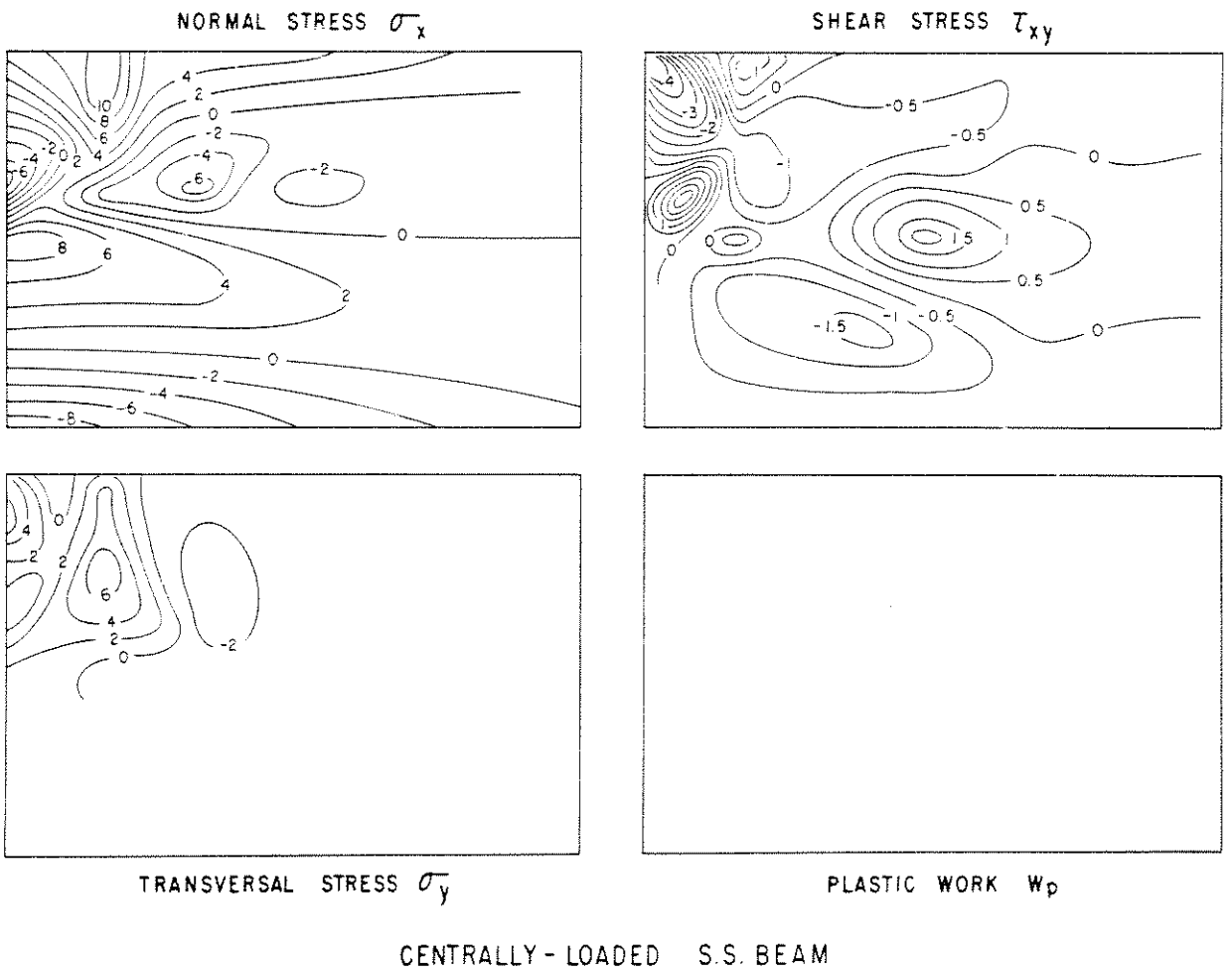
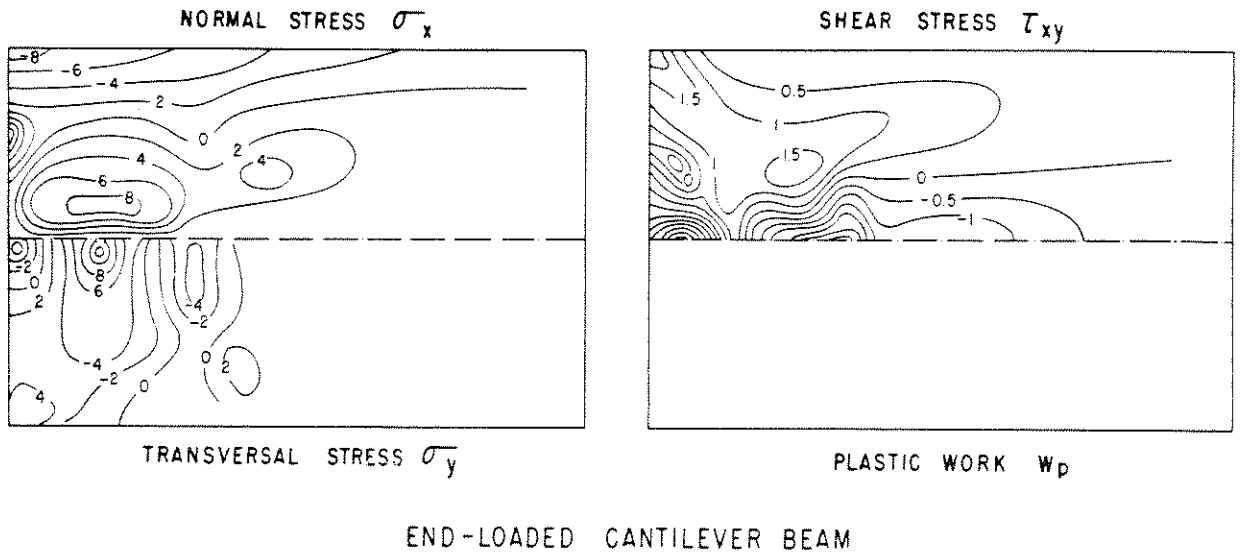
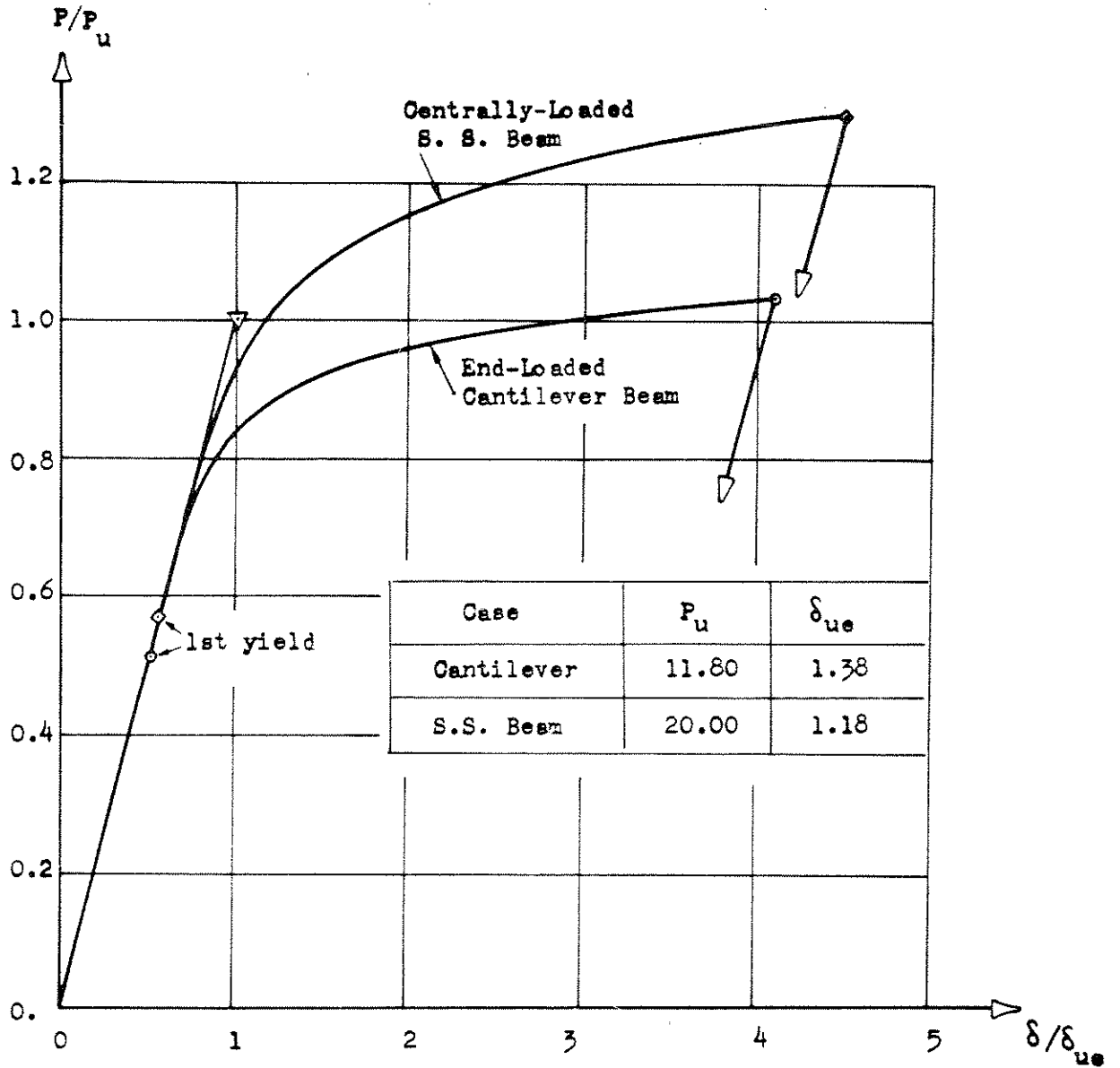


FIG. 5.26 PLASTIC HINGE FORMATION
RESIDUAL STRESSES AFTER UNLOADING



P_u is the load which would produce the theoretical plastic moment M_p at the critical section.

δ_{ue} is the elastic deflection which would take place at $P = P_u$.

δ is the displacement of the loaded point.

Fig. 5.27 - Plastic Hinge Formation: Load-Displacement Curves.

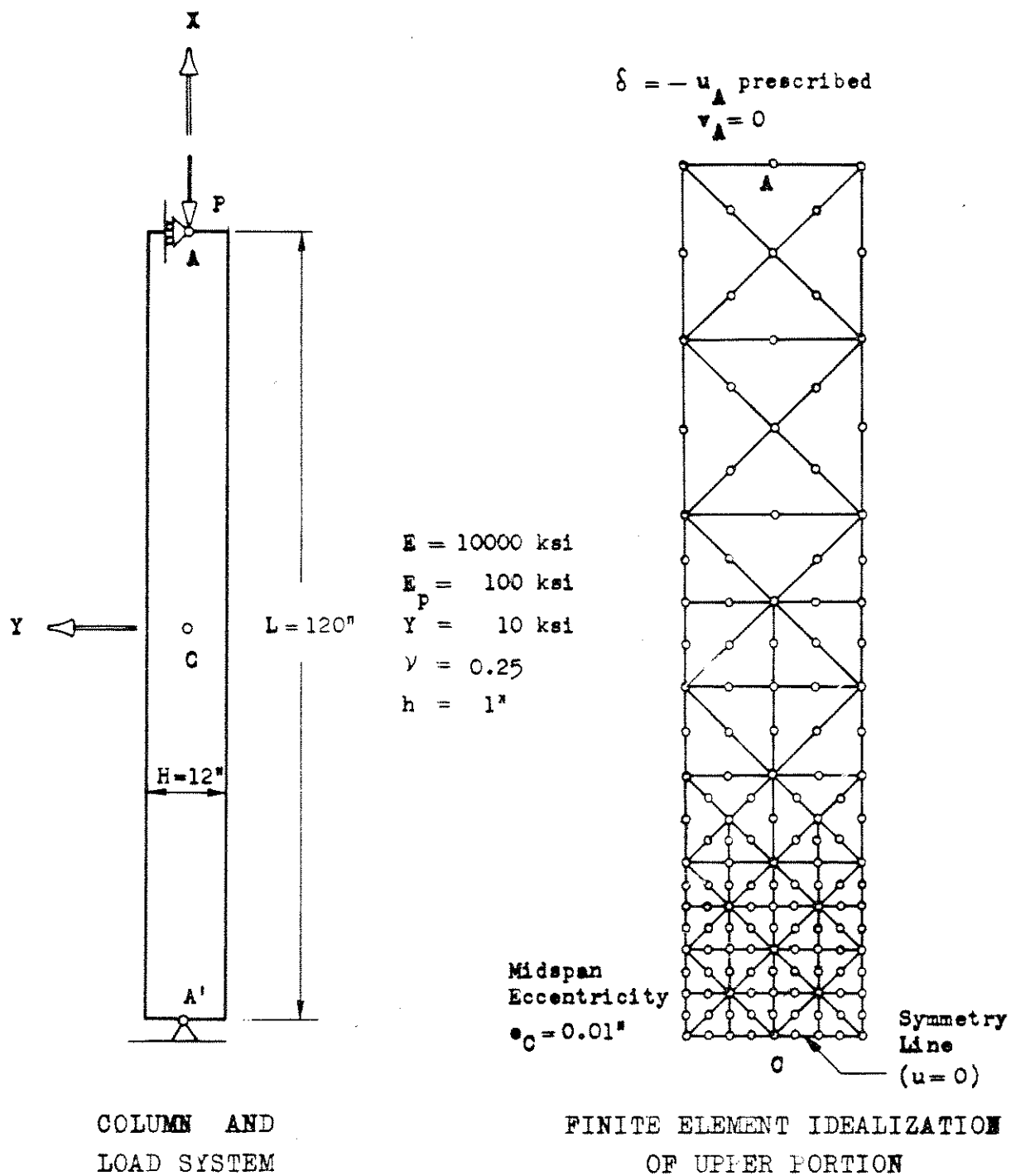


Fig. 5.28 - Plastic Buckling of a Simply Supported Column.

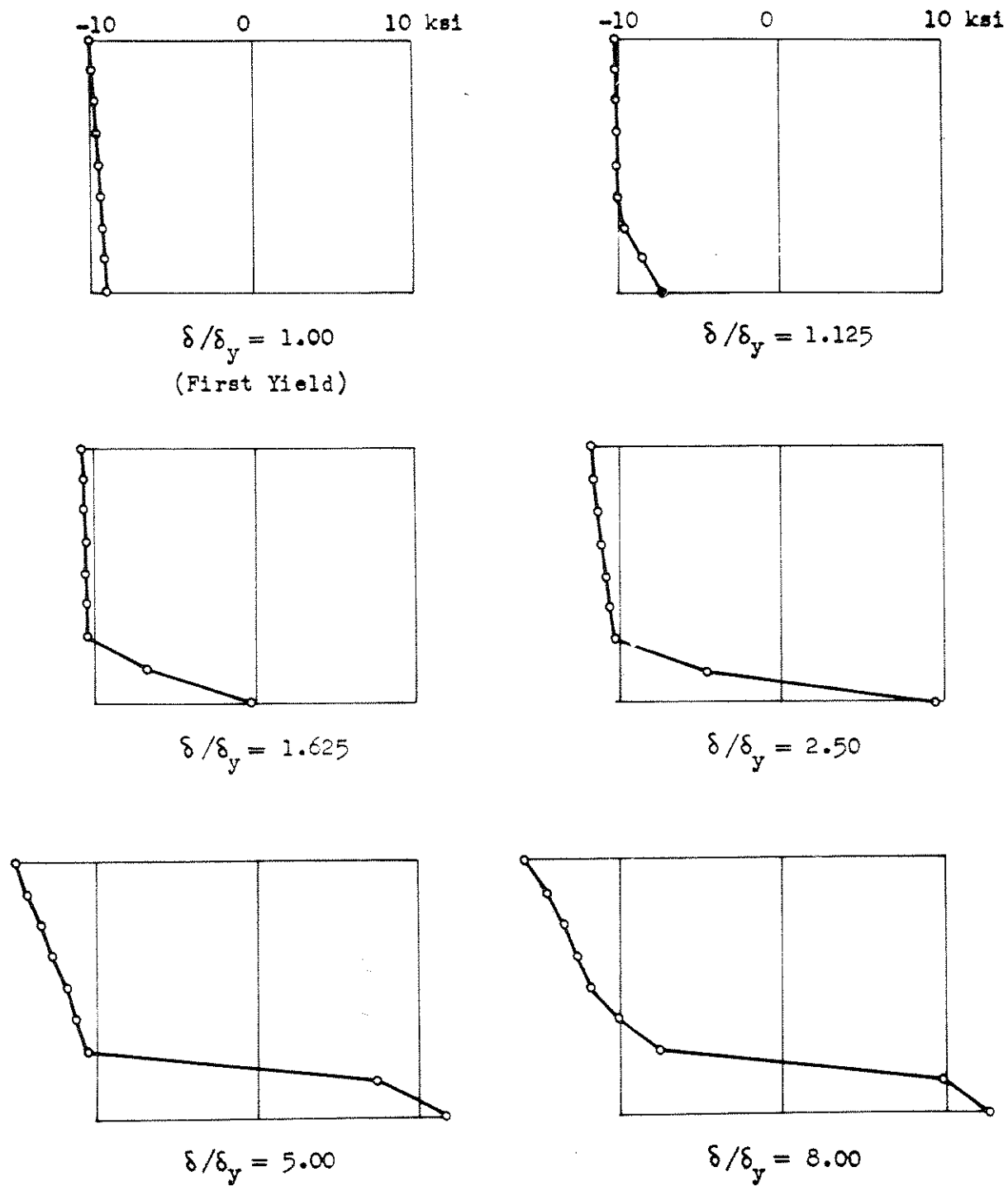


Fig. 5.29 - Plastic Buckling : Normal Stress Distribution
at Midspan Section.

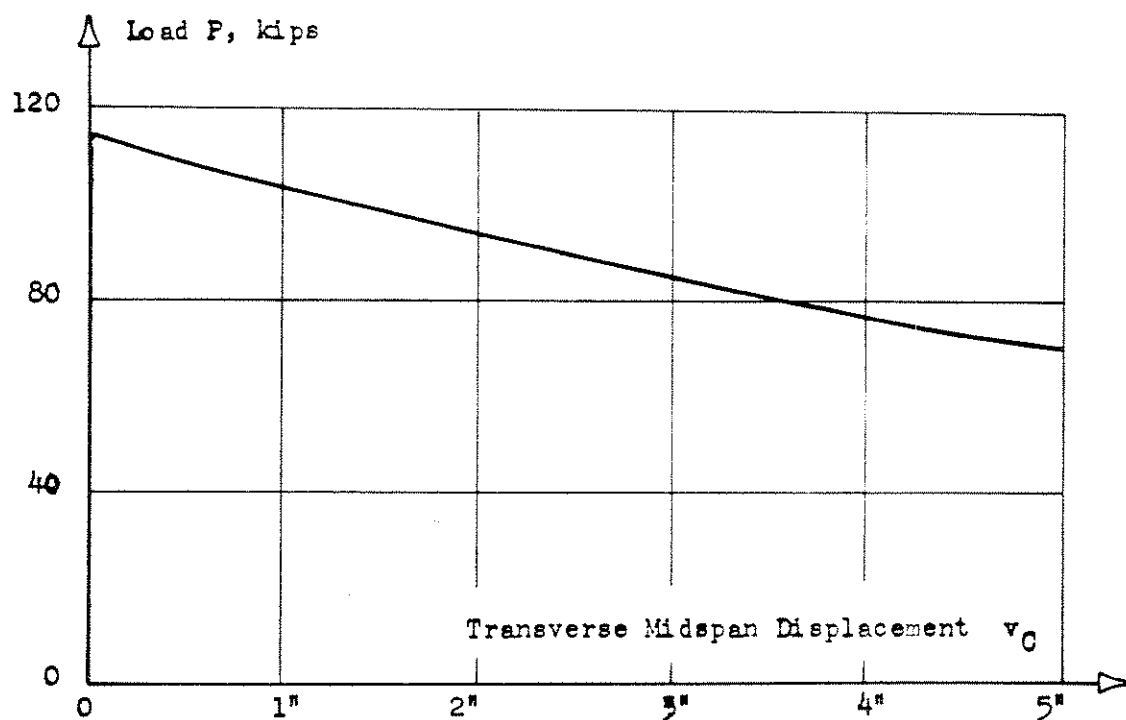
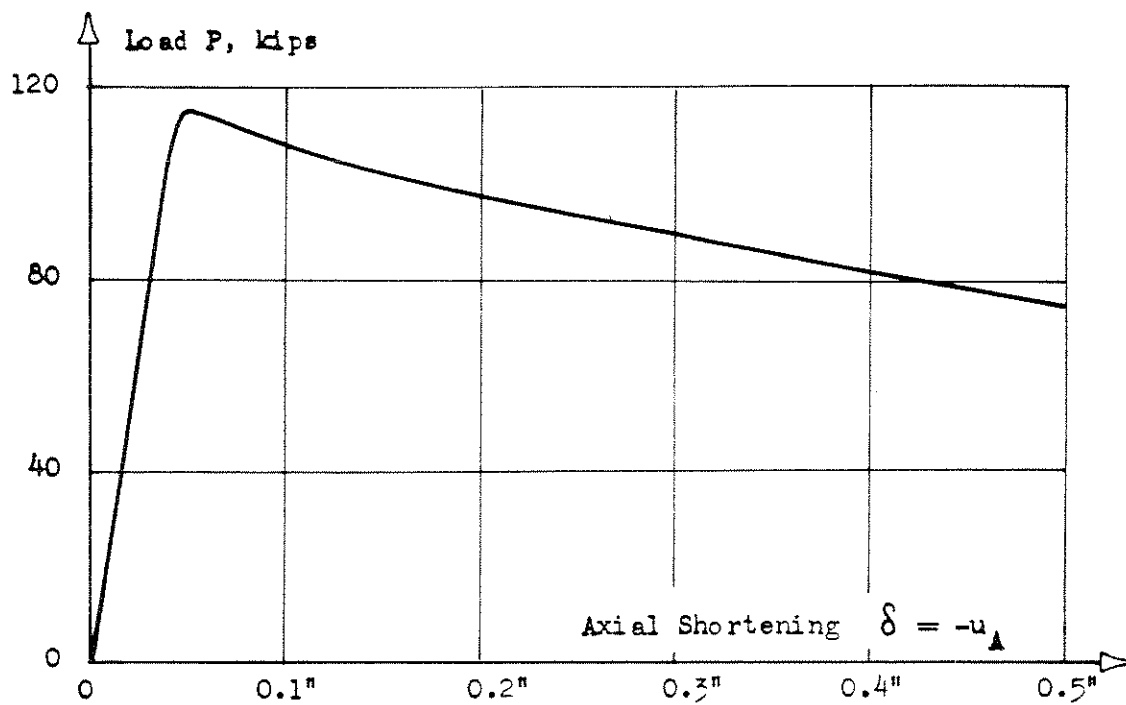


Fig. 5.30 - Plastic Buckling : Load-Displacement Curves.

V.3 ELASTIC STABILITY PROBLEMS

V.3.1 Procedure

A small program was written in order to test the application of the geometric stiffness matrix of the LST to problems of static stability of linear elastic structures in plane stress or plane strain. The external loading is assumed to be conservative and proportional to a parameter. The analysis consists of the following steps:

(a) Formation of the conventional stiffness K_C for the complete structure. Elastic displacements are determined by solving

$$K_C r = R \quad (V-1)$$

where R is the load vector of arbitrary amplitude. Elastic stresses are evaluated from these displacements.

(b) Element geometric stiffnesses are computed by using the elastic stresses and the initial geometry, in agreement with the classical formulation (see IV.3.1). The complete K_G is assembled exactly as K_C ; both are symmetric band matrices.

(c) The eigenvalue problem

$$K_C v = \lambda K_G v \quad (V-2)$$

is most conveniently solved by inverse iteration, since we seek only the smallest root $\lambda_1 = \lambda_{cr}$. The m -th step is

$$\begin{aligned} (K_C - sI) w^{(m)} &= K_G v^{(m)} \\ \lambda^{(m)} &= \max_k (w_k^{(m)}) \\ v^{(m+1)} &= w^{(m)} / \lambda^{(m)} \end{aligned} \quad (V-3)$$

where the shift "s" is applied only every 5 steps, using the estimate $0.9 \lambda^{(m)}$.

As $m \rightarrow \infty$, $(\lambda^{(m)} + s) \rightarrow \lambda_1$ and $\mathbf{v}^{(m)} \rightarrow \mathbf{v}_1$ (buckling eigenmode normalized with 1 as its largest component). When 4 digits of λ_1 are secured, the process is interrupted and the Rayleigh quotient

$$\lambda_{cr} = \frac{\mathbf{v}^T \mathbf{K}_C \mathbf{v}}{\mathbf{v}^T \mathbf{K}_M \mathbf{v}} \quad (\text{V-5})$$

provides 7 or 8 digits for λ_{cr} .

To insure that $\mathbf{v}^{(1)}$ contains components of the first mode, all its entries not restrained by kinematic boundary conditions are set to 1. It is important to impose boundary conditions on both $\mathbf{v}^{(m)}$ and $\mathbf{K}_G \mathbf{v}^{(m)}$ at each step.

V.3.2 Simply Supported Column

A simply supported column of rectangular cross section and slenderness ratio $L/r = 48$ was selected to test the program. One-half of the column was idealized by a coarse mesh of 12 LST elements (Fig. 5.31). A finer mesh of 48 elements, obtained by subdivision of each triangle into four, was also considered.

The critical value given by the beam theory, including shear correction, is

$$P_{cr} = \lambda_{cr} \frac{EI}{L^2} \quad \lambda_{cr} = \frac{\pi^2}{1 + \frac{\beta \pi^2 EI}{GA L^2}}$$

where $\beta = 6/5 = 1.2$ for rectangular cross section, and $G = E/2(1 + \nu)$

For $\nu = 0.25$, the results were

Mesh	Degrees of Freedom	λ_{cr}	Time for Complete Analysis
12 elem.	68	9.6897	6 sec.
48 elem.	244	9.6411	23 sec.
Beam theory		9.7033	

Since the critical values given by a consistent analysis with compatible finite elements are upper bounds of the exact solution, it is evident that both meshes have provided more accurate values than the simple beam theory. The latter underestimates the effect of the shear stresses, while the finite element analysis accounts for the two-dimensional nature of the problem.

The eigenvector shape differed from the sine function only in the fifth decimal place in both cases. Four cycles of iteration were necessary to get λ_{cr} within 0.01% before the Rayleigh quotient was applied.

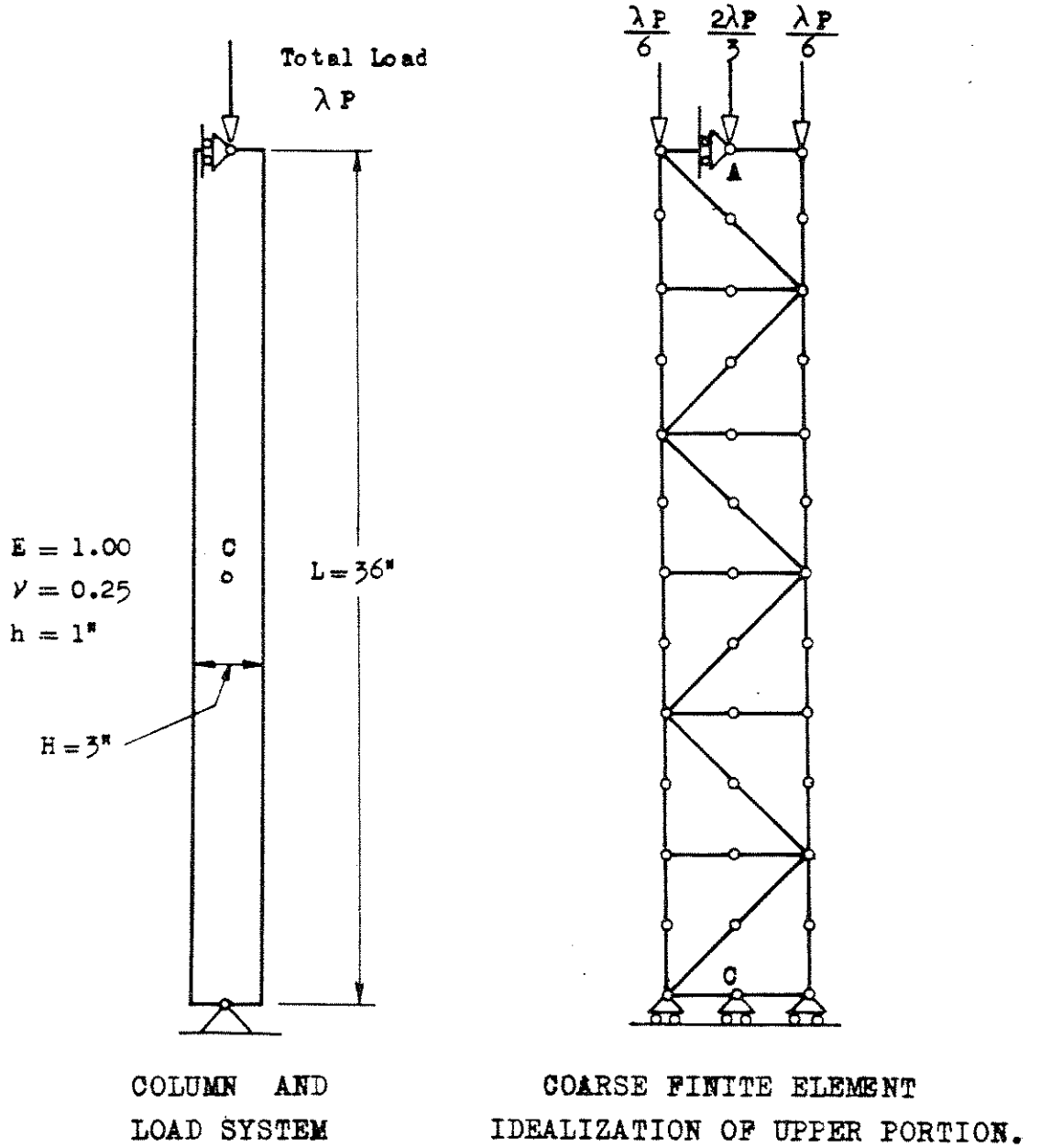


Fig. 5.31 - Elastic Buckling of a Simply Supported Column.

REFERENCES

1. Argyris, J.H., "Energy Theorems and Structural Analysis," Aircraft Eng., 26, Oct.-Nov. 1954; 27, Feb.-May 1955. Also published by Butterworths Sci. Pubs., London, 1960.
2. Turner, M.J., Clough, R.W., Martin, H.C. and Topp, L.J., "Stiffness and Deflection Analysis of Complex Structures," J. Aero. Sci., 23, pp. 805-823, 1956.
3. Adini, A. and Clough, R.W., "Analysis of Plate Bending by the Finite Element Method," NSF Report, Grant G7337, 1960.
4. Melosh, R.J., "A Stiffness Matrix for the Analysis of Thin Plates in Bending," J. Aero. Sci., 28, 34, 1961.
5. Grafton, P.E. and Strome, D.R., "Analysis of Axisymmetric Shells by the Direct Stiffness Method," AIAA Journal, 1, 10, 1963.
6. Rashid, Y., "Solution of Elastostatic Boundary Value Problems by the Finite Element Method," Ph.D. Dissertation, Univ. of California, Berkeley, 1964.
7. Clough, R.W. and Rashid, Y., "Finite Element Analysis of Axisymmetric Solids," J. ASCE, Eng. Mesh. Division, 91, No. EM-1, 1965.
8. Gallagher, R.H., Padlog, J. and Bijlaard, P.P., "Stress Analysis of Heated Complex Shapes," ARS Journal, May 1962.
9. Turner, M.J., "The Direct Stiffness Method of Structural Analysis," AGARD Meeting, Aachen, Germany, 1959.
10. Melosh, R.J., "Development of the Stiffness Method to Define Bounds on Elastic Behavior of Structures," Ph.D. Dissertation, University of Washington, 1962.
11. Melosh, R.J., "Basis of Derivation of Matrices for the Direct Stiffness Method," J. AIAA, 1, p. 1631, 1963.
12. Irons, B.H.R. and Draper, K.J., "Inadequacy of Nodal Connections in a Stiffness Solution for Plate Bending," AIAA Journal, 3,5, 1965.
13. Tocher, J.L., "Analysis of Plate Bending using Triangular Elements," Ph.D. Dissertation, University of California, Berkeley, 1963.
14. Argyris, J.H., "Continua and Discontinua," Opening paper presented at the Conference on Matrix Methods in Structural Mechanics, AFIT, Ohio, 1965.

15. Fraeijs de Veubeke, B.M., "Displacement and Equilibrium Models in Finite Element Method," Chapter 9 of "Stress Analysis," edited by O. C. Zienkiewicz and G.S. Holister, John Wiley and Sons, 1965.
16. Wilson, E.L., "Matrix Analysis of Nonlinear Structures", Proc. 2nd ASCE Conf. on Electronic Computation, Pittsburgh, Pa., Sept. 1960.
17. Wilson, E.L., "Finite Element Analysis of Two-Dimensional Structures," SESM Report No. 63-2, University of California, Berkeley, 1963.
18. Argyris, J.H., Kelsey, S. and Kamel, H., "Matrix Methods of Structural Analysis, A Precis of Recent Developments," published in "Matrix Methods of Structural Analysis," AGARDograph No. 72, edited by F. de Veubeke, Pergamon Press, 1964.
19. Fraeijs de Veubeke, B.M., "Upper and Lower Bounds in Matrix Structural Analysis," published in AGARDograph No. 72 cited in Ref. 18.
20. Herrmann, L.R., "Elasticity Equations for Incompressible and Nearly Incompressible Materials by a Variational Theorem," AIAA Journal, 3,10, October 1965.
21. Herrmann, L.R., "A Bending Analysis for Plates," paper presented at the Conference on Matrix Methods in Structural Mechanics, AFIT, Ohio, 1965.
22. Zienkiewicz, O.C. and Cheung, Y.K., "Finite Elements in the Solution of Field Problems," The Engineer, 220, pp. 507-510, Sept. 1965.
23. Clough, R.W. and Tocher, J.L., "Finite Element Stiffness Matrices for Analysis of Plate Bending," paper presented at the Conference on Matrix Methods in Structural Mechanics, AFIT, Ohio, 1965.
24. Turner, M.J., Martin, H.C. and R.C. Weikel, "Further Developments and Applications of the Stiffness Method," in AGARDograph No. 72, cited in Ref. 18.
25. Clough, R.W., "The Finite Element Method in Structural Mechanics," Chapter 7 of "Stress Analysis", cited in Ref. 15.
26. Hu-Hai-Chang, "On Some Variational Principles in the Theory of Elasticity and the Theory of Plasticity," Sci. Sinica, 4, 1, 1955.
27. Washizu, K., "On Some Variational Principles of Elasticity and Plasticity," ASRL, TR 25-18, MIT Report, 1955.
28. Indritz, J., "Methods in Analysis," MacMillan, 1963.

29. Bogner, F.K., Fox, R.L. and Schmit, L.A., "The Generation of Interelement-Compatible Stiffness and Mass Matrices by the Use of Interpolation Formulas," paper presented at the Conference on Matrix Methods in Structural Mechanics, AFIT, Ohio, 1965.
30. Pestel, E.C., "Dynamic Stiffness Matrix Formulation by Means of Hermitian Polynomials", paper presented at the Conference on Matrix Methods in Structural Mechanics, AFIT, Ohio, 1965.
31. Synge, J.L., "The Hypercircle in Mathematical Physics," Cambridge Univ. Press, 1957.
32. Hammer, P.C. and Stroud, A.H., "Numerical Evaluation of Multiple Integrals," Math. Tables Aids Comp., 12, 1958.
33. Kantorovich, L.V. and Krylov, V.I., "Approximate Methods of Higher Analysis," pp. 355-373, Noordhoff, 1958 (English translation of the 1952 Russian edition).
34. Sokolnikoff, I.S., "Mathematical Theory of Elasticity," Chapter 7, No. 112, McGraw-Hill, 1956.
35. Pian, T.H.H., "Derivation of Element Stiffness Matrices," AIAA Journal, 2, pp. 576-577, 1964.
36. Pian, T.H.H., "Element Stiffness Matrices for Boundary Compatibility and for Prescribed Boundary Stresses," paper presented at the Conference on Matrix Methods in Structural Mechanics, AFIT, Ohio, 1965.
37. Jones, R.E., "A Generalization of the Direct Stiffness Method of Structural Analysis," AIAA Journal, 5, p. 821, 1964.
38. Wissmann, J.W., "Nonlinear Structural Analysis: Tensor Formulation", paper presented at the Conference on Matrix Methods in Structural Mechanics, AFIT, Ohio, 1965.
39. Jones, R.E. and Strome, D.R., "A Survey of the Analysis of Shells by the Displacement Method," paper presented at the Conference on Matrix Methods in Structural Mechanics, AFIT, Ohio, 1965.
40. Tocher, J.L. and Hartz, W., "A Higher Order Plane Stress Element," unpublished paper, 1966.
41. Coleman, B.D. and Noll, W., "An Approximation Theorem for Functionals, with Application in Continuum Mechanics," Arch. Rat. Mech. Anal., 6, pp. 355-370, 1961.

42. Chang, T.Y., "Approximate Methods in Linear Viscoelasticity," Ph.D. Dissertation, Univ. of California, Berkeley, 1966.
43. Yoshimura, Y., "Theory of Plasticity for Small and Finite Deformations, based on Legitimate Concept of Strain," Report No. 348, Aro. Res. Inst., Tokyo University, 1959.
44. Herrmann, L.R., "A Nonlinear Two-Dimensional Stress Analysis Applicable to Solid Propellant Rocket Grains," T.M. No. 20, Aerojet Gral. Corp., 1965.
45. Biot, M.A., "Mechanics of Incremental Deformations," John Wiley and Sons, 1965.
46. Hill, R., "The Mathematical Theory of Plasticity," Oxford Univ. Press, 1960.
47. Pope, G., "The Application of the Matrix Displacement Method to Nonlinear Problems," paper presented at the Conference on Matrix Methods in Structural Mechanics, AFIT, Ohio, 1965.
48. Martin, H.C., "On the Derivation of Stiffness Matrices for the Analysis of Large Deflection and Stability Problems," paper presented at the Conference on Matrix Methods in Structural Mechanics, AFIT, Ohio, 1965.
49. Langhaar, H.L., "Energy Methods in Applied Mechanics," Chapter 6, John Wiley and Sons, 1962.
50. Bolotin, V.V., "Nonconservative Problems of the Theory of Elastic Stability," Pergamon Press, 1963.
51. Shanley, F.R., "Inelastic Column Theory," J. Aero. Sci., 14, 261, 1947.
52. Bleich, F., "Buckling Strength of Metal Structures," Chapter 1, McGraw-Hill, 1952.
53. Howland, R.C.J., Trans. Royal Soc., London, series A, 221, p. 265. 1921.
54. Abu-Ghazaleh, B.N., "Analysis of Plate Type Prismatic Structures", Ph.D. Dissertation, University of California, Berkeley, 1966.

REFINED FINITE ELEMENT ANALYSIS OF LINEAR AND
 NONLINEAR TWO-DIMENSIONAL STRUCTURES
 S.E.S.M. Report Nos. 66-22 and 66-22a

CORRIGENDA

Page 13 - Formula (I-5): the "**x**" in " $a_i \phi_i(\mathbf{x})$ " should be a bold-face (vector) symbol. Likewise for the third line from bottom, in " $(\mathbf{x}_1, \mathbf{x}_2, \dots, \mathbf{x}_m)$ ".

Page 20 - In Equations (I-15a) and (I-15b), " x_k " and " y_k " should be " x_j " and " y_j ". The last of Equations (I-16) should read

$$\frac{\partial s_i}{\partial y} = - \frac{\partial n_i}{\partial x} = - \frac{b_i}{l_i}$$

Page 29 - The name of the vector displayed at the bottom should be " ϕ_3^* ".

Page 31 - In Equation (I-30), the right hand side should be

$$\begin{pmatrix} f_4 \\ f_5 \\ f_6 \\ f_7 \\ f_8 \\ f_9 \end{pmatrix} = \dots$$

Page 37 - In the 4th line from the top, the word "cancellation" has been misspelled.

- Page 38 - In Table 4, formula no. 4, the triangular coordinates of point "f" should be 0,1,0.
- Page 39 - In Table 4 (con't), formula no. 5, the triangular coordinates of points "b", "c" and "d" (as represented in the Figure) should be
- b: $\beta_1, \beta_1, \alpha_1$
- c: $\alpha_1, \beta_1, \beta_1$
- d: $\beta_1, \alpha_1, \beta_1$
- Page 48 - The second of (II-4b) should read " $R = R_1 - K_{12} K_{22}^{-1} R_2$ ".
- Page 61 - In the fifth written line from the bottom, (" N_C ") should be (" N_ϵ ").
- Page 64 - In Equation (II-42): " u_B " and " v_B " should be represented as bold-face symbols.
- Page 65 - In Equation (II-43): symbols " ϕ_p " and " ϕ_B " should be changed to " Φ_p " and " Φ_B ".
- Page 68 - Equation (II-51) should read
- $$2T = \int_V \dot{\mathbf{r}}^T \dot{\mathbf{r}} \, dm = \dot{\mathbf{r}}^T \int_V \dots$$
- Page 70 - In Equation (II-59), " ϕ_θ " should be " ϕ_θ^T ".
- Page 71 - In the second of (II-65), an asterisk is missing on the second " \bar{q} ".

- Page 96 - In Equation (III-49), "r" should be " \bar{r} ".
- Page 99 - Line 5 should read " $(v_x + u_y)/2$ " and line 6 should read " $(v_x - u_y)/2$ ".
- Page 105 - Equation in line 7 should read " $R_f = R_f^* - K_{10} K_{00}^{-1} R_{fo}^*$ ".
- Page 114 - Fig. 4.2: there should be a factor $\frac{1}{2}$ multiplying " $\Delta^2 U$ ".
- Page 115 - In Equation (IV-3), the right hand side should read
- $$= \int_D (F^i + \Delta \bar{F}^i) \delta(\Delta u_i) dV + \int_{B_T} (T^i + \Delta \bar{T}^i) \delta(\Delta u_i) dS$$
- Page 116 - In Equation (IV-6), the subindex of " u_k " in the first term of the right hand side should be "i".
- In the right hand side of (IV-7), " F^i " and " T^i " should be " \bar{F}^i " and " \bar{T}^i ", and a Δ is missing before " u_i " in the last term.
- In second written line from the bottom, "(IV-17)" should be "(IV-7)".
- Page 120 - Second last written line: "(IV-10b)" should be "(IV-8b)".
- Page 122 - Third last written line: "(IV-17)" should be "(IV-18)".
- Page 125 - Fifth line: in the expression of J_2 , a $\frac{1}{2}$ factor should multiply " $(s_1^2 + s_2^2 + s_3^2)$ ".
- Page 128 - In Equation in line 4, a factor "h" is missing in the last right hand side.
- In Equations (IV-38) and (IV-39), the coefficient " α " should be deleted.

Page 129 - In the line following (IV-40), " $\bar{\sigma}$ " was left out.

In right hand side of (IV-43), "3" should be replaced by " $\sqrt{3}$ ".

Page 132 - In Equation (IV-57), the matrix should be labeled "symmetric".

Likewise in Equation (IV-62) on page 134.

Page 147 - Fifth written line: "awkward" has been misspelled.

Second line of second paragraph: should read "geometric" instead of "geometry".

Page 148 - First line of second paragraph: a bar over " K_G " is missing.

Page 151 - In Equation (IV-85), a transpose sign is missing for $\phi_{k,j}^T$.

Likewise in (IV-88): the last factor should be $\phi_{n,j}^T$.

Page 154 - (first line), 155 (Figs. 4.9 and 4.10) and 156 (fifth last line): the axial force "P" should be " $\frac{1}{2}(P_2 - P_1)$ " instead of " $P_2 - P_1$ ".

Page 154 - The fourth Equation should read

$$\mathbf{a}^T = \frac{1}{L} \langle -1 \quad 1 \rangle = \dots$$

Page 217 - Equation (A1-7) should read

$$\mathbf{T}_\varepsilon = \begin{bmatrix} \alpha^2 & \beta^2 & 0 & \alpha\beta \\ \beta^2 & \alpha^2 & 0 & -\alpha\beta \\ 0 & 0 & 1 & 0 \\ -2\alpha\beta & 2\alpha\beta & 0 & \alpha^2 - \beta^2 \end{bmatrix} \quad \mathbf{T}_t = \begin{bmatrix} \alpha^2 & \beta^2 & 0 & 2\alpha\beta \\ \beta^2 & \alpha^2 & 0 & -2\alpha\beta \\ 0 & 0 & 1 & 0 \\ -\alpha\beta & \alpha\beta & 0 & \alpha^2 - \beta^2 \end{bmatrix}$$

Page 218 - Equations (A1-10) should be

$$c_{11} = c_{11}^p \alpha^4 + (2c_{12}^p + 4c_{44}^p) \alpha^2 \beta^2 + c_{22}^p \beta^4$$

$$c_{22} = c_{11}^p \beta^4 + (2c_{12}^p + 4c_{44}^p) \alpha^2 \beta^2 + c_{22}^p \alpha^4$$

$$c_{44} = \dots \text{ and } c_{12} = \dots \text{ correct}$$

$$c_{14} = - \left[c_{22}^p \beta^2 - c_{11}^p \alpha^2 + (c_{12}^p + 2c_{44}^p) (\alpha^2 - \beta^2) \right] \alpha \beta$$

$$c_{24} = \left[c_{11}^p \beta^2 - c_{22}^p \alpha^2 + (c_{12}^p + 2c_{44}^p) (\alpha^2 - \beta^2) \right] \alpha \beta$$

Page 239 - Third last line should read "either J or L".

Page 240 - In Fig. A3.5, the caption should read "For single triangles, K-I is ...".

Page 243 - The FORMAT for (n) should be "(2I4,6F8.3)".

Pages 262 and 263 - (computer list of PSE-LST) have been transposed.

Page 279 - Array subscript in lines 30 and 31 should be "I" and not "1", i.e., XMIN = XORD(I) and YMIN = YORD(I).